Diese Dissertation haben begutachtet

Prof. Dr. Robert Liska

Prof. Dr. Heinz Redl

PhD Thesis

Dissertation

Development and Processing of Materials for Vascular Tissue Regeneration

ausgeführt zum Zwecke der Erlangung des akademischen Grades eines
Doktors der technischen Wissenschaften

unter der Leitung von
Ao. Univ. Prof. Dr. Robert Liska

e163
Institut für Angewandte Synthesechemie

eingereicht an der Technischen Universität Wien
Fakultät für Technische Chemie

von
Dipl.-Ing. Stefan Baudis
e0027410

Andersengasse 32/17/7, 1120 Wien

Wien, 15. Dezember 2010

Dipl.-Ing. Stefan Baudis

Nichts kann existieren ohne Ordnung.
Nichts kann entstehen ohne Chaos.

Albert Einstein (1879-1955)

Danksagung

An dieser Stelle möchte ich mich bei meinem Betreuer und Doktorvater Robert Liska für die äußerst interessante und interdisziplinäre Themenstellung bedanken. Sein ständiges Bemühen, mich fachkundig zu betreuen und stets eine angenehme Atmosphäre zu pflegen, hat die Arbeit in dieser Form erst möglich gemacht.

Besonderer Dank gilt auch allen Kooperationspartnern.

Jürgen Stampfl und Thomas Koch vom Institut für Werkstoffwissenschaft und Werkstofftechnologie der TU-Wien standen mir stets mit ihren Kompetenzen hinsichtlich generativer Fertigungsmethoden und Werkstoffprüfung zur Seite.

Auch möchte ich all den Mitarbeitern von der Medizinischen Universität Wien danken. Helga Bergmeister war bei all den Projekten von Anfang an dabei, hat die Arbeiten maßgeblich vorangetrieben und zu guter Letzt die in-vivo Studien ermöglicht. Ich danke David Bernhard, Anneliese Nigisch und Brigitta Winter für die in-vitro Tests und Heinrich Schima, Christian Grasl und Martin Stoiber für die Verarbeitung und Testung der elektroversponnenen Materialien.

Besonders wichtig war mir die Zusammenarbeit mit dem TGM. Harald Wilhelm und seine Schüler Bernhard Steyrer, Thomas Pulka, Paul Werner und Dominik Strommer haben einen wichtigen Beitrag zur mechanischen Charakterisierung der Photopolymer-Materialien geleistet, für den ich mich herzlich bedanke. In diesen Zusammenhang will ich mich auch bei Marko D. Mihovilovic bedanken, der die Zusammenarbeit mit den Schülern im Rahmen des Sparkling Science Austauschprogrammes erst ermöglichte.

Ich danke meinen Wahlpraktikanten, Bachelor- bzw. Diplomstudenten Julia Weber, Maria Schwarz Anna Ressmann und Franzi Nehl, die mir einen großen Teil der Arbeit abgenommen haben.

Außerdem möchte ich mich bei Heinz Redl bedanken, dafür, dass er sich dazu bereit erklärt hat, meine Dissertation zu begutachten.

Mein Dank gilt auch allen Kolleginnen, Kollegen und Mitarbeitern des Instituts, im Besonderen der Forschungsgruppe von Heinrich Gruber, die alle zusammen eine sehr angenehme Arbeitsatmosphäre geschaffen haben, aber mir auch produktiv zur Seite standen.
Besonders hervorheben möchte ich Christian Heller, Niki Pucher, Martin „Speidi“ Schwentenwein und vor allem Andi Mautner, der genau zum richtigen Zeitpunkt da war, um mir zu helfen!

All meinen Freunden möchte ich danken für ihre Freundschaft und ihre stete Unterstützung!
Vielen Dank, Sarah, dass du mich in den besonders schweren Monaten stets aufgemuntert und mir Zuversicht geschenkt hast!
Vielen Dank, Mama, Papa, Claudia, Oma und Opa, dass ihr immer hinter mir gestanden habt, mir eine wunderschöne Kindheit beschert habt und stets bemüht ward, mein Interesse an der Chemie zu verstehen!

Kurzfassung

Eine aufstrebende Disziplin in den Biowissenschaften ist das Tissue Engineering. Diese Disziplin beschäftigt sich mit der künstlichen Herstellung von neuem Gewebe und gilt daher als großer Hoffnungsträger für unsere Gesellschaft, die stetig älter und dadurch aber auch immer mehr von Zivilisationskrankheiten betroffen ist. Erkrankungen des Herz-Kreislaufsystems sind in diesem Zusammenhang besonders hervorzuheben.
Ziel des Tissue Engineering ist es, ein bioabbaubares, poröses Konstrukt (engl. „scaffold“) herzustellen, dass sich – sobald im Körper implantiert – durch Anregung körpereigener Regenerationsmechanismen in einem überschaubaren Zeitraum in natürliches Gewebe umformt. Nur in der ersten Phase soll das Konstrukt die volle Funktion des Gewebes übernehmen, aber dann dem neu gebildeten Gewebe weichen.
Diese Arbeit konzentriert sich auf die Entwicklung von Materialien und die Herstellung von Konstrukten für das Tissue Engineering von Blutgefäßen, im Besonderen für Koronararterien-Bypässe. Die Anforderungen für ein solches Material und die daraus hergestellten Konstrukte sind sehr hoch. Die sollen neben der Abbaubarkeit auch noch mechanische Eigenschaften ähnlich denen des zu ersetzenden Gewebes aufweisen und eine einstellbare Porosität haben, damit gleichmäßiges Einwachsen von neuem Gewebe gewährleistet werden kann.
In dieser Arbeit wurden zwei verschiedene Verarbeitungstechniken näher in Betracht gezogen: die Photopolymerisation-basierte generative Fertigung (engl. „Rapid Prototyping“, RP; „Additive Manufacturing Technologies“, AMT) und das Elektroverspinnen von thermoplastischen Elastomeren.
Mit Hilfe der generativen Fertigung ist es möglich zellulare Strukturen mit definierter Porosität und Interkonnektivität der Poren herzustellen. Um die besonders hohen Materialanforderungen zu erfüllen, muss besonderes Augenmerk auf die Netzwerkarchitektur der Photopolymere gelegt werden. Durch Einführung des Thiol-Ene-Konzepts verringert man die Sprödigkeit der Materialien, kann Abbaubarkeit induzieren und hält zudem das Molekulargewicht der Abbauprodukte niedrig. Die Photopolymere aus einer Kombination aus einem kommerziellen Urethandiacrylat, 2-Hydroxyethylacrylat und Ethylenglykolbisthioglykolat erfüllten alle mechanischen Grundvoraussetzungen (E-Modul, Reißfestigkeit, Nahtausreißwiderstand), zeigten gute Biokompatibilität und Abbaubarkeit in *in-vitro*-Tests und konnten erfolgreich mittels der generativen Fertigungsmethode DLP (engl. „Digital Light Processing“) zu zellularen Strukturen verarbeitet werden.
Beim Elektroverspinnen von thermoplastischen Elastomeren erhält man bei geeigneter Prozessführung direkt röhrenförmige Konstrukte, deren Mikrostruktur, aufgrund der zufälligen Anordnung von Nanofasern, der der extrazellulären Matrix sehr ähnelt. Deshalb wachsen Zellen auch trotz der fremden chemischen Umgebung auf diesen Oberflächen sehr gut. Kommerzielle thermoplastische Urethanelastomere (TPUs) haben bereits ausgezeichnete Eigenschaften als künstliche, elektroversponnene Blutgefäßersatzmaterialien gezeigt. Um das Wachstum einer Neoarterie zu induzieren und damit die Langzeitdurchgängigkeit zu verbessern, ist es aber nötig, dass diese Materialien bioabbaubar sind. Deshalb war es Ziel im zweiten Teil der Arbeit, abbaubare TPUs zu entwickeln. Das Konzept war der Einbau von spaltbaren Bindungen in das Rückgrat der Polymere. Der Einsatz spaltbarer Kettenverlänger (engl. cleavable chain extender, CCE) führt zu hartblock-abbaubaren TPUs. Es wurden eine Reihe von TPUs mit verschiedenen Laktat- bzw. Ethylenglykol basierten CCE synthetisiert. Die mechanischen Eigenschaften der neuen Polymere waren vergleichbar mit jenen kommerzieller TPUs, auch im versponnenen Zustand. TPUs mit verschiedenen CCE bauten mit 10 bis 200% der Rate von chirurgischem PLA ab. Die Abbauprodukte zeigten keine Zelltoxizität unter *in-vitro*-Testbedingungen bis zu einer Konzentration von 1 mmol/L. Das bestgeeignetste Material wurde im Ratten-Aorta-Modell *in-vivo* getestet. Die ersten Resultate zeigten eine gute Verträglichkeit des Materials und keine Thrombenbildung.

Abstract

An emerging discipline in life science is tissue engineering. This discipline tries the artificial generation of natural tissue and is therefore the big hope of our society which continuously grows older and therefore is increasingly concerned with life style diseases. The emphases in this context are diseases of the cardiovascular system.
The goal of tissue engineering is the fabrication of biodegradable, porous scaffolds which – as soon as grafted the body – trigger the inherent regenerative mechanism of the body and therefore are remodeled to natural tissue in a manageable period of time. Only in the short term the scaffold has to take over the whole function of the tissue but then give way to the new formed tissue.
This work is concentrated on the development of materials and the fabrication of scaffolds for vascular tissue engineering with the main focus on coronary artery bypass grafts. The requirements for such materials and the thereof fabricated scaffolds are very high. Aside the degradability the materials should have mechanical properties which match those of the tissue and possess a tailorable porosity to enable the ingrowth of new tissue.
In this work two different processing techniques were considered in detail: photopolymerization based additive manufacturing technologies (AMT) and electrospinning of thermoplastic elastomers.
By means of AMT it is possible to fabricate cellular structures with defined porosity and interconnectivity of the pores. To fulfill the high material requirements special attention has to be paid on the network architecture of the photopolymers. The introduction of the thiol-ene concept decreases the brittleness of the materials, also induces degradability and furthermore holds the molecular weight of the degradation products low. Photopolymers out of a combination of a commercial urethane diacrylate, 2-hydroxyethyl acrylate and ethylene glycol bisthioglycolate fulfilled all the basic mechanical requirements (elastic modulus, tensile strength and suture tear resistance), exhibited good biocompatibility and degradability in *in-vitro* tests and could be successfully processed to cellular scaffolds by the AMT DLP (digital light processing).
The electrospinning of thermoplastic elastomers directly leads to tubular scaffolds in case the process is conducted in suitable manner. The scaffolds possess a microstructure due to the random orientation of the nanofibers, which is very similar to the structure of the extracellular matrix. For this cells grow readily onto these surfaces despite the foreign chemical nature of the material. Commercial thermoplastic urethane elastomers (TPUs) already showed good performances as artificial electrospun vascular prosthetics. In order to induce the growth of a neo-artery and hence increase the long-term patency of the graft the use of biodegradable TPUs is beneficial. Therefore it was the aim of the second part of this work to develop degradable TPUs. The concept was to introduce cleavable bonds into the backbone of the polymers. The application of cleavable chain extenders (CCE) leads to hard-block degradable TPUs. Therefore a number of TPUs consisting of different lactide- and ethylene glycol-based CCE was synthesized. The mechanical properties of the new polymers are comparable to those of commercial TPUs, also in the electrospun application form. The TPUs with different chain extenders degraded with 10 to 200% of the rate of surgical PLA. The expected degradation products showed no cytotoxicity under *in-vitro* test conditions up to a concentration of 1 mmol/L. The most suitable material was tested in the *in-vivo* model of rat aorta. The first results showed a good compatibility of the material and no formation of thrombi.

Table of content

Introduction			
1.	**The cardiovascular system**	**1**	
2.	**Diseases of the cardiovascular system**	**2**	
3.	**Therapies**	**2**	
4.	**Tissue Engineering**	**7**	
5.	**Additive manufacturing technologies**	**14**	
6.	**Electrospinning**	**18**	
Objective		**21**	
State of the Art		**23**	
Results & Discussion		**29**	**Exp**
1.	**Photoelastomers**	**29**	**89**
1.1.	New monomers	29	89
1.1.1.	Synthesis	30	89
1.1.1.1.	Synthesis of 2-cyanoethyl acrylate (CEA)		89
1.1.1.2.	Synthesis of 2-cyano-1,1-dimethylethyl acrylate (Me_2CEA)		89
1.1.1.3.	Synthesis of 1-cyano-1-methylethyl acrylate (Me_2CMA)		90
1.1.1.4.	Synthesis of 2-cyanoethyl methacrylate (CEMA)		90
1.1.1.5.	Synthesis of N-methylcyanoethyl acrylamide (NCEA)		91
1.1.2.	Photo-differential scanning calorimetry	30	91
1.1.3.	Tests of the photopolymers	32	91
1.1.3.1.	Solubility and thermal properties	32	91
1.1.3.1.1.	Production of photopolymer specimens		91
1.1.3.1.2.	Thermal differential scanning calorimetry		92
1.1.3.2.	Biocompatibility tests	34	
1.1.3.3.	Mechanical properties	35	92
1.1.4.	Additive Manufacturing Technology: Microstereolithography	37	92
1.2.	Macromonomer based photoelastomers	39	93
1.2.1.	Polyester based photopolymers	39	93
1.2.1.1.	Synthesis of a slightly branched polyester methacrylate		93
1.2.1.2.	Determination of the hydroxyl value		93
1.2.2.	Urethane oligomer based photopolymers	40	94
1.2.2.1.	Assessment of the base monomer	40	94
1.2.2.2.	Base monomer Genomer 4215	42	

1.2.2.3.	Formulations with the monoacrylate HEA as reactive diluent	43	94
1.2.2.3.1.	Preparation of the molds		94
1.2.2.3.2.	Preparation of the formulations		94
1.2.2.3.3.	Preparation of test specimens		95
1.2.2.3.4.	Tensile test		95
1.2.2.3.5.	Suture tear resistance test		95
1.2.2.4.	The thiol-ene concept	46	96
1.2.2.4.1.	Low thiol concentrations	46	
1.2.2.4.2.	High thiol concentrations	47	
1.2.2.5.	Comparison with native material	50	
1.2.2.6.	Additive Manufacturing Technology: Digital Light Processing	52	96
1.2.2.6.1.	Viscosity measurements		96
1.2.2.6.2.	Structuring with DLP		96
1.2.2.7.	Cellular compatibility	55	96
1.2.2.7.1.	Cytotoxicity	55	96
1.2.2.7.1.1.	Preparation of the trimer		96
1.2.2.7.1.2.	Preparation of the UDA spacer		97
1.2.2.7.2.	Cell adhesion/proliferation	58	97
1.2.2.8.	Degradability	59	97
2.	**Thermoplastic urethane elastomers**	**61**	**98**
2.1.	General considerations for the synthesis of TPUs	61	
2.2.	Reproduction of Pellethane and aliphatic TPUs	62	98
2.2.1.	Purity of MDI	62	98
2.2.2.	Purity of pTHF	63	98
2.2.3.	Polymer synthesis	63	98
2.3.	Concepts for degradability and toxicological examinations	64	99
2.3.1.	Synthesis of degradation products	65	99
2.3.1.1.	1,6-Bis(hydroxyethyloxycarbonylamino)hexane (HDHC)		99
2.3.1.2.	4,4'-Bis(hydroxyethyloxycarbonylamino)diphenyl methane (MDHC)		99
2.3.1.3.	Ethyl 2-[6-[(2-ethoxy-1-methyl-2-oxo-ethoxy)carbonylamino] hexylcarbamoyloxy]-propanoate (HDLAE)		100
2.3.1.4.	3,14-Dioxa-5,12-diazahexadecanediocicacid-2,15-dimethyl-4,13-dioxo (HDLA)		100
2.3.1.5.	Acetic acid-2,2'-dimethyl-2,2'[methylenebis(4,1-phenyleneimino-carbonyloxy)] diethyl ester (MDLAE)		101
2.3.1.6.	Acetic acid-2,2'-dimethyl-2,2'[methylenebis(4,1-phenyleneimino-carbonyloxy)] (MDLA)		101

2.3.2.	Cytotoxicity tests	67	
2.4.	Cleavable chain extenders	68	102
2.4.1.	Synthesis of lactate based CCE	70	102
2.4.1.1.	Synthesis of [2-(2-(2-(2-hydroxypropanoyloxy)propanoylamino)-ethylamino)-1-methyl-2-oxo-ethyl]2-hydroxypropanoate (EDLA)		102
2.4.1.2.	Synthesis of hydroxyethyl lactate (EGLA)		102
2.4.1.3.	Synthesis of 2-[(2-ethoxy-2-oxo-ethyl)carbamoyloxy]ethyl 2-[(2-ethoxy-2-oxo-ethyl) carbamoyloxy]propanoate (ELAE)		103
2.4.2.	Synthesis of ethylene glycol based CCE	72	
2.4.3.	Synthesis of Michael adduct based CCE	73	103
2.5.	Concepts for cleavable soft blocks	75	104
2.5.1.	Synthesis of lactate extended poly(tetrahydro furan)		104
2.5.2.	Determination of the acid number		104
2.6.	Synthesis of degradable TPUs	76	104
2.7.	Tests of the TPUs	77	105
2.7.1.	Mechanical properties	77	105
2.7.1.1.	Tensile tests	77	105
2.7.1.1.1.	Non-degradable TPUs	77	105
2.7.1.1.2.	Degradable TPUs	78	105
2.7.1.2.	Dynamic mechanical analysis (DMA)	79	105
2.7.2.	Degradability	81	106
2.8.	Electrospinning and tests of electrospun grafts	83	

Introduction

1. The cardiovascular system

1.1. Heart

The ***human heart*** is the musde that provides the blood circulation through the cardiac cycle. It is one of the most vital organs in the human body. The heart consists of four chambers and four valves (Figure 1). The *superior vena cava*, *inferior vena cava*, and *pulmonary vein* are the large veins that lead into the heart, while the *aorta* and *pulmonary artery* are large arteries that exit from the heart. The *mitral valve* and *tricuspid valve* regulate the blood flow from the left or right atria and from the left and right ventricles, respectively. The blood is pumped out of the ventricles to the whole body and the lungs.[1, 2]

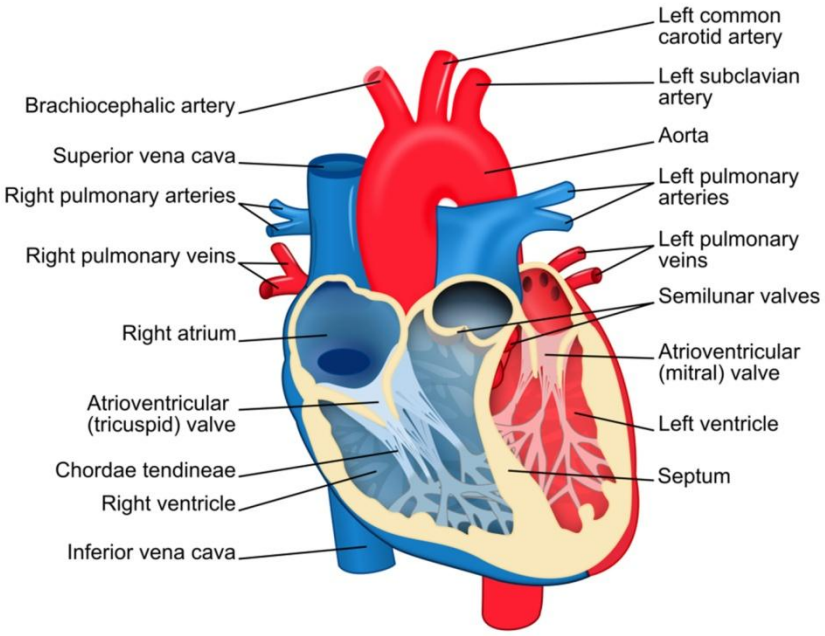

Figure 1. The human heart [1, 2]

1.2. Blood vessels

Blood vessels are an important part of the *cardiovascular system*. Their function is to transport blood throughout the body. There are three principle classes of blood vessel: *arteries*, *veins*, and *capillaries*. Arteries carry blood away from the heart and veins carry blood to the heart, while exchange of nutrients between blood and surrounding tissue takes place in thin walled capillaries. Indifferent from the location within the cardiovascular system and the diameter, all blood vessels, except the capillaries have the same basic structure.[3] They are composed of three layers (Figure 2) of distinct composition with a thickness dependent on the current and pressure conditions at the particular position within the circular system.

The *intima* is the innermost layer and lined with *endothelial cells* (EC). Its thickness is from 10 to 100 µm. The primary function of the intima is to prevent thrombogenesis. The *media* layer is composed of *smooth muscle cells* (SMC) (30-60%) that sit in a matrix of proteins (10-40% collagen and elastin). Its thickness is from 10 to 500 µm. The media provides the elastic behavior of the vessel. The SMC can contract to decrease the inner diameter of the conduits and subsequently increase the current and blood pressure, respectively. The *adventitia* is the outermost, protective layer and serves the structural integrity of the blood vessel. Its thickness is from 50 to 500 µm and it is expected to be far stiffer than the media.[4]

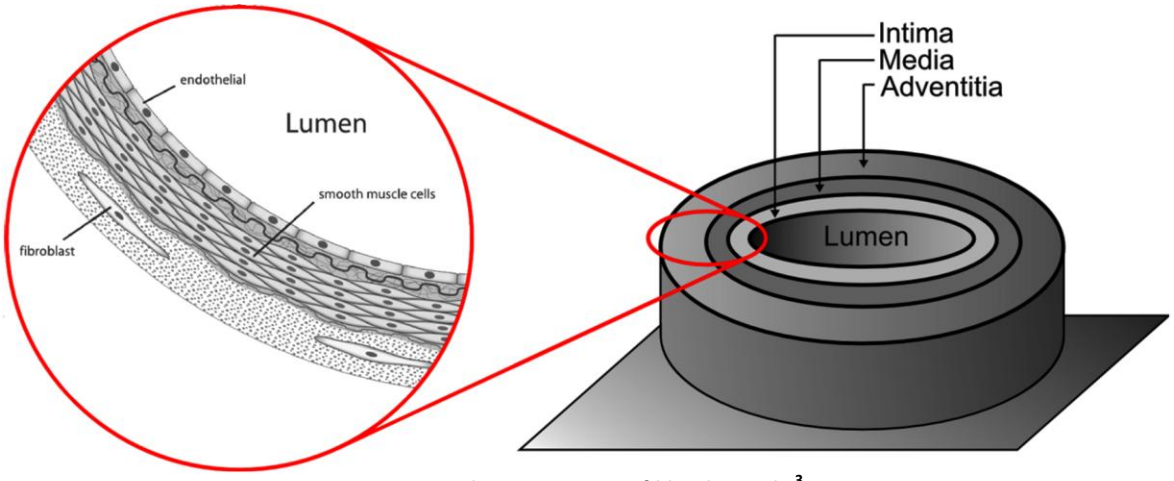

Figure 2. The composition of blood vessels [3]

2. Diseases of the cardiovascular system

Diseases of the cardiovascular system are the ***chief causes for morbidity and mortality*** in all western countries. The total direct and indirect costs of cardiovascular diseases (CVD) and stroke for 2010 are estimated at $503.2 billion for the USA alone.[5] *Coronary heart disease* (CHD) or *ischemic heart disease* (IHD) plays the most important role in the field of CVD. Typical symptoms are temporary pain (angina), irregular heart beat (arrhythmia), permanent heart muscle damage (myocardial infarction), or loss of muscle activity (heart failure). The most common risk factors of IHD, which seems to have no clear etiology, are overweight, smoking, hypertension, diabetes and hyperlipidemia. Aside from life-style sources congenital defects of the cardiovascular system also come more and more into focus. These are structural problems that arise from abnormal formation of the heart itself or of major blood vessels.

3. Therapies

A good review of this topic is given by Choi and Kim.[6] Depending on the ***severity of the IHD***, conventional therapies approach step wisely from *minimally invasive administration of drugs* – through *percutaneous intervention* (endoscopic methods) – to complex *cardiac surgeries* (Figure 3). However, in the acute situation after a cardiac infarction it is above all crucial to restore the blood supply of the myocardium; In the medium and long term it is necessary to heal the myocard (cardiomyogenesis).

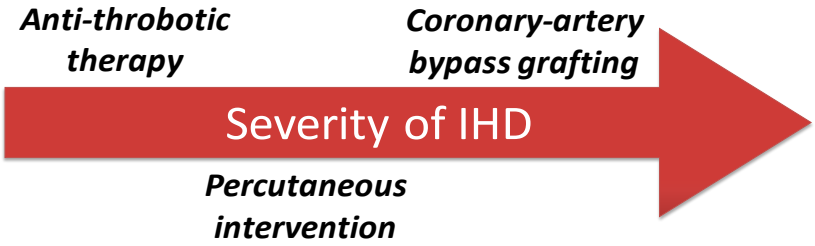

Figure 3. Conventional therapies for IHD

3.1. Conventional medical treatments

Beside real medical intervention ***life style changes*** are recommended, including weight control, smoking cessation, exercise, and a healthy diet, which, however, is discussed very controversially.[7-12]

3.1.1. Anti-thrombotic therapy

For ***acute coronary syndrome*** such as unstable angina anti-thrombotic therapy is able to lower the morbidity and mortality significantly. The suppression of the formation of *thrombin* prevents the formation of blood clots and promotes the dissolution of already existing thrombi. The administration of unfractionated *heparin* (5000 to 30000 Da) or low molecular weight heparin (<8000 Da) in combination with acetyl salicylic acid is the most common therapy to date. Another approach is the inhibition of the *hemostatis pathways* (Figure 4) [13] either by factor Xa inhibitor (Fondaparinux, Figure 5) or direct thrombin (factor IIa) inhibitor.

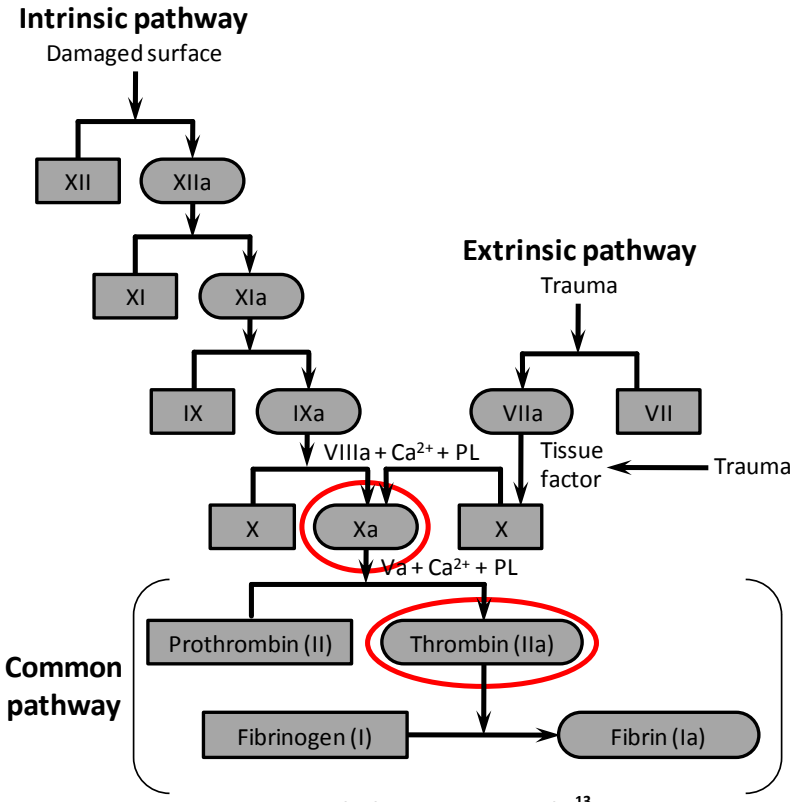

Figure 4. The hemostasis cascade [13]

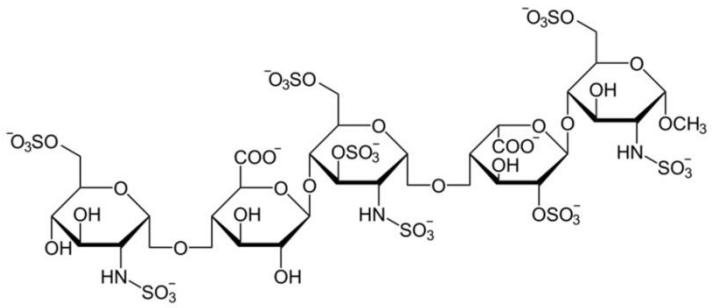

Figure 5. Fondaparinux

3.1.2. Percutaneous coronary intervention

Percutaneous coronary intervention (PCI) is applied for non-severe coronary artery disease. The occluded artery is opened by the inflation of an endoscopic introduced balloon (*balloon angioplasty*). The plaque is crushed into the wall of the artery and the normal blood flow to the heart musde is restored. This procedure is well established and is therefore also applied in very

acute situation e.g. in case of *cardiac arrest*. To avoid *restenosis,* stents, unfolding metal scaffolds, can be applied (Figure 6) s. Recently also *drug elution stents* are used.[14, 15]

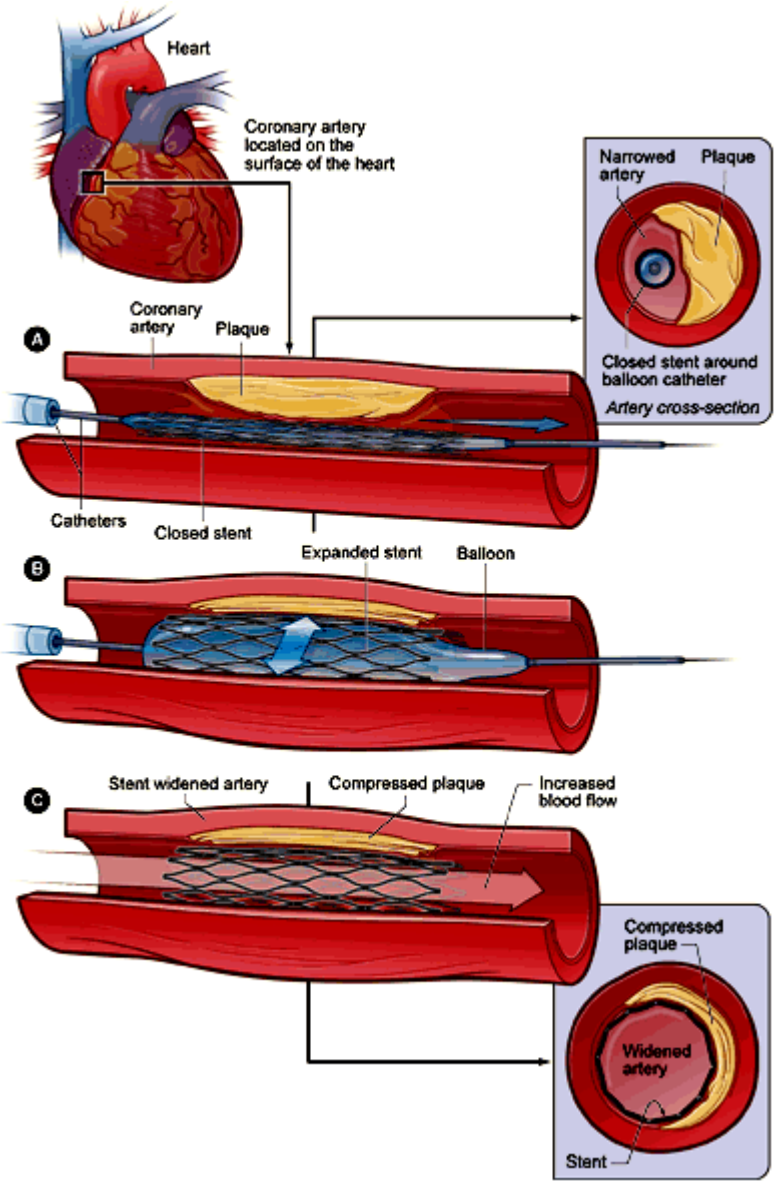

Figure 6. Balloon angioplasty with the application of metal stent [16]

Although the risks of angioplastic therapies are very low compared with bypass surgeries [17] there may be some complications during or after the percutanous intervention. Besides tearing of the artery, the release of clot fragments or the formation of in-stent blood clots that may cause myocardial infarction, or adverse/allergic reactions caused by the administrated drugs/contrast agents, restenosis is one of the most common complications of angioplasties.

3.1.3. Coronary-artery bypass grafting

Coronary-artery bypass grafting (CABG, "cabbage") is a surgical procedure that is performed to relieve angina and reduce the risk of death from coronary artery disease. Arteries or veins from donor sites of the patient's body itself, often the *saphenous vein* [18], are grafted to the coronary arteries to bypass the narrowed coronary artery (Figure 7 left) and enhance the blood supply of the myocardium. The application of cardiopulmonary bypass is necessary due to the fact that this surgery is performed with the heart stopped. Although there are also techniques available those are performed on a beating heart, so-called "off-pump" surgeries. As alternative to the saphenous

vein, the *internal thoracic artery*, one of the arteries that normally supplies the breast muscle, can be redirected to supply the heart muscle (Figure 7 right).

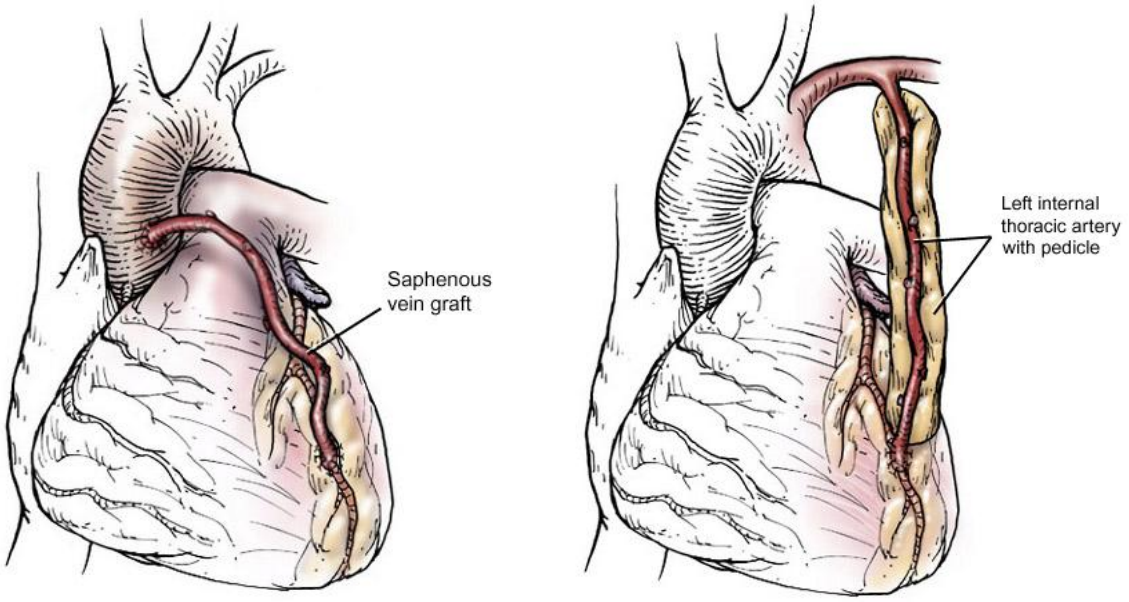

Figure 7. Coronary artery bypass grafting with saphenous vein (left) and internal thoracic artery (right) [19]

The risks of death is significantly higher for CABG as for PCI as it is for any massive invasive surgery at the open heart. Beside these complications there are also some specific issues for CABG, to be specific the non-union of the breastbone (sternum), myocardial infarction owing to embolism, hyperperfusion, or graft failure, acute kidney failure or stroke due to embolism or hyperperfusion or the vasoplegic syndrome, secondary to cardiopulmonary bypass and hypothermia.

3.1.4. Shortcomings of traditional interventions

PCI is a very important tool for the treatment of acute IHD. In the long term, however, CABG is often unavoidable due the high restenosis risk. The number of appropriate vessels for grafting though is limited in about a third of patients due to insufficient native vessels or previous vessel harvest. For particular clinical situations autologous vessels may be inadequate in diameter or length. Moreover, the use of *autografts* includes the need for *multiple surgical procedures* thus increasing risks (*donor site morbidity*) and costs.
Alternative therapies and the tissue engineering approach try to overcome this problem by the manipulation of the malfunctioning processes at the cellular level and even beneath.

3.2. Alternative therapies

3.2.1. Protein therapy

Aside from their structural function proteins act as ***enzymes*** or ***growth factors*** (GF) and therefore have a very important role. Diseases are closely related to the malfunctioning of particular proteins, so, therapies that take this approach are very promising. Various proteins of therapeutical interest can be produced with relative ease and cost-effectively by means of recombinant DNA technology. However, efficient cargo-carriers have to be found so that the proteins are able to penetrate cells (cell penetrating peptides, CPP). The most important therapeutic proteins for the IHD are derived from *HIV-TAT protein* (trans-activator of transcription), coupled with the anti-cell death protein FNK or BH4.
Heat shock proteins protect other proteins from aggregation, refold damaged proteins or lead to degradation of severely damaged proteins. The cardio protective effect of these proteins might be attributed to the direct inhibition of the *caspase cascade* which generally leads to apoptosis of the cells.

Beside these functional proteins, ***angiogenic growth factors*** [20] are valuable therapeutic agents. *Fibroblast growth factors* (FGF) possess binding sites for EC, SMC, myoblasts and therefore stimulate the proliferation of these cell types. *Vascular endothelial growth factors* (VEGF) are the most studied GF. They improve the vitality of EC, play a key role in angiogenesis (the formation of new capillaries) of fetal myocardium and ischemic limbs, in wound healing, and in the coronary collateral development. Also a synergic effect with FGF can be observed. So both GF are often applied in combination.

3.2.2. Cell therapy

Cell therapy is the ***transplantation of human or animal cells*** to replace or repair damaged cells or tissues, generally the promotion of *endogenous regeneration mechanisms*. The applied cell types are manifold. The most frequently used cell types for the cell therapy of IHD are ***bone marrow derived cells*** like *hematopoetic progenitor* cells (HPC) that are able to differentiate into all types of blood cells, *mesenchymal stem cells* (MSC), that differentiate into multiple phenotypes and additionally possess a very low immunogenicity and may therefore be of allogenic origin *endothelial progenitor cells* (EPC) that home to sites of ischemia, stimulate neovascularization and differentiate to endothelial cells and possible to cardiomyocytes.[21] Particular the EPC seem to have a high potential as measured on the number of new publications in the field of cardiac repair.[21-37]

An important other classes are *embryonic stem cells* (ESC) that posses unlimited proliferation capacity, differentiate to all cell types, but with the risk of formation of tumors.[38-40]

3.2.3. Gene therapy

While the basic idea may sound very similar to protein therapy gene therapy is a completely different approach. Instead of the administration of therapeutic proteins, ***genes are infiltrated into cells*** of the affected tissues that express these proteins, predominately GF such as VEGF and FGF.[41] This infiltration is done by means of *viral* or *non-viral vectors* (plasmids), carriers that penetrate into the genome of the cells and bear the code of the corresponding protein. The therapeutic outcome of gene therapy depends on the on the efficient insertion of therapeutic genes without causing cell injury, mutations, or an immune response.

4. Tissue Engineering

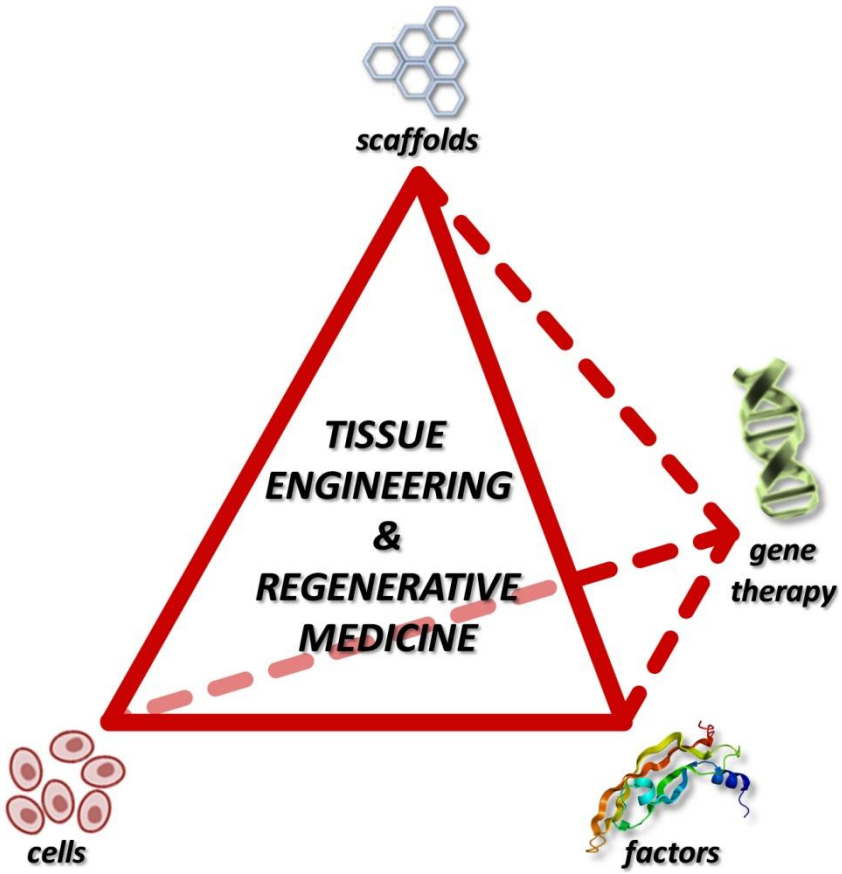

Figure 8. Tissue engineering tetrahedron

As a comprehensive approach that combines all therapy concepts, ***tissue engineering*** (TE) has emerged as a novel therapeutic strategy to repair damaged tissue and organs *in-vitro* or in-vivo.[42] TE has been defined as the application of ***interdisciplinary sciences*** (*medicine*, *chemistry* and *mechanical engineering*) to repair, restore and regenerate the function of a tissue or a whole organ.[43-45] A good review covering the achievements of this approach is given by Atala [39], one of the pioneers of TE. This new approach is destined to understand the cellular mechanisms of tissue formation and regeneration and to induce new functional tissues. Three basic building blocks are utilized in TE to regenerate new tissue: ***scaffolds***, ***cells*** and ***(growth)factors*** (Figure 8).[46] Generally, scaffolds are made of ***biomaterials***. Among biomaterials currently under investigation one can find inorganic as well as organic scaffolds. Composite systems, combining the advantages of both, seem to be a promising choice, in particular for hard tissue replacements. A good overview is provided by Laurencin *et al.*[47], Eisenbarth [48] and Buchmeiser [49]. Cells can be seeded on the scaffold ***in-vivo*** and ***in-vitro***. Generally, in-vivo-seeding is preferable. Because this means that the shaped scaffold is just implanted and new tissue will grow automatically because of the high biocompatibility of the material. But – unfortunately – this is a very rare case. Normally the scaffold has to be seeded before implantation. Under ideal conditions the desired tissue can grow without any side effects. The scaffold adopts a more or less neutral position. To adjust the biological function of an engineered tissue different factors are needed. Those factors promote *cell growth* (growth factors), *cell adhesion* (integrine analogues), and *differentiation* of stem cells or inhibit inflammation and so on. *Gene therapy* which is of course strongly associated with the cells is an up-and-coming new tool for TE that has not yet fully established but might produce relief in several issues of TE.[50-53]

4.1. Approaches for Vascular Tissue Engineering (VTE)

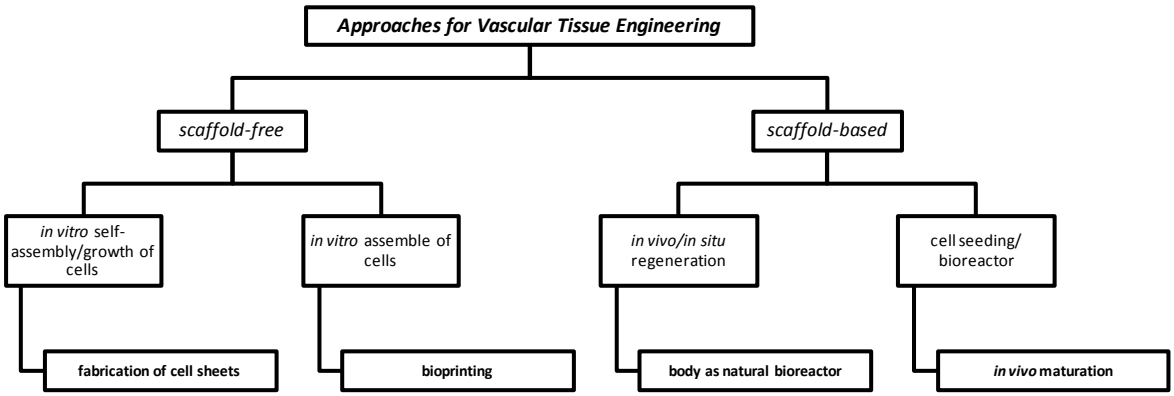

Figure 9. Approaches for VTE

Figure 9 depicts different design approaches available for VTE.[54-56] Although TE commonly is associated with the application of *scaffolds* for guided cell growth[43], several approaches for *scaffold-free VTE* are described. For example *SMC sheet* were grown in vitro, rolled up to conduits and used as grafts[57]. Other research groups succeeded in *bioprinting* of cells to generate tailored tissues[58, 59] There are also concepts of printing whole organs.[60] However, the *scaffold-based* approach is the more preferred route by far.[61] In this case it can be distinguished between in situ regeneration – the biomaterial scaffold in just implanted and cells settle in vivo – and the cell seeding or *bioreactor* approach respectively.[62] In the latter case the scaffold is treated with cells and growth factors under static or even dynamic conditions to mimic the environment of the human body in a very reproductive manner. The construct is implanted after this procedure. In some cases the degradable scaffold has already been fully converted into living tissue.[63] However, while the bioreactor approach provides prostheses with high patient-specific cell content, which is very beneficial for the whole curing process, the *in-situ* regeneration may be preferred because some patients cannot wait for the time consuming fabrication of a bioreactor graft in a case of emergency e.g. after a cardiac infarction. In addition, insertion of the regenerated tissue requires a second operation.

The material requirements for the in situ regeneration are very high. The material has to fulfill (1) ***mechanical*** and (2) ***structural*** requirements specific to the tissue it is replacing, (3) it has to be ***biocompatible***, (4) it should ***degrade*** in a beneficial manner, and (5) it should be ***easily manufactured*** and ***sterilized***.

(1) The mechanical properties of the material are very crucial. Generally they should *comply* with the properties of native blood vessels.[64-66] *Modulus mismatch* can cause less laminar flow at the junction site and therefore possibly lead to stenosis.[67] Additionally the seams of the junction induce stress peaks that may lead to failure.

(2) Since tissues are *3-dimensional constructs*, the scaffolds should also have a 3-dimensional structure.[68] A high porosity with interconnectivity provides an ideal substrate for the ingrowth of new tissue and the exchange of nutrients.[69]

(3) Biocompatibility of the material means at least that it must not provoke any adverse effects e.g. thrombi or immune reactions.[70, 71] It should also provide a suitable surface for the *adhesion of blood vessel specific cells*.[35]

(4) *Biodegradability* is a very important feature of scaffolds for VTE.[72] While the tissue regenerates, the material has to disappear. Ideally, the degradation should promote and not restrict growth of new tissue (Figure 10).

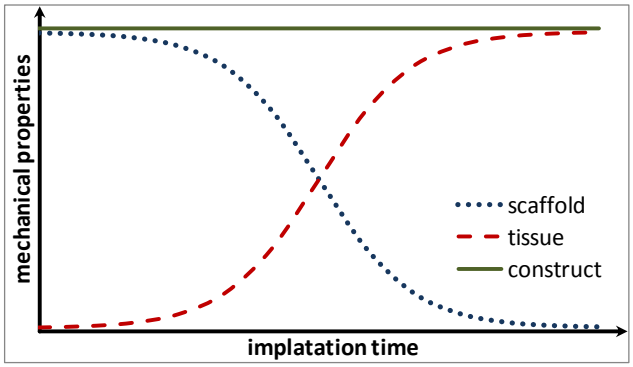

Figure 10. Ideal mechanical behavior during degradation (qualitatively drawn)

Recently Roh *et al.* [73] described very conclusively the *in-vivo* remodeling of polyester-based porous vascular grafts [74] as mature blood vessels via an inflammation-mediated process (Figure 11).[75]

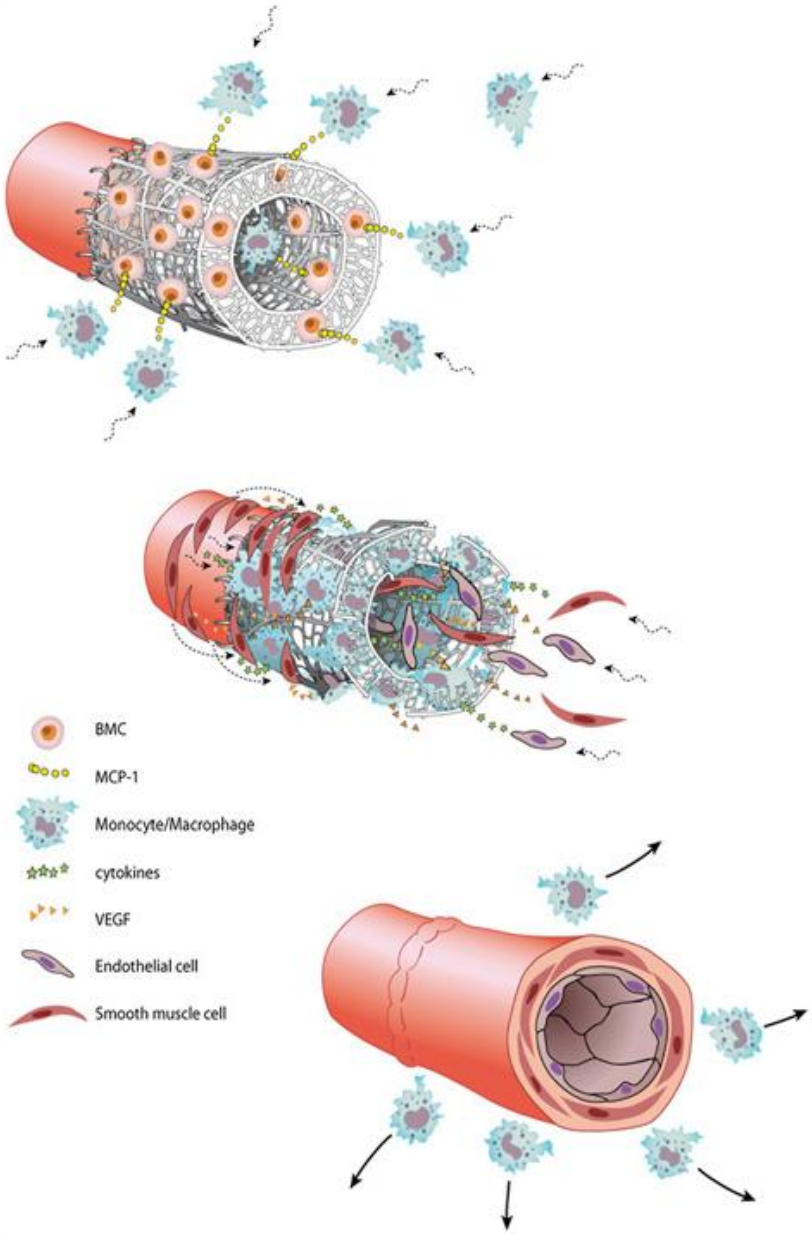

Figure 11. In-vivo regeneration of blood vessel aided by tissue-engineered vascular graft [73]

4.2. Biomaterials for Scaffold-based VTE

As seen in Figure 12 there are two important ***classes of biomaterials for VTE*** – *natural* and *synthetic*. Beside the categorization regarding origin and chemical structure, other aspects like biocompatibility and -degradability, mechanical compliance, and processability – just to name a few – play a decisive role for the suitability as material for scaffolds [61] for VTE.

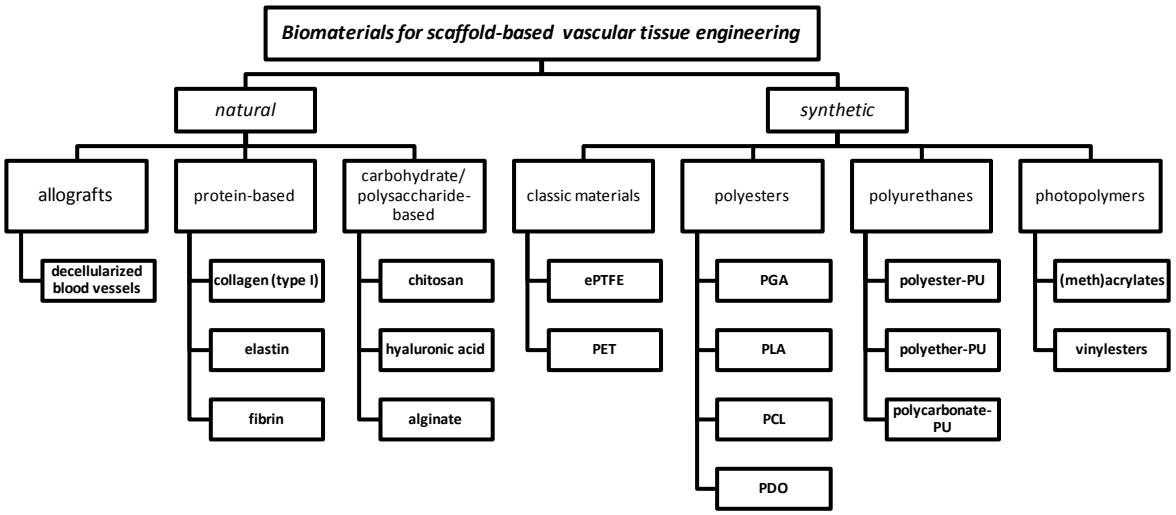

Figure 12. Biomaterials for VTE

4.2.1. Bioderived Materials for Vascular Grafts

The most straight forward alternative if ***autologous grafts*** with sufficient quality are not available would be the use of ***allogenic materials***.[76, 77] However, in spite of being decellularized by means of detergents and enzymatic extraction methods, *allografts* or even *xenografts* often provoke an immune response.[78-80]

The application of ***protein-based biomaterials*** aims to have all the advantages of allografts, especially concerning biocompatibility and remodeling capacity, without their shortcomings regarding immunogenicity.

Type-I-collagen is the main component of the extracellular matrix (ECM) and can easily be extracted in large quantities for example from human placenta.[81] The main challenge when using collagen as biomaterial is to overcome its low mechanical integrity. One possibility is to reinforce the material with a mesh e.g. from Dacron (a plastic with existing approval in vascular applications, see also later). Another possibility is to crosslink collagen to enhance the mechanical properties. With a combination of glutaraldehyde, dimethyl suberimidate, dimethyl 3,3'-dithiobispropionimidate, and acyl azide for example[82] covalent links between the collagen fibers are formed.

Elastin is the structural protein of artery walls and should therefore be a suitable biomaterial for vascular grafts. Indeed, the mechanical properties of scaffolds made of elastin – often in combination with collagen – are contrary to the expectations and even worse than collagen alone. However, it has been reported that elastin regulates the cell growth and inhibits the hyperplasia of SMC which is often an issue.[83] In combination with a degradable synthetic polymer the mechanical properties can be enhanced decisively.[84, 85]

Fibrin is an insoluble protein that is involved in the blood clotting process (Figure 4). It has already proved to be a good agent for tissue glues and seals[86], applied for surgeries of very soft organs e.g. liver. The main advantage of fibrin as biomaterial is, that it can be produced out of the patients own blood. Therefore immunogenicity will not be an issue. Beside the application as scaffolds for vascular grafts [87, 88], fibrin is often used as coating to enhance the hemocompatibility of surfaces.[89] It was also found that fibroblasts and SMCs produce even more collagen in a fibrin than in a collagen matrix.

In addition to the protein-based materials, polysaccharide-based biomaterials are considered to be suitable scaffolds for VTE.
Chitosan is derived from chitin, the main component of the cutide of insects and crustacean. A specialty of chitosan is its inherent antimicrobial activity.[90] It has also been reported that human coronary endothelial and SMC attach strongly to the surface of chitosan-based scaffolds. In combination with its very low immunogenicity and its ability to inhibit SMC hyperplasia, those properties make chitosan a very promising candidate as a biomaterial for VTE. However, the major drawback of chitosan is its very poor mechanical properties and poor solubility in most solvents. So, it will likely be combined (blended) with other polymers e.g. poly(caprolactone).[91]
Hyaluronic acid is an important component of many tissues of the human body. It has already captured the market of cosmetics but it is also very prominent as biomaterial to repair articular cartilage[92] and other tissues.[93] In spite of the fact that cells only attach weakly to its surface several studies were done to examine strategies to increase the suitability of the material for vascular grafts.[94] Nevertheless, at this point in time hyaluronic acid-based biomaterials seem not to be very promising for VTE.
Alginate is obtained from brown seaweeds. Due to its biocompatibility, low toxicity and convenient gelation behavior it is often used for several biomedical applications. It suits perfectly as localized delivery vehicle for angiogenic molecules (e.g. VEGF or FGF) to promote new blood vessel formation.[95]

4.2.2. Synthetic Materials for Vascular Grafts

Classic materials – *expanded poly(tetrafluoro ethylene)* (ePTFE, Figure 13) and *woven/knitted poly(ethylene terephthalate)* (PET) – are most suitable for large-caliber vascular grafts.[96, 97]

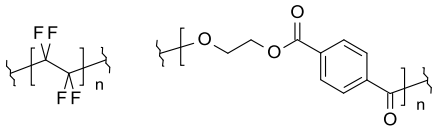

PTFE **PET**

Figure 13. Structure of PTFE and PET

Unfortunately they fail to act as *small-diameter grafts* mostly due to thrombosis. Patency rates are already very low after a few weeks from implantation.[98] To improve the performance of these materials several efforts were undertaken to increase the *long-term patency*. Surface modification is the key to success.[99] For example the attachment of *anticoagulant* or *antithrombotic* agents e.g. heparin to the grafts improved the patency in the rat model.[100]
However, to really regenerate new vascular tissue it is necessary that the synthetic biomaterial give way to the new cells settling down. Therefore biodegradability is an important requirement for scaffold-based tissue engineering.[72] Biodegradation predominantly rest upon the hydrolytic cleavage of the ester bond of polyesters. That is why the class of polyesters is very important in the field of biomaterials.[101-103]
Poly(glycolic acid) (PGA, Figure 14) is synthesized by the ring-opening polymerization of glycolide.[104, 105] Depending on the implantation site it degrades within 4 weeks and 6 months and is eliminated to water and carbon dioxide. It has been shown that seeding with SMCs or ECs leads to a very homogenous distribution of the cells in the constructs. Due to the very fast degradation rate PGA is often used as scaffold for the bioreactor-based TE approach.[62]
Poly(lactic acid) (PLA) is obtained by the ring-opening polymerization of lactide. Due to the chiral nature of lactic acid the crystallinity and the degradation rate, respectively, can be tailored by the ratio of the both enantiomers within the polymers.[106] Racemic PLA, however, is amorphous and degrades fastest. The additional methyl groups as side chain of the polymer cause the lower hydrophilicity of PLA compared to PGA. PLA therefore degrades slowly.[101] The already very good tendency to attach vascular cells and to guide the ingrowth of new tissue can even be improved by the conjugation with bioactive molecules like fibronectin.

The main disadvantage of both PGA and PLA is the catastrophic degradation mechanism (bulk erosion).[107] The initial degradation rate is very low, but as soon as the material is interspersed with water the scaffold collapses very fast which is contrary to the more or less linear growth of the new tissue. Additionally high amount of acid is released and the low pH can cause necrosis.
Poly(ε-caprolactone) (PCL) degrades significantly slower than PGA or PLA. This is due to the hydrophobic aliphatic chain. It exhibits excellent cell compatibility [108] and also has better mechanical properties.[109] However, the very slow degradation rate involves a very low remodeling capacity.[108]
Poly(dioxanone) (PDO) is similar to PGA and is synthesized analogous but it is more slowly resorbed. PDO has already proved its value as suture material; Therefore it was also considered as a biomaterial for VTE. It demonstrated spontaneous endothelialization and a patency rate of 100% after 1 year from implantation in the rabbit aorta model.[110]

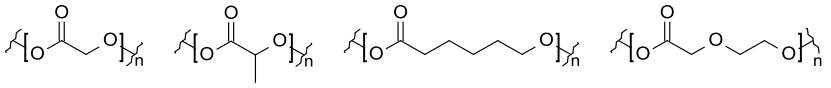

Figure 14. Polyester based biomaterials

Polyurethanes (PUs) are the most popular elastomeric materials in this research field. Their mechanical properties comply better with those of native blood vessels and therefore they are thought to be more appropriate materials for VTE.[111]
PUs may further be classified as polyester-PUs, polyether-PUs and polycarbonate-PUs, depending on the prepolymers/softblocks applied for the synthesis of the PUs.[112, 113]
Unfortunately polyester- as well as polyether-PUs exhibit adverse degradation behavior in vivo although they initially demonstrated good biocompatibility.[114] Polyester-PUs are subjected to (enzymatic) hydrolysis while polyether-PUs are degraded by an oxidative mechanism that leads to catastrophic failure of the grafts (environmental stress cracking).[113, 115-117]
In contrast, polycarbonate-PUs show a quite good performance[118, 119] although the first clinical studies had very disappointing results.
A complete other class of biomaterials are *photopolymers*. While all above mentioned materials are processed in the polymer form (see also section 4.3), photopolymers are polymerized during processing.[120-122] The considerations here are limited to radical polymerization. The most common monomers in this case are *(meth)acrylates*. For soft tissues the state-of-the-art materials are photopolymer hydrogels from poly(ethylene glycol) acrylates (PEG acrylates).[123-125] PEG exhibits an inherent resistance to protein adsorption or cell adhesion.[71] This is a major advantage in this case because specific cell attachment is induced by the conjugation with integrine analogs. For example the peptide REDV is specific for endothelial cells.[126, 127] The major drawback of (meth)acrylate based photopolymers is the toxicity of residual monomer and the degradation product of the polymer. Therefore other classes of monomers were developed.[128] Although *vinylesters* demonstrate a lower reactivity regarding photopolymerization, this disadvantage is more than compensated. The toxicity of the monomers is orders of magnitude lower than that of acrylates and the non-toxic degradation products can easily be removed from the implantation site as they are low-molecular and water soluble.[129]

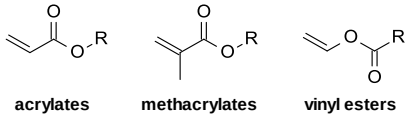

Figure 15. Monomers for photopolymerization

The major advantage of photopolymers is that they can be processed by ***additive manufacturing technologies*** (AMT, see also in section 4.3) to produce scaffolds with arbitrary geometries.[122, 130-132] AMT will further be discussed in section 5.

4.3. Fabrication Techniques/Application Forms of Scaffolds for VTE

Beside the chemical nature of the biomaterial the ***microscopic structure*** of the scaffold strongly influences its bioactivity. This was clearly demonstrated using the example of fibrin clots.[133] Therefore the technique of fabrication or the form of application, respectively, must also be considered.[134] Figure 16 depicts the most common application forms of scaffolds at a glance.

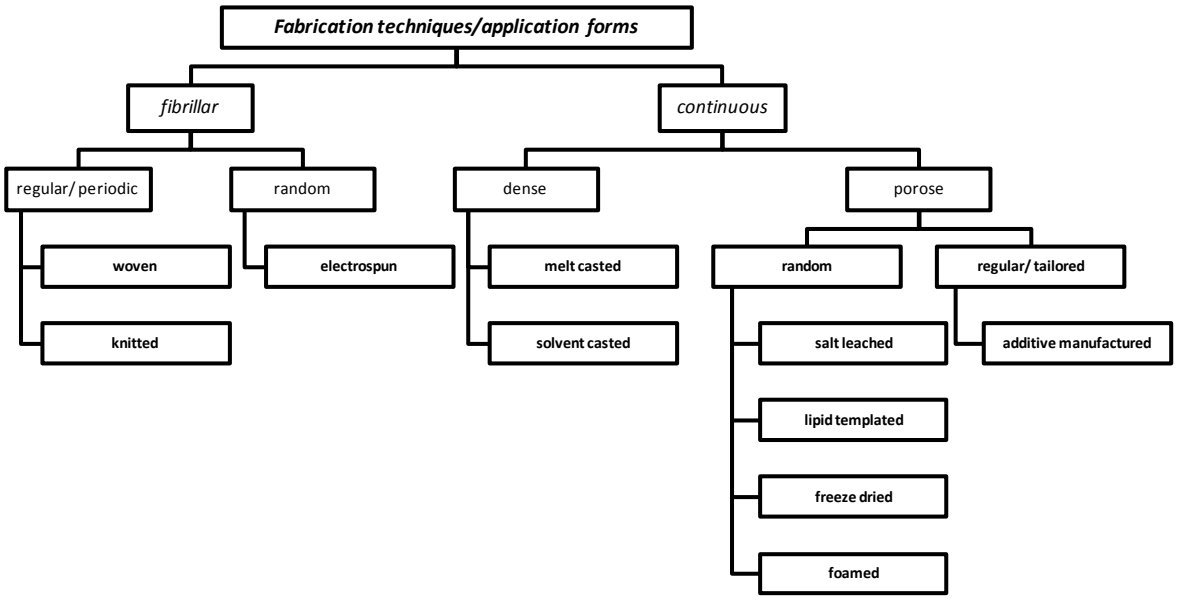

Figure 16. Application forms of scaffolds for VTE

A good overview for the processing of *thermoplastics* (for the case of PLA) is provided by Lim and Rubino.[135] Although it seems to be a question of philosophy whether woven or knitted fibrillar scaffolds are applied (warp knitted Dacron grafts, however, generally are more compliant than woven or weft knitted grafts), there is a consensus regarding the fact that random orientation of polymer nanofibers mimics the ECM better.[136] Therefore ***electrospinning*** has become an important tool for the fabrication of scaffolds.[137-139]

In case of continuous materials dense scaffolds whether *melt* or *solvent* casted are of minor importance unless they are equipped with a special surface structure.[99] To manufacture porous scaffolds the polymeric material can be mixed with other phases – the porogens – which are removed after processing like it is performed during salt leaching[140] or lipid templating.[141] Other techniques namely freeze drying and gas foaming generate porosity by means of phase transitions.[142] All these techniques work very empirical and porosities can only be adjusted within a certain range. Absolute interconnectivity of the pores is also not given.

Additive manufacturing technologies also known as rapid prototyping technologies, however, can fabricate arbitrary structures with defined porosity and interconnectivity of the pores [143] already established as tool to fabricate scaffolds for tissue engineering [144] including vascular conduits [145].

This work tracks two approaches – ***additive manufactured photoelastomers*** and ***electrospun thermoplastic urethane elastomers***.

5. Additive manufacturing technologies

Moldless manufacturing techniques known as *Additive Manufacturing Technology* (AMT), *Solid Freeform Fabrication* (SFF) or *Rapid Prototyping* (RP) allow the fabrication of complex 3D structures with defined and interconnected pores (Figure 17). AMT builds objects by selectively adding materials, layer by layer, as specified by a CAD (*computer aided design*) file.

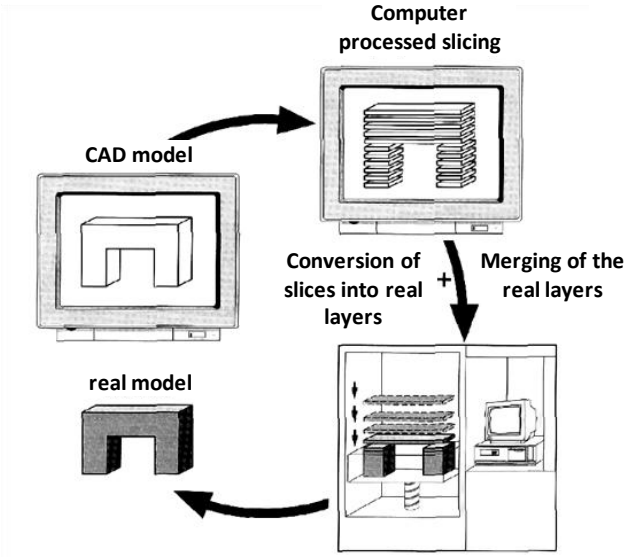

Figure 17. Principle of the layer-by-layer AMT techniques [146]

Good reviews about this topic are given by Leong *et al.* [147] and Hutmacher *et al.* [148]. Depending on the mechanism of the formation of solid material it can be distinguished between three categories of AMT: *melt and dissolution techniques*, *particle bonding techniques*, and *photopolymerization of photosensitive resins*. All these techniques have key benefits compared to traditional manufacturing methods: no tools or masks are needed because the parts are built layer by layer and the shape complexity of the fabricated parts is virtually unlimited (Figure 18).

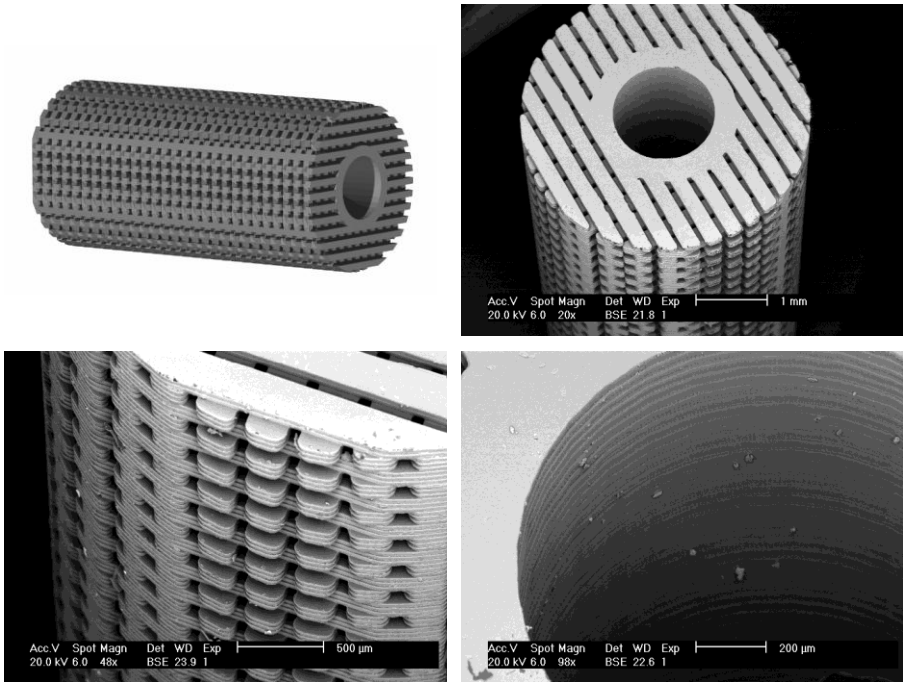

Figure 18. Example for an additive manufactured part: CAD model (up left) and SEM micrographs of the part

In this work only the ***photopolymerization methods*** are applied. Therefore this chapter is dedicated to these methods, exclusively. They are based on the selective solidification of a photocurable resin by light. The different methods of photopolymerization based AMT are *stereolithography* (SLA), *digital light processing* (DLP) and *inkjet based systems*. The feature resolutions of commercially available SLA- and DLP-systems are around 50 µm. In case of SLA the photopolymerization is initiated by a scanning UV laser beam, DLP works with a digital mirror device in combination with a Hg-high-pressure lamp. Inkjet based systems, however, in contrast to DLP or SLA do not work by means of the selective photopolymerization of a homogenous monomer layer but it selectively deposits the monomers for each layer of the part before the whole layer is cured with an UV lamp. The main advantage of this method is the possibility to generate multi-materials; however the drawback is the need of support material, even for simple geometries, and the resulting poor surface quality.
The resins are cured by the aid of ***photoinitiators*** (PI).[149] PIs form a large amount of initiating radicals when irradiated with light of particular wavelength. Those radicals start the free radical polymerization chain reaction. The liquid formulation is converted into solid material (Figure 19).

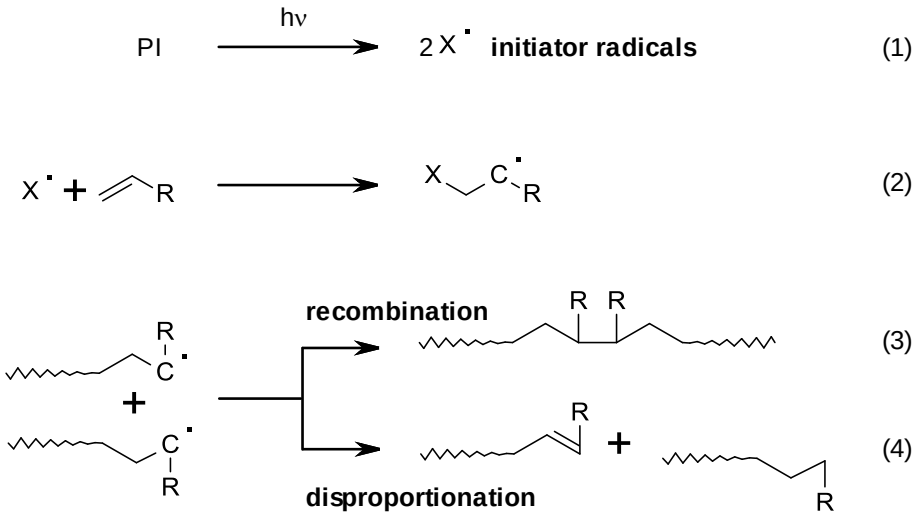

Figure 19. Principle of photopolymerization

In the first step (*initiation*) (1), the PI dissociates into *radicals* (X•) due to absorption of light. Those radicals add onto monomer molecules to start the *chain reaction* (2). During the chain growth reaction (*propagation*) the addition of other monomer molecules occurs whereas chain termination takes place because of *recombination* or *disproportionation* (3, 4).
Since all the applied monomers are very reactive and polymerize easily owing to thermal stress, it is necessary to use *inhibitors* that scavenge accidentally formed radicals before they start the polymerization. A simplified mechanistic scheme of hydroquinone monomethylether (MEHQ) is shown in Figure 20.

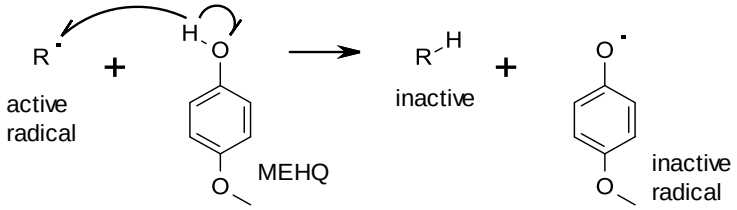

Figure 20: Function of MEHQ

The PI is the key substance of such formulations because it is UV or VIS sensible and therefore converts the radiation energy into chemical energy while forming radicals that start the

polymerization. This can happen through photo-fragmentation as a result of *α-cleavage* (*Type I*) or through *hydrogen abstraction* or *electron transfer* from a donor molecule (*Type II*).

α-Cleavage of Type I initiators commonly take place next to the carbonyl group. So benzoyl radicals often start the polymerization. Some examples for Type I initiators are benzoin ethers, dialkoxy acetophenones, hydroxyalkyl phenones, benzoylphosphine oxides and morpholino ketones. To demonstrate the principle of cleavage, a bisacylphosphine oxide based PI (BPO, Irgacure 819®) from the company Ciba SC is displayed in Figure 21. In this case not only the benzoyl radical but also the phosphorus radical initiates the polymerization.

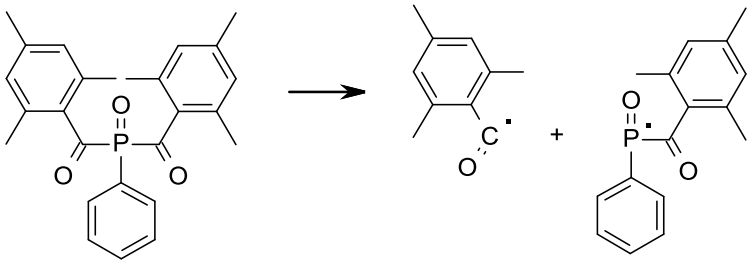

Figure 21: Cleavage of Type I PI Irgacure 819®

PIs which form radicals through hydrogen abstraction from a co-initiator belong to Type II initiators. They react *bimolecularly* by an electron-proton transfer from the co-initiator to the excited ketone. Examples for such PIs are benzophenones, thioxanthones, anthraquinones, xanthones, fluorenones, benziles, ketocoumarines and camphor quinones. Amines are often used as suitable donors. They transfer an electron to the excited ketone and therefore form a radical pair intermediately. In the second step the reactive radicals are finally generated by proton transfer. Figure 22 displays the mechanism by the means of the system camphor quinone (CQ)/ethyl dimethylamino benzoate (DMAB) that is used for biomaterial applications.[150]

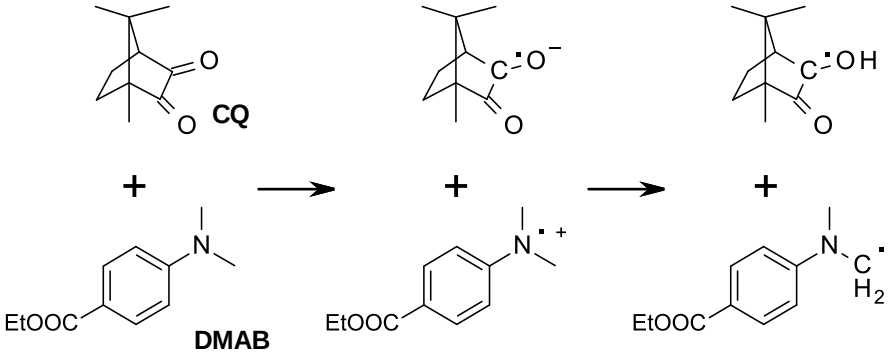

Figure 22: Electron and proton transfer of Type II initiators

Oxygen can cause inhibition of the radical polymerization. Due to its bi-radical character it can attach to the reactive ends and therefore stop the propagation (Figure 23).

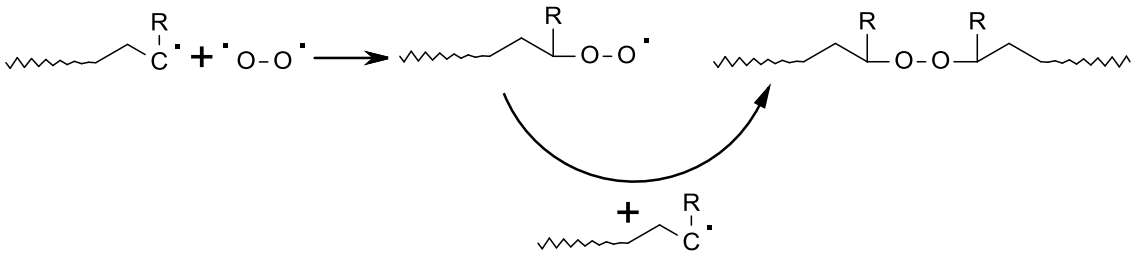

Figure 23: Inhibition due to oxygen

Therefore care has to be taken to reduce the amount of oxygen present, since lower double bond conversion can result in migratables which are unwanted in biomedical applications.
Photopolymer resins for technical applications are often of *higher molecular weight* and contain various other *functional groups* within the spacer to tune the material properties (Figure 24).

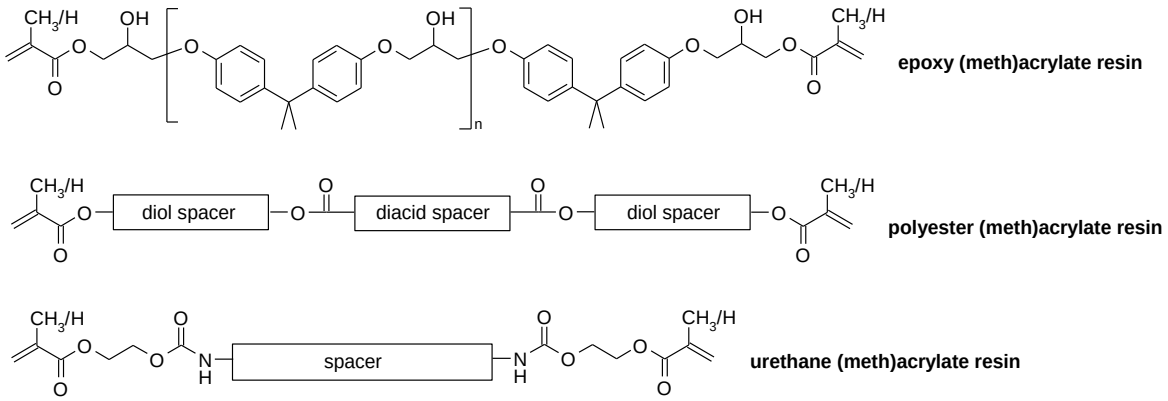

Figure 24. Photopolymer resins with functional groups

Epoxy (meth)acrylate resins are overwhelmingly based on bis-phenol A. The rigid aromatic rings and the additional π/π stacking of these structures lead to very hard but brittle materials. Depending on the different spacers of *polyester* (*meth*)*acrylate* and *urethane* (*meth*)*acrylate* resins a wide spectrum from soft to hard materials can be obtained. The *urethane group*, however, has an additional effect on the mechanical properties due to the formation of very strong (intermolecular) H bonds (Figure 25) which contributes to (micro)phase separation that also toughens the material. Combinations of epoxy and urethane methacrylate resins are applied as dental filling materials.[151]

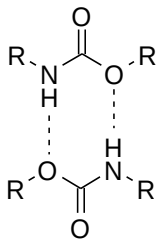

Figure 25. Urethane H bonds

Most of these base monomer possess *high viscosities* owing to their high molecular weight and the functional groups that might even promote crystallization. Therefore *low molecular weight monomers* are mixed to the formulations to lower the viscosity and enable the processability of the resins. Common monomers for these purpose are 1,6-hexandiol diacrylate (HDDA),

trimethylolpropane triacrylate (TTA) and pentaerythritol tri-/tetraacrlylate (Figure 26), often referred to as “reactive diluents”.

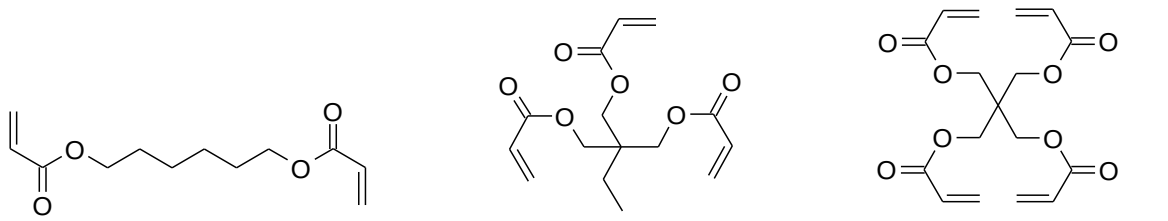

HDDA TTA Pentaerythritol tetracrylate

Figure 26: Common monomer for photopolymerization

6. Electrospinning

Contrary to the photopolymer concept described above, ***electrospinning*** processes linear polymers and does not contribute to increased molecular weight. ES has attracted the interest of biomedical research as it is possible to manufacture seamless, non-woven, fibrous structures which are able to mimic the ECM.[152, 153] A good review on the application of ES for regenerative medicine and *cardiovascular tissue engineering* is given by Sell and Bowlin.[139] By varying the process parameters it is possible to create various geometries, sizes and microstructures.

For ES the polymer solution is applied in a syringe fitted with a blunt tip cannula (Figure 27). The application of a large electric potential (10-30 kV) to overcome the surface tension generates a fine jet of the solution towards the grounded target.[154] The solvent evaporates and the *fibers* (50 nm-10µm diameter) deposit on the spinning/translating mandrel which coils the fibers. Due to the residual solvent the fibers possess adhesive surfaces and fuse to *conduits*.[137]

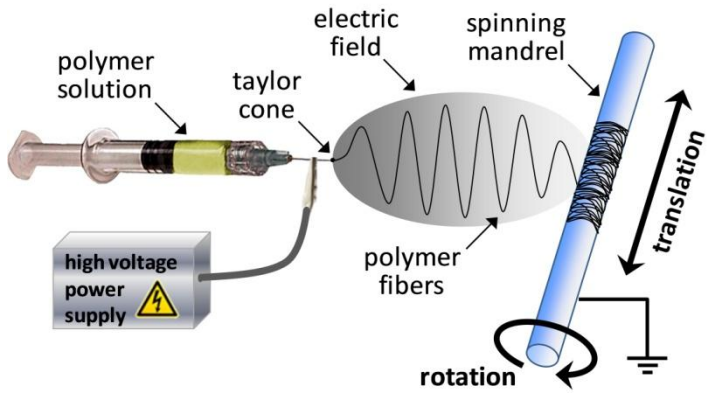

Figure 27. Principle of electrospinning

Another worthy specialty of ES is that *composites* can easily be fabricated by co-spinning or sequential/layered spinning of different materials whereat one of the materials often acts as support of the other component which enhances the biocompatibility.[155]

As for all materials for VTE biodegradability plays a central role. *Biodegradation* of electrospun materials predominantly rest upon the hydrolytic cleavage of the ester bond of polyesters. That is why the class of polyesters is such an important class of biomaterials [101] and they are frequently used as materials for electrospun vascular grafts. In fact all biomedical *approved polyesters* were already attempted as materials for artificial blood vessels (PGA [62, 156], PLA [88], PCL [84, 109], PDO [110, 157, 158]). The polyester-based biomaterials are often applied as combination with each other – as blend or (block-)co-polymers. With different ratios of the polymers within the polymer blends it is possible to tailor the properties, especially the *degradation rate* and the *mechanical* behavior. Another possibility to modify the mechanical properties and the degradation characteristics is to photocrosslink the fibers during the ES process, which was done by Tan and

Burdick with acrylate conjugated poly(β-amino esters)[159] and by Ifkovits and Burdick with acrylated poly(glycerol sebacate)[160]. Aside the *synthetic polymers* sometimes also *natural polymers* are processed with ES for the use as small-diameter vascular grafts. For example *fibroin* was used of a combination of electrospun and spumed material.[161]
However, it is often reported that *compliance mismatch* – the deviant mechanical properties of the constructs compared to native blood vessels – can cause less laminar flow at the junction site and therefore possibly lead to *stenosis*.[67, 162] Although this hypothesis has not yet been proved properly in experiment this assumption stands to reason. Therefore, this concern has prompted the research of more elastic polymers. *Polyurethanes* (PUs) are the most popular elastomeric materials in this research field. Contrary to the polyesters described above PUs are always *block-co-polymers* (with ***hard***- and ***soft*** segments), from the formal perspective ***polyaddition*** products of macrodiols with diisocyanates.
However, there are two different, important classes of TPUs: the *non-chain-extended* and the *chain extended* type TPUs.[163] The latter are synthesized by means of a *one-shot method* (Figure 28, left), the former by the *prepolymer method* (Figure 28, right).

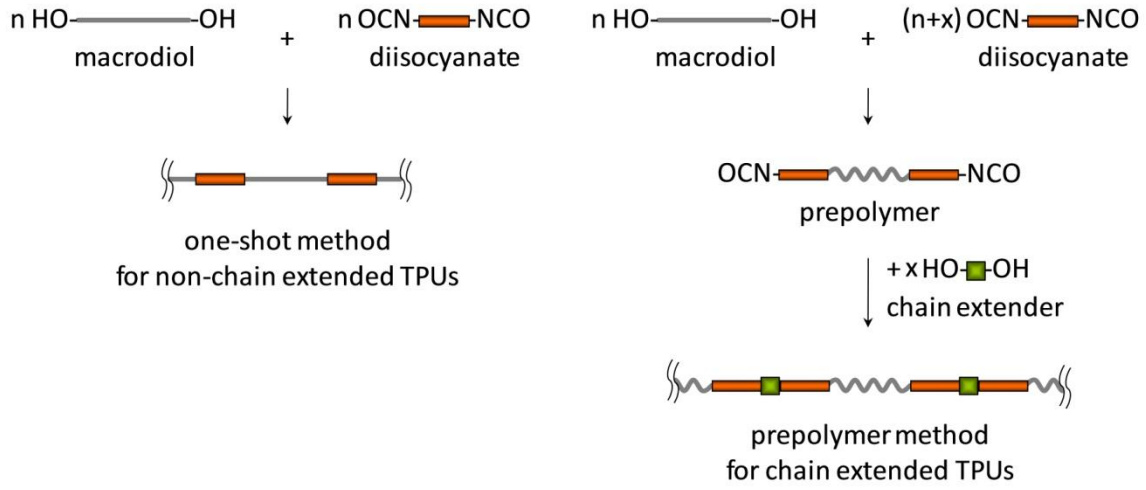

Figure 28. Scheme of the syntheses of non-chain extended TPUs (left) and chain extended TPUs (right)

In both cases hard- as well as soft-blocks are formed (Figure 29, left). The hard-blocks consist of the rigid urethane group containing moiety, while the soft-blocks consist of very flexible polyether or polyesters and in some cases polysiloxanes [164]. In the solid state the hard blocks aggregate thus *microphase separation* is observed (Figure 29, right), which is the central principle for the special mechanical properties of TPUs.

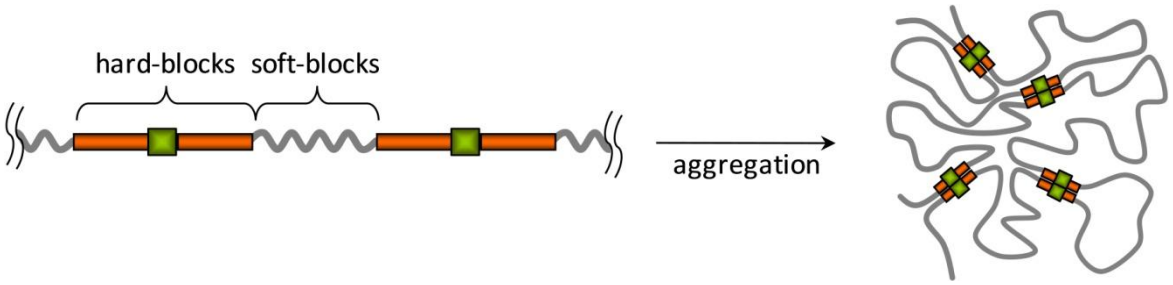

Figure 29. Polymer architecture of TPUs, single polymer chain (left) and aggregation (right)

Hard-block formation, however, is promoted for chain extended TPUs owing to the higher percentage of urethane groups. It has to be mentioned that beside diols, diamines or dithiols can be used as nucleophiles of the chain extenders. In these cases, however, poly(ureas) and poly(thiourethanes), respectively, are formed.

A typical TPU is the commercially available ***Pellethane***™ (Dow). It consists of *methane 4,4'-diphenyl diisocyanate* (MDI), *poly(tetrahydro furan)* (pTHF) and *1,4-butandiol* (BDO) (Figure 30).

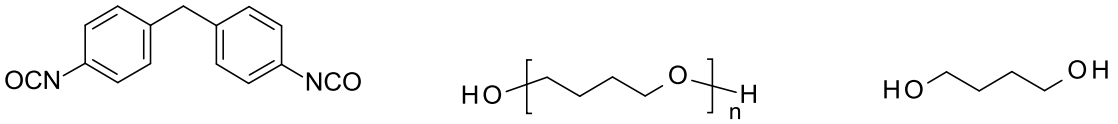

MDI **pTHF** **BDO**

Figure 30. Components of Pellethane™

TPUs have proved to be biocompatible in previous tests and should therefore be a suitable material for VTE.[118, 165-171] However, recent studies showed that the ingrowth of new tissue and the revascularization, respectively, is ***hindered by non-degradable material***. Thus it should be beneficial to combine the properties/concepts of polyesters and TPUs and create new ***degradable*** polymers.[172]

Objective

The tissue engineering of cardiovascular grafts is even after decades of research a field with manifold concepts but few achievements as measured by the clinical outcomes and the benefits for the patients. Therefore two very different approaches – the additive manufacturing of photoelastomers and electrospinning of thermoplastic urethane elastomers – should be conducted. This work should focus on the chemistry and the material properties of the new designated biomaterials and structure-property relationships should be established to easily tailor the properties for the specific task.

From recent work we have promising results for cyanoethyl acrylate as biomaterial for vascular grafts. In this work the surprising mechanical properties of this system should be studied by the examination of similar compounds. Additionally a biocompatible, mechanically complying material should be manufactured by stereolithography.
An alternative concept using urethane acrylates as base monomers should be developed. Again, the mechanical properties of the new system should be studied and modified by different additives. The optimized material should

- mimic the mechanical properties of native blood vessels
- be degradable, similar as established biodegradable polymers
- be manufactured by means of a suitable additive manufacturing technology
- have excellent biocompatibility (including low cytotoxicity of the degradation products)

As a second, alternative approach, new degradable thermoplastic urethane elastomers as material for electrospun vascular grafts should be developed. Pellethane, a FDA approved non-degradable thermoplastic urethane elastomer, should be taken as bench mark, as it was already used as material for electrospun vascular grafts. The molecular structure of Pellethane should be used as a template that will specifically modified to give a TPU that is

- degradable
- non-toxic (including degradation products)
- mechanical sufficient
- capable for electrospinning

In this context the focus should be on the concept of a cleavable chain extender to introduce the degradability of the TPUs.

State of the Art

1. Photopolymers for soft tissue engineering

In the last decade, ***photopolymers*** more and more came into the focus of ***biomedical research*** [123, 173-176] as they exhibit a wide spectrum of properties [130] and they have already been established as *bone cement* [177] and *dental filling material* [151] for several decades. Furthermore they can be processed by *additive manufacturing technologies* (AMTs) to fabricate structures with defined pore geometry which makes them very attractive for the application as tailored scaffolds for tissue engineering [178] especially for hard tissue regeneration e.g. bone repair [120-122, 179, 180]. In the last years, our research group undertook also several attempts to apply these concepts for VTE.[131, 181]

One of the first spacers between the polymerizable groups that was considered to be biocompatible was the commercially available *poly(ethylene glycol)* (PEG).[182] Owing to its uncharged and hydrophilic properties it inherently repels an unspecific protein adhesion in aqueous media.[183] An additional advantage of PEG is the ability to form *hydrogels* which improves the biocompatibility. Good reviews for the biomedical application of photopolymerizable hydrogels are given by Bryant and Anseth [184], as well as by Nguyen and West [185]. Metters and Lin focus on the biodegradability of hydrogels.[186] (Meth)acrylated PEG chains of various length have been used for many applications e.g. the encapsulation of chondrocytes for cartilage regeneration [187], osteoblasts for bone TE [173], vascular smooth muscle cells [188] and mesenchymal stem cells [189, 190]. Using (meth)acrylated PEG hydrogels containing short peptide sequences for selective cell adhesion is a frequently used approach to improve biocompatibility of photopolymers. [123, 191-193] For example tetrapeptide RGDS (Arg-Gly-Asp-Ser, Figure 31) can be conjugated to the scaffold.[124]

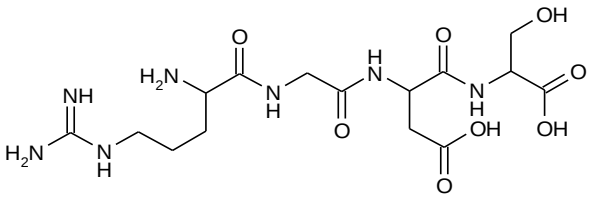

Figure 31. RGDS peptide

RGD-sequences have been used previously to improve the biocompatibility of biomaterials. [127, 194] For vascular scaffolds it has been shown that the REDV peptide (Figure 32) is specific for endothelial cells.[126]

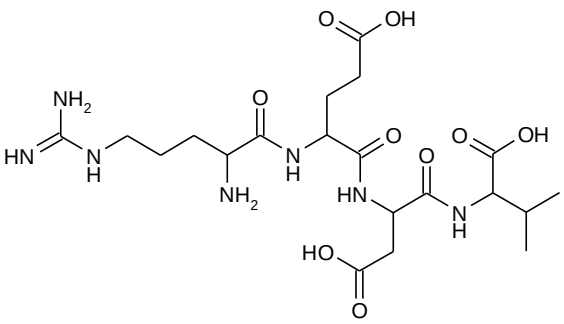

Figure 32. REDV peptide

Those *cell attachment promoting peptides* work best when they are not integrated inside the polymer chain but protruding from the surface of the polymer scaffold. Therefore a PEG spacer is the ideal approach.[173]

As a direct consequence of the need of tissue engineering for degradable scaffolds, the use of *completely biodegradable photopolymers* has found its way into the biomedical materials research field.[195] Beside the use for TE, the application for drug delivery system is very important.[196]

The design of novel multifunctional monomers and macromers that give degradable crosslinked polymers upon free radical polymerization is an interesting task for synthetic chemistry. The different concepts are reviewed by Ifkovits and Burdick [197] as well as Baroli [198]. Two representative examples are shown in Figure 33. They are obtained by ring-opening polymerization of a multivalent alcohol (e.g. PEG) to yield telechelic ABA blockcopolymers with PGA, PLA, PCL or PTMC that are end-capped with (meth)acrylates.[150, 199-203]

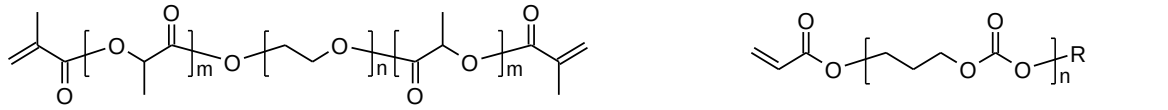

methacrylate end-capped PEG-PLA **acrylate end-capped poly(trimethylene carbonate)**

Figure 33. Different monomers for biodegradable photopolymers

However, for the *in-situ* scaffold-based VTE the material requirements are very specific and most of the materials discussed before and summarized by Schuster *et al.* [120, 121] fail to have proper mechanical properties. The most frequently used photopolymers for soft tissue regeneration are crosslinked polyethylene glycol diacrylates (PEGDA) [123, 173-175, 193], often applied as hydrogel (Figure 34, top). Those polymer networks have a high crosslink density along the polymer backbone. Therefore, these materials are very sensitive to cracks as they cannot dissipate energy by gliding of the polymer chains. Loading immediately leads to crack formation and thus minimize the strength as well as elongation.

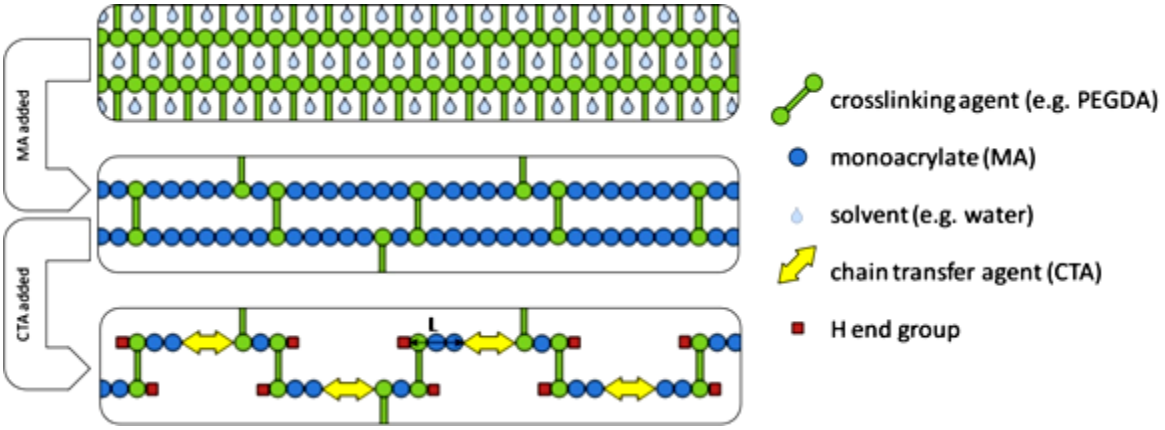

Figure 34. Idealized network architectures: crosslinked PEGDA hydrogel (top), network with, monoacrylates (middle), thiol-ene system (bottom)

To modify the networks and to have more control over the polymer architecture monoacrylates and *chain transfer agents* are added (Figure 34, middle and bottom). Thiols are an often used class of CTA due to their rapid tendency to radically add to alkenes. *Thiol-ene systems* were already in use in the early fifties [204, 205] but a lot of problems arose from the storage stability and odor [206]. However, in the last decade the thiol-ene click-reaction was intensively reexamined first of all by Charles E. Hoyle and Christopher N. Bowman.[207] Thiols are very reactive to hydrogen abstraction, and form sulfur radicals in the initiation step (Scheme 1a). These radicals propagate the polymerization. (Scheme 1b, c) When work with activated vinyls such as acrylates thiol-ene

propagation occurs at a rate similar to that of acrylate homopolymerization (Scheme 1d) [208]. Termination is possible by recombination or disproportion of two radicals.

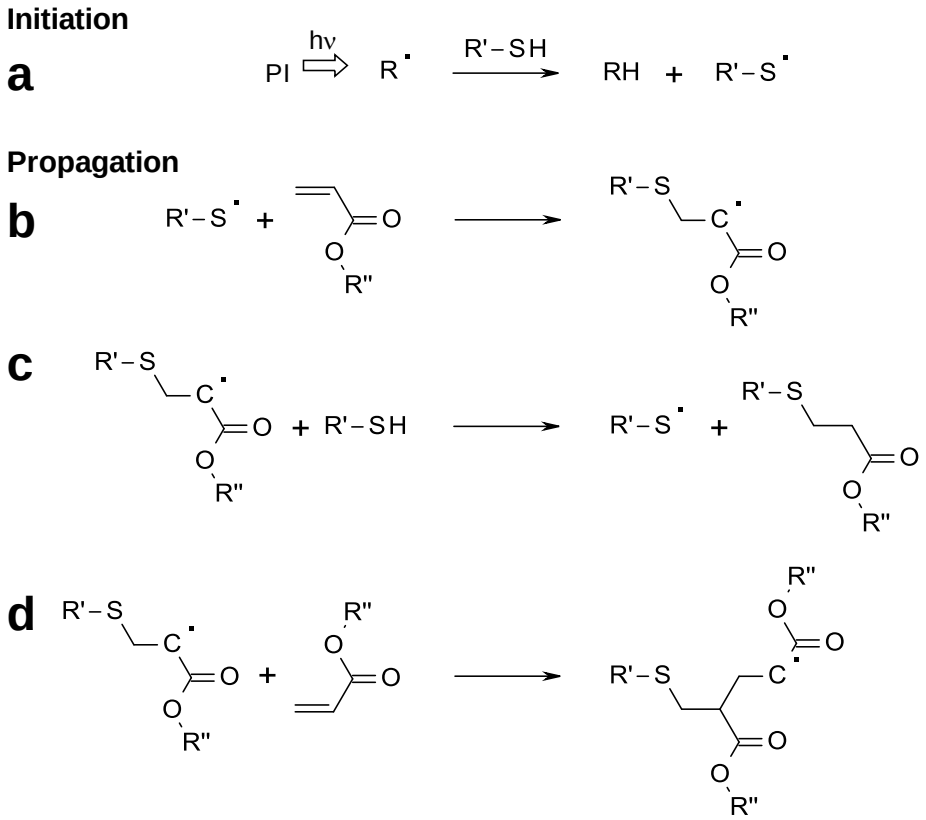

Scheme 1. Thiol-ene click-reaction with acrylates

Thiol-ene chemistry has already been applied for the development of new bio-responsive materials predominantly as hydrogels.[209-213] The step-growth like mechanism of the thiol-ene click-reaction and the high uniformity of the network leads to totally different architectures and mechanical properties from acrylate systems.

2. Degradable thermoplastic urethane elastomers

A good overview about (bio)degradable polyurethanes is given by Guelcher [214] and Santerre [113]. To design degradable thermoplastic urethane elastomers *cleavable bonds* are incorporated in the backbone of the polymers. Cleavable bonds can either be *esters*, *peptids* or *disulfids*. While peptides and disulfides are predominantly cleaved by enzymes [215-220], esters can be cleaved hydrolytically [47] and enzymatically [221] (Figure 35). A review about the design and synthesis of biodegradable and enzymatically cleavable polyurethanes is provided by Matsumura *et al.*[222] Herein the enzymatic and isocyanate-free synthesis of polyurethanes is also described.

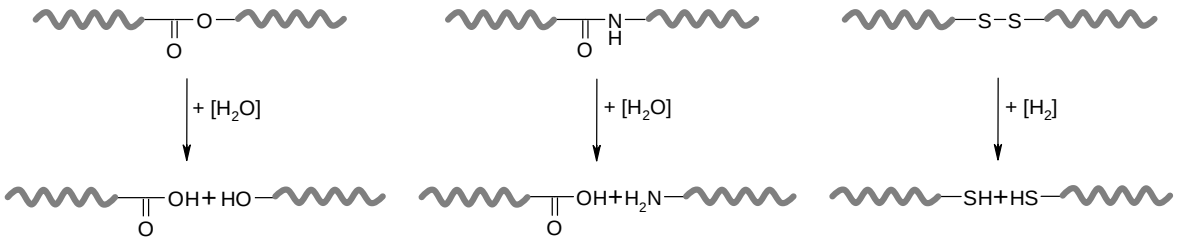

Figure 35. Cleavable bonds: esters (left), peptides (middle) and disulfids (right)

Soft-block degradability is often achieved by the application of polyester macrodiols, predominately derived from glycolic acid (GA)/glycolid, lactic acid (LA)/lactid, caprolactone (CL) or trimethylene carbonate (TMC) by a ring opening polymerization, initiated by (small) diols like (di)ethylene glycol or 1,4-butanediol.[223-226] By copolymerization the properties of the polymers can be influenced.[227, 228]

The most prominent concept is the use of CL-(co)-polymer diols [229-245], followed by LA-(co)-polymer diols [246-251] and TMC-(co)-polymer diols [252, 253]. Another approach is the use of classic AABB polyester, e.g. poly(tetramethylene succinate)diol [254].

To introduce *hard-block degradability*, it is necessary to apply a ***cleavable chain extender*** (CCE) for the prepolymer method. A CCE is a small molecule (m.w. < 500 g/mol) with two terminal hydroxyl/amino/thiol groups connected linearly by at least one deavable bond.[238] In literature a large variety of different (cleavable) chain extenders are used for the synthesis of degradable TPUs (Table 1). Beside the choice of the chain extender also the selection of the *diisocyanate* (DI) is crucial. Generally aromatic diisocyanates like MDI or toluene diisocyanate (TDI) are avoided for medical applications because of the toxicity of the corresponding diamines.[255-257]. Commonly used DI can be seen in Table 2.

Most of these degradable TPUs are not designated for a special application but most of the authors claim the suitability of their developed TPU for biomedical applications. However, some references also describe a special application. In fact, the whole spectrum from hard- to soft tissue engineering is covered. This is possible due to the tailorable wide range of mechanical properties of the TPU. For *bone tissue engineering* very tough but hard materials are needed [231, 234, 258], while for *cartilage repair* [234, 240, 259] and even *softer tissues* materials with rather low moduli and high elongations are required. [235, 237, 239, 260] Of course, some of the materials are used for *vascular* or *cardiac tissue engineering*.[233, 245, 261] Aside the application for tissue engineering the application of degradable TPUs for *controlled release* of *drugs* has also high impact in literature. [231, 237, 243, 250, 262, 263]

Table 1. Chain extender used for biodegradable poly(urethanes)

chain extender	*structure*	
ethylene glycol (EG)	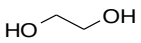	242, 258
butanediol (BDO)	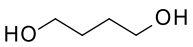	236, 237, 249, 254
putrescine	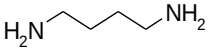	233, 245
lysine ethyl ester	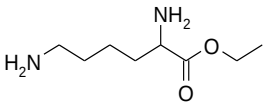	233, 235, 237
ornithine ethyl ester	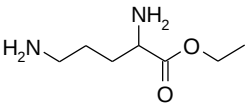	235
2-amino-1-butanol (2AB)	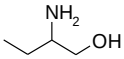	229-231
2-mercaptoethyl ether (2MEE)	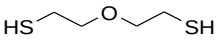	229, 230
2,2'-(methylimino)diethanol (MIDE)	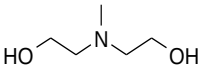	236, 241
N,N-bis(2-hydroxyethyl)-sulfamic acid (BES)	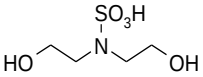	241
2,2-dimethylol propionic acid (DMPA)	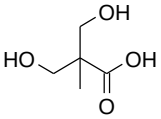	243, 264
2-hydroxyethyl lactate (EGLA)	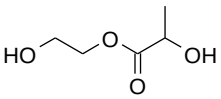	238
2,2'-dithiobisethanol (DIT)	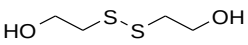	220
desaminotyrosyl tyrosine hexyl ester (DTH)	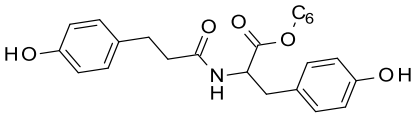	244
dianhydro-D-sorbitol (ISO)	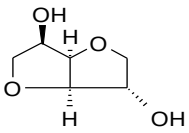	234, 240, 259
1,4-cyclohexanedimethanol bis(phenyl alanine) ester (PCE)	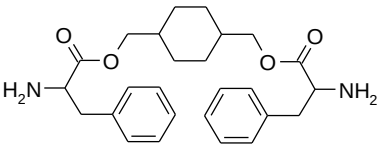	232, 261
morphine sulfate	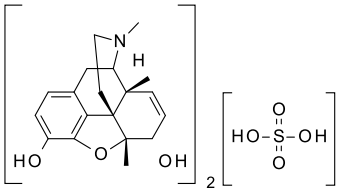	263

Table 2. Diisocyanates for biodegradable poly(urethanes)

diisocyanate	*structure*	
hexamethylene diisocyanate (HMDI)	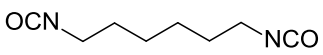	220, 229, 230, 238, 240, 244, 247, 248, 251, 252, 259
2,2,4-trimethylhexamethylene diisocyanate (TMDI)	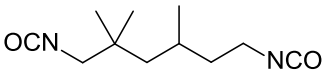	246
tetramethylene diisocyanate (BDI)	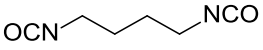	169, 233, 245, 249, 265
4,4‘-dicydohexylmethane diisocyanate (H_{12}MDI)	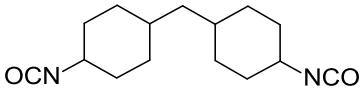	242, 254, 258
Isophorone diisocyanate (IPDI)	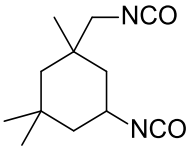	229-231, 237, 243, 264
lysine diisocyanate (LDI	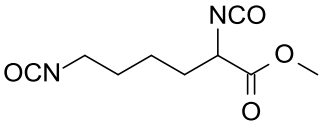	232, 235, 250, 253, 266

To enhance the mechanical properties, especially the suture tear retention TPUs can also be crosslinked after processing. Tran *et al.* fabricated porous scaffolds by the salt leaching method and added a thermal crosslinking step.[267] The crosslinking occurs by an intermolecular transesterification mechanism.[268] An alternative crosslinking method is the incorporation of zwitterionic moieties into the polyurethanes. After mixing with gelatin beads both components crosslink by the interaction of the ionic groups which improves the properties of the material.[269]

Results & Discussion

1. Photoelastomers

"Photoelastomers" actually is a very new and not yet established term for photopolymers with a very low crosslink density and with similar properties to conventional elastomers. Classical elastomers have polymer architectures of very long, coiled polymer chains that are (reversibly or covalently) crosslinked by only a few laterally connections. During elongation the chains are de-coiled and arrange in strain direction (Figure 36). The highly aligned polymer chains are in an entropic unfavorable condition. Therefore the elasticity of elastomers is driven by entropy (entropic/rubber elasticity) unlike those of other materials (energy elasticity).

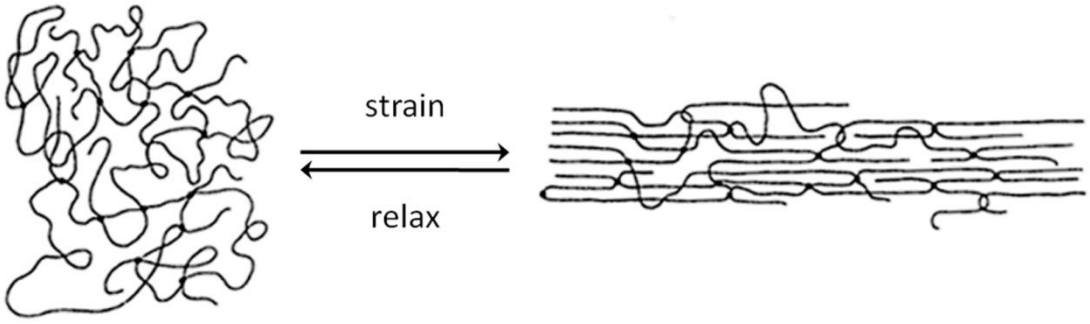

Figure 36. Elasticity of elastomers

Another important and distinct difference to other materials is that elastomers are always applied above their glass transition temperature (Tg). For bioelastomers this means that the Tg is lower than body temperature.[270] So, very low Tg's are necessary even though not sufficient requirements for elastomers. The glass transition temperature can be determined by thermal-differential scanning calorimetry (ThermDSC)[271] or dynamic mechanical analysis (DMA)[272].

1.1. New monomers

In preliminary studies we were able to build structures with geometries desired for artificial vascular grafts out of a mixture of trimethylolpropane triacrylate (**TTA**) and ethoxylated trimethylolpropane triacrylate (**ETA**) with Irgacure 2959® [273] as biocompatible PI. Unfortunately, this formulation and most of the photopolymers known from literature, where some of them were examined concerning their biocompatibility in preliminary experiments [120, 121], turned out to be not suitable because of their hard and brittle material behavior. One exception was poly(2-cyanoethyl acrylate) (poly-**CEA**) that showed similar mechanical properties to native blood vessel. To see if an optimization of the mechanical properties is possible it was of interest to investigate different analogous compounds (Figure 37). It was unclear whether the electronic influence of the cyano groups, the cyano group itself or crosslinking by chain transfer reactions during polymerization was responsible for these properties. Mechanical characterization should indicate the optimum base monomer for the formulation.

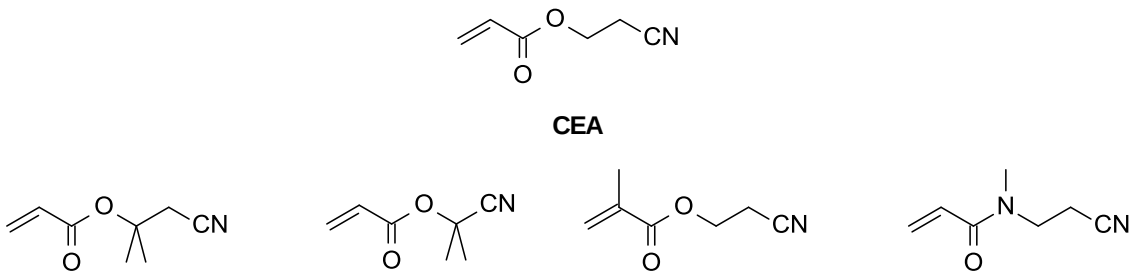

Figure 37. CEA-derived monomers

1.1.1. Synthesis

Due to the excellent mechanical properties of poly-**CEA** it was of interest to investigate several CEA-analogous compounds to tune the reactivity and the mechanical properties of the polymer and to investigate the reason for the surprising mechanical properties. The β-blocked acrylate **Me$_2$CEA** as well as the α-blocked acrylate **Me$_2$CMA** [274, 275] were synthesized to investigate the influence of the hydrogen atoms next to the oxygen of the ester or the nitrile group in **CEA** concerning abstraction reactions during polymerization. It was expected that a small amount of chain transfer reactions lead to a slightly crosslinked polymer network similar to rubber-like materials. The methacrylate **CEMA** [276, 277] should have a better store stability and a lower toxicity due to the slower Michael addition on this molecule. The acrylamide **NCEA** [278, 279] was synthesized since it should have a higher reactivity and the amide bond eventually promotes cell adhesion [120]. Conversion of (meth-)acryloyl chloride with the corresponding hydroxyl compound or the amine, respectively (Scheme 2) and purification by distillation gave the desired products in a yield ranging from 22 to 72%.

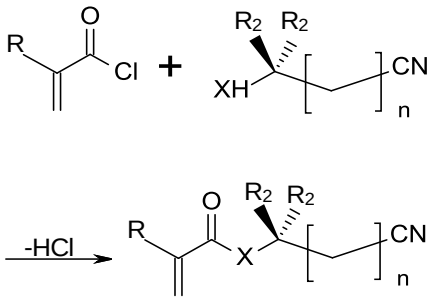

	R_1	*R_2*	*X*	*n*	*Yield*
CEA	-H	-H	-O-	1	69%
Me$_2$CEA	-H	-Me	-O-	1	26%
Me$_2$CMA	-H	-Me	-O-	0	22%
CEMA	-Me	-H	-O-	1	72%
NCEA	-H	-H	-N(Me)-	1	43%

Scheme 2. Synthesis of CEA analogous compounds

1.1.2. Photo-differential scanning calorimetry

A very important property of new monomers that are designated to be structured by means of photolithographic AMT techniques is their photoreactivity. To investigate the photopolymerization behavior, different techniques are used in literature, where real time Fourier transformation infra red (RT-FTIR), photo-differential scanning calorimetry (photo-DSC), pyrometry, photo-rheology or dilatometry [280] are frequently used methods. As photo-DSC is a method with high efficacy which provides all relevant information within one simple measurement, this technique was selected to evaluate the monomers.[281] The heat flux between a pan filled with monomer formulation with a PI and a reference pan is measured while both pans are irradiated with light of specific wave length. The pan with the monomers warms due to the exothermic polymerization reaction. However, the temperature of both pans is kept at the same level and the difference of power consumption is directly related to the imaginary heat flux between the samples.

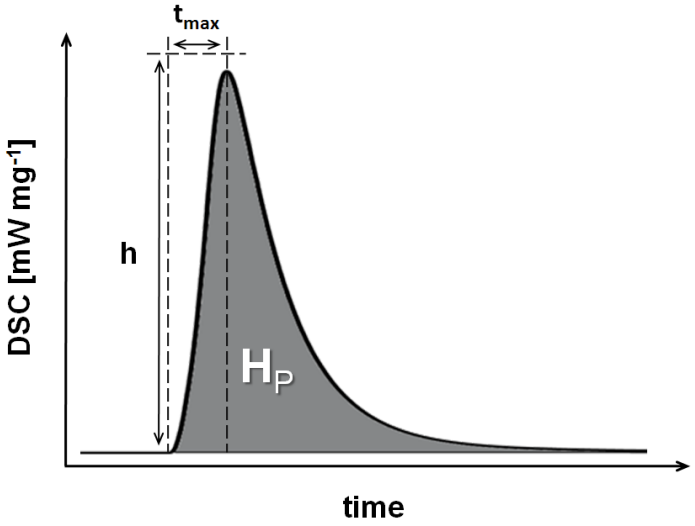

Figure 38. Schematic Photo-DSC plot

By evaluation of the DSC plots, the time to reach the maximum polymerization heat flux t_{max}, the double bond conversion DBC and the rate of polymerization R_P can be obtained (Figure 38).[282] For the DBC and the R_P, the theoretical heat of polymerization $\Delta H_{0,P}$ has to be known. With the value of the area of the peak and the theoretical heat of polymerization of the monomer known from literature the double bond conversion can be calculated by the aid of eq. 1 and 2, respectively.

$$DBC = \frac{\Delta H_P}{\Delta H_{0,P}} \quad (1)$$

ΔH_P.....heat of polymerization [J·g^{-1}]
$\Delta H_{0,P}$.....theoretical heat of polymerization [J·mol^{-1}]

$$\Delta H_{0,P} = \Delta H_{0,DB} \cdot \sum \frac{w_i}{M_i} x_i \quad (2)$$

$\Delta H_{0,DB}$..... theoretical heat of polymerization of the double bond [J·g^{-1}]
w_i.....weight fraction of the monomer i [ ]
M_i ..... molecular weight of the monomer i [g·mol^{-1}]
x_i.....number of polymerizable groups [ ]

R_P can be calculated from the height of the peak at t_{max} according to eq. 3.

$$R_p = \frac{h \cdot \rho}{\Delta H_{0,P}} \quad (3)$$

R_p .....rate of polymerization [mol·L^{-1}·s^{-1}]
h ..... specific heat flow at maximum [mW·mg^{-1}]
ρ .....density of the resin [g·L^{-1}]

Table 3. Theoretical heat of polymerization [283]

monomer	$\Delta H_{0,P}$ [kJ·mol^{-1}]
acrylate	80.0
methacrylate	60.0

The photo-DSC plots of all monoacrylates with 0.5% (w/w) of **BPO** as PI are displayed in Figure 39, t_{max}, R_p and DBC are listed in Table 4.

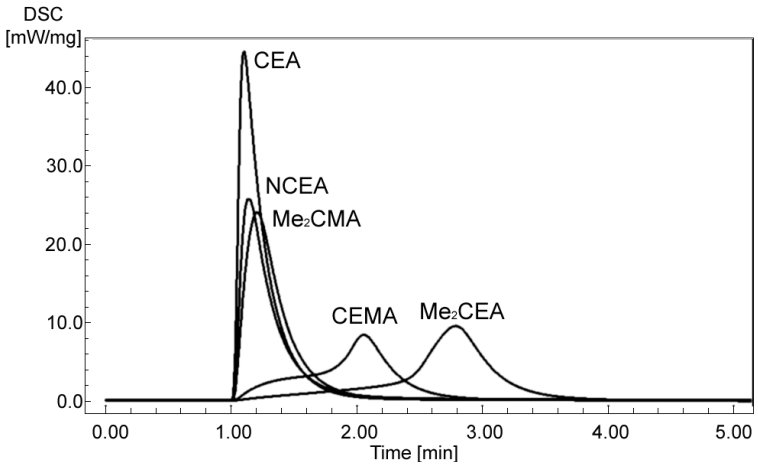

Figure 39. Photo-DSC plots of monoacrylates with 0.5% (w/w) of Irgacure 819® as PI

Table 4. Photo-DSC data of monoacrylates with 0.5% (w/w) of Irgacure 819® as PI

	t_{max} [s]	DBC [%]	$R_P \times 10^3$ [mol·L^{-1}·s^{-1}]
CEA	6	86	500
Me_2CEA	110	76	121
Me_2CMA	12	85	311
CEMA	64	75	140
NCEA	8	80	331

The acrylate **CEA** is a highly reactive monomer not only from the viewpoint of the extraordinarily high R_p but also t_{max} and DBC are outstanding. The acrylamide **NCEA** and the α-blocked acrylate **Me_2CMA** have a lower R_p (but within the same order of magnitude) while the methacrylate **CEMA** and the β-blocked acrylate **Me_2CEA** have a rather low reactivity especially in respect of the high values for t_{max}. Reactivities of the methacrylate **CEMA** and the acrylamide **NCEA** are as expected for such functional groups.[120, 121] The differences between the two H-blocked monomers indicate differences in the polymerization mechanism.

1.1.3. Tests of the photopolymers

1.1.3.1. Solubility and thermal properties

To explain the differences in the polymerization mechanism of the new monomers, the solubility of the photopolymers was examined. Whereas poly-**NCEA** and poly-**Me_2CMA** are soluble in different solvents as expected, poly-**CEA**, poly-**CEMA** and poly-**Me_2CEA** are completely insoluble. Therefore it can be assumed that the acrylamide based poly-**NCEA** and the α-blocked acrylate based poly-**Me_2CMA** are linear or branched polymers while poly-**CEA**, poly-**CEMA** and poly-**Me_2CEA** are crosslinked photopolymers. As the different solubility there is also a distinct difference in the mechanical properties of the photopolymers. The two soluble and therefore

linear or branched polymers based on **NCEA** and **Me_2CMA** are brittle while poly-**CEA**, poly-**CEMA** and poly-**Me_2CEA** however are flexible and have elastomeric properties.
As explained earlier the glass transition temperature (Tg) is a very important characteristic for elastomers. Tg of poly-**CEA** seems to be below room temperature, while in case of poly-**CEMA** and poly-**Me_2CEA** the Tg's are at higher temperatures. To investigate the different values of Tg also thermal DSCs were performed.
ThermDSC [284] works similar to photoDSC with the same arrangement of two pans, filled with the substance and a reference, respectively. Both pans are heated with a defined rate (1 to 10°C/min) and the difference of heat flux demanded by the both pans is plotted against the temperatures. Exothermic or endothermic transitions of 1st order (recrystallization, melting, decomposition) become apparent as peaks with curvatures of opposite sign. Glass transition, however, is a transition of 2nd order and therefore only observable as a step of the DSC curve (Figure 40).

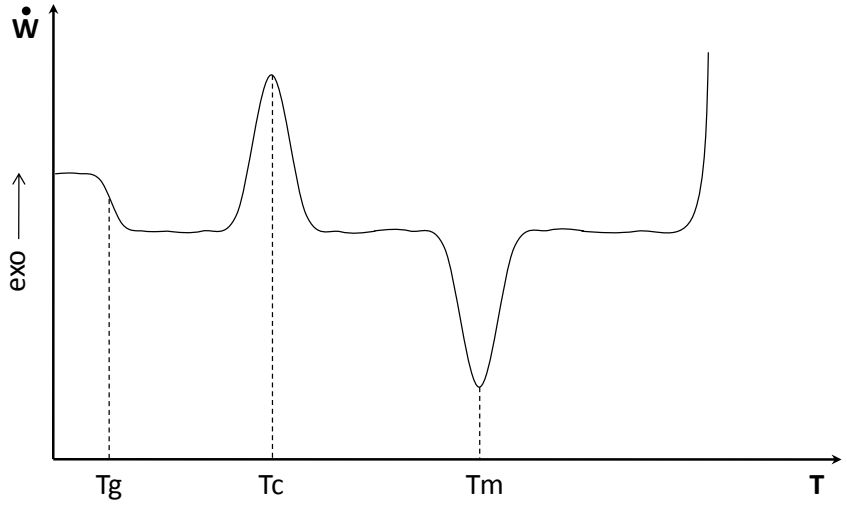

Figure 40. Typical ThermDSC plot

For the ThermDSC measurements, the insoluble polymers were extracted and the soluble polymers were reprecipitated in order to remove residual monomer. Table 5 summarizes all the different properties of the photopolymers.

Table 5. Properties of the photopolymers

		Reactivity	*Solubility*	T_g
CEA	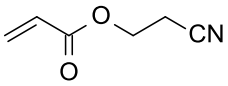	+	insoluble	11°C
Me_2CEA	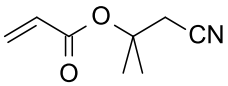	-	insoluble	52°C
Me_2CMA	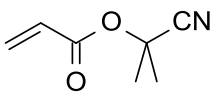	+	soluble	134°C
CEMA	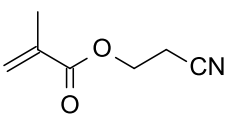	-	insoluble	112°C
NCEA	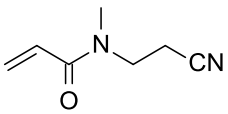	+	soluble	130°C

Considering the structure-properties relationship, it can be concluded that the elastomeric behavior of the polymers of **CEA**, **CEMA** and **Me_2CEA** seems to be caused by crosslinking via hydrogen abstraction of the hydrogen atoms next to the cyano group. Similar to natural rubber a crosslinking density of about 0.1 to 1 per 100 monomer units leads to elastomeric properties.
In sight of reactivity and mechanical properties at physiological temperatures **CEA** has the most promising properties by far.

1.1.3.2. Biocompatibility tests

In preliminary tests, dense poly-**CEA** specimens were investigated using a formazan based cell proliferation and cytotoxicity assay. The rather poor results have forced us to the application of hydrogels, [123, 173-175, 193, 285] crosslinked by a broad variety of different amounts of two crosslinking agents as selected above. The hydrogels could not be produced directly because of the insolubility of **CEA** in water. Therefore alcogels were made with ethanol and the solvent was exchanged with water afterwards. Generally, **CEA**-hydrogels containing different percentages of **ETA** showed rather poor results in cell culture. For example, no cell attachment was observed when human endothelial cells were seeded onto cryostat sections of a **CEA**-hydrogel with 5% (w/w) **ETA** (Figure 41a) while a hydrogel with 10% (w/w) **ETA** showed a slightly improved cell adhesion (Figure 41b). In contrast, when **PEGDA** was used as crosslinking agent, endothelial cell attachment and proliferation was strongly enhanced (Figure 41c and Figure 41d). These morphologic findings are corroborated by the results of cell proliferation and cytotoxicity assay EZ4U which revealed that increasing the amount of crosslinker **PEGDA** in the formulations improves endothelial cell proliferation on the photopolymers. Therefore **ETA** was rejected as crosslinker in further experiments. It has to be noted that from this broad set of experiments it cannot be concluded whether the cell adhesion is improved by the changed mechanical properties or the chemical structure of the crosslinker. The latter aspect seems to be less relevant as PEGDAs are known to give poor cell adhesion.[286]
In the detailed subsequent studies we also had to exchange the solvent for the test specimen preparation as the stereolithography process requires solvents with high boiling points. Therefore polyethylene glycol 400 (**PEG400** with $\overline{M}_n = 400$ g/mol) was added instead of ethanol in the monomer mixture. After extraction with water to form hydrogels out of the PEG-gels, proliferation rates comparable to those observed on tissue culture treated plastic coverslips were attained. It can be summarized that the application of hydrogels with carefully selected crosslinker is crucial to achieve good biocompatibility.

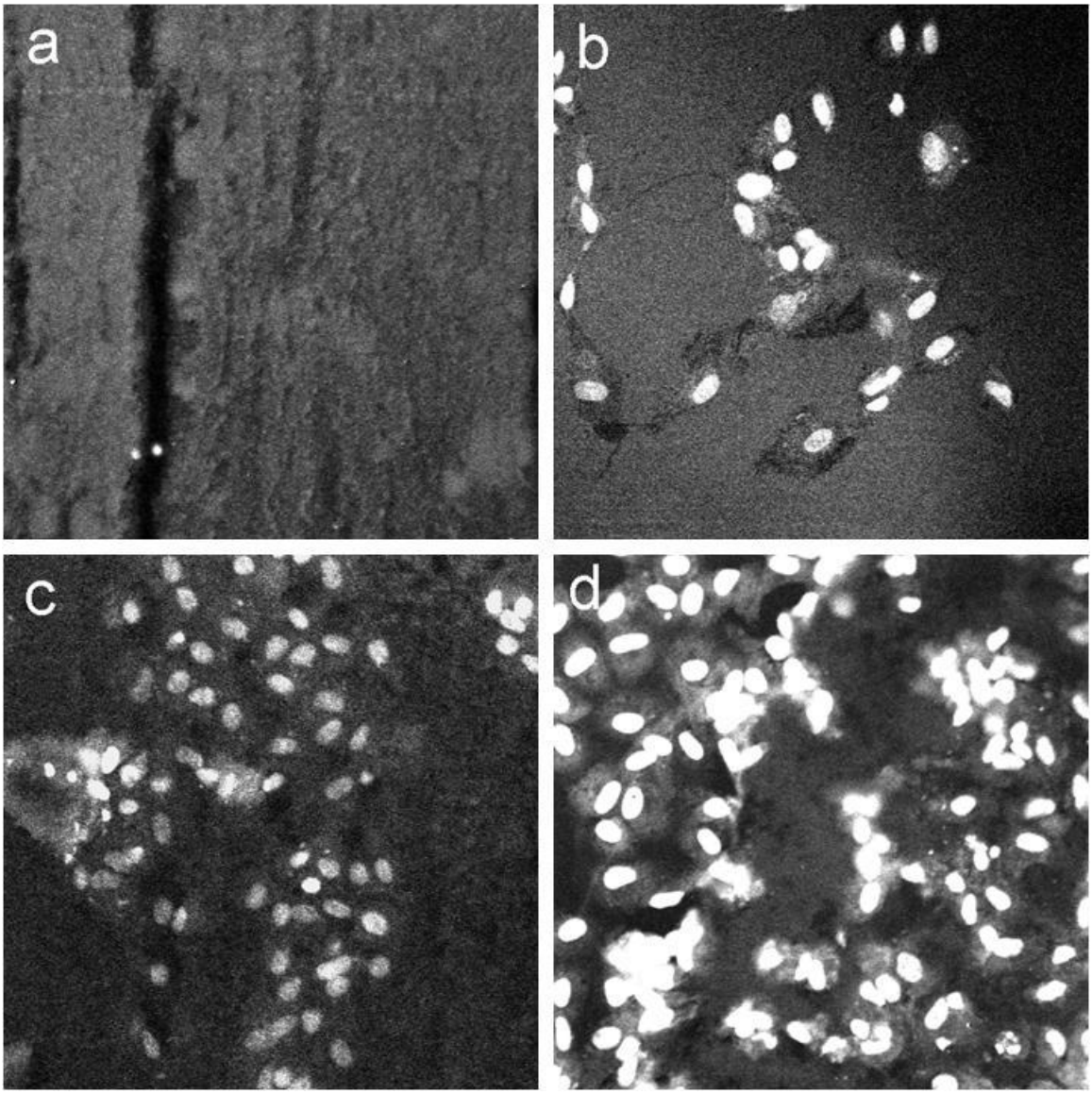

Figure 41. Morphology of HUVECs seeded onto cryostat sections of CEA hydrogels made from a: 50% CEA/5% ETA/45% EtOH, b: 50% CEA/10% ETA/40% EtOH, c: 15% CEA/15% PEGDA/70% EtOH, d: 15% CEA/14% PEGDA/80% EtOH (TOPRO-3 staining, laser scanning microscopy x 400)

1.1.3.3. Mechanical properties

To investigate the mechanical properties of natural blood vessels [287], an ovine arteria carotis was tested in tension. In circumferential direction the elastic modulus (E) of the blood vessel ranged from 350 to 550 kPa, the tensile strength (S) was between 900 and 1100 kPa while the strain at break (ε_b) varied from 100 to 150%.

As the biocompatibility tests indicated that the application of hydrogels with **PEGDA** as crosslinker improves the cell attachment of the examined test specimens and also a sufficient reactivity has been found in the photo-DSC measurements, **PEGDA** was chosen as the most suitable crosslinking agent for further studies. Therefore the mechanical properties of **PEGDA**-crosslinked poly-**CEA** hydrogel systems were investigated in a wider scope. Three different resin formulations (A-C, Table 6) were produced, cured in a silicone mould, extracted three times overnight in distilled water and specimens according to ISO 527-1/5A were punched. The specimens were tested with a tensile testing machine (Zwick Z050) with a strain rate of 25 mm/min.

Table 6. Resin formulations with 48.5% (w/w) PEG400 as solvent and 1.5% (w/w) Irgacure 819® as PI for mechanical tests

Formulation	*% (w/w) CEA*	*% (w/w) PEGDA*	*E [kPa]*	*S [kPa]*	*ε_b [%]*
A	49	1	215 ± 17	138 ± 12	98 ± 11
B	48	2	316 ± 18	121 ± 6	81 ± 10
C	45	5	410 ± 22	151 ± 19	67 ± 8

As it could be seen in Figure 42, *E* increases continuously with the content of the crosslinker PEGDA. E of formulation C lies well within the range of natural blood vessels. Figure 42 also depicts the dependency of ε_b of the material on the crosslinking ratio. As expected, with increasing amount of crosslinker ε_b decreases. S of the material is more or less independent of the crosslinking ratio (Table 6).

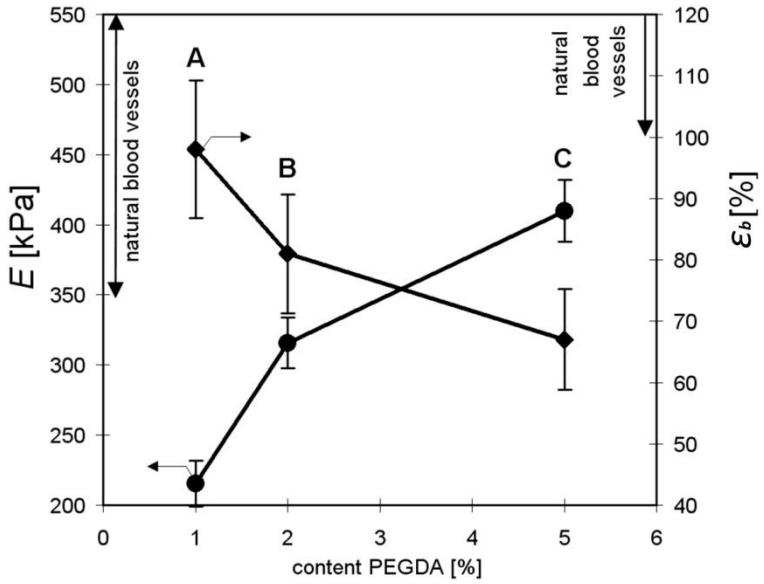

Figure 42. Dependency of the elastic modulus and the strain at break on the content of crosslinker PEGDA

Formulation C fits best with the elastic modulus of natural blood vessels, which is the most important mechanical property for artificial blood vessels. The ultimate strain as well as the tensile strength are still in need of improvement. By changing the solvent content and the spacer length of the crosslinker, these parameters can be optimized. Nevertheless, these results are of sufficient quality to perform first attempts for the structuring of artificial blood vessels by microstereolithography.

1.1.4. Additive Manufacturing Technology: Microstereolithography

Microstereolithography is a rapid prototyping technique that allows the fabrication of complex 3-dimensional structures by curing a photosensitive resin layer by layer.[130] After slicing the CAD model into virtual layers the photosensitive resin is selectively solidified according to the layer information. By stacking up the individual layers the final part is built (Figure 43).

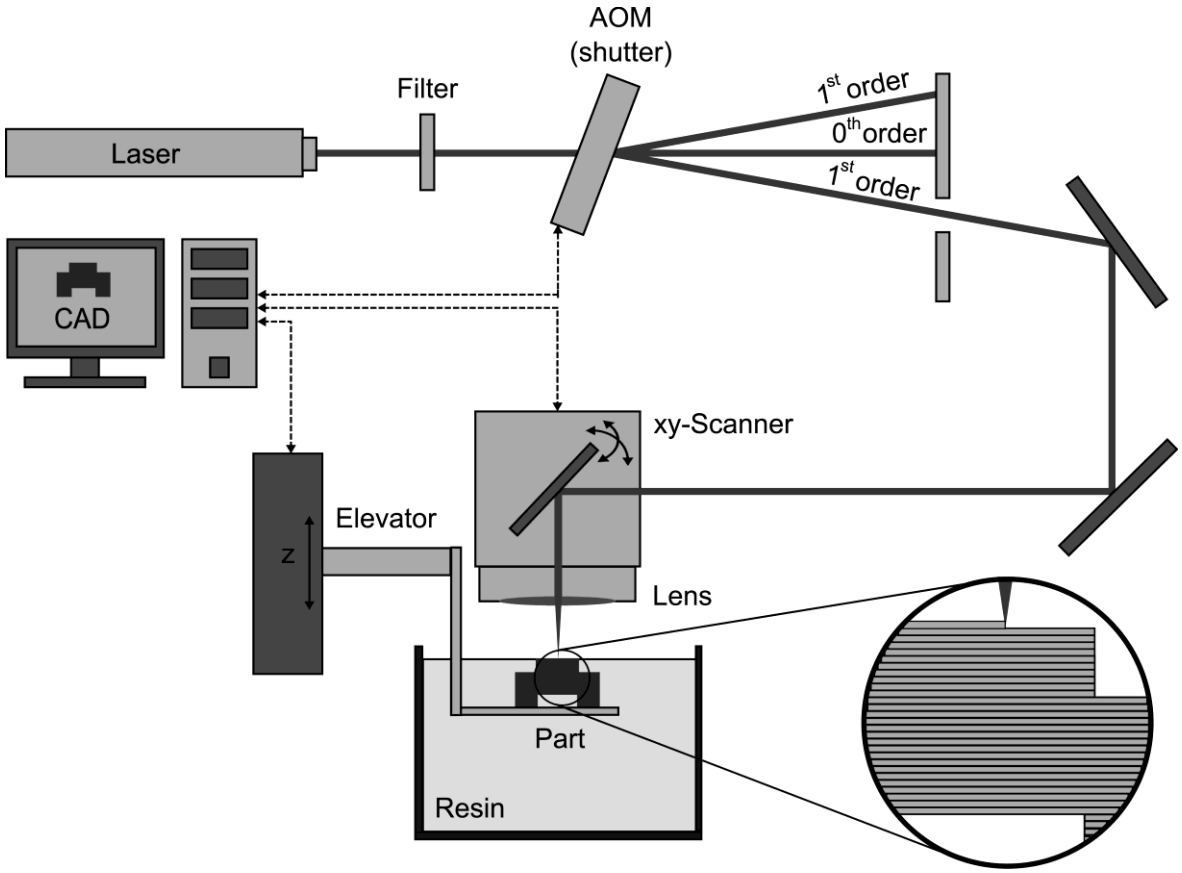

Figure 43. Microstereolithography system

The laser generates a continuous beam of monochromatic (355 nm) light that pass through the acousto-optic modulator which can deflect the beam with a very high frequency (MHz-GHz). The system of mirrors is arranged in such a way that only the deflected light can pass through the slit and continue to the scanning system where it is reflected to scan above the surface of the resin and cure the current layer. Once a whole layer is cured the part is lowered by an elevating system into the bath of resin, the wiper of the coating system (not shown in Figure 43) covers the surface with new monomer before the next layer is cured. The applied laser is a neodymium doped yttrium aluminum garnet ($Y_3Al_5O_{12}$) laser (Nd:YAG). This is the most popular solid state laser.[288] In the yttrium aluminum garnet about 1% of the Y^{3+}-Ions are exchanged by Nd^{3+}-Ions. The laser transition accords a wavelength of 1064.1 nm. Pulsed laser types with the frequency multiplied wavelength of 532 nm (doubled), 355 nm (tripled) and 266 nm (quadruplicated) are available. The acousto-optic modulator (AOM) is used as the shutter of the microstereolithography system. In fact it does not turn the beam on and off, it only generates diffraction pattern. The different orders (1^{st}, 2^{nd}, 3^{rd} etc.) of the beam leave the device in different angles shifted by 2Θ.[289] In the off-mode only the non-deflect 0^{th} order appears. The mirrors of the system are arranged in such a manner that only the 1^{st} order pass the slit (Figure 43). The AOM is composed of a piezo crystal with a high frequency (HF) generator, the Bragg-glass and an acoustic absorber. The HF generator induces the vibration of the piezo crystal that causes a supersonic wave within the Bragg-glass. This suspends the optical isotropy of the glass. The phonons within the glass let it act as grating which diffracts the light according to Bragg's law and therefore generate the different orders of diffraction. Unfortunately the 0^{th} order will always have the highest intensity. So, one loses the

bulk of the photons. However, the distribution of the different orders of diffraction according to the light intensity depends on the direction of polarization of the light. Using a $\lambda/2$-delay platelet which is also integrated in the microstereolithography system, it is possible to rotate the direction of polarization [288] and therefore to optimize – that means to maximize – the intensity of the 1st order. The used scanner consists of 2 tiltable mirrors – driven by galvanometer actuators – and a lens. The beam enters the scanner at the access aperture, is deflected by the first (y-direction) and then the second mirror (x-direction) and focused by the lens. To cure a structure the scanner guides the laser beam through the surface of the photocurable resin in a special manner. First the contour then an orthogonal cross hatching is drawn. Beside the optical components of the microstereolithography system, some other non-optical components are important. The platform, the compensation volume as well as the wiper have to be driven with a very high accuracy (sub-µm) to achieve the high resolution of microstereolithography. Therefore it is necessary to apply multiphase motor elements that can be controlled digitally. Linear piezoelectric motors comply with these requirements. They are composed of a locking crystal group and a motive crystal group that are both attached to the carriage. Sequential triggering of the different groups generates movement. This movement is recorded and controlled by a linear measurement system.
Based on the findings in the previous chapters a resin system containing **CEA** (45% (w/w)), **PEGDA** (5% (w/w)) and **PEG400** (48.45% (w/w)) fulfills the basic requirements for artificial vascular grafts. Preliminary penetration tests were carried out to find the optimal process parameters for microstereolithography. To limit the penetration depth of the Laser beam and therefore increase the resolution in z-direction it is necessary to add an absorber to the formulation. For this purpose 2,2'-hydroxy-4,4'-methoxybenzophenone (**HMB**) was used. Due to the perfect overlapping with the laser wavelength and the high extinction coefficient (ε_{355nm}= 15200 L·mol^{-1}·cm^{-1}) only very low concentrations of this absorber are necessary. Variation of amount of PI and absorber gave an optimum balance at 1.5% (w/w) **BPO** and 0.05% (w/w) **HMB**.
By means of microstereolithography small diameter conduits were built. After rinsing with 2-propanol and post-curing under the UV lamp, the part was extracted (Figure 44).

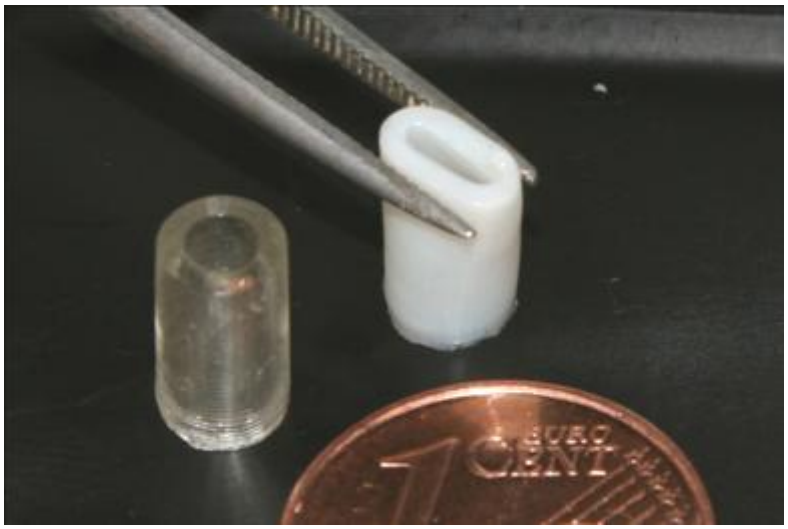

Figure 44. Conduits out of CEA based resins, unextracted (left) and extracted (right)

Concluding it can be said that although **CEA** based formulations fulfill the basic requirements for materials for scaffold-based VTE and it can be manufactured by SLA there are too many drawbacks especially regarding the applicability of these materials. The first experiences of the surgeons with the material emphasized its incapability for being sewed, which is the exclusive implantation method. In the end this material does not possess any degradability aside from the cleavability of the ester bonds whose cleavage would, however, not lead to low molecular compounds that could be eliminated by the body. Therefore other materials were investigated.

1.2. Macromonomer based photoelastomers

An intensive preliminary study of different acrylate based monomer systems showed that even if the specific network architecture of common elastomers is adjusted by the carefully combination of crosslinking agents and reactive diluents the typical elastomeric behavior could not be obtained.

1.2.1. Polyester based photopolymers

In this preliminary study, for example a multifunctional polyester methacrylate was synthesized in two steps. In the first step a **slightly branched polyester** was prepared by an acid catalyzed polycondensation of 1 eq polyethylene glycol (200 g/mol, **PEG200**), 1 eq adipic acid and 0.88 eq glycerol in toluene (Scheme 3). This polyester should introduce the degradability of the photopolymer and acts as wide meshed crosslinking agent. The approximate molecular weight of the polyester was assessed by determination of the hydroxyl value (OH value). The most common method to determine the OH value is the conversion of the hydroxyl end groups with an excess of acetylic anhydride and the back titration with a KOH titer solution. The OH value of the polyester was 0.0005 mol/g. By simplifying and assuming a linear polyester the molecular weight would be approximately 4000 g/mol

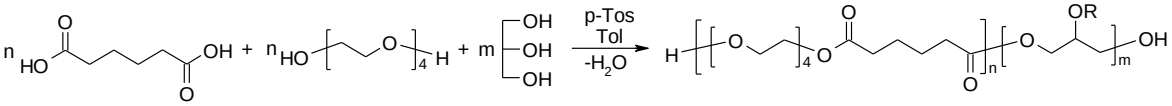

Scheme 3. Synthesis of a slightly branched polyester

To introduce polymerizable end groups the **slightly branched polyester** was converted with 1.2 eq (regarding the hydroxyl end groups) methacryloyl acid chloride with 2 eq triethyl amine as acid scavenger in DCM (Scheme 4). The methacrylate group modified polyester was purified by acid extraction and drying in vacuo.

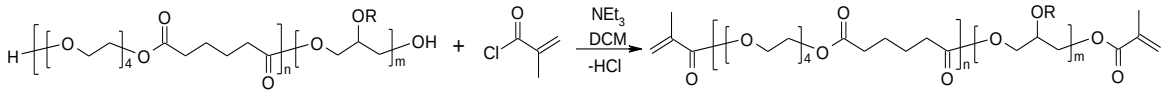

Scheme 4. Introduction of methacrylate groups

To simulate the network architecture of elastomers, the synthesized polyester methacrylat was combined with different monoacrylates (**HEMA**, **HEA**, **DPA**, **CEA**, **BEA** and **BA**, Figure 45) at different molar ratios (1, 5, 20, 50, 80% (n/n) of polyester methacrylate groups). The formulations also contained 1% (w/w) **BPO** as PI.

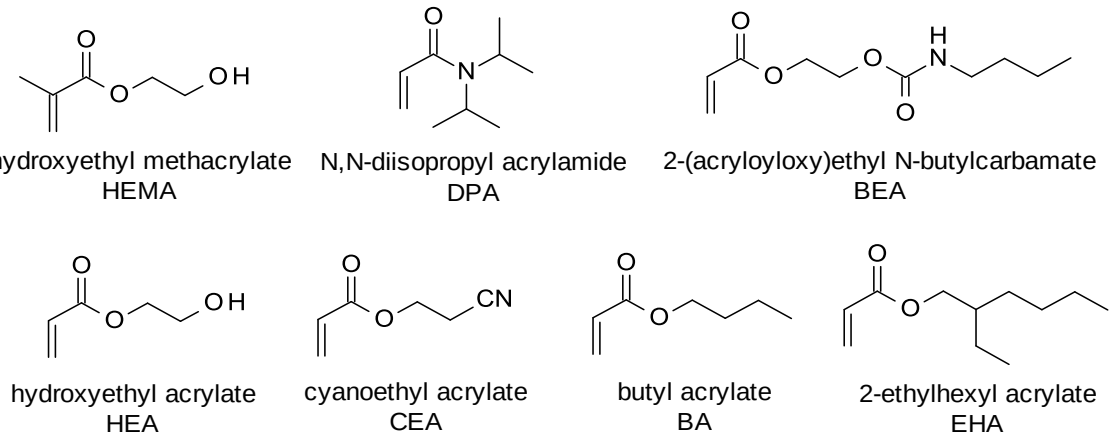

Figure 45. Frequently used mono(meth)acrylates

The formulations were cured as described above and tested manually. The best results after all could be obtained with rather high ratios of the polyester methacrylate (50, 80% (n/n)) with the monoacylates **HEA** and **CEA**. Samples of these formulations could be bent without tearing and elongated to a certain extent before breaking. However, none of the samples really had satisfactory mechanical properties and exhibited very brittle behavior. As already mentioned in the introduction, for technical applications often urethane based resins are used. The additional interaction of these groups improves the toughness of the materials. Different commercially available urethane acrylate resins were tested for their suitability for the desired application.

1.2.2. Urethane oligomer based photopolymers

1.2.2.1. Assessment of the base monomer

Three different commercial urethane acrylate monomers were examined in this study (Table 7).

Table 7. Base urethane acrylate monomers.

abbr.	*brand (company)*	*description*	*functionality*	*mol. wt. [g/mol]*
UMA	Genomer 4188/EHA (Rahn)	Urethane monoacrylate in 20% EHA	1[d]	-
UDA	Genomer 4215 (Rahn)	Aliphatic polyester urethane diacrylate	2[d]	1500[d]
UTA	Photomer 6210 (Cognis)	Aliphatic urethane acrylate oligomer	3[c]	1400[d]

[d] information from data sheets [290-292]

[c] calculated

The information from the data sheets were checked and complemented by the titration of the acrylate groups. A very fast and accurate method for that is the mercaptan method. The acrylates are converted with dodecyl mercaptan to the according Michael adduct (Scheme 5a) and the excess of dodecyl mercaptan is titrated with an iodine titer solution (Scheme 5b).

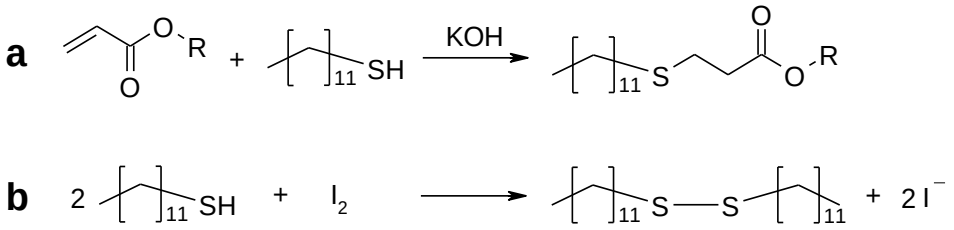

Scheme 5. Mercaptan method

Therefore about 1 g (with 1 mg accuracy) was dissolved in 50 mL 1:1 toluene/ethanol and treated with 20 mL of a solution of dodecyl mercaptan (5% (w/w) in ethanol) and 3 mL of an ethanolic solution of KOH (5% (w/w)) under nitrogen atmosphere for 5 min at r.t. under stirring. The acetatic solution was titrated with 0.1 M iodine titer solution with starch as indicator. The determinations were done in triplicates with parallel blank samples only containing the reagents without the monomers.
The double bond value (DB value, the amount of double bonds in [mol] per [g] monomer) was calculated according eq. 4.

$$DB\ value = \frac{1}{1000} \cdot \frac{f \cdot c}{m} \cdot (B - A) \tag{4}$$

A .....consumption for sample [mL]
B ..... consumption for blank [mL]
f ..... titer factor [ ]
c.....concentration of titer solution [mol/L]
DB value .....double bond value [mol/g]
m ..... weight [g]

The relationship between the molecular weight, the functionality and the DB value of the monomer is described by eq. 5.

$$M = \frac{n}{DB\ value} \tag{5}$$

M..... molecular weight [g/mol]
n ..... functionality [ ]

Table 8 sums up the results of the titrations.

Table 8. Results of double bond titration

Abbr.	*functionality*	*mol. wt. [g/mol]*
UMA	1	773±4*
UDA	2	1629±4
UTA	3	1429±3

* average mol.wt. of resin components

The urethane acrylate resins were cured in their pure form and as formulations with the monoacrylates **BEA**, **EHA**, **HEA** and **CEA** (Figure 45) with different molar ratios regarding the double bonds (1:1, 1:5, 1:10, 1:20). All formulations contained 1% (w/w) **BPO** as PI. The polymer samples were extracted in chloroform, methanol and distilled water for each 15 min in a supersonic bath and tested manually.
Samples from **UMA** exhibited high solvent uptake during the extraction due to the non-crosslinked polymer architecture and broke during this procedure. Polymers with **UTA**, however, were very brittle and could not be elongated without cracking. The best results were

obtained for **UDA**, especially in combination with **HEA**. Therefore **UDA** was selected as base monomer for all upcoming examinations.

1.2.2.2. Base monomer Genomer 4215

The commercial urethane diacrylate Genomer 4215 (**UDA**) was reported to have very low irritancy [293] and toxicity [290] (LD50 (oral, rat) > 5 g/kg). This especially makes it favorable for the application as a component for biophotopolymers. The exact composition of this resin, however, was still unknown. So, NMR examinations were conducted to reveal the structure.
Generally the structure determination of high molecular resins is rather complicated, but with the knowledge of the standard synthesis concept of polyester urethane diacrylates the determination could be simplified.
The synthesis of polyester urethane diacrylates is very similar to that of TPUs. The polyester prepolymer is either synthesized by a ring opening polymerization of lactones initiated by small diols like ethylene glycol or by an AABB polycondensation of diacids with diols with an excess of diol, because hydroxyl end groups are obligatory. The molecular weight of the prepolymer can be controlled by the ratio of the components. In the second step the macrodiol is converted into a macrodiisocyanate by the reaction with an excess of diisocyanate. Contrary to the chain extension with small diols in case of the TPUs and the high increase of molecular weight, the chain extension for diacrylates is done with HEA in the third step (Figure 46).

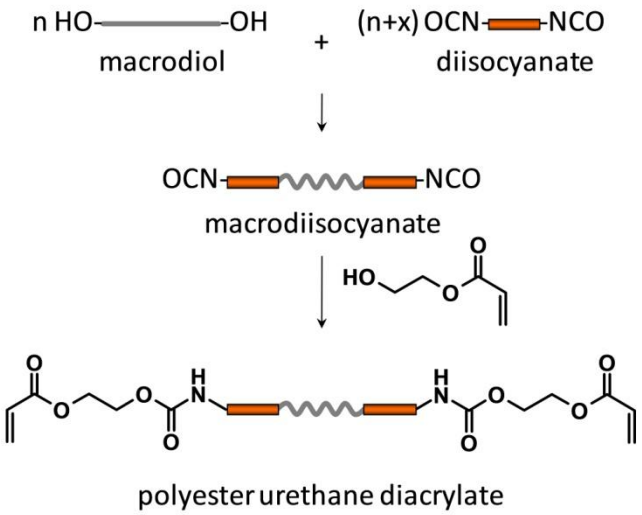

Figure 46. Synthesis of polyester urethane diacrylates

Keeping this is mind the ^{1}H-NMR (Figure 47) of Genomer 4215 can easily be interpreted.

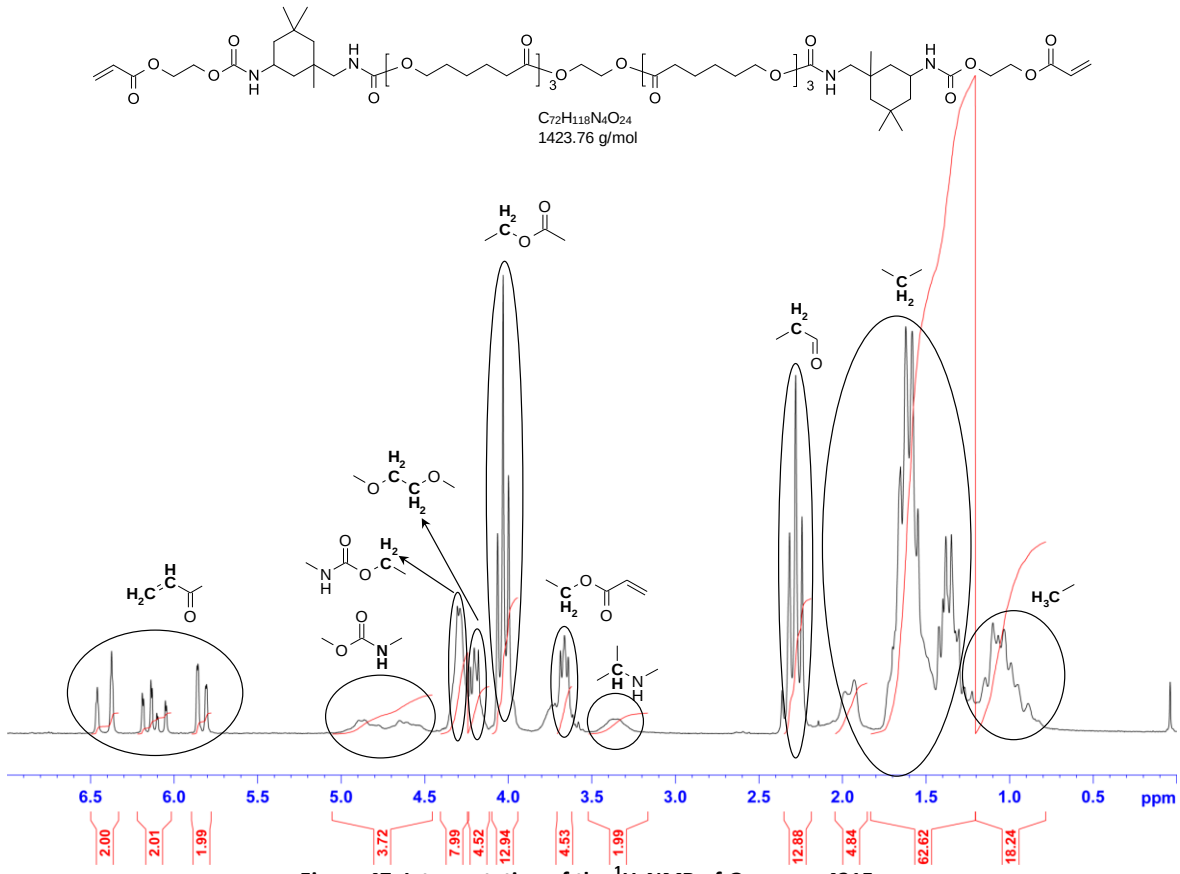

Figure 47. Interpretation of the ^{1}H-NMR of Genomer 4215

The peaks on the high shift end of course belong to the terminating acrylate groups. The characteristic peaks at 1.0 ppm indicate isophorone diisocyanate as diisocyanate component of the resin. The rather broad peaks at about 4.7 and 3.3 ppm correspond to the two different NH groups of the urethanes. From the ratio of the high and low shifted CH_2 groups at about 1.6, 2.3 and 4.0 ppm it can be derived that **PCL** was used as prepolymer. From the ratio of the CH_2 groups belonging to **PCL** and the acrylate end groups it can be derived that in sum there are about 6 units of caprolactone. The remaining CH_2 peaks belong to the initiating diol (properly ethylene glycol) and to **HEA**. The constructed molecule also shown in Figure 47 has a molecular weight of about 1500 g/mol which is in good compliance with the information from the data sheet.
An important conclusion of this examination is that **UDA** itself already contains a degradable moiety and **PCL** is an approved material for biomedical application.[108] On the other hand isophorone diisocyanate is frequently used as diisocyanate component for biocompatible urethane materials.[229-231, 237, 243, 264]

1.2.2.3. Formulations with the monoacrylate HEA as reactive diluent

UDA in combination with **HEA** had the best mechanical properties in the first screening of different urethane acrylate base monomers and monoacrylates as reactive diluent. For this reason, this combination was examined in a wider context of testing. Again formulations with different molar ratios of these components (Table 9) were produced, also containing **BPO** as PI, and cured as described above. Tensile tests were performed to assess the elastic modulus (E), the tensile strength (S) and the elongation at break (ε_b). The results of these tests can be seen in Figure 48.

Table 9. Formulations of UDA and HEA

Formulation	***a***	***b***	***c***	***d***	***e***
X [a)]	*5*	*15*	*20*	*25*	*30*
n (UDA) [mmol]	37.58	20.07	16.27	13.69	11.81
n(HEA) [mmol]	375.8	602.0	651.0	684.4	708.6
% (w/w) (UDA)	56.4	30.1	24.4	20.5	17.7
% (w/w) (HEA)	43.6	69.9	75.6	79.5	82.3

[a)] molar ratio of double bonds in HEA:UDA

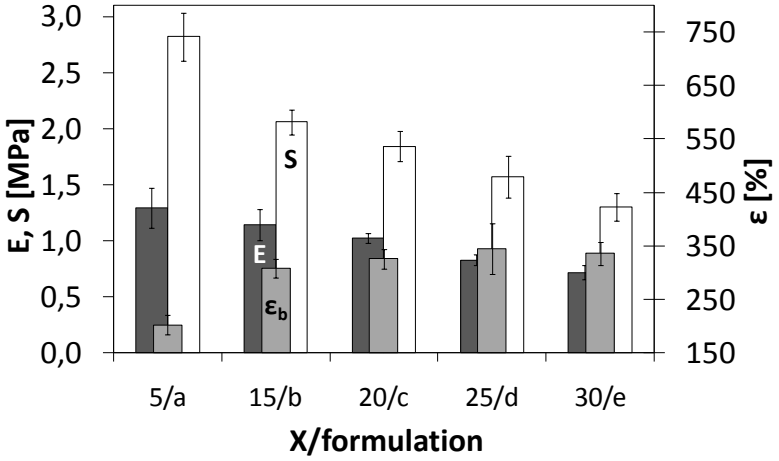

Figure 48. Mechanical properties of photopolymers of UDA with HEA

The mechanical properties of the photoelastomers within this series change in a very traceable manner. The network density is decreased from formulation a to e as crosslinks are removed by the addition of more monoacrylate (Figure 49).

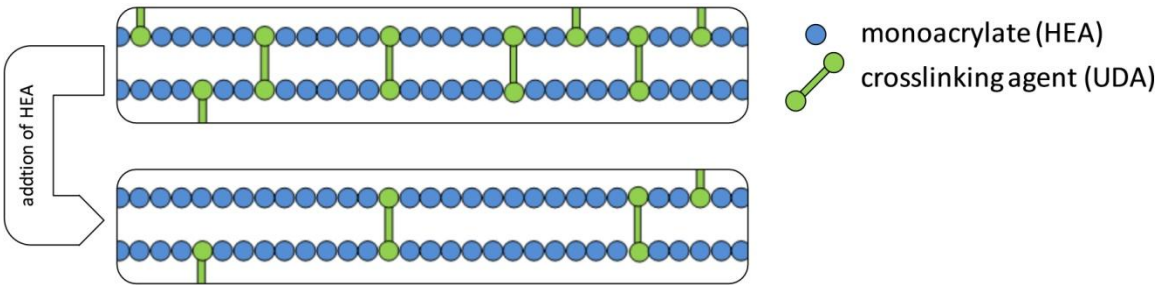

Figure 49. Decrease of the network density by addition of monoacrylate

Therefore S as well as E are decreased. ε_b, however, is increased. Formulation ***b*** is in best compliance with the mechanical properties of native blood vessels.

But the loading situation of the tensile test is quite idealized and especially crosslinked polymer systems are known to be very sensitive to cracks.[294] This might be a chief disadvantage as the artificial graft will be sutured during transplantation. So, there is a special mechanical loading situation at the junction site of the grafts. To simulate this situation, also suture tear resistance tests were carried out. To assess the suture tear resistance of the photopolymers, molded specimens (2x10x20 mm^3) were cut in the half with a knife (to avoid edge effects), provided with a seam of surgical suture by the aid of a special gauge (seam distance 4 mm from the edge), clasped into a modified tensile testing arrangement (Figure 50) and loaded with a speed of 50 mm/min. A very similar method was also applied by Mine *et al.*[295] A typical curve of the tear resistance test is shown in Figure 51. In the initial phase – at low elongations – only elastic/reversible deformations occur. At higher elongations cracks appear and propagate to the final tearing event.

Figure 50. Tear resistance test method

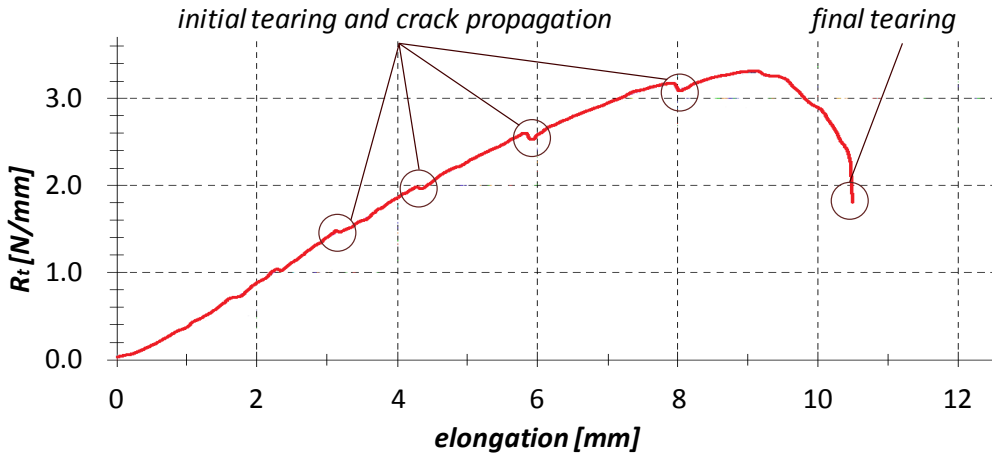

Figure 51. Typical curve of a suture tear resistance test

The suture tear resistance is calculated according to eq. 6.

$$R_t = \frac{F}{d} \tag{6}$$

R_t ..... suture tear resistance [N/mm]
F ..... peak force [N]
d ..... depth of specimen [d]

The suture tear resistance tests were also conducted with porcine coronary arteries as reference. As suspected the suture tear resistance of the highly crosslinked photopolymer from formulation ***b*** is very low (R_t = 0.72±0.15 N/mm) compared to those of native material (R_t = 2.75±0.53 N/mm). Hence, concepts have to be found to decrease the crosslink density without just increasing the monoacrylate, because the neat acrylate polymer backbone in materials causes very brittle material behavior.

1.2.2.4. The thiol-ene concept

In a previous paper it was described that the combination of urethane based monomers with thiols contributes to materials with high elongations and toughness [296]. Hence, the thiol-ene concept was also integrated in this study. Contrary to classical chain growth mechanism of the radical polymerization thiol-ene systems exhibit a large portion of step-growth mechanism (Figure 52 right) and entirely different network structures are formed (Figure 52 left).[297, 298]

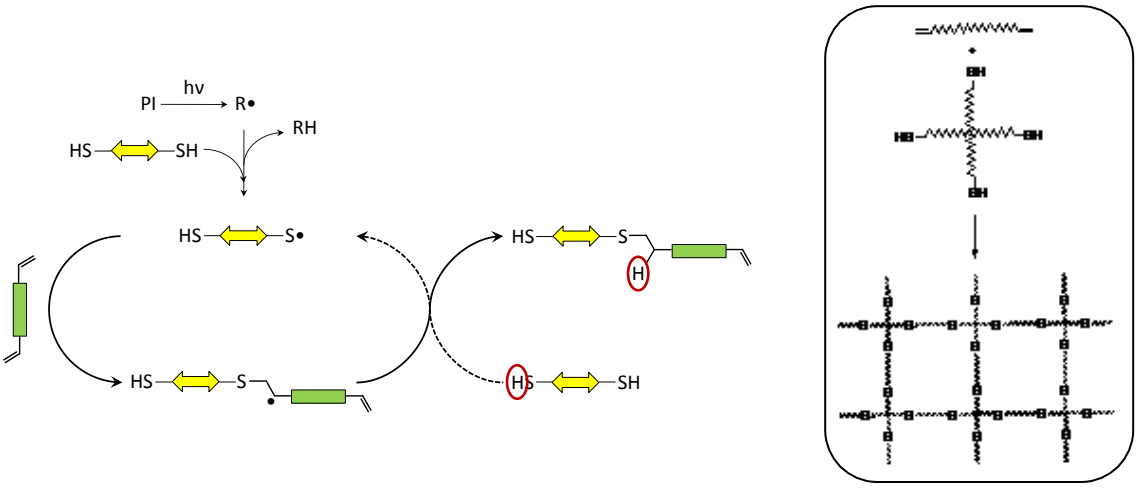

Figure 52. Thio-ene step growth mechanism (right) and network structure (left)

In this study two difunctional thiols were applied - 3,6-dioxa-1,8-octan-dithiol (**DOD**) [176] and ethylene glycol-bis-thiogycolate (**TGEG**, Figure 53)

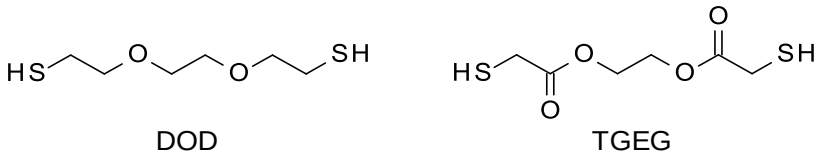

Figure 53. Dithiols as chain transfer agents

DOD was taken for the first experiments. For further investigations **TGEG** was used. The two cleavable bonds of the molecule should introduce degradability in the photopolymers.

1.2.2.4.1. Low thiol concentrations

Again formulations containing **UDA** and **HEA** were used and all tests were done as described above but this time the formulations also contained increasing amount of the CTA **DOD** (Table 10). The results of the tensile tests can be seen in Figure 54.

Table 10. Formulations with DOD.

Formulation[b]	***f***	***g***	***h***	***i***
Y[c]	*128*	*64*	*32*	*21*
n (UDA) [mmol]	19.88	19.71	19.36	19.02
n(HEA) [mmol]	596.5	591.2	580.7	570.7
n(DOD) [mmol]	4.97	9.85	19.36	28.53
% (w/w) (H1)	29.8	29.6	29.0	28.5
% (w/w) (HEA)	69.3	68.6	67.4	66.3
% (w/w) (DOD)	0.9	1.8	3.5	5.2

[b] Formulation b with a ratio of functional groups in HEA to UDA of 15 was taken as basis.

[c] Molar ratio of double bonds to thiol groups in the resin.

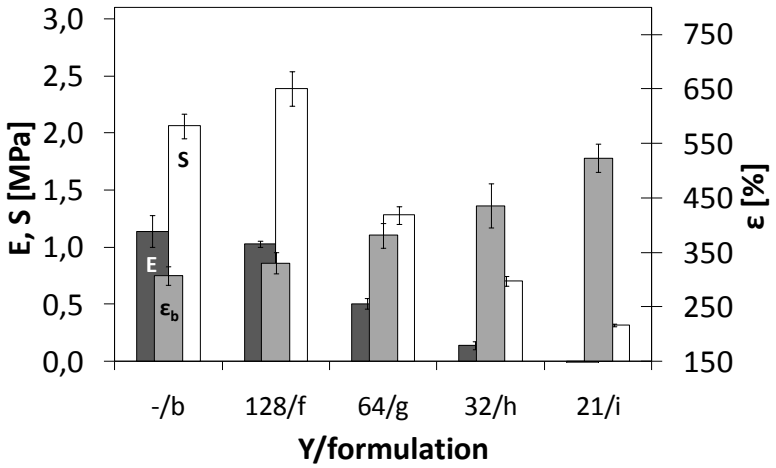

Figure 54. Mechanical properties of photopolymers of UDA with HEA and DOD

The mechanical properties of the photoelastomers also change in a very traceable manner within this series. However, in this case the decrease of strength and modulus and the increase of ultimate strain, respectively, can be attributed to the decreased chain length of the backbone of the photoelastomers (Figure 55).

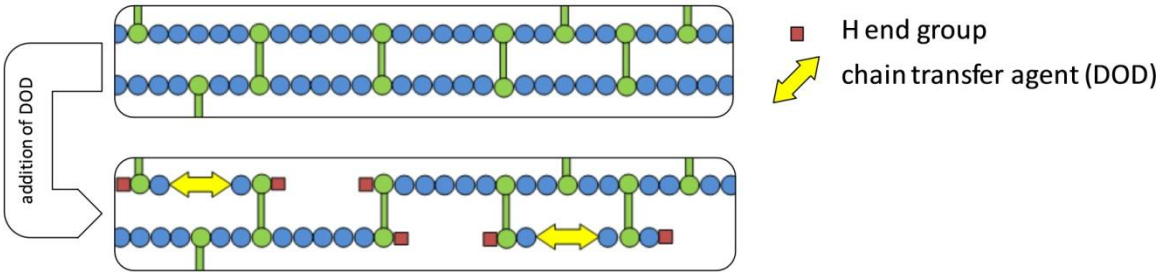

Figure 55. Decrease of the acrylate backbone length by addition of chain transfer agent

At a certain molar ratio Y of double bonds to thiol groups in the resin the mechanical properties drop dramatically. In this context it has to be considered that only 1 of 16 double bonds belongs to the diacrylate **UDA** (derived from the ratio of functional groups in **HEA** to **UDA** of 15). This means if the content of dithiol is increased (which is equivalent to a decrease of Y) and therefore more and more H end groups are introduced the backbone of the polyacrylate becomes shorter and shorter. However, if Y would be decreased to values below 16 the probability of the incorporation of a double bond belonging to UDA drops beneath 1, which means that low molecular weight blocks are formed without any links to the network. These obtained oligomers have only poor material properties. On the other hand, the high content of **HEA** causes a very high water-uptake of the material which corrupts the material properties additionally. Hence, to overcome these problems the content of diacrylate has to be increased. Such experiments are described in the next chapter.

1.2.2.4.2. High thiol concentrations

The emphasis of the previous experiments was that both, the ratio of the total double bonds and the thiols as well as the ratio of double bonds of the diarylate, have to be taken into account. By using diacrylates (DA) and dithiols as chain transfer agents (CTA) with a small amount of monoacrylate (MA) as reactive diluent with a molar ratio of diacrylate:dithiol near to but >1, almost linear, slightly branched but hardly crosslinked photopolymers with short oligo(acrylate) blocks are obtained. The idealized network architecture can be described by the statistical block length (L, eq. 7) and the DA content (R, eq. 8), the average number of diacrylates within these blocks.

$$L = \frac{mol\ MA + 2 \cdot mol\ DA}{2 \cdot mol\ CTA} \quad (7)$$

$$R = \frac{mol\ DA}{mol\ CTA} \quad (8)$$

These polymers have very similar architecture as elastomers and should therefore have ideal mechanical properties for the intended application. Degradability of these photopolymers can either be introduced by cleavable bonds in the spacer of the DA and/or in the CTA.[176] The DA used in this study already contains a degradable moiety – **UDA** was synthesized out of the prepolymer **PCL**. However, **PCL** degrades with a rather low rate. Therefore the CTA **DOD** was exchange by **EGTG**. The incorporation of the additional well cleavable bonds into the acrylate backbone of the polymers should enhance the degradability considerably.

A practical complication, however, by using very high amounts of thiols in these acrylate based formulation is the premature gelation of the resin due to the high reactivity of the thiol-ene system towards spontaneously formed radicals. Therefore also a stabilizer has to be added to the formulations. 1,2-Dihydroxy-4-tert-butylbenzene (DBB) inhibits radical polymerizations and therefore improves the storage stability of thiol-ene formulations.[299] The monomer formulations always had a composition following the code CTA:MA:DA which is the molar ratio of chain transfer agent, monoacrylate and the diacrylate. Since both CTA and DA within this study are difunctional the ratio of the reactive groups is 2·CTA:MA:2·DA. The monomer formulations always contained 1% (w/w) PI **BPO** and 1% (w/w) stabilizer DBB. The composition of the monomer system **EGTG/HEA/UDA** was varied to assess the optimal ratio and to see the limits of the thiol-ene system (Table 11). Three by three different formulations with different block lengths L and DA contents R were prepared. The block length was kept constant while the content of DA was increased and therefore the number of branches and crosslinks were also raised.

The characterization of the material properties ε_b, E and S have been performed using a tensile testing machine (Zwick, Z050). For preparation of the specimen the formulation was poured into a silicon mold and then cured as described above. The cured plates were used for punching out the dog-bone specimens. The extraction process were carried out just before punching out the specimens to guarantee the precise measurements as the material swells while taking up a small amount of water. Due to the soft material the tensile tests were performed without way transducer to prevent a predetermined breaking point. ε was analyzed by the change of cross-beam travel. S was determined from the peak force.

The tensile behavior and the results of the suture tear resistance tests of the monomer system **EGTG/HEA/UDA** are displayed in Figure 56 and Figure 57.

Table 11. EGTG/HEA/UDA formulations

	low block length (L = 2)		*med. block length (L = 5)*		*high block length (L = 21)*	
low DA content	***j***	1 : 2 : 1 (R = 1.00)	***m***	1 : 8 : 1 (R = 1.00)	***p***	1 : 40 : 1 (R = 1.00)
med. DA content	***k***	1 : 1.8 : 1.1 (R = 1.10)	***n***	1 : 7.2 : 1.4 (R = 1.40)	***q***	1 : 38 : 2 (R = 2.00)
high DA content	***l***	1 : 1.6 : 1.2 (R = 1.20)	***o***	1 : 6.4 : 1.8 (R = 1.80)	***r***	1 : 34 : 4 (R = 4.00)

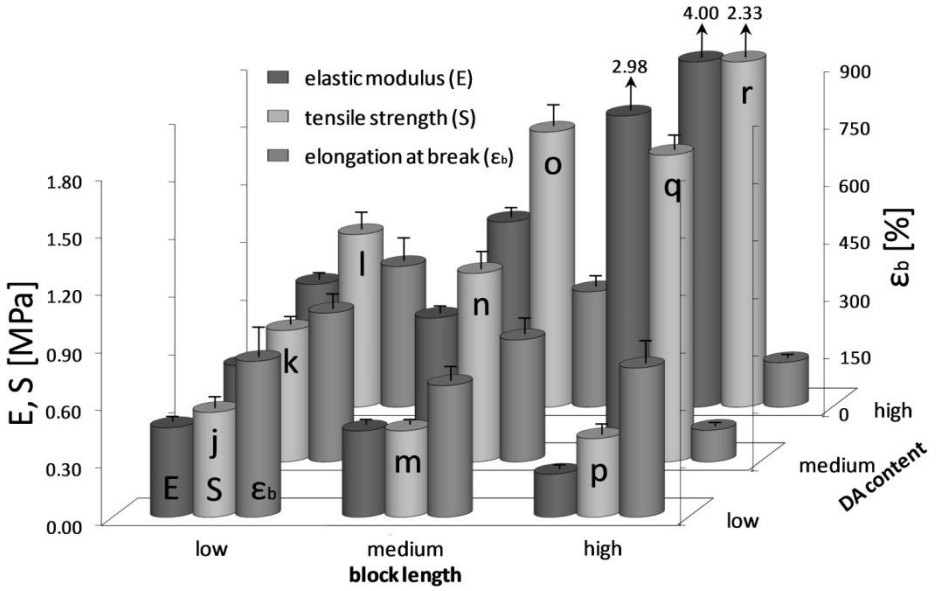

Figure 56. Tensile behavior of the formulations with UDA, HEA and EGTG

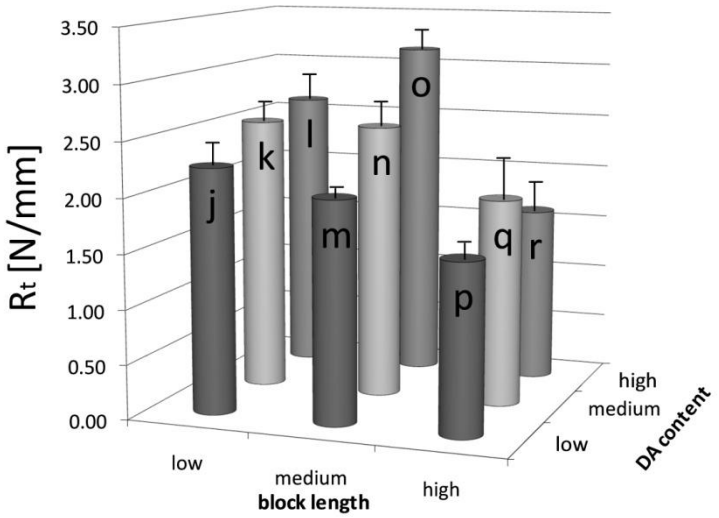

Figure 57. Suture tear resistance of the formulations with UDA, HEA and EGTG

Certain trends were observed. Increasing the DA content R at a constant block length L in case of the sample set ***j***⇨***k***⇨***l*** leads to an increase of E, S and R_t. The same trend with an even higher significance was observed for the sample set ***m***⇨***n***⇨***o***. This is due to the increase of the quantity of branches, crosslinks and the number of possible hydrogen bonds, respectively. Therefore the materials grow harder as also observed for classic, thiol-free systems.[131, 181] However, in case of the set ***p***⇨***q***⇨***r*** the medium and high R leads to the very brittle materials ***q*** and ***r*** with exceptional low ε as well as R_t and high E as well as S. It seems that certain ratios are beyond the application frame of thiol-ene chemistry and the characteristic network architecture cannot be formed sufficiently. This can be explained by homopolymerization of **HEA** [208] combined with a high crosslink density (R = 2, 4) that leads to brittle materials.
In the orthogonal direction the block length L is increased using a higher content of MA in the formulation (Figure 58). The sample set ***j***⇨***m***⇨***p*** exhibits a decrease of E, S and R_t with increasing L.

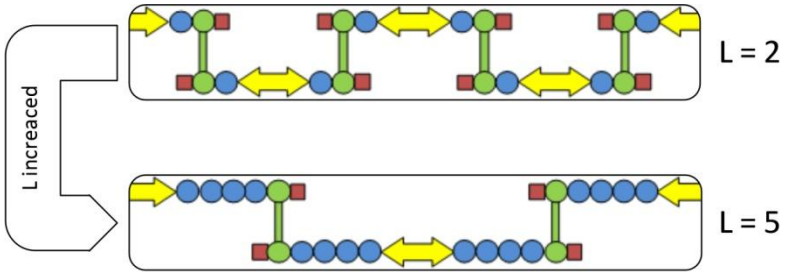

Figure 58. Idealized polymer architectures for R = 1

Beside the flexible prepolymer of **UDA**, the urethane groups of the spacer exhibit strong association tendency owing to hydrogen bonds. It is most likely that aggregates of two or more **UDA** molecules are already formed in the (non-cured) liquid state which is one reason for the high viscosity of the base resin. However, those aggregates also remain in the (cured) solid state and act like reversible crosslinks. This motif is also applied for thermoplastic urethane elastomers. Increasing the block length L at constant DA content R reduces the content of urethane groups of the polymer. This and the higher content of **HEA** that probably increases the water uptake leads to softer materials in case of the set ***j***⇨***m***⇨***p***.
However, this trend is unincisive or even reversed in case of the sample sets ***k***⇨***n***⇨***q*** and ***l***⇨***o***⇨***r***; ***q*** and ***r*** again have to be considered as outliners. This reversal trend can be attributed to the additional increase of the DA content R which seems to overcompensate the effect of the increase of the block length L.
The lower degree of crosslinking due to the addition of the dithiol and the concurrent high amount of **UDA** enable the emergence of the function of the urethane groups. The advantage of the reversible crosslinks formed by these urethane groups is that the network can be reorganized when strained and gliding of the polymer chains dissipates a large quantity of deformation energy. This effect enables the material to be tougher.[294] The classic system, only containing **UDA** and **HEA**, which was examined above has only values of R_t = 0.7 N/mm at relatively high moduli of E = 1.1 MPa. So, the thiol-ene concept proved to improve the material properties for the designated application.

1.2.2.5. Comparison with native material

Generally, it is only possible with limitations to reproduce the mechanical properties of the native, anisotropic composite material with an isotropic photopolymer.[169, 300] Blood vessels are fiber reinforced materials. The mechanical integrity of blood vessels is predicated on the tunica media [301] that is formed by the SMCs that sit in a matrix of structural proteins. The fibers are formed by the myofilaments of the SMC and elastin. The compliance of the elastic modulus is very important to avoid modulus mismatch at the anastomosis.

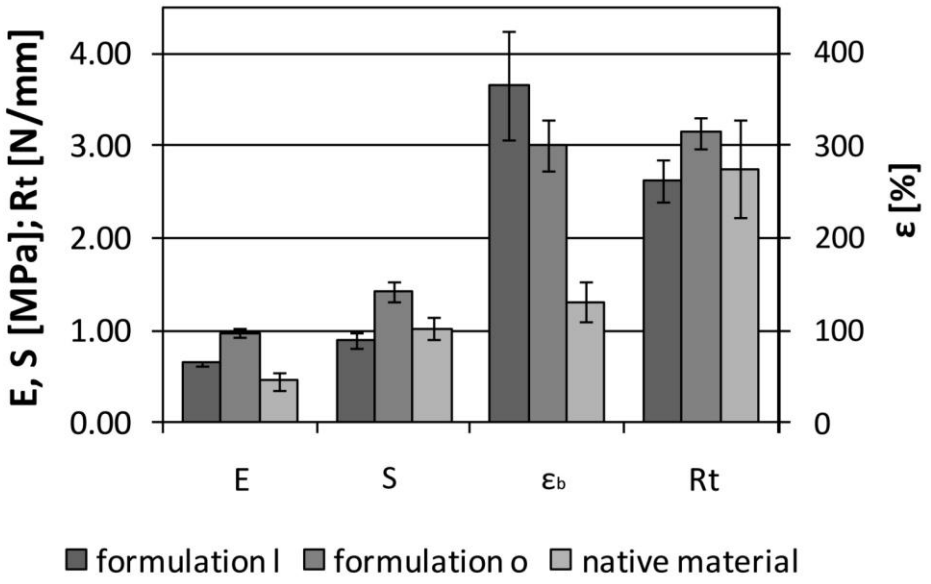

Figure 59. Comparison of the mechanical attributes of photopolymer and native material

The photopolymers of formulation ***l*** and ***o*** match well with native material concerning the elastic modulus, tensile strength as well as the suture tear resistance (Figure 59). The ultimate elongations, however, are about three times larger than those of blood vessels. This is due to the alignment of the fibers in case of the blood vessels and the subsequent progressive increase of the stress level. So, the tensile strength is already attained at relatively low elongations (Figure 60).

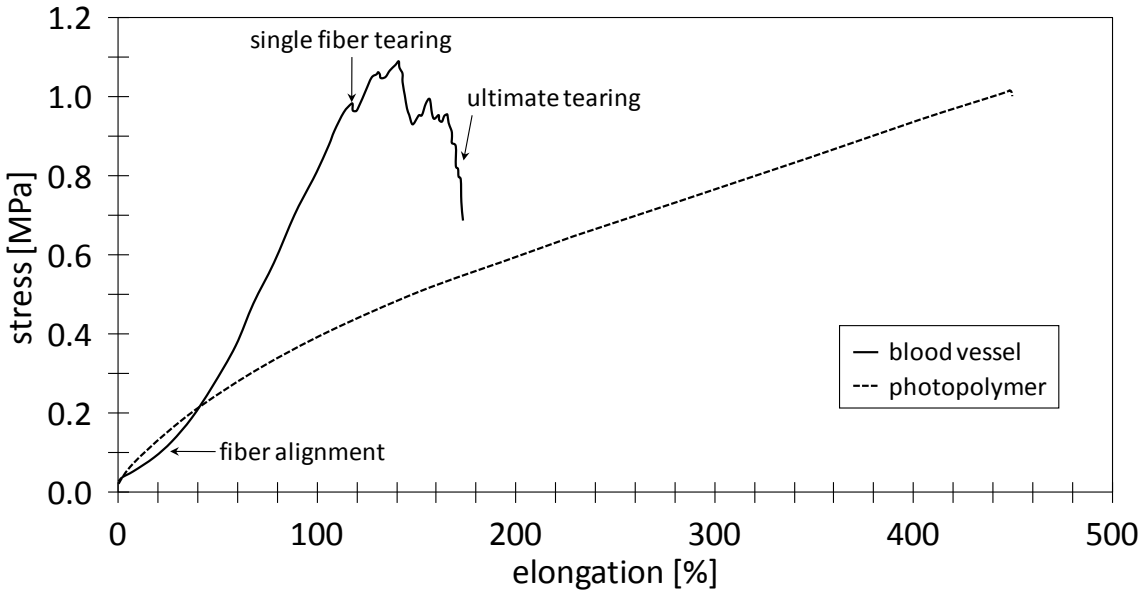

Figure 60. Tensile test curves of blood vessels and photopolymers

From classic engineering it is known that the circumferential stress σ_c within the walls of a hydrostatic pressure (p) loaded rotation-symmetric body with given inner diameter d and wall thickness s can be calculated by eq. 9.

$$\sigma_c = \frac{p \cdot d}{2 \cdot s} \tag{9}$$

To estimate the circumferential elongation ε_c the elastic modulus E can be introduce to obtain eq. 10.

$$\varepsilon_c = \frac{p \cdot d}{2 \cdot s \cdot E} \cdot 100\% \tag{10}$$

Considering the pressure conditions of the artery (d = 3 mm, s = 0.5 mm, E = 0.5 MPa) of a hypertonic patient (p = 180 mm Hg = 0.024 MPa) circumferential elongations of about 14% can be expected. In this physiologic range the photopolymers show a very good compliance.

1.2.2.6. Additive Manufacturing Technology: Digital Light Processing

To create artificial vascular grafts with a defined outer and inner structure it is necessary to apply powerful manufacture technologies. AM provides the technologies for this purpose. For this study the digital light processing (DLP) method was applied [178]. The photosensitive resin is irradiated from the bottom through the window of the reservoir according to the 2D information of the current slice as a thin layer beneath the already printed part or the substrate, respectively. This way the whole part is built up layer by layer (Figure 61).

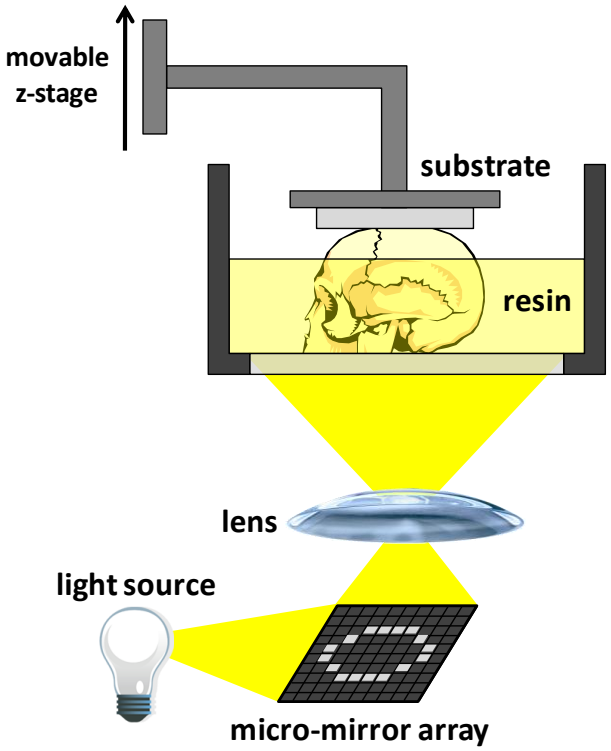

Figure 61. Principle of DLP

The applied device is a commercial system purchased from Envisiontech, type Perfactory® SXGA$^+$ Mini Multi Lens (Figure 62).

Figure 62. Envisiontech™ Perfactory® (www.envisiontec.de)

The optimization of the formulation to this point was focused only on aspects concerning the mechanical behavior of the photopolymers. However, it is also necessary to optimize the formulation for the additive manufacturing process where the viscosity is an important parameter. Commercial resin formulations for the DLP process have viscosities around 1 Pa·s [302] but resins with viscosities up to 5 Pa·s were also already successfully manufactured in a stereolithographic process.[303] Therefore we aim to have a viscosity between 1 and 5 Pa·s.
Photopolymers out of formulation ***l*** have excellent mechanical performance. The high viscosity of this formulation (about 60 Pa·s), however, makes it impossible to apply the designated additive manufacturing technique. To reduce the viscosity without changing the final mechanical properties significantly a higher content of reactive diluent and/or non-reactive diluent can be used.

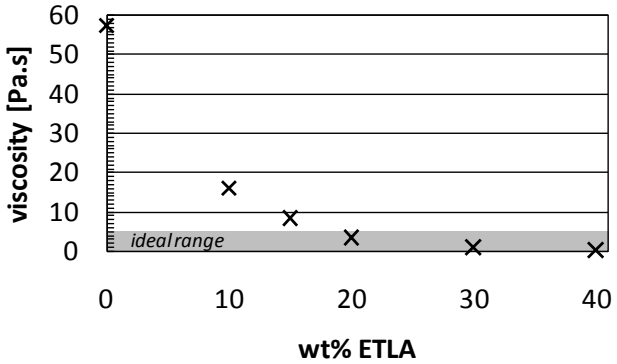

Figure 63. Dependence of the viscosity on the content of the solvent ETLA

The viscosity of formulation ***l*** decreases very fast if for example ethyl lactate (**ETLA**) is added (Figure 63). High solvent contents of **ETLA**, however, would lead to very fragile photopolymers which is critical for the additive manufacturing process and should therefore be avoided, although we have found that the mechanical properties recover after extraction. But, as the initial testing of the mechanical properties indicated that an increase of L and therefore a higher content of the low viscous **HEA** from formulation ***l*⇨*o*** had no disadvantageous effects on the mechanical properties we combined both thinning concepts and finally came to the slightly modified formulation ***j*** (Table 12). Formulation ***j*** corresponds to a ratio of 1:2.7:1.2 (**EGTG**/**HEA**/**UDA**, L = 2.6, R = 1.2) and has a viscosity of 3.3 Pa·s (20°C).

Table 12. Comparison of the optimized formulation (*s*) with the formulation (*l*) and (o)

	l	*o*	*s*	
EGTG	9.4	5.7	7.2	% (w/w)
HEA	8.3	19.9	10.9	
UDA	80.3	72.4	62.1	
ETLA	0.0	0.0	17.8	
BPO	1.0	1.0	1.0	
DBB	1.0	1.0	1.0	

In addition to viscosity the penetration depth of light is also an important AMT parameter. To limit the penetration and therefore increase the resolution in z-direction an absorber has to be added to the formulation. To determine the optimal concentration, penetration tests have to be performed. Therefore a transparency film was arranged at the window of the DLP device and small amounts of the resins with different concentrations of the commercial absorber CGL097 (Ciba SC, **ABS**) were exposed with different process parameters. The uncured resin was washed from the transparency film and the depth and quality of the cured circles was assessed.
In contrast to resins of hard and highly crosslinked photopolymers, resins of soft and more linear photopolymers need, despite comparable photoreactivities, longer gelation times to form layers of sufficient mechanical integrity. At a intensity of 750 mW/dm^2 and an absorber concentration of 0.25% (w/w) no sufficient gelation was observed even after 30 s of exposure. For high resolution building procedures low exposure times are necessary. Therefore the intensity was raised to 1000 mW/dm^2, which gave already good gelation after only 20 s. However, the penetration depth was over 200 µm. Hence the absorber concentration was increased to 0.5% (w/w), decreasing the penetration depth beneath 200 µm after 25 s of exposure. Using these optimized process parameters, a 3D cellular test structure was manufactured (Figure 64).

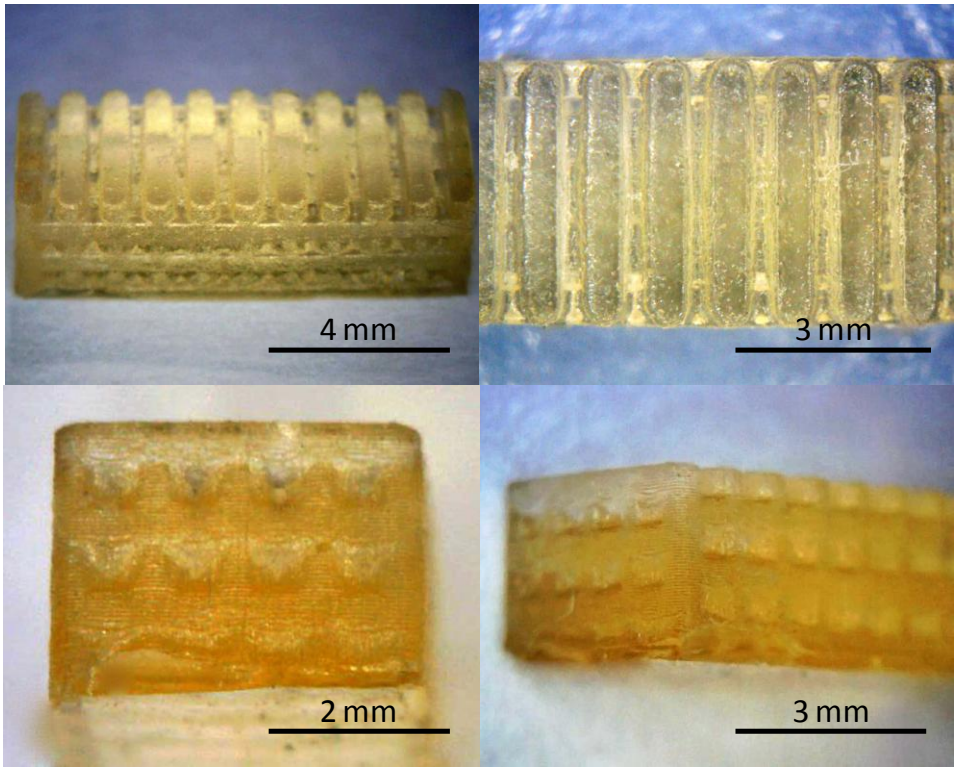

Figure 64. Images of the test structure (cross structure)

The basic structure of the cellular cross structure is represented in a sufficient quality in this manufactured part; however, there was still room for optimization. Therefore the PI system as

well as the concentration of the stabilizer, which of course decrease the reactivity of the formulation, was reconsidered.
For that, the PI **BPO** was combined with the Type I PI system of an equimolar mixture of camphorquinone (**CQ**) and N,N-dimethylaminobenzoic acid ethyl ester (**DMAB**) in the ratio 1:1 (w/w) (Table 13) and the penetration tests were repeated. All formulations again contained 0.5% (w/w) of the absorber **ABS**.

Table 13. Penetration depths [µm] for formulation s with different PI systems at different exposure times

	exposure time [s]					
formulation	***5***	***10***	***15***	***20***	***25***	***30***
s (1% (w/w) BPO)	-*	-*	110	160	180	240
s (BPO/CQ/DMAB (1%))	-*	-*	-*	30	30	60
s (BPO/CQ/DMAB (3%))	-*	-*	60	100	130	180
s (BPO/CQ/DMAB (5%))	-*	40	90	150	190	230

*insufficient polymerization

From the penetration test is can be seen, that using higher concentration of photo initiator the polymerized thickness of the specimen can be decreased. Figure 65 shows more structures of the optimized formulation at optimized process parameters.

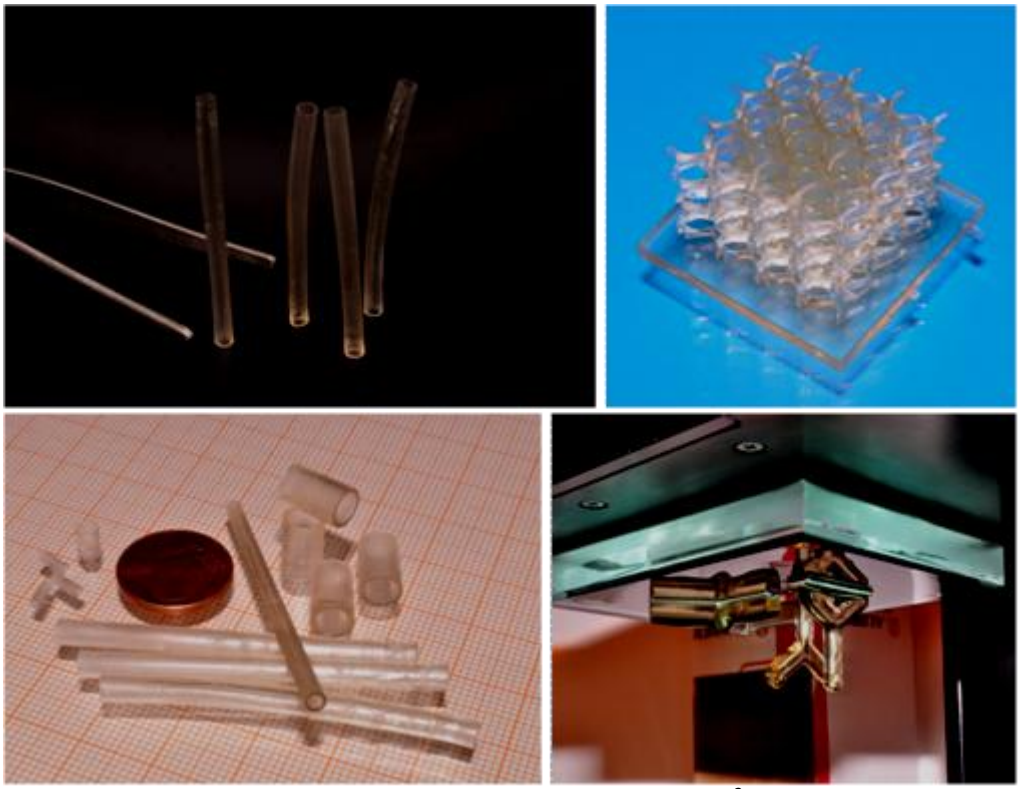

Figure 65. More test structures: 25 s exposure time, 1000 mW/dm^2, voxel depth 50 µm

1.2.2.7. Cellular compatibility

1.2.2.7.1. Cytotoxicity

To evaluate the cellular compatibility of the new photoelastomers it is necessary to assess the cytotoxicity of residual components of the formulation as well as the degradation products.
The degradation products were tested on one hand as a concentrated solution of a degradation experiment (**DG**) and on the other hand as solution of defined substances assumed to be formed during degradation (Figure 66).

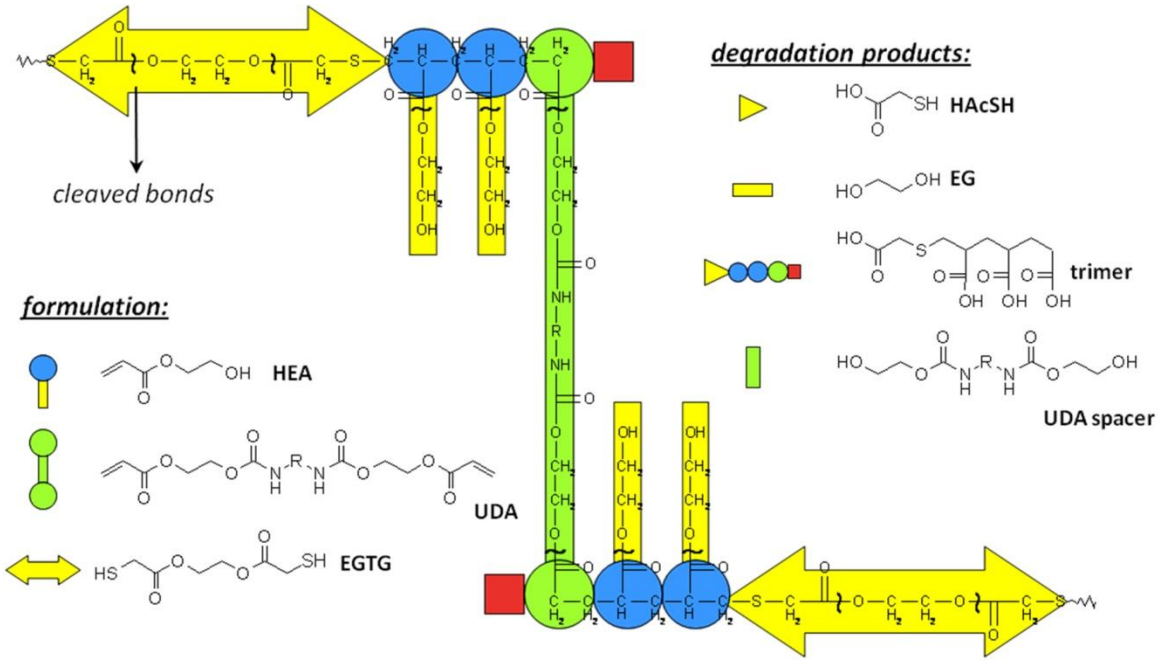

Figure 66. Substances for the cytotoxicity tests

The **trimer** was prepared by the idealized photoreaction of thioglycolic acid (HAcSH) with 3 eq. acrylic acid (**AA**) with **BPO** as PI (Scheme 6).

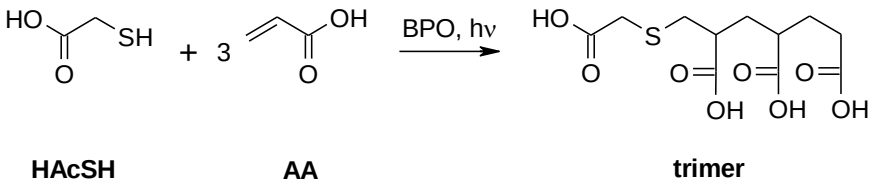

Scheme 6. Synthesis of the trimer

The **UDA spacer** was obtained by the alkaline hydrolysis of **UDA** and subsequent extraction. The NMR spectra confirm the successful cleavage and removal of the acrylate groups while the signals of the spacer remained nearly unaffected (Figure 67).

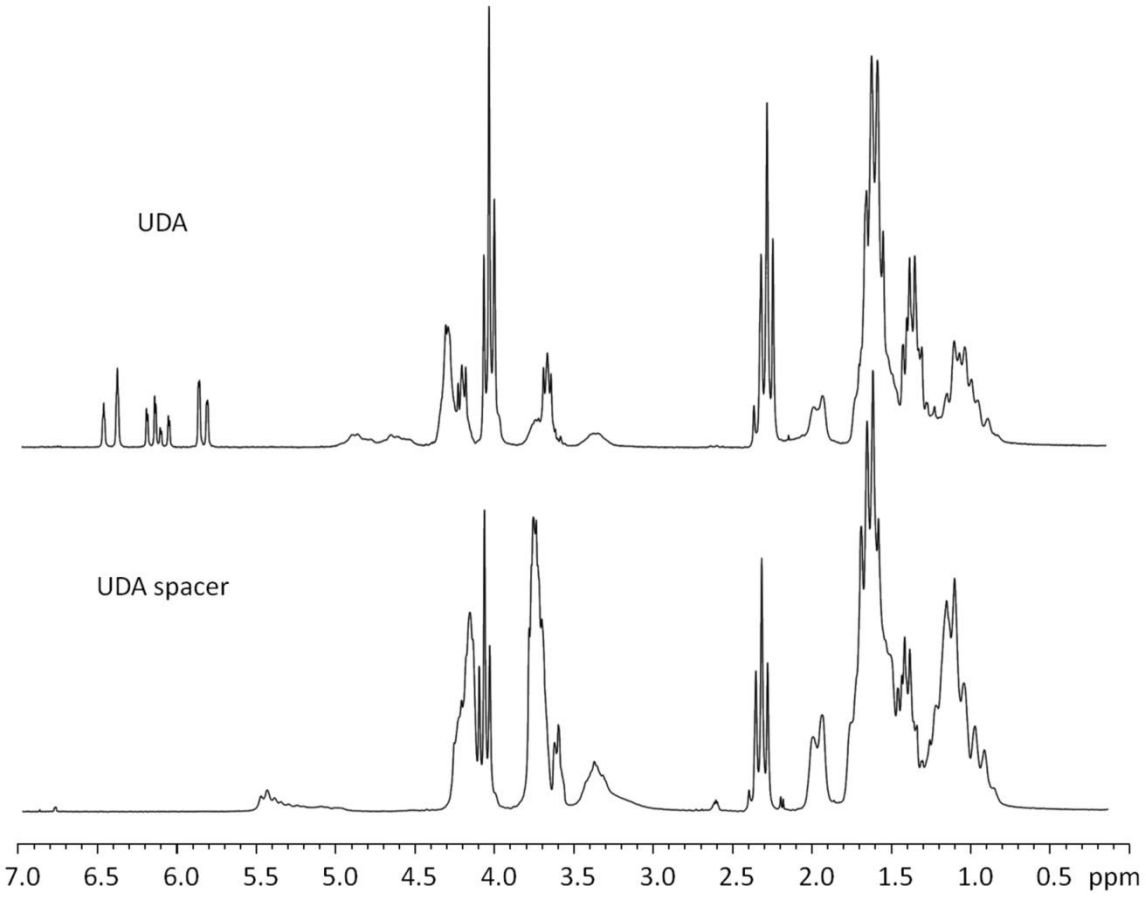

Figure 67. 1H-NMR spectra of the UDA and the UDA spacer in CDCl3/d6-DMSO

Stock solutions of every single substance (**HEA, UDA, EGTG, ETLA, HAcSH, EG, trimer and UDA spacer**) in DMSO with concentrations of 1 mmol/mL (≡ 1 M) were produced (in case of **UDA** and **UDA spacer** only concentrations of 0.1 mM were possible). HUVECs were cultured, proliferated on plastic coverslips and treated with increasing concentrations (10, 50, 100 and 1000 µM) of the examined substances from dilution series. The viability of the cells was assessed by a formazan based assay after 24 h of proliferation at 37°C. For reference blank samples only containing the same amount of DMSO were performed.

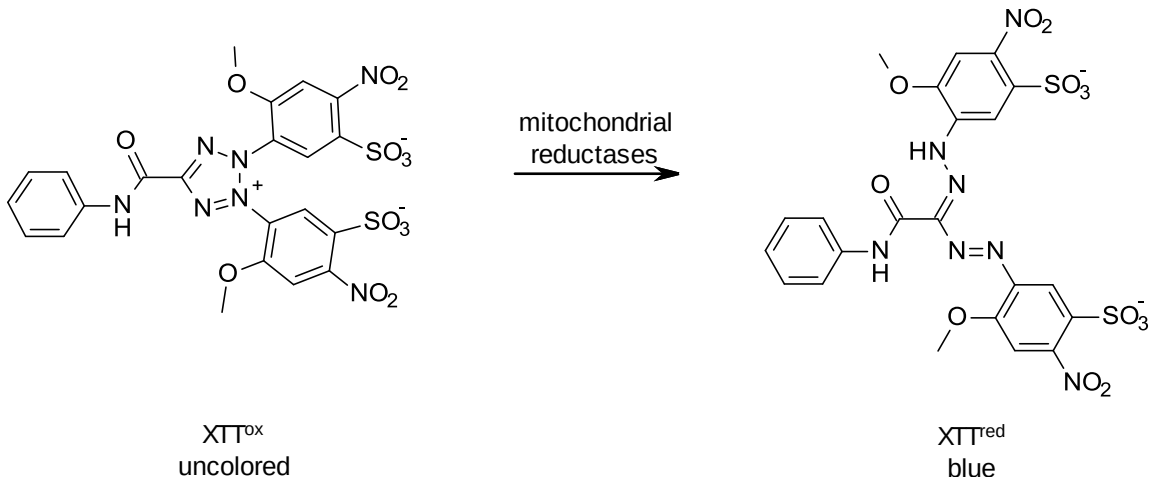

Scheme 7. XTT reduction

The non-radioactive cell proliferation and toxicity assay was developed by Biomedica Vienna [304] and works with the sodium salt of (2,3-bis-(2-methoxy-4-nitro-5-sulfophenyl)-2H-tetrazolium-5-

carboxanilide) (XTT, Scheme 7). XTT is reduced by reductases of the mitochrondrium of viable cells only and the intensely colored formazan derivative is formed which can be quantified by means of photometric measurements at 450 nm. The absorbance at 450 nm is directly related to the cell viability.
The cytotoxic concentration of the substances (c_{tox}) was defined as the concentration, the viability of the cells dropped significantly. Table 14 gives an overview of the obtained results.

Table 14. Cytotoxic concentration of resin components and degradation products

substance	c_{tox} *[µM]*
HEA	50
UDA	50
EGTG	-*
ETLA	-*
HAcSH	-*
EG	-*
trimer	-*
UDA spacer	50

* no cytotoxicity observed

It was expected that the acrylates (**HEA** and **UDA**) have a significant cytotoxicity, however it can be assumed that concentrations of 50 µM will not be attained by the release of the monomers after the vigorous extraction procedure. All other components/degradation products with the exception of the **UDA spacer** showed no cytotoxic effects at test conditions. However, due to the high molecular weight of the **UDA spacer** and its relative poor solubility in water it is also not expected that the cytotoxic concentration will be reached during degradation.
To test possible toxicologic interactions the substances, the extract of a real degradation experiment (**DG**) was tested for cytotoxicity, too. No toxic effects were observed.

1.2.2.7.2. Cell adhesion/proliferation
The photopolymer test specimens had a disc-like shape with a diameter of 13 mm and a thickness of about 1 mm – fitting perfect into a 24 well plate. To manufacture these specimens the resin was cured in teflon molds according the procedure already described for the mechanical tests. After demolding, the specimens were extracted to remove residual monomer and solvent. Therefore, the material was placed into methanol and water each thrice overnight.
HUVECs ($4{\cdot}10^4$ cells/cm^2) were either seeded onto cell-culture treated Thermanox™ plastic coverslips (Nunc, Rochester, NY, USA) precoated with a 1% (w/v) solution of bovine gelatin (Sigma, St. Louis, USA) or onto the disc-shaped polymeric test specimens. Cells were kept under static conditions in a humidified incubator (37°C, 5% CO_2) for 24h. The specimens were removed from the well plate and carefully prepared for SEM imaging. Figure 68 shows representive SEM images cell seeded surface of both coverslip control and photopolymer. The attached cells exhibit by the typical cobblestone-like morphology of EC.

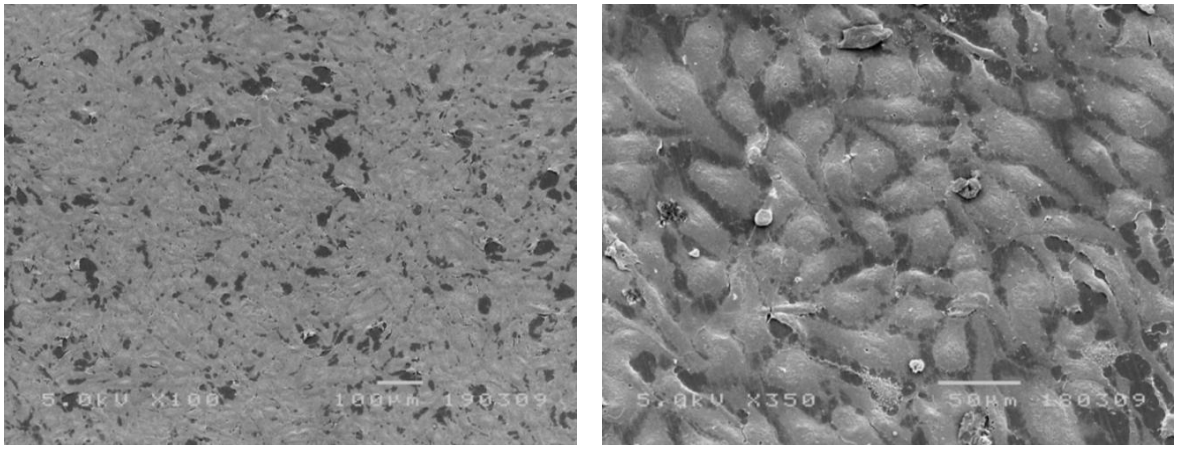

Figure 68. Cell adhesion of HUVECS: coverslip control (left), photopolymer (right)

1.2.2.8. Degradability

The degradation of artificial biomaterials for tissue regeneration is a crucial point in the regeneration of native tissue. By incorporation of cleavable bonds into the polymer backbone we aimed to introduce degradability of the photopolymers. Degradation tests were performed in phosphate buffered saline solution (PBS) at different temperatures and mass loss as well as water uptake were assessed after certain periods of degradation. The end point of every experiment was defined as the point when the specimens totally fell apart. Figure 69 (left) depicts the mass loss curves of the photopolymers during the degradation test at the different temperatures. As it can be seen, the degradation is heavily influenced by the temperature. At 110°C the end point was already observed after a mass loss of about 30%. However, in every case there was a residue that turned out to be non-degradable which was identified in ^{1}H-NMR experiments as nearly exclusive the spacer of **UDA**.

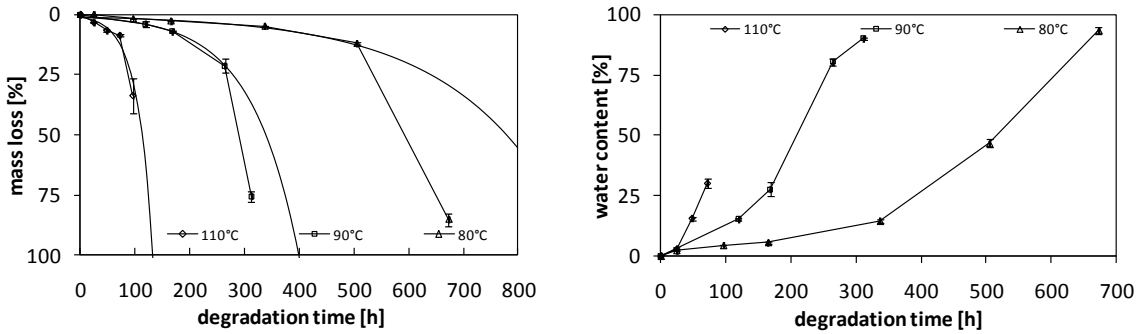

Figure 69. Mass loss curves with exponential trend lines (left) and water content curves (right) of the polymers of formulation s during degradation

The degradation involves swelling of the polymer specimens (Figure 70). The water content curves have a very similar shape as the degradation curves (Figure 69, right), although the water content curve for 90°C indicates a sigmoidal trace that reflects the reality better.

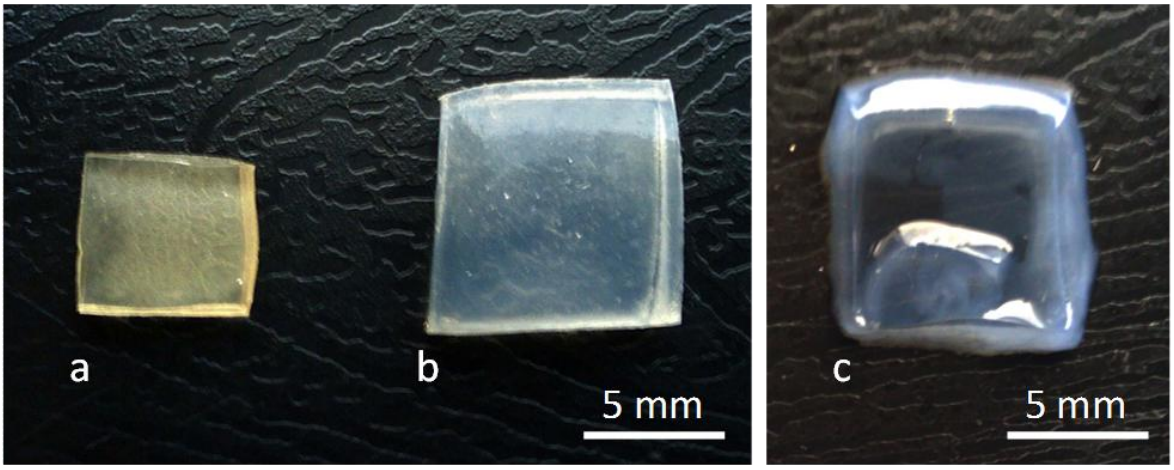

Figure 70. Specimen after degradation for a period of (a) 5 d, (b) 11 d and (c) 13 d at 90°C

The progressive degradation curves indicate a bulk erosion mechanism [107, 305]. The curves, however, do not have an exponential but an even steeper trace (Figure 69). This observation might be attributed to several effects. First of all the mass loss is a very convenient but complicated monitoring parameter as the progressive hydrolysis of the ester bonds of the polymer network does not reflect in the erosion. In the initial phase of degradation cleaving single bonds at different sites of the network does not lead to any mass loss. The mass of the network will not decrease before the fragments are small enough to be washed away. But as soon as the molecular weight of the cleavage products drops beneath a certain level the mass loss increases dramatically. Another effect is the change-over of the velocity determining steps. In the initial phase the velocity of hydrolysis is determined by the (slow) diffusion of water into the network. As soon as the network is interspersed with water the hydrolysis rate grows fast.

It can be concluded intermediately that photopolymers with well considered polymer architecture can be tailored to comply with the mechanical requirements for vascular tissue regeneration. The developed materials also possess sufficient suture tear resistance and endothelial cells readily attach to the surface. The photopolymers degrade in a manner which is very similar to surgical **PLA** and there are no toxic products released. Finally the photopolymers can be manufactured by DLP to fabricate cellular scaffolds for tissue engineering.

2. Thermoplastic urethane elastomers

2.1. General considerations for the synthesis of TPUs

The synthesis of thermoplastic urethane elastomers is a polyaddition between diols (A) and diisocyanates (B). For all polyadditions, Carothers law (eq. 11) is valid.

$$\overline{P_n} = \frac{1+q}{1+q-2qp} \tag{11}$$

$$q = \frac{n_A}{n_B} \tag{12}$$

$$p = \frac{n_0 - n}{n_0} \tag{13}$$

$\overline{P_n}$.....degree of polymerization [ ]
q .....ratio of reactive groups (q ≤ 1)[ ]
p .....conversion [ ]
n_A .....amount of substance A [mol]
n_B ..... amount of substance B [mol]

In the stoichiometric case (q = 1) eq 13 simplifies to eq. 14. A plot of eq. 14 can be seen in Figure 71.

$$\overline{P_n} = \frac{1}{1-p} \tag{14}$$

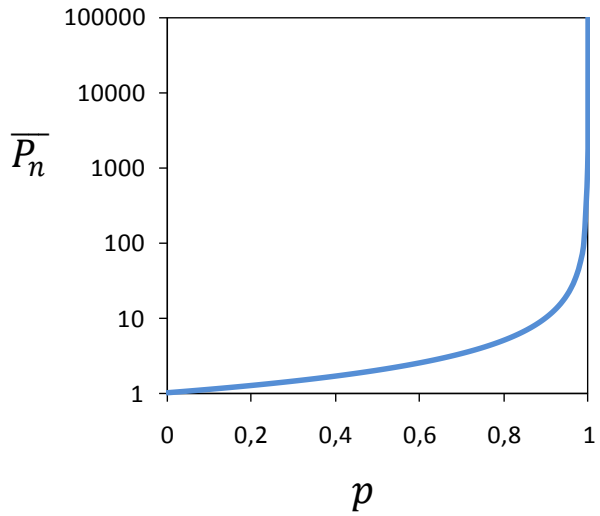

Figure 71. Dependency of the degree of polymerization $\overline{P_n}$ on the conversion p (q = 1)

A very similar relation is obtained for complete conversion (p = 1) (eq. 15).

$$\overline{P_n} = \frac{1+q}{1-q} \tag{15}$$

To obtain high degrees of polymerization and molecular weights, respectively, it is necessary to have both p and q near to 1. This means one needs very good conversions and stoichiometric reaction conditions. The purity of the starting materials therefore is crucial.
In case of polyurethanes the absence of water is particularly important, because water reacts with isocyanates and the non-stable carbamide acid that form can decompose to the corresponding amine and carbon dioxide. The amine again reacts with the isocyanates to form ureas (Scheme 8). This means 1 mole of water consumes 2 moles of isocyanates and therefore q is decreased which

has a large impact on the molecular weight of the obtained polymers. While undesired in our case, industrially this reaction is used in the formation of polyurethane foams (by volume the most important application for polyurethanes).

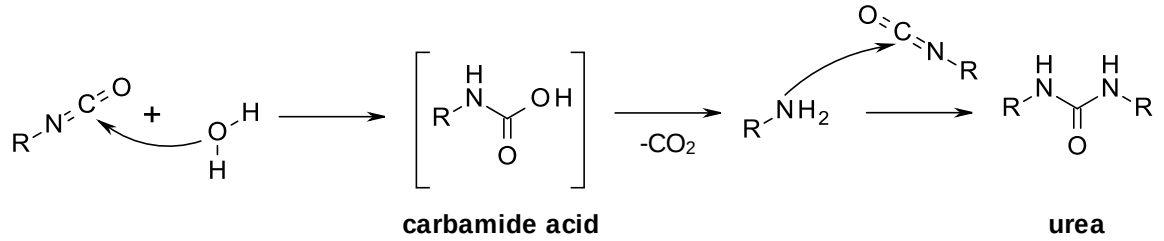

Scheme 8. Reaction of isocyanates with water

2.2. Reproduction of Pellethane and aliphatic TPUs

Pellethane (**Pell**) is a commercially TPU and approved by the FDA. Recently this materials was already applied as electrospun vascular grafts.[171] It is composed of the diisocyanate **MDI**, the prepolymer **pTHF** and the chain extender **BDO** (Figure 72).

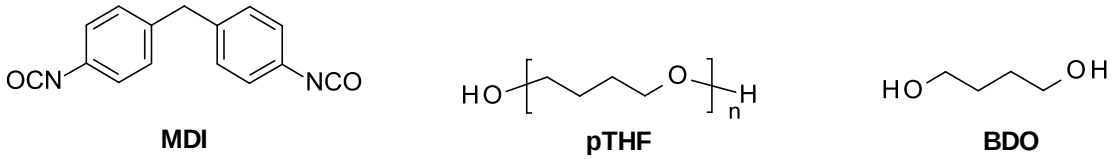

Figure 72. Components of Pellethane™

In the first part of this study **Pell** should be reproduced to develop a method for the synthesis of TPUs, to investigate the ratio and molecular weight of the components, and to be able to modify the different components to obtain non-toxic, degradable TPUs. In this context especially the substitution of the aromatic **MDI** (and the questionable inherent aromatic amines) with aliphatic correspondents was in the foreground.

TPUs out of the components of **Pell** have been described by Eisenbach *et al.*[306] They used **pTHF** with a molecular weight of 2000 g/mol with ratios **MDI**/**pTHF**/**BDO** 2:1:1, 3:1:2 and 4:1:3. In this study different molecular weights of **pTHF** as well as different ratios were applied (Table 17).

However, before the synthesis the purity of the starting materials was checked and the necessary purification steps were conducted.

2.2.1. Purity of MDI

The purity of **MDI** was assessed by a back titration of the isocyanate groups [307]. Therefore the isocyanate groups were converted to the according urea with an excess of di-n-butyl amine (**DBA**, Scheme 9). The remaining **DBA** was titrated with a titer solution of HCl.

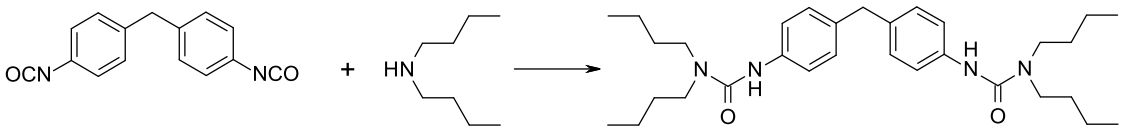

Scheme 9. Conversion of MDI with DBA

The results showed that the applied **MDI** possessed only 97% of the theoretic isocyanate activity. Some of the isocyanate groups might already be converted to ureas owing to humidity. Therefore the MDI was distilled by means of a kugelrohr distillation at fine vacuum.

2.2.2. Purity of pTHF

To confirm the molecular weight of **pTHF** the hydroxyl value (OH value) of both batches were determined. The OH value is defined as the molar amount (mmol) of the hydroxyl end groups in 1 g polymer. The most common method to determine the OH value is the conversion of the hydroxyl end groups with an excess of acetylic anhydride and the back titration with a KOH titer solution.

Table 15. Hydroxy number of pTHF

m.w. of pTHF [g/mol]	*theoret. OH value [mmol/g]*	*actual OH value [mmol/g]*	*actual m.w. [g/mol]*	*deviation*
1000	2.000	1.965	1018	1.8%
2900	0.690	0.678	2950	1.7%

The deviation from the product specifications in both cases was rather low and was therefore negligible.

Another important parameter for the purity of the **pTHF** batches for the synthesis of TPUs is the water content (c_w). The water content of **pTHF** can be assessed by Karl Fischer (KF) titration. This method can quantify water in very low quantities. For KF titration the substance is titrated with a dry methanolic solution containing iodine, sulfur dioxide and an excess of pyridine (**Py**) as base. Crucial for this method is the fact that the following reaction (Scheme 10) works only in presence of water.

$$CH_3OH + SO_2 + Py \longrightarrow (PyH)CH_3OSO_2$$

$$(PyH)CH_3OSO_2 + \boldsymbol{H_2O} + I_2 + 2\,Py \longrightarrow (PyH)CH_3OSO_3 + 2\,(PyH)I$$

Scheme 10. Karl Fischer titration

Sulfur dioxide, iodine and water react in a molar ratio of 1:1:1. The end point of the titration can be detected by coulometric techniques.

Samples of the **pTHF** batches were dissolved in dry THF to obtain solutions of about 10% (w/w) (weight percentages were calculated with a density of THF of 0.8892 g/mL). The c_w of this solutions and the pure dry THF was determined by KF titration. The c_w of the dry THF was 37 ppm

Table 16. Water content of untreated pTHF batches

m.w. of pTHF [g/mol]	*mass in 10 mL THF [g]*	*percentage of solution [% (w/w)]*	*c_w (solution) [ppm]*	*c_w (pTHF) [ppm]*	*molar c_w [% (n/n)]*
1000	0,9640	10,7	59	241	1,34
2900	0,9689	10,8	62	265	4,26

The c_w of the untreated samples was quite high (Table 16), especially for the high molecular weight **pTHF** when measured by the molar ratio. The c_w had to be decreased about to the level of common c_w of the extra dry solvents used for the synthesis that lies at about 50 ppm. Recommended drying procedures for prepolymers for the synthesis of TPUs is their treatment in vacuo at elevated temperature under magnetic stirring. The THF batches were dried at 90°C/5 mbar overnight. After this procedure values of c_w<30 ppm were obtained.

2.2.3. Polymer synthesis

Before the real polymer synthesis, a kinetic study with the non-chain extended polyurethane of **MDI** and **pTHF1000** was conducted. **MDI** (0.92 mmol, 1 eq) in dry dioxane was added to a stirred solution of dried **pTHF** in dry dioxane at 90°C in a dry argon atmosphere. Three drops of tin octoate (SnOct) were added and samples were taken after 1, 2, 3, 4.5, 6.5, 22.5 and 30.5 hours

and examined by means of GPC. After a polymerization time of 1 hour already 90% of the final molecular weight was attained. The polymerization can be considered as complete after 3 hours as also recommended in literature.[247, 248] However, overnight reactions should be done, whenever possible.
For the synthesis of the polymers the preliminary dried **pTHF** that was stored over $CaCl_2$ in a desiccator was dried for another hour directly prior the reaction. Dry dioxane was added before **MDI** in dioxane and 3 drops of SnOct were added in a dry Ar atmosphere. After 1 h of stirring at 90°C the formation of the macrodiisocyanate should be complete and freshly distilled **BDO** was added to the reaction mixture. Generally the viscosity of the solution increased dramatically and more dry solvent was added ensure a sufficient mixing. The polymerization was continued overnight at 90°C. The reaction mixture was diluted with solvent so as to be able to add the solution drop wisely to the 5-fold amount of petroleum ether under vigorous stirring. The precipitated polymer was filtered off and dried in vacuo. Molecular weights of the obtained polymers were assessed by GPC (Table 17).

Table 17. Reproduction of Pellethane and aliphatic TPU

Polymer ID	*diisocyanate*	*m.w. of pTHF [g/mol]*	*ratio DI/pTHF/BDO*	*m.w. [kDa]/Pd*
P01	MDI	1000	3:1:2	24/1.7
P02	MDI	2900	3:1:2	32/1.6
P03	MDI	1000	2:1:1	36/2.1
P04	HMDI	1000	3:1:2	15/1.3
Pell	MDI	-*	-*	36/1.7

*unknown

For the design of (bio)degradable TPUs it has to be considered that every single building block will be subjected to metabolism. The degradation products will be transported within the organism, chemically modified and maybe accumulated at certain organs. Long term effects, however, cannot be predicted at all.
So, to play it safe it is recommended to avoid components with inherent potential to form substances of toxic relevance. **MDI**, among all other aromatic diisocyanates, is one of these components, as the corresponding diamines are known for their toxicity.[255-257]
Therefore, one of the first modifications of **Pell** was the substitution of **MDI** with **HMDI**. To observe the impact on the mechanical properties of the polymers, a TPU containing **HMDI** instead of **MDI** was synthesized and compared with the replicate of **Pell** and **Pell** itself, respectively.
Polymerizations were performed as described for the aromatic TPUs. But as the solubility of the aliphatic polymers in dioxane was insufficient, extra dry DMF was used instead. Reprecipitation was done in methanol.

2.3. Concepts for degradability and toxicological examinations

Degradability of TPUs can be introduced either in the soft- or the hard-blocks (or both) (Figure 73). A good overview of this topic is given by Shi and Tian[270].

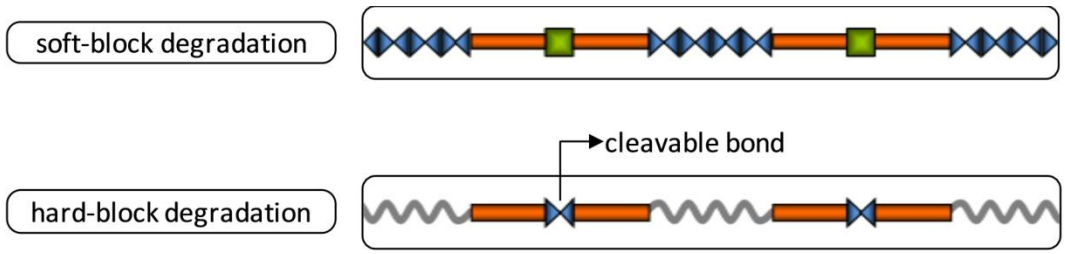

Figure 73. Introduction of degradability

In this work only ester bonds are considered as cleavable bonds. Independent from the fact whether cleavable soft-blocks or hard-blocks are introduced, the first concept for the degrading moiety should be moieties with lactate or ethylene glycol end groups.

Table 18. Concepts for soft- & hard-block degradability (R...low molecular weight residue)

end groups	*prepolymer for soft-block degradable TPUs*	*chain extender for hard-block degradable TPUs*
ethylene glycol	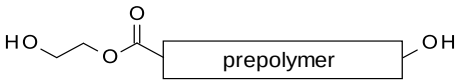	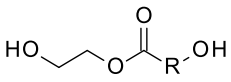
lactate	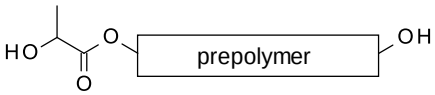	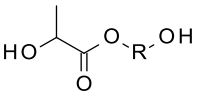

The free hydroxyl groups add to the isocyanates to form the urethane groups during the polymer synthesis, while the ester groups are cleaved during the degradation of the polymers (Figure 74).

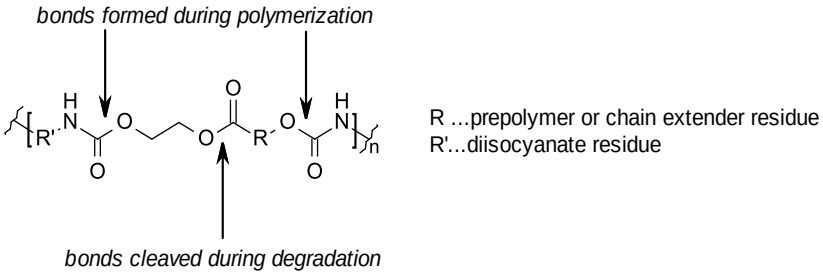

Figure 74. Bonds formed/cleaved for the example of ethylene glycol terminated moiety

So, during degradation predominantly two different classes of cleavage products, beside the polymeric moieties (hydroxyl- or carboxyl-terminated soft-blocks or parts of it), would be formed – the ethylene glycol and lactate extended diisocyanate (Figure 75).

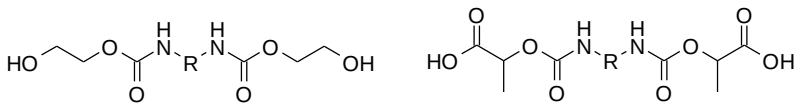

Figure 75. Ethylene glycol extended (left) and lactate extended diisocyanate (right)

Those substances should have the main impact of the toxic effects during degradation.

2.3.1. Synthesis of degradation products

To investigate the acute toxic effects of the degradation products of degradable TPUs based on aromatic and aliphatic diisocyanates the according substances derived from **MDI**- as well as **HMDI** were synthesized and tested. Table 19 shows the 4 substances assumed to be formed predominately during the degradation of the conceptual TPUs described above.

Table 19.Degradation products of MDI- as well as HMDI-based TPUs

end groups	*MDI*	*HMDI*
ethylene glycol	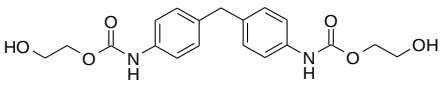 **MDHC**	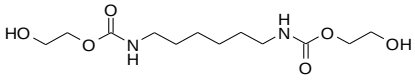 **HDHC**
lactate	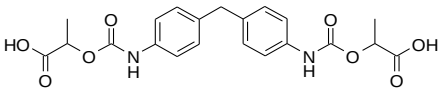 **MDLA**	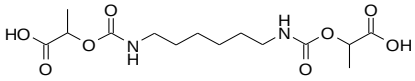 **HDLA**

The synthesis of 1,6-bis(hydroxyethyloxycarbonylamino)hexane (**HDHC**) was already described in literature [308, 309] and was done by the catalyzed ring-opening of ethylene carbonate with hexamethylene diamine (Scheme 11). Therefore 2 eq ethylene carbonate in DCM were added to a solution of 1 eq hexamethylene diamine in DCM at r.t. with stirring. After the addition of one drop SnOct the product precipitated. The reaction was continued overnight and the product was recrystallized from acetone. **HDHC** was obtained with a yield of 66% as a white powder.

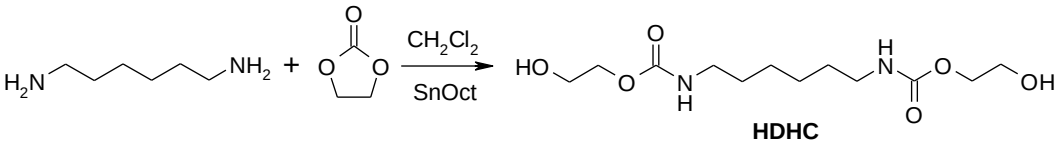

Scheme 11. Synthesis concept of HDHC

The synthesis of 4,4'-bis(hydroxyethyloxycarbonylamino)diphenyl methane (**MDHC**) was attempted in the analogous way (Scheme 12). 2 eq ethylene carbonate in DCM were added to a solution of 1 eq 4,4'-diphenyl methane diamine in DCM at r.t. under stirring. After the addition of one drop SnOct, however, no precipitation was observed. Even after several days TLC indicated no conversion.

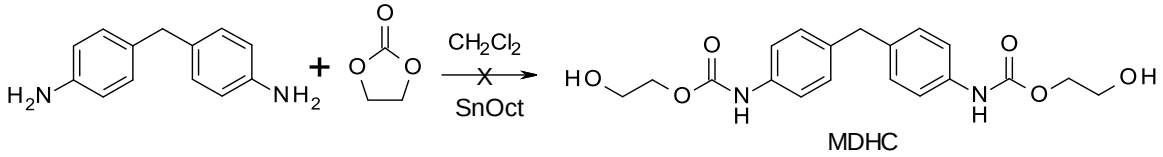

Scheme 12. Synthesis concept of MDHC

Another approach for the synthesis of **MDHC** is the classic extension of **MDI** with an excess of ethylene glycol (Scheme 13). Therefore 1 eq of **MDI** in dry dioxane was added drop wisely to 4 eq of freshly distilled ethylene glycol in dry dioxane under stirring and Ar atmosphere. After the addition of one drop of SnOct the solution was stirred for 2 h at 90°C. The product was precipitated in the 10-fold amount of distilled water and recrystallized from ethanol. **MDHC** was obtained with a yield of 47% as a pale yellow powder.

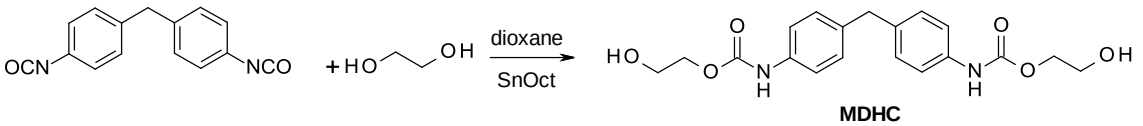

MDHC

Scheme 13. Synthesis concept of MDHC

The syntheses of **MDLA** and **HDLA** had to be done in 2 steps as the free acids would interfere with the chain extension (Scheme 14). Therefore 1 eq **MDI** or **HMDI** in dioxane were added drop wisely to 2.2 eq ethyl lactate in dioxane under stirring and Ar atmosphere. After the addition of one drop of SnOct the solution was stirred for 2 h at 90°C. The intermediate products were precipitated in the 10-fold amounts of distilled iced water. Recrystallization from ethanol gave 92% acetic acid-2,2'-dimethyl-2,2'[methylenebis(4,1-phenyleneiminocarbonyloxy)]-1,1'-diethyl ester (**MDLAE**) and recrystallization from water gave 89% 3,14-dioxa-5,12-diazahexadecanediocic acid-2,15-dimethyl-4,13-dioxo-1,16-diethylester (**HDLAE**), respectively.

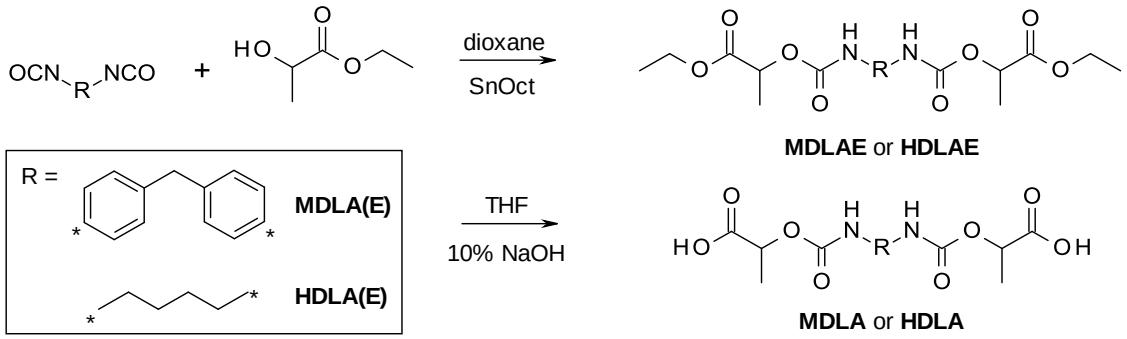

MDLAE or **HDLAE**

MDLA or **HDLA**

Scheme 14. Synthesis concepts of MDLA and HDLA

For the hydrolysis, a solution of 1 eq of **MDLAE** or **HDLAE**, respectively, in THF was stirred, cooled with an ice/water bath and 10 eq NaOH were added as a 10% (w/v) aqueous solution. After one hour of stirring the aqueous solution was acidified with (1:5) diluted HCl and the products precipitated. Recrystallization from methanol gave 55% acetic acid-2,2'-dimethyl-2,2'[methylenebis(4,1-phenyleneiminocarbonyloxy)] (**MDLA**) and recrystallization from water gave 35% 3,14-dioxa-5,12-diazahexadecanediocic acid-2,15-dimethyl-4,13-dioxo (**HDLA**), respectively.
MDLA was obtained with an overall yield of 51% and **HDLA** with 31%.

2.3.2. Cytotoxicity tests

Stock solutions of every single substance (**MDHC**, **MDLAE**, **MDLA**, **HDHC**, **HDLAE** and **HDLA**) in DMSO with concentrations of 1 mmol/mL (≡ 1 M) were produced. Human umbilical vein endothelial cells (HUVEC) were cultured, proliferated on plastic coverslips and treated with increasing concentrations (0.1, 1, 5, 10, 50, 100, 500 and 1000 µM) of the examined substances from dilution series. The viability of the cells was assessed by a formazan based assay after 24 h of proliferation at 37°C. For reference blank samples only containing the same amount of DMSO were performed.
All 6 substances showed no significant decrease of the cell viability even at highest concentration of 1 mmol/L. Such a high concentration will not be achieved in vivo during the degradation of the vascular grafts. Therefore acute cytotoxicity of these degradation products was considered to be negligible. However, long term effect of secondary products, accumulation or systemic effects, especially in case of the inherent existing aromatic amines of **MDI** derived could not be assessed within the framework of this study. Hence **MDI** was excluded from further considerations.

2.4. Cleavable chain extenders

Cleavable chain extenders (CCE) are relatively small molecules (m.w.<500 g/mol) with two nucleophilic groups (OH, NH_2, SH) connected linearly by at least one cleavable bond. In this work only ester bonds are considered as cleavable bonds. The concepts for this study can be divided into three groups: lactate derived CCE, ethylene glycol derived CCE and Michael adducts. Table 20 sums up the concepts and target molecules.

Table 20. Concepts for CCE

lactate derived	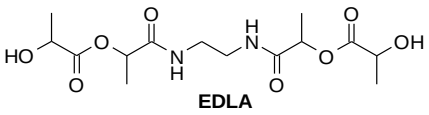 **EDLA** 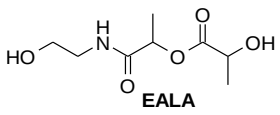 **EALA** 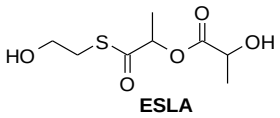 **ESLA** 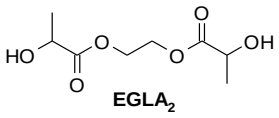 **$EGLA_2$** 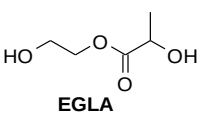 **EGLA**
ethylene glycol derived	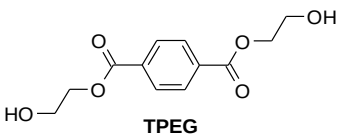 **TPEG** 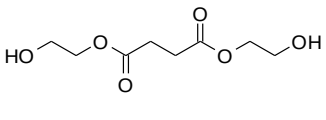 **SUEG** 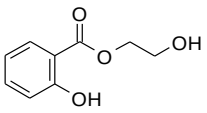 **SAEG** 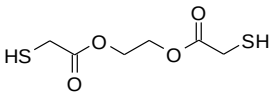 **TGEG** 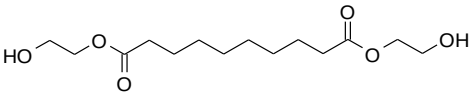 **SBEG**
Michael adducts	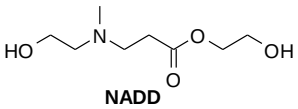 **NADD** 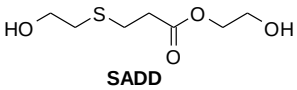 **SADD** 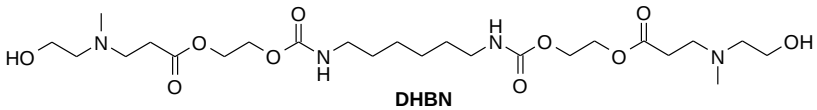 **DHBN** 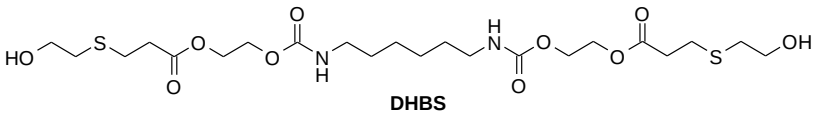 **DHBS**

CCEs were designed with the stipulation having simple methods for the synthesis (e.g. avoidance of protecting group techniques) with purification steps (e.g. distillation or recrystallization) that are also suitable for the high quantities of material required for mechanical characterization, for the optimization of the electrospinning process, and for subsequent in vivo studies. **TPEG** and **TGEG**, however, are commercially available and can be purified by distillation and recrystallization, respectively.

Aside this it was planned to use salicylic acid derived CCE like **SAEG**. Therefore model reactions for the chain extension with salicylic acid derived nucleophiles should be performed, since reactivity of this substance class toward isocyanates is insufficiently described in literature. Salicylic acid derivatives are known to have blood thinning effects.[6, 310, 311] Antithrombotic medication is a fundamental part of every IHD therapy. The degrading graft could therefore also have the function of a reservoir for controlled drug release.

Therefore 1 eq of **HMDI** in dry dioxane was added to a solution of 2.1 eq ethyl salicylate in dry dioxane. After the addition of three drops of SnOct the solution was stirred overnight at 70°C (Scheme 15). During work-up an insoluble fraction was formed that emerged to be the urea formed from unconverted **HMDI** with humidity. Unfortunately, the conversion seemed to be far from suitable for chain extension of TPUs. So the concept of salicylic acid derived chain extenders was rejected.

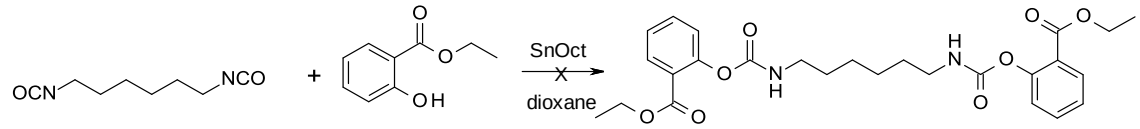

Scheme 15. Model reaction for the chain extension with salicylates

2.4.1. Synthesis of lactate based CCE

The concept for the synthesis of [2-(2-(2-(2-hydroxypropanoyloxy)propanoylamino)ethylamino)-1-methyl-2-oxo-ethyl]2-hydroxypropanoate (**EDLA**) was encouraged by the good conversion und selectivity of the ring opening addition of hexamethylene diamine with ethylene carbonate for the synthesis of (**HDHC**, section 2.3.1). The higher nucleophilicity of the nitrogen of ethylene diamine compared to the secondary hydroxyl group should avoid ring opening polymerization (ROP) (Scheme 14).

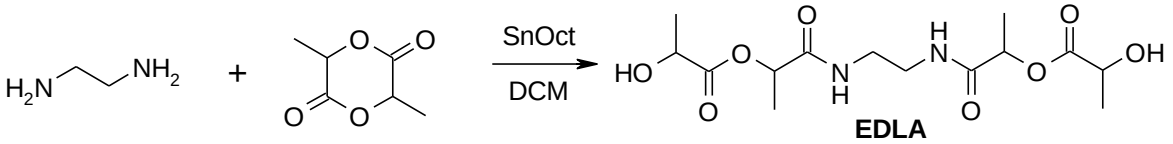

Scheme 16. Synthesis concept for EDLA

For the synthesis of **EDLA**, 1 eq freshly distilled ethylene diamine was reacted with 2 eq lactide at r.t. in DCM in the presence of SnOct as catalyst. The crude product was precipitated as an oily substance in petroleum ether. The purity was checked by means of TLC. Multiple substances where detected. It seems ROP could not be avoided completely. The purification was performed with silica gel column chromatography. This turned out to be very laborious and time-consuming and only low quantities (20%) of **EDLA** as pale yellow oil could be afforded.

Another approach was the use of 2-aminoethanol instead of the diamine and the synthesis of [2-(2-hydroxyethylamino)-1-methyl-2-oxo-ethyl] 2-hydroxypropanoate (**EALA**, Scheme 17)

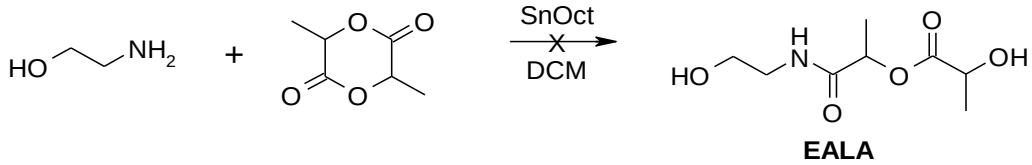

Scheme 17. Synthesis concept for EALA

1.2 eq of freshly distilled 2-aminoethanol were converted with 1 eq lactide in DCM at r.t. in the presence of SnOct as catalyst. The crude product was precipitated as an oily substance in petroleum ether. The purity was checked by means of TLC and multiple substances where detected. In addition, the crude product was very viscous, which indicated multiple ring opening.

The reaction was repeated in the same manner, without using the catalyst, in order to reduce the reactivity and avoid ROP. However, TLC showed the same result. Based on prior difficulties from chromatographic purification of **EDLA** no further attempts were carried out to prepare **EALA**.

The problem with multiple ring opening might arise from the fact that the basic amines could probably catalyze ROP, which would also explain the same result of the non-catalyzed conversion of 2-aminoethanol with lactide. Thus, a new chain extender with a thiol instead of an amine was investigated (Scheme 18).

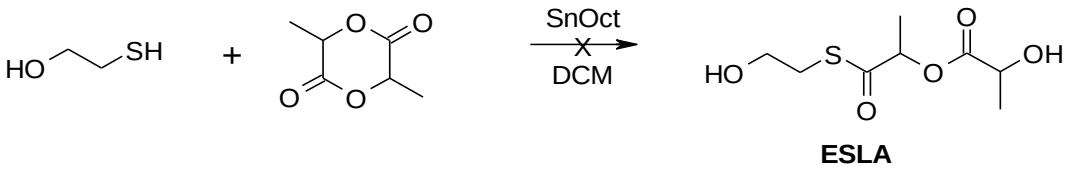

ESLA

Scheme 18. Synthesis concept for ESLA

For the synthesis of [2-(2-hydroxyethylthio)-1-methyl-2-oxo-ethyl] 2-hydroxypropanoate (**ESLA**) 1 eq of freshly distilled 2-mercaptoethanol was converted with 0.9 eq lactide in DCM at r.t. in the presence of SnOct as catalyst. The crude product was examined by NMR, but only the starting materials could be detected.

Ring opening of lactide did not seem to be a good approach for the synthesis of high quantities of lactate based CCE. Hence, other concepts were developed. The direct application of lactic acid, ethyl lactate or even PLA was attempted.
For the synthesis of ethylene lactate (**$EGLA_2$**) 1 eq ethylene glycol was reacted with 2.2 eq lactic acid in toluene under sulfuric acid condition in a water separator arrangement overnight. After neutralization and evaporation of the solvent a crude product NMR indicates the successful conversion and the desired product. Distillation, however, led to decomposition and polymerization of the product.

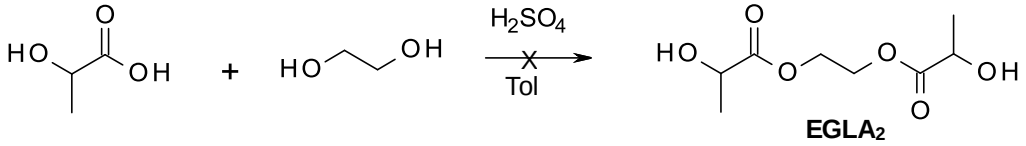

$EGLA_2$

Scheme 19. Synthesis concept for $EGLA_2$

Instead of using an excess of lactic acid to account for disubstitution of ethylene glycol the reaction was attempted with an excess of ethylene glycol. Hydroxyethyl lactate (**EGLA**, Scheme 20) would be the desired product. At least 5 eq ethylene glycol were reacted with 1 eq lactic acid or ethyl lactate in toluene in the presence of p-toluenesulfonic acid (p-Tos). Water/ethanol was distilled off. After neutralization and evaporation of the solvent and the excess of ethylene glycol distillation again led to polymerization in both cases.

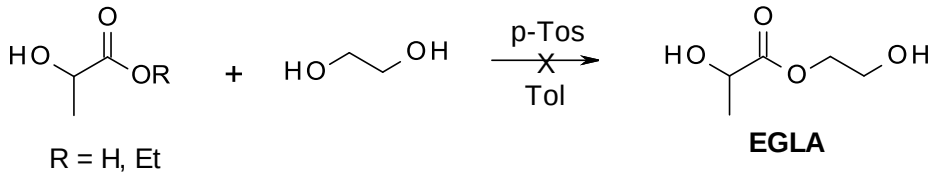

EGLA

Scheme 20. Synthesis concept for EGLA

Acid catalyzed (trans)esterification seems to be unfeasible for the synthesis and purification (by distillation), respectively, of the desired small, hydroxyl group terminated esters. Traces of the catalyst or lactic acid after work-up are enough to catalyze the intermolecular transesterification during the distillation. Spontaneous transesterification (without catalyst) occurs only at high temperatures (200°C and above) with sufficient velocity. However, such a temperature can only be realized in an autoclave as the boiling point of the starting material at atmospheric pressure is too low. The separation of ethanol to obtain high conversion in this autoclave arrangement is not possible at lab scale.
Another approach would be the depolymerization of **PLA** with ethylene glycol as the boiling point of ethylene glycol should be high enough for a rapid transesterification (Scheme 21).

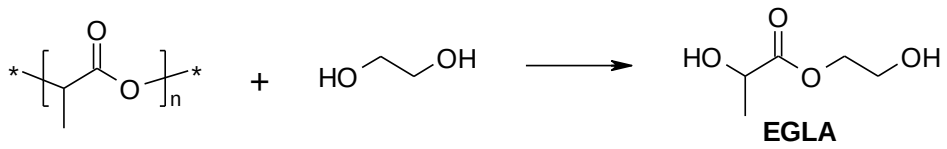

Scheme 21. Depolymerization of PLA with ethylene glycol

1 eq **PLA** (with respect to the lactic acid units) was refluxed with 5 eq ethylene glycol overnight. The successive decrease of viscosity of the solution indicated the progress of depolymerization. After the evaporation of the excess of ethylene glycol the product could be distilled in vacuo. **EGLA** was obtained as colorless oil with a yield of 48%. Unfortunately the storage stability of **EGLA** is very low. It has to be stored in the fridge and freshly distilled prior use.

To test the suitability of **EGLA** as chain extender a model reaction using a monoisocyanate was conducted (Scheme 22). Therefore 2 eq of isocyanatoacetic acid ethyl ester in dry dioxane was added to EGLA in dry dioxane under Ar atmosphere and stirred overnight at 70°C in the presence of SnOct. ELAE was precipitated in petrol ether and dried in vacuo to obtain the white powder with a yield of 87%.

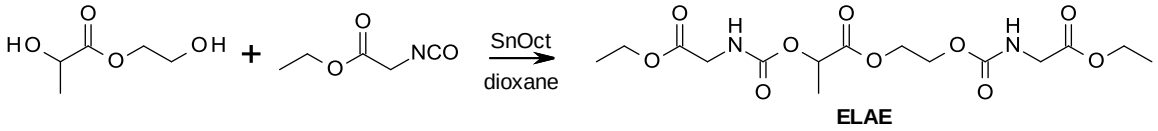

Scheme 22. Model reaction for the chain extension with EGLA

2.4.2. Synthesis of ethylene glycol based CCE

As assumed, the acid catalyzed conversion of 1 eq succinic acid with 10 eq ethylene glycol in toluene with water separation (Scheme 23), incurred the same problems observed for the previous (trans)esterifications. The polymerization due to intermolecular transesterifications led to polymerization of the product during distillation which makes purification impossible.

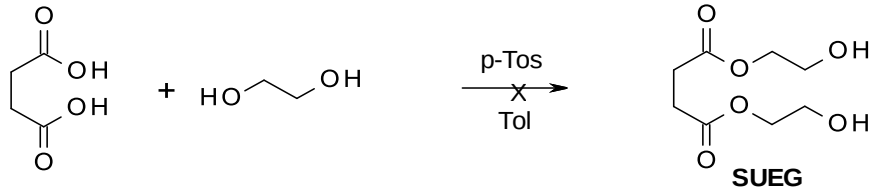

Scheme 23. Synthesis concept for SUEG

An alternative is the application of the succinic acid dichloride instead of the free acid. 1 eq succinic acid dichloride in DCM was added drop wisely under stirring to a solution of 5 eq ethylene glycol and 2.5 eq triethyl amine at -10°C. After one hour of stirring the solution was extracted with diluted HCl solution. Unfortunately the product dispersed into the aqueous phase and could not be re-extracted into the organic phase with reasonable amounts of DCM or chloroform.

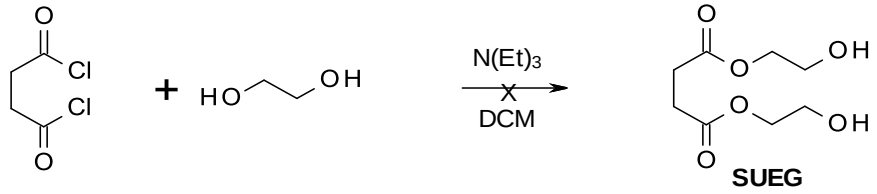

Scheme 24. Synthesis concept for SUEG

The higher melting points of bis(hydroxyethyl)esters of dicarboxylic acids with higher molecular weights could be used to recrystallize the products for purification instead of a distillation (as in case of **TPEG**) and therefore avoid the complication of intermolecular transesterifications.

Therefore, the synthesis of bis(hydroxyethyl)sebacate (**SBEG**, Scheme 25) was attempted as sabacic acid was also already considered as component of biodegradable polyester materials.[312]

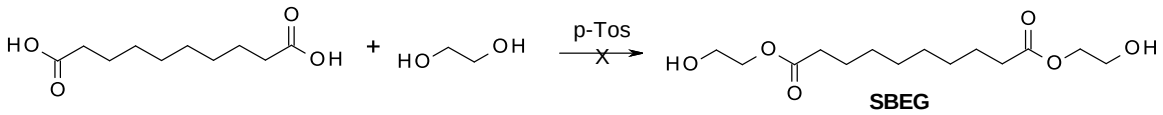

Scheme 25. Synthesis concept for SBEG

1 eq sabacic acid was converted with 10 eq ethylene glycol, which was also used as solvent, at the presence of p-toluenesulfonic acid under stirring at 100°C. The formed water was distilled of by a successive decrease of pressure. The mixture was stirred overnight at 100°C/100 mbar. After all water was distilled off, the product crystallized at r.t. overnight. The product was filtered off, washed with water, dried and recrystallized from diethyl ether. The product was obtained with a theoretical yield of 32%. Unfortunately NMR indicated oligomers.

2.4.3. Synthesis of Michael adduct based CCE

In literature the successful Michael addition of diethanolamine with acryloyloxyethyl-2-bromoisobutyrate is decribed.[313] The similar reaction was described for 2-amino ethanol with ethyl acrylate.[314] Therefore, it should be possible to synthesize 2-hydroxyethyl-3-(2-hydroxy-ethyl(methyl)amino)propanoate (**NADD**) by a Michael addition of N-methyl-2-aminoethanol with 2-hydroxyethylacrylate (Scheme 26).

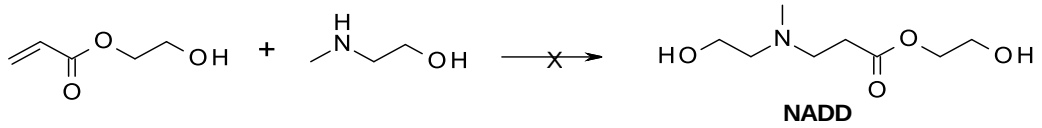

Scheme 26. Synthesis concept for NADD

1.2 eq N-methyl-2-aminoethanol were reacted with 1 eq of 2-hydroxyethyl acrylate under stirring at r.t. overnight. For purification, the crude product was distilled twice, but still some contamination, that was most likely ethylene glycol, could be detected in the NMR. Ethylene glycol probably is formed during distillation due to an intra-/intermolecular rearrangement.
Therefore, again the exchange of the nucleophile was attempted and 2-mercaptoethanol was used instead of N-methyl-2-aminoethanol (Scheme 27).

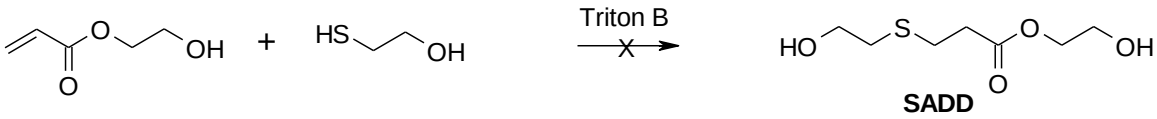

Scheme 27. Synthesis concept for SADD

In literature the synthesis of methyl-β-hydroxyethylmercaptopropionate is described by a Michael addition of 2-mercaptoethanol with methyl acrylate in the presence of benzyltrimethylammonium hydroxide (Triton B) as catalyst.[315] Based on that, for the synthesis of 2-hydroxyethyl-3-(2-hydroxyethylsulfanyl)propanoate (**SADD**) 1 eq 2-mercaptoethanol was converted with 2 eq of 2-hydroxyethyl acrylate in the presence of Triton B. The crude product was a viscous and clear substance. Unfortunately, the product could not be purified by distillation, and the substance became more viscous and yellowish and presumably decomposed.
Again, the high temperature treatment of the substances during distillation led to the decomposition of the products in both cases. So, as an alternative approach is was attempted to directly prepare the degradable hard-blocks. This means to conduct the chain extension before the Michael addition (Scheme 28). These substances should crystallize due to the urethane interaction and could therefore be purified by recrystallization.

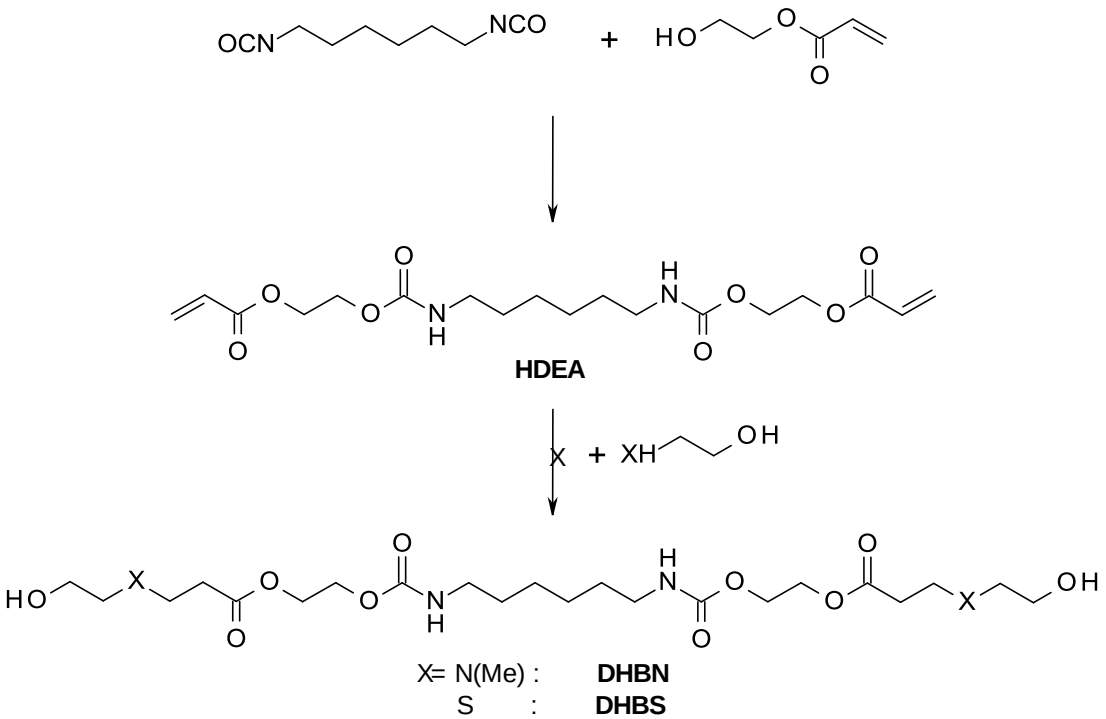

Scheme 28. Synthesis concepts for degradable hard-blocks

The intermediate product, N,N'-bis[(2-acryloyloxyethoxy)carbonyl]-1,6-hexanediamine (**HDEA**), was prepared by standard extension reaction of **HMDI** with **HEA** (Scheme 29). Therefore, 1 eq **HMDI** in dry dioxane was added to a solution of HEA in dry dioxane under stirring and Ar atmosphere. After the addition of one drop of SnOct the solution was stirred overnight at 70°C. The product was precipitated in the 10-fold amount of ice water, filtered, washed and dried in vacuo over $CaCl_2$.

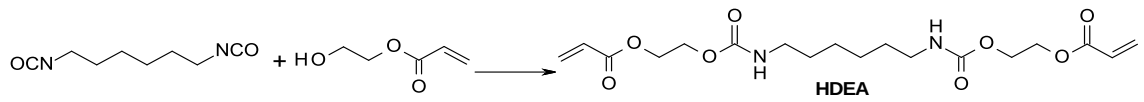

Scheme 29. Synthesis concept of HDEA

The Michael addition of N-methyl-2-aminoethanol with **HDEA** to obtain **DHBN** was done similar as described above.

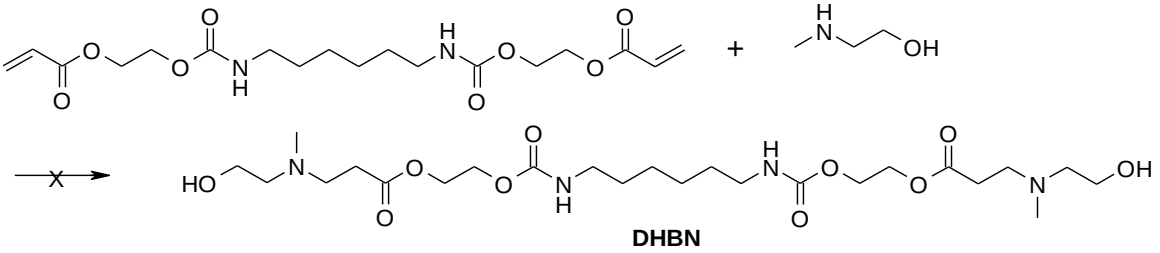

Scheme 30. Michael addition of N-methyl-2-aminoethanol with HDEA

Therefore, 2.2 eq N-methyl-2-aminoethanol were converted with 1 eq **HDEA** at r.t. in methanol under Ar atmosphere. After work-up, a crude product NMR showed only the product of aminolysis.

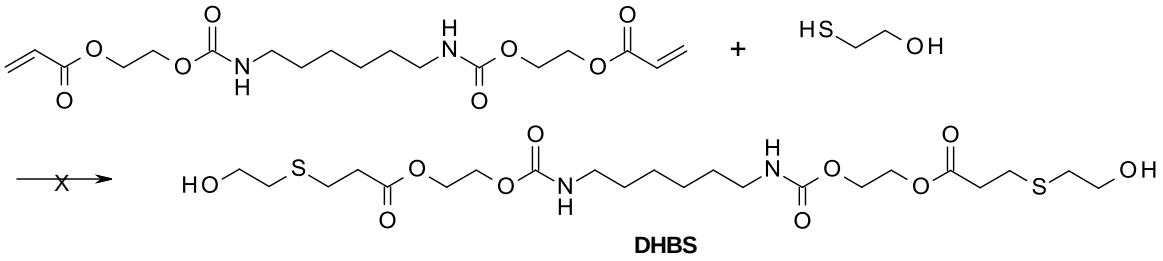

Scheme 31. Michael addition of 2-mercaptoethanol with HDEA

The same procedure was performed with 2-mercaptoethanol as nucleophile with a little amount of MEHQ to avoid radical thiol-ene reaction. After work-up a crude NMR still showed residues of acrylate. So, the reaction was repeated with an even higher excess of 2-mercaptoethanol and mild, elevated temperatures. The crude NMR this time only indicated traces of acrylate, but many unidentified signals of side products. However, the desired product never crystallized.

2.5. Concepts for cleavable soft blocks

This work was focused on the hard-block degradation of TPUs. Never the less, some concepts for cleavable soft-blocks were examined. The easiest way to convert polyether urethanes (like **PeII**) into a degradable TPU is the application of polyethers, extended with just a few units of a ring opening polyester, e.g. **PLA** or **PCL**, thus ABA block-co-polymers.

E.g. for the synthesis of poly[(D/L-lactide)-co-(tetrahydrofuran)-co-(D/L-lactide)]-diol (Scheme 32) 1 eq of dry poly(tetrahydrofuran) (**pTHF**, m.w. 2000 g/mol, n = 28) was heated with 4 eq of D/L-lactid to 130°C at Ar atmosphere and stirred for 9 hours at the presence of SnOct. For purification, the polymer was reprecipitated from a solution in toluene in petroleum ether. The desired ABA-block-co-polymer was obtained with a yield of 64%. The block length m = 3 was determined by means of NMR.

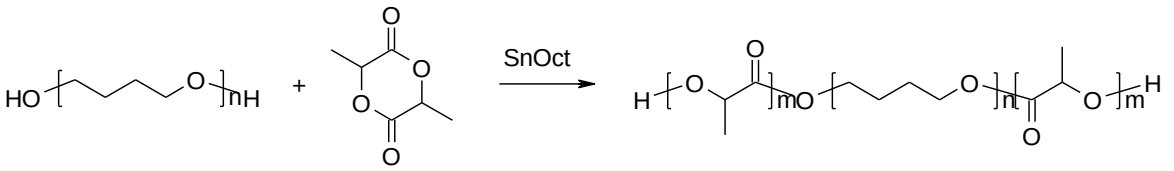

Scheme 32. Ring opening polymerization of lactide with pTHF

Ring-opening of lactide with water leads to carboxylic acid groups. Therefore the acid number is a perfect monitoring parameter. The acid number is defined as the mg KOH equivalent of the acid endgroups in 1 g polymer. The most common method to determine the acid number is the titration with a methanolic KOH titer solution. The acid number of the synthesized block-co-polymer was determined to be less than 1 and therefore sufficiently low.

Beside the classic polyester as (cleavable) soft blocks, recently also polycarbonates are described in literature to have several advantages.[118, 119, 253, 316] Poly(trimethylene carbonate) (**pTMC**) undergoes a typical but different degradation mechanism. While polyesters like **PLA** or **PGA** suffer from the bulk erosion mechanism [107], a catastrophic, autocatalytic event (Figure 76), **pTMC** undergoes enzymatic surface erosion.[317]

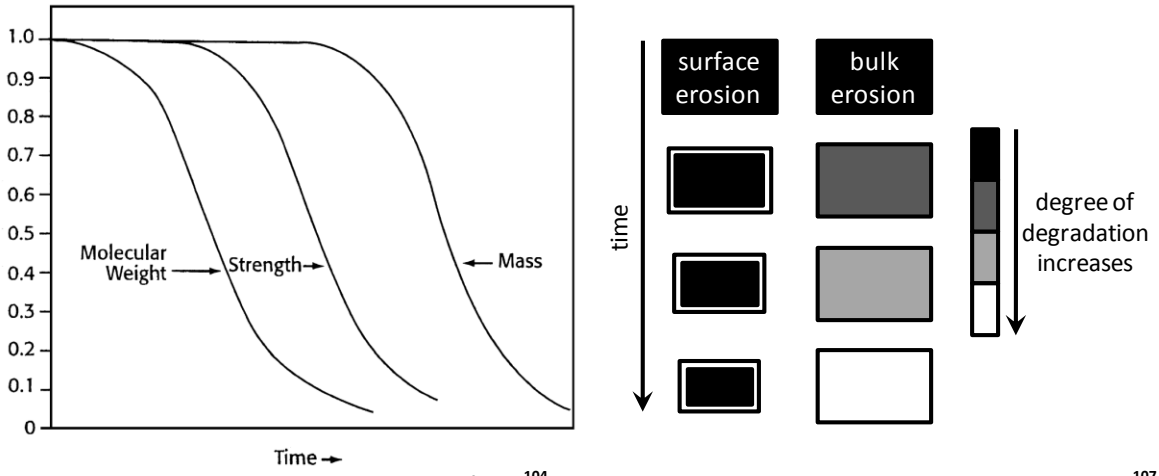

Figure 76. Typical degradation behavior of PLA/PGA [104] (left), difference between surface and bulk erosion (right) [107]

pTMC diols can be synthesized by ROP of **TMC** with a low molecular weight diol (e.g. ethylene glycol) to obtain "pure" **pTMC** or again by ROP with macrodiols to obtain ABA-block-co-polymers. This way, the degradation behavior of the soft block can be tailored.[270]
In this study another polycarbonate was used. Poly(hexamethylene carbonate) (**pHMC**) is synthesized by the ROP of ethylene carbonate with hexamethylene diol [223] and is commercially available.

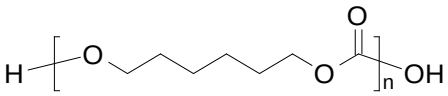

pHMC

Figure 77. Structure of poly(hexamethylene carbonate)

pHMC is presumed to be hydrolytically stable. However, due to the chemical similarity to **PCL** it might be degraded by enzymes, e.g. lipases that are specialized to cleave bonds next to long hydrophobic chains.

2.6. Synthesis of degradable TPUs

All synthesized TPUs assumed to be degradable consisted of **HMDI** as DI component. The prepolymer and the chain extender, respectively, as well as the ratio of diisocyanate, prepolymer and chain extender (DI:P:CE) were varied. The TPU were synthesized by the prepolymer method in DMF with SnOct as catalyst, as already described for the aliphatic (non-degradable) TPU in section 2.2.3. Table 21 arises all synthesized TPUs, their composition and their molecular weight assessed by GPC.

Table 21. TPUs with cleavable bonds

Polymer ID	*prepolymer/m.w.*	*chain extender*	*ratio DI:P:CE*	*m.w.[kDa]/Pd*
P05	pTHF1000	TPEG	3:1:2	30/1.6
P06	pTHF1000	TPEG	2:1:1	27/1.7
P07	pTHF1000	EDLA	3:1:2	21/1.4
P08	pTHF1000	EGLA	3:1:2	32/1.7
P09	pTHF1000	EGLA	2:1:1	25/1.8
P10	pTHF1000	TGEG	3:1:2	14/1.9
P11	pHMC860	BDO	3:1:2	12/1.7

2.7. Tests of the TPUs

The different polymers **P1** to **P11** were subjected to different characterization methods. The polymers for the reproduction of **Pell P1** to **P4** were classically tested by tensile tests. The best of this selection were electrospun and tested as tubular grafts (see section 2.8).
The polymers, assumed to be degradable, were also tested by tensile tests, however with an adapted method of specimen fabrication to avoid premature degradation.
A selection of them was also tested by dynamic mechanical analysis (DMA) to obtain more specific data. Additionally these polymers were tested for their degradability in accelerated degradation tests. Then again, the best of these polymers were electrospun and tested as grafts.
All tests were made with **Pell** as reference and bench mark.

2.7.1. Mechanical properties

For TE the mechanical properties of the applied scaffolds are of special interest. Depending on the tissue that should be regenerated the requirements on the polymers can differ over a broad range. The spectrum ranges from rather soft and elastic materials like blood vessels or skin to materials with hard material behavior such as bone.
A sufficient strength is the basic requirement to prohibit material failure. Therefore, classic tensile testing measurements should be performed. From selected polymers dynamic mechanical analysis (DMA) can give information about the viscoelastic properties and the temperature dependency of mechanical properties.

2.7.1.1. Tensile tests

Tensile test is a quasi-statically testing procedure for materials.[272] The specimen is loaded until a given strain is reached (e.g. failure of specimen). The two important testing parameters are stress σ [MPa] (eq x) and strain ε [%] (eq y).

$$\sigma = \frac{F}{A_0} \tag{16}$$

$$\varepsilon = \frac{\Delta L}{L_0} \cdot 100\% \tag{17}$$

σ ..... tensile stress [MPa]
F ..... tensile force [N]
A_0 ..... initial cross section [mm^2]
ε ..... tensile strain [%]
ΔL ..... elongation
L_0 ..... initial length

The specimen is fixed by two clamps and strained with a constant velocity while the stress-strain plot is recorded. The measurement is stopped until the specimen breaks or a given strain is reached. Testing materials for artificial blood vessels, 3 important mechanical parameters can be obtained evaluating the stress-strain plots: the elastic modulus E [MPa], the tensile strength S [MPa] and strain at break ε_B [%].

2.7.1.1.1. Non-degradable TPUs

The non-degradable TPUs **P1** to **P4** where hot-pressed to obtain sheets of the materials. Hot-pressing is a very fast and effective method to generate thin layers of thermoplastics with a very good surface quality and constant thicknesses. Therefore a hot-press type Collin P200P was applied with a temperature/pressure program illustrated in Figure 78.

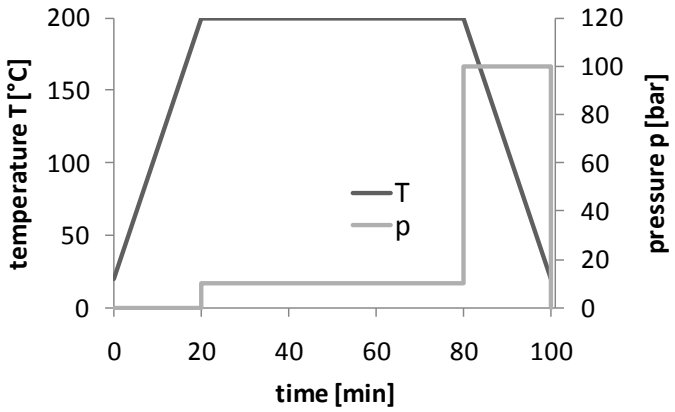

Figure 78. Temperature/pressure program for the hot-press

Dog bone specimens according to the standard ISO 527-1 type 5A (equivalent to ASTM D638 type IV) were punched out of the obtained foils and tested in a tensile testing machine type Zwick Z050 with a testing velocity of 50 mm/min at least quintuplicated. Table 22 shows the results of these measurements.

Table 22. Results of the tensile tests of non-degradable TPUs

Polymer ID	*composition*	*E [MPa]*	*S [MPa]*	ε_b *[%]*
P01	MDI/pTHF1000/BDO 3:1:2	45±3	41.3±0.6	900±25
P02	MDI/pTHF2900/BDO 3:1:2	9.0±0.3	5.9±0.3	769±41
P03	MDI/pTHF1000/BDO 2:1:1	12.5±0.2	4.06±0.08	262±11
P04	HMDI/pTHF1000/BDO 3:1:2	88±2	23.2±0.2	848±17
Pell	commercial product	20.44±0.05	35.9±0.2	1301±87

The mechanical properties of the different TPUs change according to their hard/soft block ratios.[318] The soft block content can be increased by a longer prepolymer (pTHF2900 instead of pTHF1000) or by a decrease of chain extender content (a ratio of 2:1:1 instead of 3:1:2). Increasing the soft block content leads to lower moduli and strengths compared to the bench mark **Pell**. Therefore the application of pTHF1000 in the TPUs with a ratio of 3:1:2 yield the best results for the **Pell** replicate **P01**. Hence this composition was also used for the aliphatic TPU **P04**. The aromatic diisocyanate was substituted by the aliphatic **HMDI**. As expected the general mechanical performance of the polymer is decreased by this substitution as the aromatic structures within the backbone of **P01** or **Pell** support the hard block formation. However, the tensile strength of **P04** was only reduced by one-third compared with the bench mark **Pell** and this seems to be the price of the avoidance of toxic components.

2.7.1.1.2. Degradable TPUs

Polymers that are assumed to be degradable by a hydrolytic mechanism must not be treated thermally because at elevated temperatures already the air humidity can cause cleavage of the bonds. Therefore another specimen preparation had to be performed for the degradable TPUs. Solution-casting (a.k.a. solvent-casting) is frequently applied to obtain films for the (mechanical) characterization of thermally non-stable polymers.[109, 135, 227, 228, 316] Therefore the polymers are dissolved in suitable solvents which are then evaporated in molds to form the compact films. For technical application solvents with rather high volatilities (acetone, THF, ether, DCM) are preferred to speed up the process.[319] However, in this study the obtained film quality was unsatisfactory when THF was used as solvent. This is maybe due to the very high evaporation rate compared to the very low diffusion of residual solvent to the surface of the film. Hence there is a difference between the shrinkage of the material at the surface and the material within the mold. This leads to very deformed films that are unsuitable for the mechanical characterization. For this

reason DMF was used as solvent. As molds, cavities (40x60x2 mm^3) of PTFE were used, fabricated by milling and finally smoothed by polishing.
The TPUs were cast from solutions of about 10% (w/w). In some cases the concentration had to be decreased because cracks were formed during evaporation of solutions with high concentrations. After 24 h the films were dried in vacuo and specimens according to the standard ISO 527-1 type 5B were punched out and tested in a tensile testing arrangement as described above. The results can be seen in Table 23.

Table 23. Results of the tensile tests of degradable TPUs

Polymer ID	*composition*	*E [MPa]*	*S [MPa]*	*ε_b [%]*
P05	HMDI/pTHF1000/TPEG 3:1:2	-*	-*	-*
P06	HMDI/pTHF1000/TPEG 2:1:1	35±14	17±1	1379±137
P07	HMDI/pTHF1000/EDLA 3:1:2	-♦	-♦	-♦
P08	HMDI/pTHF1000/EGLA 3:1:2	36±15	4.7±0.2	181±28
P09	HMDI/pTHF1000/EGLA 2:1:1	-★	-★	-★
P10	HMDI/pTHF1000/TGEG 3:1:2	-*	-*	-*
P11	HMDI/pHMC860/BDO 3:1:2	15±3	9.0±0.2	63±8
Pell	commercial product	11±3	20±4	891±145

* material too brittle
♦ material in to low quantities
★ material properties insufficient

P05, **P07**, **P09** and **P10** could not be tested for several reasons. **P05** and **P10** exhibited very brittle behavior and all films, solution-cast from different concentrations, showed severe cracks. This is probably due to high chain extender contents. **P07** could only be obtained in a low amount as the CCE applied for the synthesis can only be prepared in very low quantities owing to the laborious purification procedure. The reduction of the chain extender content in case of **P09** led to very soft materials with insufficient mechanical properties. However, the polymers **P08** and **P11** show acceptable and **P06** superior mechanical properties near to or even above the bench mark **Pell**.

2.7.1.2. Dynamic mechanical analysis (DMA)

All polymers show frequency and temperature dependent mechanical properties when exposed to an external load.[272, 284] This is called the viscoelasticity of polymers.
To assess the viscoelastic properties of the polymers, stripe specimens were tested in a tensile DMA at increasing temperature. The samples were exposed to an external co-sinusoidal stress σ(t), resulting in strain ε(t) (Figure 79). Depending on the viscoelasticity of the materials a phase shift from $\delta = 0$ (ideal elastic properties) to $\delta = \pi/2$ (ideal viscous properties) between those periodic curves can be observed.

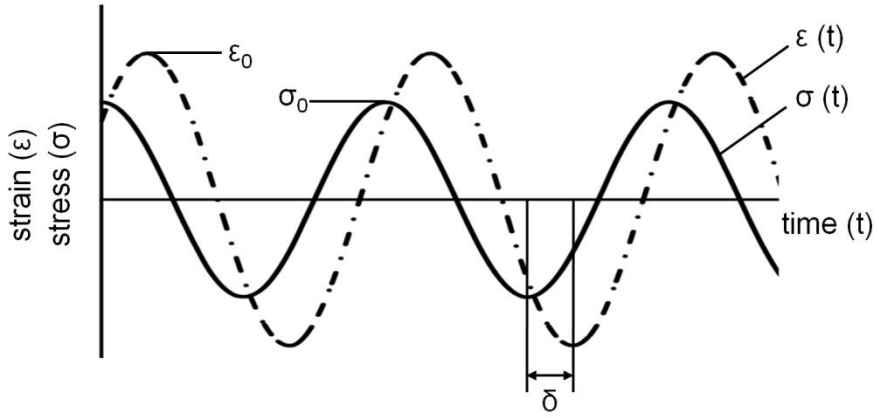

Figure 79. Schematic plots for stress and strain during a DMA experiment

$$\sigma(t) = \sigma_0 \cdot \cos(\omega \cdot t) \tag{18}$$

σ_0 ..... stress amplitude [MPa]
ω ..... angular frequency [s^{-1}]
t ..... time [s]

$$\varepsilon(t) = \varepsilon_0 \cdot \cos(\omega \cdot t - \delta) \tag{19}$$

ε_0 ..... strain amplitude [MPa]
δ ..... phase shift [ ]

Similar to classical tensile test a complex modulus (E*) can be calculated according to eq. 20.

$$E^* = \frac{\sigma(t)}{\varepsilon(t)} = \frac{\sigma_0}{\varepsilon_0} \cdot \frac{\cos(\omega \cdot t)}{\cos(\omega \cdot t - \delta)} \tag{20}$$

E^* ..... complex modulus [$J \cdot g^{-1}$]

This term can be transferred into a complex numbers expression, separating the complex modulus into a real part, the storage modulus, and into an imaginary part, the loss modulus (eq. 21).

$$E^* = \frac{\sigma_0}{\varepsilon_0} \cdot \cos\delta + i \cdot \frac{\sigma_0}{\varepsilon_0} \cdot \sin\delta = E' + i \cdot E'' \tag{21}$$

E' ..... storage modulus [MPa]
E'' ..... loss modulus [MPa]

The storage modulus is a term for the quantity of stored energy during the deformation and therefore the elastic behavior, whereas the loss modulus, however, represents the dissipated energy, the viscous behavior.
Especially important for (semi)crystalline materials, like TPUs, is the fact, that in the range of the glass transition a dramatic decrease of the storage modulus can be observed (Figure 80). The value of E'', however, runs through a relative maximum at the glass transition temperature. Therefore, the Tg can be obtained from the inflection point of the storage modulus curve as well as from the relative maximum of the E'' curve. Both values of Tg differ a little from each other and it is a matter of philosophy which value is stated. In this study Tg was determined at the maximum of E''.

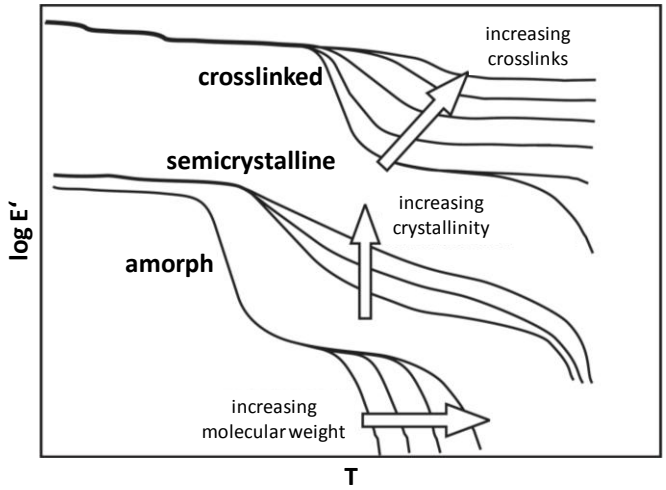

Figure 80. Temperature dependency of the storage modulus [272]

Two degradable polymers with good mechanical performance during the tensile tests (**P06** and **P08**) and Pell were selected for the DMA measurements. Therefore films were solution-cast as described before and stripe specimens with a length of about 20 mm and widths of about 2 mm were cut. Clamping lengths were about 1.5 mm. The specimens were tested with an angular frequency of $\omega = 1\ \mathrm{Hz}$, a strain amplitude of $\varepsilon_0 = 0.1\ \%$, within the temperature range of -100 to 50°C, with a heating rate of 3°C/min at least in duplicate. Table 24 sums up the results (for detailed information see appendix).

Table 24. Results of the tensile DMA measurements

Polymer ID	*composition*	*E [MPa]/20°C*	*E [MPa]/37°C*	*Tg [°C]*
P06	HMDI/pTHF1000/TPEG 2:1:1	87±1	76±1	-60±3
P08	HMDI/pTHF1000/EGLA 3:1:2	84±5	74±5	-60±1
Pell	commercial product	26±2	23±3	-44±1

The aliphatic TPUs have higher moduli as already seen in classical tensile tests. The Tg that is predominately determined by the soft-block is significantly lower in case of the self-synthesized TPUs **P06** and **P08**. This may indicate that the prepolymer in **Pell** has a lower molecular weight than the **pTHF** used for the synthesis. However, decreasing the length of the **pTHF** will also lead to increased moduli and this is unfavorable because the moduli of the aliphatic TPUs are already quite high. So, in addition, the chain extender content has to be decreased too.

2.7.2. Degradability

The remodeling capacity of materials used for tissue regeneration is mainly determined by their ability to degrade *in-vivo* and to induce new tissue formation. This is the main idea of tissue engineering and also circumvents follow-up surgeries to remove the implant due to a failures or long-term adverse effects. The biodegradability of most of the materials in clinical use rest upon the cleavage of ester bonds as found in polymers like **PLA**.[47] The synthesized TPUs contain very similar structures, therefore it was expected that the degradation will occur in time ranges as also certificated for surgical **PLA** material.

Usually, degradation *in-vivo* and *in-vitro* can hardly been compared, as there are too many factors that influence the behavior in real life. Nevertheless, *in-vivo* degradation behavior of biomaterials is commonly simulated by hydrolysis *in-vitro* under physiological conditions at pH 7.4 using PBS at 37°C. The degradation time in these cases can be up to several years.[46] Therefore different methods are used in literature to accelerate this process. This can be either done by increasing the pH-value [129, 312, 320, 321], the use of elevated temperature [320] or by enzymatic catalysis [322]. In this study, the approach of elevated temperature was used. Degradation tests of all materials, except **P09**, were conducted, regardless of the fact whether mechanical data could be assessed or not.

Therefore small platelets of the material were immerged into PBS solutions that were then applied to an autoclave at 110°C. The mass erosion (m_{eros}, eq. 22, Figure 81 left) as well as the drop of molecular weight (M_{drop}, eq. 23, Figure 81 right) of the materials were assessed. Pell and surgical PLA were used as references.

$$m_{eros}(\mathrm{t}) = \frac{m_t - m_o}{m_o} \cdot 100\% \tag{22}$$

$$M_{drop}(\mathrm{t}) = \frac{M_t - M_o}{M_o} \cdot 100\% \tag{23}$$

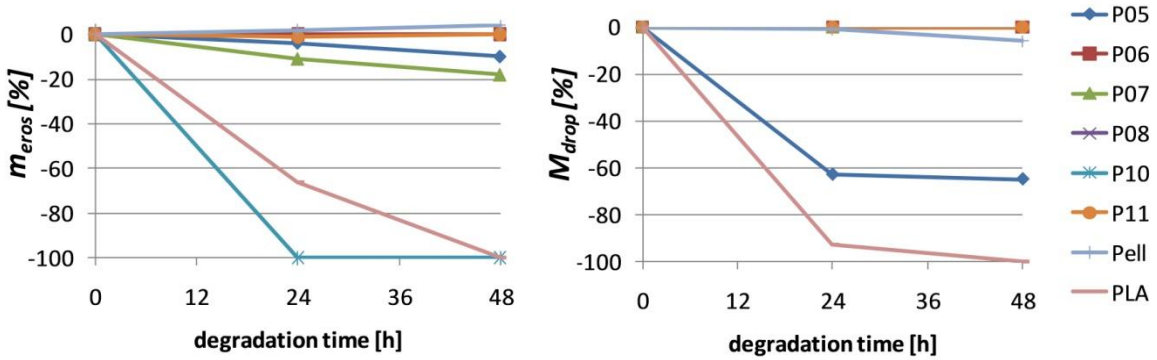

Figure 81. Degradation curves of the TPUs

The mass erosion progressed in an approximately linear fashion, so degradation rates ($\dot{m}_{eros}$, eq. 24) can be defined to easily compare the different degradation velocity (Table 25).

$$\dot{m}_{eros} = -\frac{1}{n} \cdot \sum_n \frac{m_{eros}(\mathrm{t})}{\mathrm{t}} \tag{24}$$

Table 25. Degradation rates

material	*P05*	*P06*	*P07*	*P08*	*P10*	*P11*	*Pell*	*PLA*
$\dot{m}_{eros}$ ***[%/h]***	0.2	0.0	0.4	4.2	4.2	0.0	0.0	2.4

As expected, the polymer **P05**, containing high amount of the terephthalic acid based CCE has a rather low degradation rate owing to the relative high stability of the aromatic ester bonds. It is interesting, however, that **P06**, which contains the same CCE with a decreased ratio, showed no mass loss at all. It was expected, that the reduction of chain extender (to tune the mechanical properties) in case of P06 would only have a small impact on the degradability. The polymer with the lactamide groups containing CCE **EDLA**, **P07** degrades faster than **P05**. This is due to the fact that the aliphatic ester bonds can be cleaved more easily. However, the additional H bonds from the lactamide groups within the hard blocks seem to retard the degradation process because **PLA** possesses the same ester bonds but in a different chemical environment. Surprisingly the polymers with the small lactate based CCE **EGLA**, **P08**, or the sulfur containing CCE **TGEG** degraded fastest and with approx. the doubled speed of the surgical bench mark **PLA**. The polymer with the polycarbonate soft block, **P11**, exhibited no mass loss under the degradation test conditions. This was expected because the carbonate group is known to have high hydrolytic stability. **Pell** exhibited no degradation at the tested conditions; the gain of mass can be attributed to swelling. **PLA** degraded within 48 h.

The drop in molecular weight could only be determined for the polymers that were not already degraded after the first run. For a mass erosion of 100% the drop of molecular weight was defined as 100%. The most interesting result is that **P05** with terephthalic acid based CCE and **PLA** both have a distinct drop in molecular weight while the polymer with the lactamide groups containing CCE **EDLA**, **P07**, had no drop at all. This might indicate surface erosion instead of a bulk erosion mechanism as observed for **PLA** and **P05**, maybe also caused by the lactamide groups of the CCE.

Again there is a clear difference between chemically similar polymers **P05** and **P06**. The molecular weight of **P05** drops visibly while **P06** seems to remain unchanged.

2.8. Electrospinning and tests of electrospun grafts

The electrospinning (ES) process can provide scaffolds with micro- to nanoscale topography and high porosities, and can therefore mimic the natural extracellular matrix.[152-154] It is a very easy but empirical process that can be perform with comparably low technical effort. Vascular grafts were fabricated with an ES device consisting of a high-voltage power supply, a custom-made infusion pump, a syringe, a rotating mandrel, and a back electrode.[171] The syringe was filled with the polymer solution and was fitted with a blunt-ended needle which was connected to ground. The polymer solution was pressed through the syringe at a flow rate of 0.01 mL/min. The grafts were made from solutions of about 5% (w/w) of the TPUs in 1,1,1,3,3,3-hexafluoro-2-propanol. The mandrel was rotated at 200 rpm and oscillated 150 mm in the transverse direction at a speed of 8 mm/s. The grafts were spun with a voltage of 20 kV to the back electrode and had an inner diameter of 2.1 mm, lengths of about 140 mm, and wall thicknesses of about 100 µm that were controlled by the spinning time.

The grafts were tested in circumferential direction in a special tensile testing arrangement according to Figure 82.[171] Again, Pell was taken as bench mark.

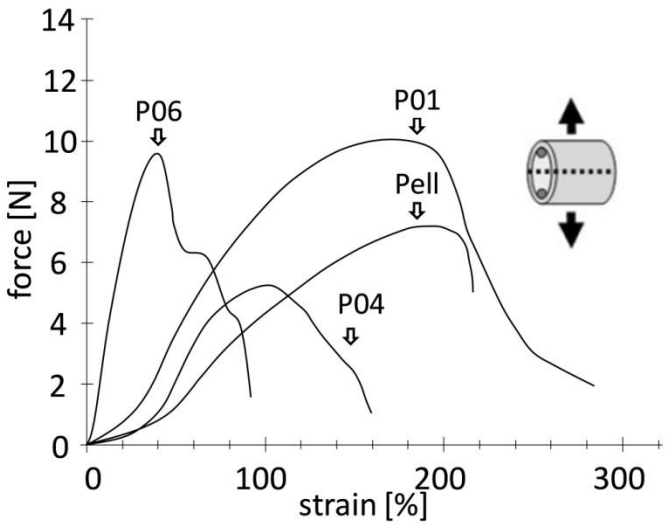

Figure 82. Tensile test results of tubular grafts

In Figure 82 the results of the tensile tests can be seen. The relevant range of the circumferential elongation was already discussed in section 1.2.2.5 and is up to about 14%. The aliphatic TPU **P04** shows a very good compliance within this range, however, it has only about 66% of the strength of the commercial **Pell**. The replicate of **Pell P01** exhibits a better performance as measure by the ultimate force and elongation. However, very good strength could be obtained for the polymer P06 containing the CCE **TPEG**. For this **P06** was considered for the first in vivo tests with rats. The rat aorta model is suitable to simulate the fluid dynamic conditions of human coronary arteries as the flow rate and the diameter are in a comparable range.

Detailed information concerning the outcome of the *in-vivo* tests cannot be provided to date. However, the first animals were sacrificed after 6 months after implantation to extract the artificial blood vessels for the histological examinations (Figure 83). The extracted graft indicated no signs of the formation of thrombi which is a very good preliminary result.

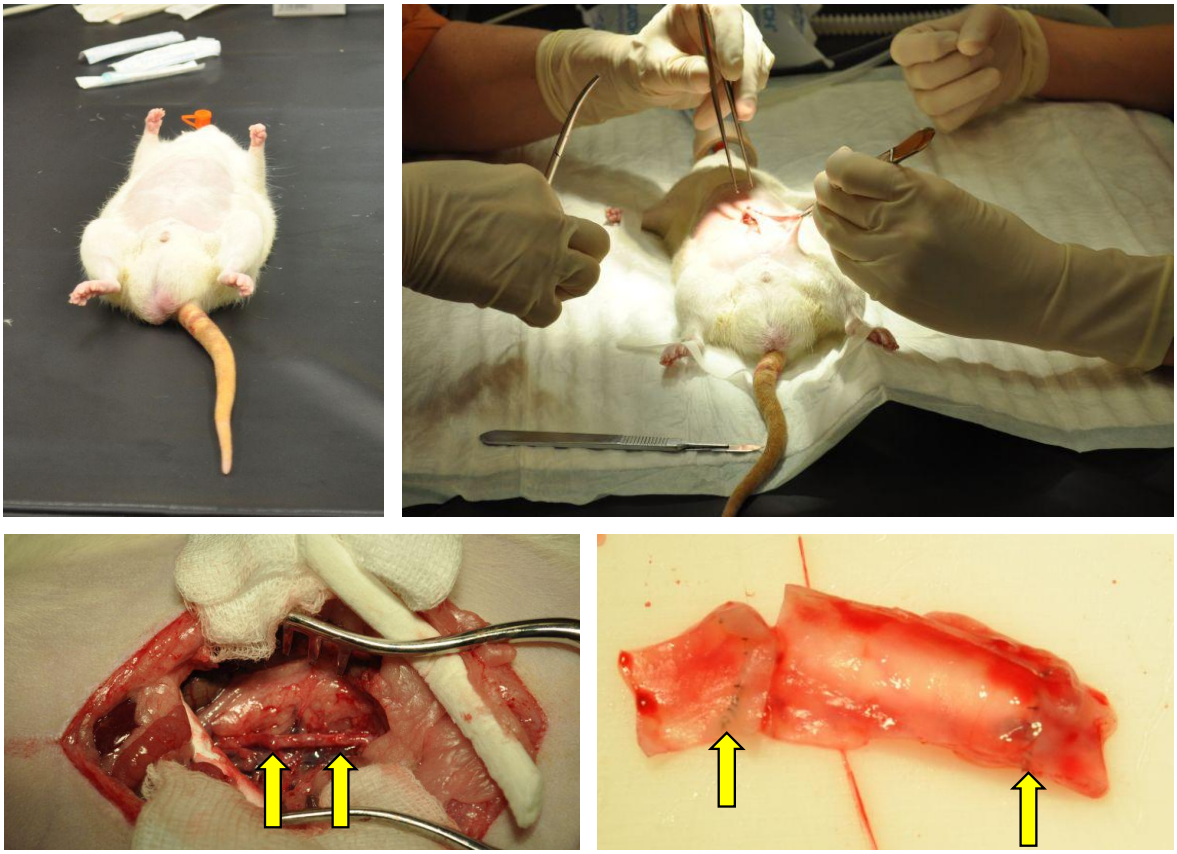

Figure 83. Rat aorta *in-vivo* investigation of the electrospun grafts consisting of the developed degradable TPU; Both anastomoses are marked with yellow arrows

Conclusion

Cardiovascular diseases are the chief cause of mortality in industrial countries. Especially elderly but also young people due to unhealthy life style are concerned, however, the elderly population suffers from the fact that the state-of-the-art material for bypass surgeries to cure ischemic heart disease still is of autologous origin. This means that it has to be harvested from the patient himself. Aside the complications that might occur owing to the multiple surgery procedure it is not at all certain, that elderly patients can donor sufficient materials themselves. Considering using artificial vascular material, one is faced with the issue that both biomedical approved materials (PTFE and PET) are not suitable for the long term application as coronary artery bypass graft. Advances in tissue engineering – especially of bone and cartilage tissues – has prompted the research for materials for vascular restoration. However, tissue engineering makes great demands on the materials used for the scaffolds for the guided cell growth.
In this work two different approaches were attempted to develop new materials for vascular tissue regeneration. On one hand Additive Manufacturing Technologies (AMT), particularly Microstereolithography (µSLA) and Digital Light Processing (DLP) – which both are based on the layer-by-layer fabrication of a photosensitive resin cured by photopolymerization – enable the fabrication of 3D scaffolds with defined shapes, pore sizes and interconnectivity of the pores which is favorable for all tissue engineering applications. On the other hand the very simple method of Electrospinning (ES) has emerged to be a very powerful tool to directly fabricate porous conduits out of (biocompatible) thermoplastics with a microstructure that perfectly mimics the extracellular matrix. Therefore suitable materials for both manufacturing methods were developed.
In previous work the surpassing material properties of poly(cyanoethyl acrylate) (poly-CEA) were studied. It was unclear whether the electronic influence of the cyano groups, the cyano group itself or crosslinking by chain transfer reactions during polymerization was responsible for these properties. Therefore different analogous compounds were synthesized to investigate the exceptional behavior of these polymers.

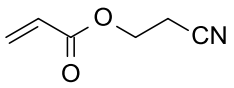

CEA

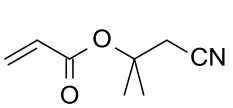

Me_2CEA

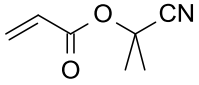

Me_2CMA

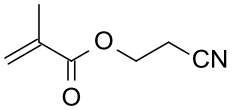

CEMA

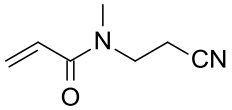

NCEA

From the subsequent study of the photoreactivity of the monomers and the mechanical/thermal properties and solubility of the polymers it could be assumed that the elastomeric behavior of the polymers of CEA, CEMA and Me_2CEA seems to be caused by crosslinking via hydrogen abstraction of the hydrogen atoms next to the cyano group. Similar to natural rubber a crosslinking density of about 0.1 to 1 per 100 monomer units leads to elastomeric properties. In sight of high reactivity and mechanical properties at physiological temperatures CEA was still the most promising substance. Therefore CEA based monomer formulations were optimized for µSLA and the biocompatibility of the system was improved by application of hydrogels. However, the first experiences of the surgeons with the material emphasized its incapability for being sewed, which is the exclusive implantation method. In the end this material does not possess any degradability aside from the cleavability of the ester bonds whose cleavage would, however, not lead to low

molecular compounds that could be eliminated by the body. Therefore other materials were investigated.
Materials containing urethane groups are known to have very good (elastic) properties and also possess sufficient biocompatibility. Therefore urethane acrylate systems were studied in a wider context. Different commercially available urethane oligomer acrylates were tested in combination with a large variety of monoacrylates as reactive diluents. The best preliminary results were obtained with an urethane oligomer diacrylate (UDA) from the company Rahn in combination with hydroxyethyl acrylate (HEA). However, to adjust the material properties to match those of native blood vessels high contents of HEA were needed but the obtained material had insufficient suture tear resistance. This was due to the very low content of urethane groups. To increase the amount of urethane groups in the material the content of UDA had to be increased. However, the tightly crosslinked photopolymers would be to stiff for the designated application. Therefore dithiols were added to the formulations. Thiol-ene polymer systems are known to have rather low moduli but high elongations and strengths. This way the urethane group content could be increased significantly with obtaining hard materials. The optimized photosensitive resins contained UDA, HEA and ethylene glycol bisthioglycolate (EGTG) as chain transfer agent.

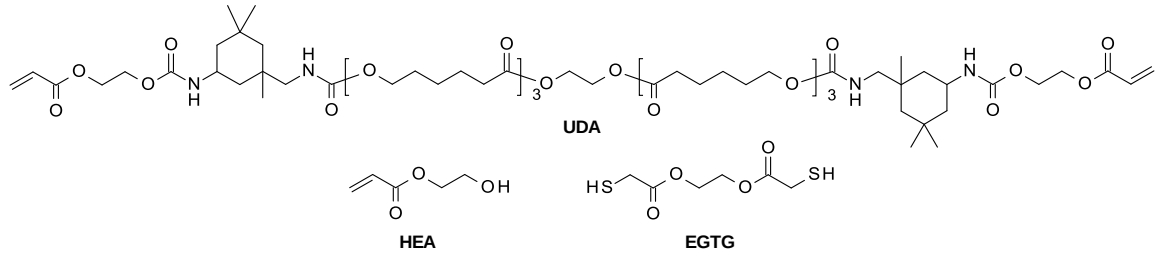

The components were combined in a ratio that predominantly linear, slightly branched but hardly crosslinked photopolymers were formed. The high content of urethane groups causes a high density of reversible crosslinks due to H bonds. These bonds can be cleaved and regenerated during the deformation of the material. With this polymer architecture the material had elastomeric properties comparable to native vascular tissue and showed good performance in suture tear resistance tests. Additionally these polymers possessed an inherent degradability owing to the (hydrolytically) cleavable ester bonds along the back bone (introduced through EGTG) and the branches/crosslinks (introduced by the poly(caprolactone) spacer of UDA) of the polymers which was comparable to those of surgical poly(lactic acid). Specimens of this material exhibited a good endothelial cell attachment which is crucial for the long term performance of the vascular grafts (Figure 84).

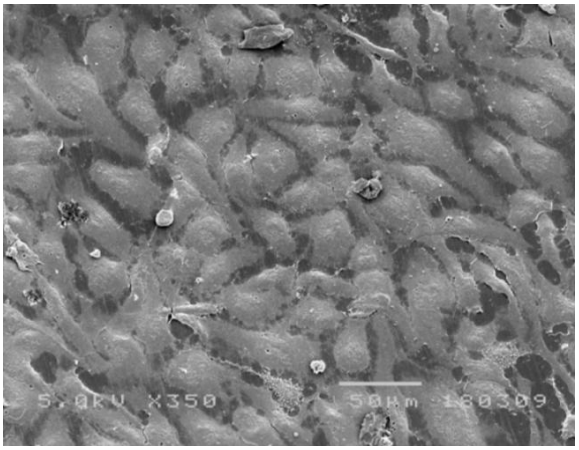

Figure 84. Human umbilical vein endothelial cell attachment on polymer specimen

The photopolymers could also be processed by the desired AM technology DLP and cellular structures as well as conduits were fabricated (Figure 85).

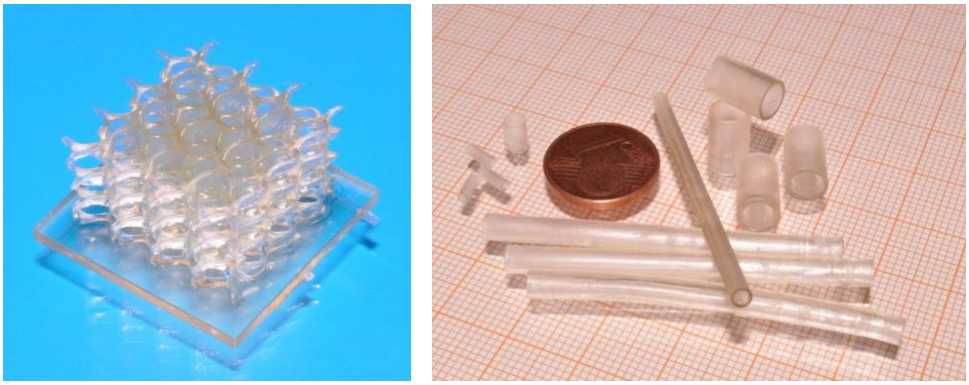

Figure 85. Manufactured parts of biocompatible, degradable photopolymer

On the other hand degradable thermoplastic urethane elastomers (TPU) for ES were developed. The commercial TPU Pellethane which has already shown good performance as electrospun vascular grafts in rats was taken as bench mark. Modeled on Pellethane different segmented TPUs should be synthesized which possess (bio)degradability. Pellethane is composed of the diisocyanate methylene diphenyl diisocyanate (MDI), the macrodiol poly(tetrahydrofuran) (pTHF) and the chain extender 1,4-butandiol (BDO). To develop a method for the synthesis of TPUs and assess the exact composition of Pellethane, the commercial polymer was replicated in a separate preliminary study.

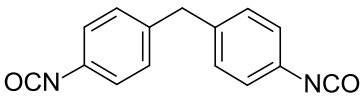

MDI

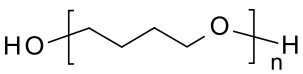

pTHF

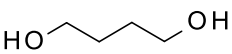

BDO

For the design of degradable TPUs for biomedical applications it is important to consider all cleavage products that might be liberated during degradation. From MDI derived degradable TPUs aromatic diamines could probably form. For this the first modification towards degradable TPUs was the exchange of MDI with the aliphatic hexamethylene diisocyanate (HMDI). The tensile strength of aliphatic copies of Pellethane decreased to about 66% of those of Pellethane itself but should still be sufficient for the application. In the subsequent step the chain extender BDO was exchanged with cleavable chain extenders (CCE) to introduce hydrolytic degradability. The CCE were based on either ethylene glycol or lactate. The two best CCE were hydroxyethyl lactate (EGLA) and bis(2-hydroxyethyl) terephthalate (TPEG).

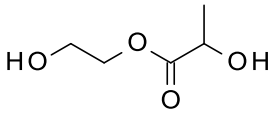

EGLA

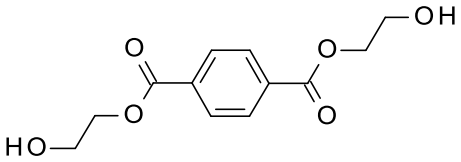

TPEG

TPUs containing EGLA as chain extender exhibited an *in-vitro* degradability with the double rate of surgical poly(lactic acid) (PLA) while TPUs with TPEG degraded only with rates of about the tenth of PLA. This result was expected due to the relative high hydrolytic stability of the aromatic ester bonds. The cleavage products assumed to be form during polymer degradation (HDHC and HDLA) were synthesized and tested for their cytotoxicity but no acute toxic effects were observed.

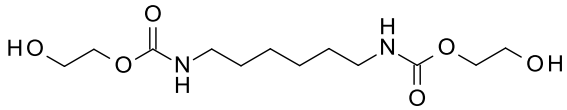

HDHC

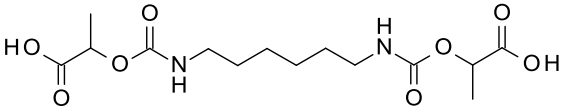

HDLA

Interestingly, the aromatic groups – introduced by the rather harmless terephthalic acid – within the backbone of the polymers containing TPEG improved the mechanical properties of the material compared to the neat aliphatic TPUs. The electrospun conduits of these degradable TPUs had tensile strengths comparable to the bench mark Pellethane.

Encouraged by the very good mechanical performance of the material as electrospun conduits *in-vivo* tests were started. The conduits were grafted to the aortae of rats. 6 month after implantation no sign of the formation of thrombi were observed (Figure 86) what makes this material to a promising candidate for vascular tissue regeneration.

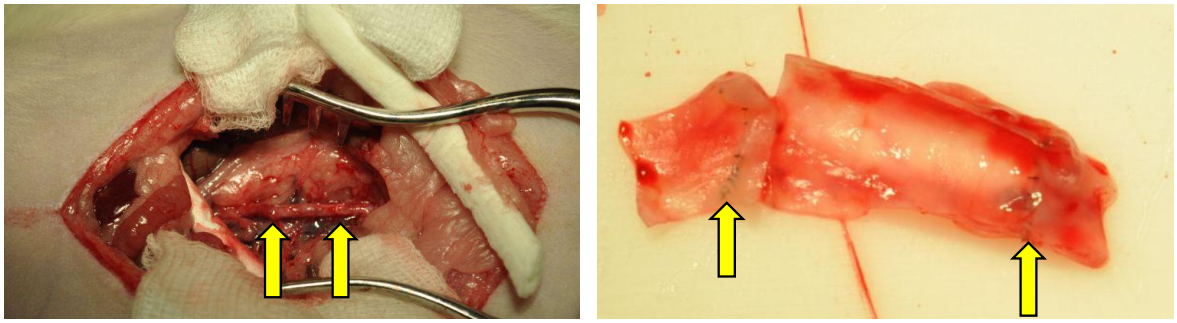

Figure 86. In-vivo tests: rat aorta graft (left) and explanted, opened conduit (right)

Experimental

1. Photoelastomers

1.1. New monomers

1.1.1. Synthesis

1.1.1.1. Synthesis of 2-cyanoethyl acrylate (CEA)[323]

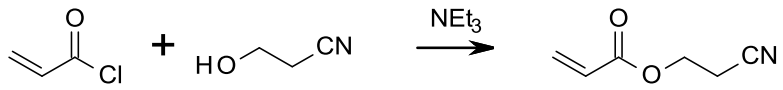

CEA

[90.51] [71.08] [125.12]

Reagents	2-hydroxypropionitrile	5.00 g	70.3 mmol
	triethylamine	12.10 g	119.6 mmol
	acryloyl chloride	7.60 g	84.4 mmol

Procedure
A solution of 2-hydroxypropionitrile and triethylamine in 50 mL of dichloromethane was cooled to -10°C. Acryloyl chloride in 30 mL of dichloromethane were added dropwise while stirring so that the temperature did not exceed -5°C. The solution was stirred overnight at room temperature, filtered, extracted with 1M aq. HCl (3 x 100 mL) and 10% (w/v) aq. NaOH (100 mL), dried over anhydrous Na_2SO_4 and filtered. After the addition of 5 mg hydroquinone monomethyl ether as stabilizer the solvent was evaporated in vacuo. Purification by distillation (b.p. 52-54°C, $9 \cdot 10^{-3}$ mbar; 108°C, 12 torr [323]) gave 6.1 g(69%) of **CEA** as a colorless liquid.
^{1}H NMR ($CDCl_3$): δ (ppm) = 6.46 (1H, dd, J = 17.0, 1.6 Hz, H(H)C=C), 6.13 (1H, dd, J = 17.2, 10.4 Hz, HC=C), 5.90 (1H, dd, J = 10.4, 1.6 Hz, H(H)C=C), 4.35 (2H, t, J = 6.4 Hz, O-CH_2), 2.73 (2H, t, J = 6.4 Hz, -CH_2-CN);
^{13}C NMR ($CDCl_3$): δ (ppm) = 165.44, 132.24, 127.40, 116.87, 58.79, 18.00;
GC-MS: 3.50 min, m/z = 54.10, 55.06, 70.06, 72.04, 85,04.

1.1.1.2. Synthesis of 2-cyano-1,1-dimethylethyl acrylate (Me_2CEA)

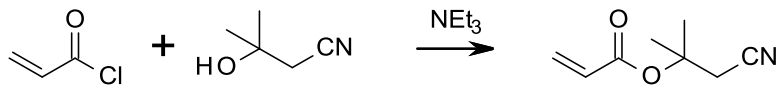

Me_2CEA

[90.51] [99.13] [153.18]

Reagents	3-hydroxy-3-methylbutyronitrile	5.00 g	50.4 mmol
	triethylamine	8.66 g	85.7 mmol
	acryloyl chloride	5.47 g	60.5 mmol

Procedure
Me_2CEA was obtained from 3-hydroxy-3-methylbutyronitrile and acryloyl chloride according to the procedure described for **CEA** as a colorless liquid with a yield of 26%.

B.p.: 42-45°C ($1.5 \cdot 10^{-1}$ mbar);
^{1}H NMR ($CDCl_3$): δ (ppm) = 6.37 (1H, dd, J = 17.1 Hz, 1.7 Hz, H(H)C=C), 6.06 (1H, dd, J = 17.1 Hz, 10.3 Hz, HC=C), 5.82 (1H, dd, J =10.4 Hz, 1.6 Hz, H(H)C=C), 2.96 (2H, s, CH_2), 1.63 (6H, s, CH_3);
^{13}C NMR ($CDCl_3$): δ (ppm) = 165.20, 131.14, 129.02, 116.66, 78.16; 29.59, 25.92;
GC-MS: 3.12 min, m/z = 55.2, 73.2, 81.3, 82.3, 113.2.

1.1.1.3. Synthesis of 1-cyano-1-methylethyl acrylate (Me_2CMA)

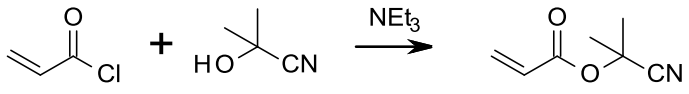

Me_2CMA

[90.51] [85.10] [139.15]

Reagents	2-hydroxy-2-methylpropionitrile	5.00 g	58.8 mmol
	triethylamine	10.11 g	99.9 mmol
	acryloyl chloride	6.38 g	70.5 mmol

Procedure
Me_2CMA was obtained from 2-hydroxy-2-methylpropionitrile and acryloyl chloride according to the procedure described for **CEA** as a pale yellow liquid with a yield of 22%. B.p.: 39-40°C ($3 \cdot 10^{-1}$ mbar); ^{1}H NMR ($CDCl_3$): δ (ppm) = 6.47 (1H, dd, J = 17.0 Hz, 1.6 Hz, H(H)C=C), 6.09 (1H, dd, J = 16.9 Hz, 10.5 Hz, HC=C), 5.92 (1H, dd, J =10.4 Hz, 1.6 Hz, H(H)C=C), 1.79 (6H, s, CH_3); ^{13}C NMR ($CDCl_3$): δ (ppm) = 163.98, 132.72, 127.49, 119.29, 68.51; 26.90; GC-MS: 2.94 min, m/z = 55.01, 56.07, 67.07, 68.06, 72.99, 84.03.

1.1.1.4. Synthesis of 2-cyanoethyl methacrylate (CEMA)

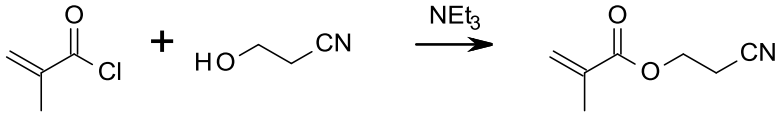

CEMA

[104.54] [71.08] [139.15]

Reagents	2-hydroxypropionitrile	5.00 g	70.3 mmol
	triethylamine	12.10 g	119.6 mmol
	methacryloyl chloride	8.82 g	84.4 mmol

Procedure
CEMA was obtained from 2-hydroxypropionitrile and methacryloyl chloride according to the procedure described for **CEA** as a colorless liquid with a yield of 72%. B.p.: 54-56°C ($1.5 \cdot 10^{-2}$ mbar) (42-43°C, 0.45 torr [324]); ^{1}H NMR ($CDCl_3$): δ (ppm) = 6.17 (1H, m, H(H)C=C), 5.63 (1H, m, H(H)C=C), 4.35 (2H, t, J = 6.3 Hz, O-CH_2), 2.75 (2H, t, J = 6.3 Hz, -CH_2-CN), 1.94 (3H, m, CH_3); ^{13}C NMR ($CDCl_3$): δ (ppm) = 166.72, 135.42, 126.95, 116.89, 58.95; 18.19, 18.07; GC-MS: 4.26 min, m/z = 54.02, 55.08, 68.02, 69.05, 70.07, 85.98.

1.1.1.5. Synthesis of N-methylcyanoethyl acrylamide (NCEA)

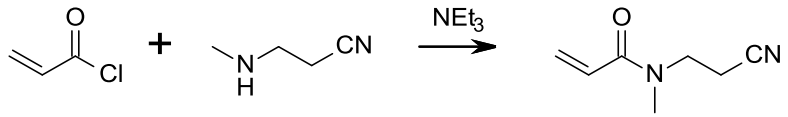

NCEA

[90.51] [84.12] [138.17]

Reagents	N-methylcyanoethyl amine	8.00 g	95.1 mmol
	polyvinyl pyridine	12.10 g	190.0 mmol*
	acryloyl chloride	10.30 g	114.1 mmol
			*active sites

Procedure
A solution of N-methylcyanoethyl amine in dichloromethane (100 mL) was cooled to -10°C and polyvinyl pyridine was added under argon atmosphere. After stirring for 5 min, a solution of acryloyl chloride in dichloromethane (80 mL) was added dropwise. The reaction was stirred for 17 h. The mixture was filtered and the solid washed with dichloromethane (200 mL). After the addition of 3 mg hydroquinone monomethyl ether the solvent was evaporated in vacuo. Purification by distillation (b.p.: 102-105°C, $1 \cdot 10^{-2}$ mbar) gave 5.6 g (43%) of **NCEA** as a colorless liquid.
^{1}H NMR ($CDCl_3$): δ (ppm) = 6.56 (1H, dd, J = 10.2 Hz, 16.7 Hz, HC=C), 6.33 (1H, dd, J = 2.05 Hz, 16.8 Hz, H(H)C=C), 5.73 (1H, dd, J = 2.1 Hz, 10.2 Hz, H(H)C=C), 3.66 (2H, t, J = 6.5 Hz, N-CH_2-), 3.21 (s, 3H, N-CH_3), 2.67 (2H, t, J = 6.5 Hz, -CH_2-CN);
^{13}C NMR ($CDCl_3$): δ (ppm) = 166.56, 128.82, 127.00, 118.30, 45.08; 36.91, 16.02;
GC-MS: 5.73 min, m/z = 54.09, 55.05, 69.06, 98.01, 99.08, 138.06, 139.09.

1.1.2. Photo-differential scanning calorimetry

About 5 mg of the monomer (-mixture) containing 1% (w/w) photoinitiator (Irgacure 819®) were weighed in accurately into an aluminum pan taking care that the drops always have a similar shape. If the accruing heat exceeded the capacity of the device less monomer was weighed in. This pan was positioned at the right sensor of the measuring cell. The left sensor was occupied with a pan with about the same amount of already cured polymer as reference. Subsequently the cell was equipped with a special aluminum cylinder. The light guide was inserted into the hole of the cylinder and the chamber was purged with nitrogen (50 mL/min) for about 5 minutes while the system also equilibrated. The DSC device was switched into the record mode and after 1 minute the irradiation was activated and deactivated as soon as a steady state has been observed or after 30 minutes.

1.1.3. Tests of the photopolymers

1.1.3.1. Solubility and thermal properties

1.1.3.1.1. Production of photopolymer specimens

To manufacture the silicone mould to cure the resins, a special silicone resin from the company Wacker (Elastosil M 4470) was used. About 3 g of the curing agent T40 were weighed in and about 97 g silicon resin were added. The components were mixed using a glass rod before it was degassed within a vacuum chamber.
The desired specimen shape was manufactured using the Rapid Prototyping system called Perfactory from the company Envisiontech. The positive-moulds were glued on an aluminum foil and a ring was applied to form a cavity. The mixed formulation was poured into the cavity taking

care not to enclose bubbles. Manufacture's data declare that the resin is cured after about 12 hours. But generally 24 h were necessary before the mould was removed from the cavity and stored for a period of 12 h in the vacuum oven at 60°C. The positive-mould can be recycled.
After all components of the photo resin were weighed in and mixed the resin was filled into the silicon mould by the aid of a pipette and the cavities of the mould were covered with a glass plate. The UV lamp was activated and 5 minutes were waited to let the lamp warm up. Ventilation fans start automatically but the water cooling had to be activated manually. The nitrogen chamber was placed onto the transportation belt and transferred into the UV chamber. The curing time was 5 minutes. For demolding the parts the silicone mould can be bent. Subsequently the specimens were irradiated for 5 minutes from the other side. The mould was cleaned after every curing process with acetone.

1.1.3.1.2. Thermal differential scanning calorimetry
Thermal DSC measurements were carried out with a Netzsch DSC 204 F1 device with an Intracooler type ETK100/A. About 5 mg of the polymer were weighed into an aluminum pan. The polymer samples were heated to 200°C and cooled to 0°C with rates of 2°/min before the real DSC measurement was started from 0 to 200°C with a rate of 2°/min. The glass transition temperatures were calculated by means of the software provided by Netzsch.

1.1.3.3. Mechanical properties
The carotid artery of a sheep obtained from the Medical University of Vienna was cut into rings of about 5mm length using a scalpel. Those rings were cut to open them as little cuboid specimen. Width and thickness were measured very carefully using a sliding caliper.
The tensile testing machine (Zwick Z050) was equipped with a very sensitive 1 N load cell and two small clamps with sand paper to avoid slipping through of the specimens. Unfortunately no extensometer system due to the very small necessary clamping width could be applied. After calibrating the elevating system the clamps were driven to a clamping width of 5 mm and one of the prepared specimens were clamped in orthogonally. After the dimensions of the specimen were entered into the software shell the measurement was started. The real measurements with a crosshead velocity of 5 mm/min began when a pre-load of 0.05 N was achieved. The measurements were aborted when the specimens apparently were broken.
As described above, specimens of the photopolymers for the mechanical tests were produced by curing of the desired resin in suitable moulds. To achieve a higher accuracy the specimen had a width of about 10 mm and a thickness of about 1 mm. Specimens of CEA/ETA (1% (w/w)) hydrogels with 50, 40 and 30 % water were produced and extracted twice with EtOH and four times with water each over night. The clamps of the tensile testing machine were also equipped with sand paper to avoid slipping. After the system was calibrated the clamps were driven to a clamping width of 10 mm. The specimens were clamped in and the dimensions were entered into the software shell. Before the measurements with a crosshead velocity of 10 mm/min were started the specimens were pre-loaded with 0.1 N. The measurements were aborted when the specimens apparently were broken.

1.1.4. Additive Manufacturing Technology: Microstereolithography
With the parameters optimized by penetration tests, conduits were printed onto an aluminum support plate with a laser power of 2 mW and optimized laser speed. The CAD model of the target structure was sliced into equidistant layers of 50 µm; the hatching and the line reduction were adjusted in order to obtain optimum results. The non-cured resin was removed by rinsing with 2-propanol and a post curing step under the UV lamp was performed.

1.2. Macromonomer based photoelastomers

1.2.1. Polyester based photopolymers

1.2.1.1. Synthesis of a slightly branched polyester methacrylate

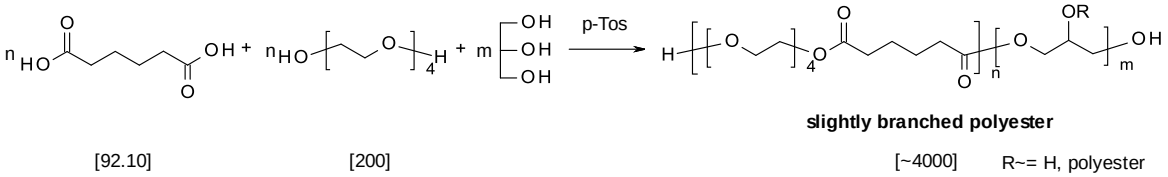

[92.10] [200] [~4000] R~= H, polyester

Reagents	polyethylene glycol (200 g/mol)	10.00 g	50.0 mmol
	adipic acid	7.30 g	50.0 mmol
	glycerol	0.40 g	4.4 mmol

Procedure
A solution of polyethylene glycol, adipic acid, glycerol and 0.5 g p-toluenesulfonic acid in 100 mL toluene was refluxed for 4 h using a water distilling trap. The solvent was evaporated in vacuo, the residue was dissolved in chloroform and extracted thrice with distilled water. The organic phase was dried with sodium sulfate, filtrated and the solvent was evaporated in vacuo. 17.95 g of the intermediate polyester was obtained as a pale yellow viscous mass.
^{1}H-NMR ($CDCl_3$): δ(ppm) = 4.16 (4H, t, J = 0.1 Hz, CH_2-O-CO), 3.78 - 3.54 (approx. 17H, m, -O-CH_2-CH_2-O-), 2.41 - 2.25 (4H, m, -O-CO-CH_2-), 1.77 - 1.58 (4H, m, -O-CO-CH_2-C$\underline{H}_2$-);
OH value: 0.0005 mol/g.

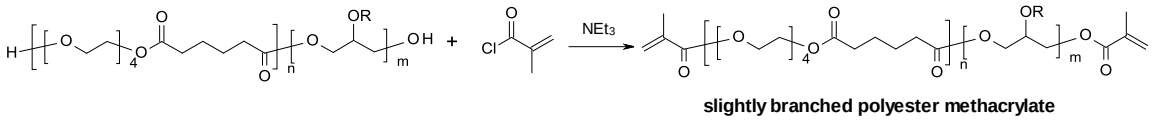

[~4000] [104.54] [~4150] R = methacrylate, polyester

Reagents	polyester (4000 g/mol)	17.95 g	4.5 mmol
	triethylamine	1.80 g	17.8 mmol
	methacryloyl chloride	1.14 g	10.9 mmol

A solution of the obtained polyester and triethylamine in 50 mL of dichloromethane was cooled to -10°C. Methacryloyl chloride in 30 mL of dichloromethane were added dropwise while stirring so that the temperature did not exceed -5°C. The solution was stirred overnight at room temperature, filtered, extracted with 1M aq. HCl (3 x 100 mL) and 10% (w/v) aq. NaOH (100 mL), dried over anhydrous Na_2SO_4 and filtered. The solvent was evaporated in vacuo. The polyester methacrylate was obtained as a pale yellow viscous mass with a yield of 13.93 g (76%).
^{1}H-NMR ($CDCl_3$): δ(ppm) = 6.14 – 6.07 (1H, m $\underline{H}$-CH=C), 5.60 -5.52 (1H, m, H-C$\underline{H}$=C), 4.20 (4H, t, J = 4,5 Hz, CH_2-O-CO), 3.74 -3,56 (approx 17H, m, -O-CH_2-CH_2-O-), 2.40 - 2,27 (4H, m, -O-CO-CH_2-), 1.94 – 1.90 (3H, t, J = 0.6 Hz, CH_3-C=CH_2), 1.74 - 1.55 (4H, m, -O-CO-CH_2-C$\underline{H}_2$-).

1.2.1.2. Determination of the hydroxyl value
The hydroxyl value was determined according to the standard DIN 53240. About 1 g of polymer (mg accuracy) was stirred with 1 mL of acetylation reagent, made out of 70 g of distilled pyridine and 30 g of distilled acetic anhydride, and 10 mL pyridine, for 70 min at approximately 110°C. Then the samples were titrated with 0.5 N potassium hydroxide titer solution against

phenolphthalein. A blank sample, not containing polymer, was treated analogous. The OH value can be calculated by eq. 25.

$$OH\ value = \frac{f \cdot c}{m} \cdot (B - A) \quad (25)$$

A.....consumption for sample [mL]
B..... consumption for blank [mL]
f.....titer factor [ ]
c.....concentration of titer solution [mol/L]
OH value..... hydroxyl value [mol/g]
m .....weight [g]

1.2.2. Urethane oligomer based photopolymers

1.2.2.1. Assessment of the base monomer

Determination of the double bond value
1 g (with 1 mg accuracy) of the acrylate resin was dissolved in 50 mL of a 1:1 mixture of toluene and ethanol, treated with 20 mL of a solution of dodecyl mercaptan (5% (w/w) in ethanol) and 3 mL of an ethanolic solution of KOH (5% (w/w)) under nitrogen atmosphere for 5 min at r.t. under stirring. The acetatic solution was titrated with 0.1 M iodine titer solution with starch as indicator. The double bond value (DB value) was calculated according eq. 26.

$$DB\ value = \frac{1}{1000} \cdot \frac{f \cdot c}{m} \cdot (B - A) \quad (26)$$

A..... consumption for sample [mL]
B.....consumption for blank [mL]
f .....titer factor [ ]
c ..... concentration of titer solution [mol/L]
DB value..... double bond value [mol/g]
m .....weight [g]

1.2.2.3. Formulations with the monoacrylate HEA as reactive diluent

1.2.2.3.1. Preparation of the molds

The molds for the tests of the mechanical properties of the photopolymers were made out of crosslinked polysiloxanes. In case of the molds for the suture tear resistance test specimens (20x10x2 mm^3), the positive pattern were printed by means of an Objet Eden 260 3D printer. The positive pattern for the molds for the large plates to punch out the specimen for the tensile tests was a glass plate (115x95x4 mm^3).
The positive patterns were glued to an aluminum foil and a border frame out of plasticine was placed around the arrangement. The freshly prepared polysiloxane casting mixture was poured into the mold after vacuum degassing and cured for 24 h at r.t.. After removing the plasticine, the aluminum foil and the positive pattern, the mold was stored for another period of 12 h in the vacuum oven at 60°C to complete the curing process and remove any volatiles.

1.2.2.3.2. Preparation of the formulations

For the preparation of the formulations the solid components (BPO, DBB) were first dissolved in the low viscosity MA and solvent (if used) before the thiol was added. Then, the solution was mixed with the highly viscous UDA. Bubbles were removed within a vacuum chamber before the formulation was poured into the mold and cured.

1.2.2.3.3. Preparation of test specimens

After the formulations were homogenized and all bubbles were removed, the monomer mixture was poured into the molds and the cavity was covered with a glass plate to reduce the effect of oxygen inhibition, the formation of a meniscus and to obtain an even surface. The filled molds were applied to the UV system. After 5 min exposure the cured part was demolded and irradiated for another 5 min from the other side.

The dog bone specimens (total length: 80 mm, measuring length: 15 mm, width 10 mm) for tensile tests were punched from plates (115x95x4 mm^3) while the specimens for the suture tear resistance tests (20x10x2 mm^3) were molded directly. Before the mechanical tests were performed, the specimens were extracted twice overnight in methanol and in distilled water to remove residual monomer/solvent (if used). Initially a supersonic bath was used. The tests were carried out in the wet condition to simulate the environment of the final application.

For the tests of native material fresh porcine coronary and ovine carotid arteries were used. Depending on the test procedure – tensile or tear resistance – the native blood vessels were prepared differently. Tensile tests (Figure 87a) were performed in circumferential direction which is the main loading situation of the blood vessel owing to the blood pressure. Suture tear resistance tests (Figure 87b), however, were performed in axial direction according to the anastomosis.

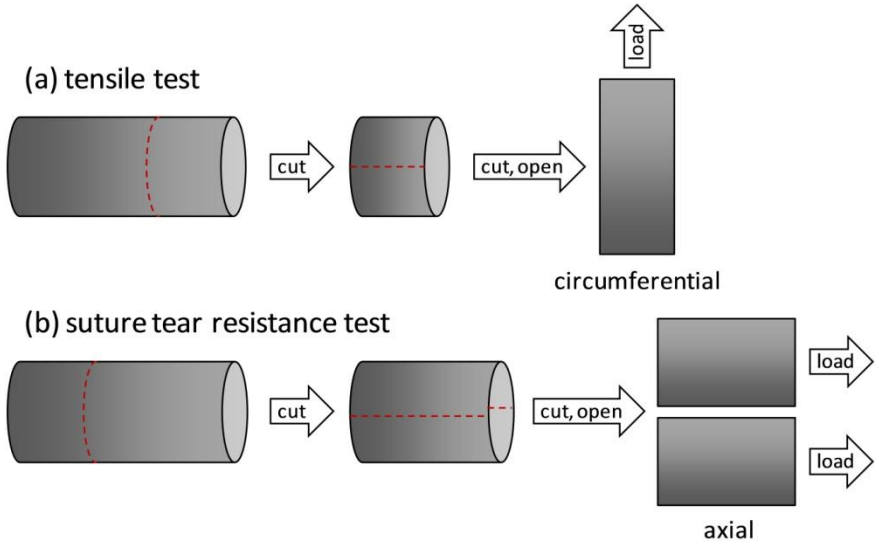

Figure 87. Preparation of the native blood vessels for the mechanical tests

1.2.2.3.4. Tensile test

The tensile tests were performed with a tensile testing machine type Zwick Z050. The elongation (ε) was determined from the cross-beam travel. The elastic modulus (E) was determined as secant modulus between an elongation of 0.05 and 0.5% while the tensile strength (S) was calculated from the peak force. All results were obtained at least in quintuplicate.

1.2.2.3.5. Suture tear resistance test

The molded specimens for the suture tear resistance tests were cut in the half with a knife (to avoid edge effects), supplied with a seam of surgical suture by the aid of a special gauge (seam distance 4 mm from the edge), clasped into a modified tensile testing arrangement (Figure 50) and loaded with a speed of 50 mm/min. The suture tear resistance (R_t) is calculated from the peak force (F) and the specimen depth (d) according to eq. 3.

$$R_t = \frac{F}{d} \tag{3}$$

All results were obtained at least in quintuplicate. Tests of the native blood vessels were performed analogous.

1.2.2.4. The thiol-ene concept

All tests were performed analogous to section 1.2.2.3.

1.2.2.6. Additive Manufacturing Technology: Digital Light Processing

1.2.2.6.1. Viscosity measurements

To determine the rheological properties, the dependency of the viscosity on shear rate was examined, using a Physica MCR 300 from the company Anton Paar with a cone-plate arrangement (25 mm diameter, 1° angle) at different shear rates and constant temperature (20°C).

1.2.2.6.2. Structuring with DLP

The fabrication of the 3D-parts was done using an EnvisionTec Perfactory® Mini Multi Lens with a resolution of 1400 x 1050 and a PTFE vat. Structures were built with a layer thickness of 50 µm at a lamp power of 1000 mW/dm². After completion of the structuring process, the prototype was rinsed with ethanol, followed by post-curing under the UV lamp and subsequent extraction with methanol and water for each 24 h.

1.2.2.7. Cellular compatibility

1.2.2.7.1. Cytotoxicity

All resin components as well as the degradation products were tested regarding their cytotoxicity. All substances (as far as possible) were prepared as a 1 M stock solution in DMSO.

1.2.2.7.1.1. Preparation of the trimer

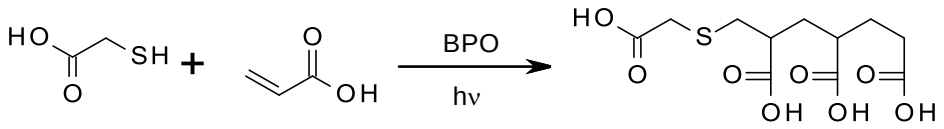

trimer

[92.12] [72.06] [308.30]

Reagents	acrylic acid	0.72 g	10.0 mmol
	mercaptoacetic acid	0.35 g	3.3 mmol

Procedure

The **trimer** was prepared by mixing acrylic acid with mercaptoacetic acid and 11 mg BPO. The mixture was irradiated according to the same procedure applied for the photopolymers but without additional treatment or work-up.

GPC measurements indicated that the potential **trimer** has a molecular weight of about 500 g/mol (theoretical value about 300 g/mol)

1.2.2.7.1.2. Preparation of the UDA spacer

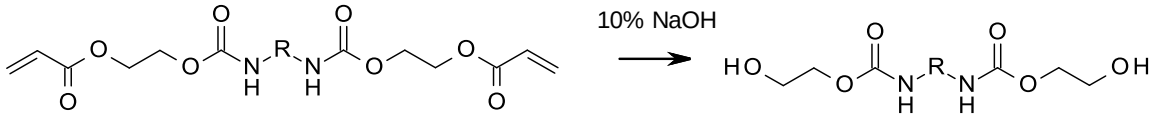

UDA
[~1500]

UDA spacer
[~1400]

Reagents	sodium hydroxide	1.00 g	20.0 mmol
	urethane diacrylate	5.00 g	3.3 mmol

Procedure
A solution of NaOH in 10 mL water was added to a solution of **UDA** in 10 mL THF. The mixture was stirred vigorously over night at 50°C. After evaporation of THF in vacuo, water was added to the residue and the product was extracted with chloroform. The organic phase was dried over sodium sulfate, filtered and the solvent was evaporated in vacuo. The pale yellow, waxy product was dried in vacuo to give 2.23 g (49%) of the **UDA spacer**.

1.2.2.7.2. Cell adhesion/proliferation

Preparation of the polymer specimens
The photopolymer test specimens had a disc-like shape with a diameter of about 13 mm and a thickness of about 1 mm—fitting perfectly into a 24-well-plate. To manufacture these specimens the resin was cured analogue to the procedure described for the specimens for the mechanical study. The extraction, however, was done more vigorous – thrice overnight in methanol and thrice overnight in distilled water, after an initial time of 10 min in methanol in the supersonic bath.

1.2.2.8. Degradability

Degradability test procedure
The degradability tests were performed in phosphate buffered saline solution (PBS, consisting of 18.3 g $Na_2HPO_4 \cdot 2H_2O$, 2 g KH_2PO_4, 2 g KCl and 80 g NaCl in 1000 mL distilled water) at different elevated temperatures to accelerate the process. The specimens were prepared according to the procedure for the preparation of the specimens for the mechanical tests. The dimensions of the specimens were 6x6x1 mm^3 and they had a mass of $m_0 = 36 \pm 5$ mg. All results were obtained at least in triplicate.
Degradation tests at 110°C were performed in an autoclave in covered eprouvettes for each specimen with 10 mL PBS. Samples were removed every 24 h. Heat-up and cool-down phase took about 2 h in sum and were conducted reproducible. The pH value of every sample was checked to be at 7.4 before the samples were extracted in distilled water and weighed to assess the mass at the swollen state ($m_{wet,t}$). After drying at 40°C in the vacuum oven overnight the dry weight ($m_{dry,t}$) was determined.
Tests at 90 and 80°C were done in an ordinary oven in closed glass vials for each specimen with 6 mL PBS. Samples were removed every 3-5 d and treated as described above.
The water content (c_w) and the mass loss (m_{loss}) are calculated according to eq. 4 and eq. 5, respectively.

$$c_w(t) = \frac{m_{wet,t} - m_{dry,t}}{m_{wet,t}} \cdot 100\% \quad (4)$$

$$m_{loss}(t) = \frac{m_0 - m_{dry,t}}{m_0} \cdot 100\% \quad (5)$$

2. Thermoplastic urethane elastomers

2.2. Reproduction of Pellethane and aliphatic TPUs

2.2.1. Purity of MDI

Titration of isocyanate groups

About 50 mg portions of MDI were weighed into glass flasks with 15 mL 0.1 M dibutyl amine solution in toluene. The blanks only contained the dibutyl amine solution. All the flasks were placed in an ultrasonic bath to dissolve all components. 70 mL of isopropanol and 3–4 drops of bromophenol blue indicator solution were then added to each of the flasks and the content was titrated with 0.1 M HCl titer solution. The end point was a color change from blue to pale yellow. The determinations were done in triplicates. The isocyanate activity can be calculated according eq. 27.

$$a = \frac{2 \cdot 10^5 \cdot m}{M_{MDI}} \cdot \frac{1}{(B-A) \cdot c \cdot f} \quad (27)$$

A..... consumption for sample [mL]
B.....consumption for blank [mL]
f .....titer factor [ ]
c ..... concentration of titer solution [mol/L]
a .....isocyanate activity [%]
m .....weight [g]

2.2.2. Purity of pTHF

The hydroxyl value was determined according to the procedure described in section 1.2.1.2.

Determination of the water content

To determine the water content of polymer samples a solution with a percentage by weight (x) of about 10% (w/w) (with an accuracy of 0.1%) of polymer in dry THF was prepared. About 1 g (with mg accuracy) was injected to the measuring cell of an automated Karl Fischer titration device. The water content (c_w [ppm]) was calculated automatically from the consumption of titer solution and the entered sample weight. The water content of the neat polymer sample can be calculated by means of eq. 28.

$$c_{w,polymer} = \frac{100 \cdot c_{w,solution} - c_{w,solvent} \cdot (100 - x)}{x} \quad (28)$$

2.2.3. Polymer synthesis

General polymer synthesis

Preliminary, the prepolymer was dried overnight at 90°C in vacuo (5 mbar) under magnetic stirring; Water contents were below 50 ppm. A solution of the distilled diisocyanate (x eq) in dry solvent was added to the prepolymer (y eq, about 3.5 g) under stirring and Ar atmosphere. Afterwards about 2 drops stannous octoate (SnOct) were added as catalyst. After 2h of stirring at 90°C a solution of the chain extender ([x-y] eq) in dry DMF was added and the polyaddition was

continued overnight. The viscous solution was diluted with solvent and the TPU was precipitated in the suitable solvent, filtered, washed and dried in vacuo.

2.3. Concepts for degradability and toxicological examinations

2.3.1. Synthesis of degradation products

2.3.1.1. 1,6-Bis(hydroxyethyloxycarbonylamino)hexane (HDHC)[309]

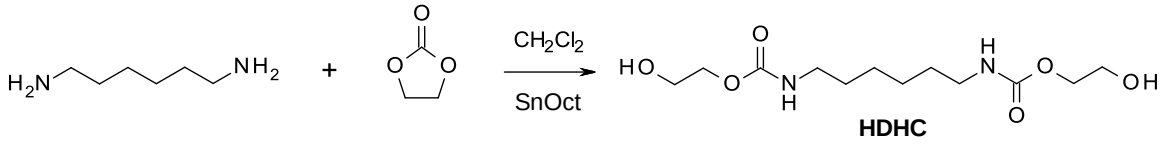

[116.21] [88.06] [292.33]

Reagents	hexamethylene diamine	5.81 g	50.0 mmol
	ethylene carbonate	8.80 g	100.0 mmol

Procedure
For the synthesis of **HDHC**, hexamethylene diamine was dissolved in 10 mL DCM. After the addition of 1 drop of SnOct a solution of ethylene carbonate in 10 mL DCM was added dropwise with stirring. The formation of the white product as a precipitate occurred within minutes but the reaction was continued overnight. Filtration and purification by recrystallization from acetone gave 9.6 g (66%) of **HDHC** as a white powder (m.p. 93-95°C, lit.: 93-94°C[309]).
^{1}H NMR (200 MHz, DMSO-d_6): δ (ppm) = 7.06 and 6.71 (t, J = 5.3 Hz, 2H, NH), 4.68 (t, J = 5.2 Hz, 2H, OH), 3.92 (t, J = 5.2 Hz, 4H, CH_2-O), 3.51 (dt, J_1 = 5.0 Hz, J_2 = 5.1 Hz, 4H, C$\underline{H}_2$-OH), 2.93 (dt, J_1 = 6.2 Hz, J_2 = 6.4 Hz, 4H, C$\underline{H}_2$-NH), 1.48-1.03 (m, 8H, CH_2).

2.3.1.2. 4,4'-Bis(hydroxyethyloxycarbonylamino)diphenyl methane (MDHC)

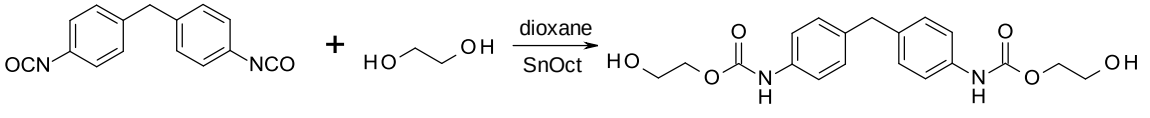

MDI **MDHC**

[250.26] [62.07] [374.40]

Reagents	ethylene glycol	2.00 g	32.2 mmol
	methane 4,4'-diphenyl diisocyanate	2.00 g	8.0 mmol

Procedure
For the synthesis of **MDHC,** ethylene glycol was dissolved in 10 mL dry dioxane under Ar atmosphere. After the addition of 1 drop of SnOct the mixture was heated to 90°C and a solution of methane 4,4'-diphenyl diisocyante in dry dioxane was added under stirring. After 2h the product was precipitated in ice/water, filtered off and recrystallized from ethanol. Drying in vacuo gave 1.40 g (47%) of MDHC as a pale yellow powder (m.p. 148-151°C).
^{1}H NMR (DMSO-d_6): δ (ppm) = 9.64 and 9.57 (s, 2H, NH), 7.35 (d, J = 8.4 Hz, 4H, ar-H), 7.08 (d, J = 8.4 Hz, 4H, ar-H), 4.80 (t, J = 5.3 Hz, 2H, OH), 4.07 (t, J = 5.1 Hz, 4H, CH_2-O), 3.77 (s, 2H, CH_2-ar), 3.60 (q, J = 5.2 Hz, 4H, CH_2-OH),
^{13}C NMR (DMSO-d_6): δ (ppm) = 153.65, 137.14, 135.43, 128.83, 118.35, 65.88, 59.32.

2.3.1.3. Ethyl 2-[6-[(2-ethoxy-1-methyl-2-oxo-ethoxy)carbonylamino] hexylcarbamoyloxy]-propanoate (HDLAE)

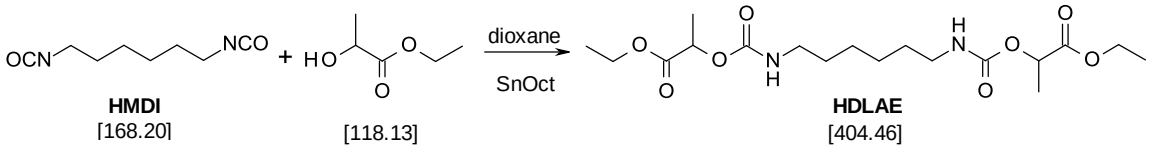

Reagents	ethyl lactate	5.75 g	48.7 mmol
	hexamethylene diisocyanate	3.72 g	22.1 mmol

Procedure

For the synthesis of **HDLAE**, ethyl lactate was dissolved in 10 mL dry dioxane under Ar atmosphere. After the addition of 1 drop of SnOct the mixture was heated to 90°C and a solution of hexamethylene diisocyanate in dry dioxane was added under stirring. After 2h the product was precipitated in ice/water, filtered off and recrystallized from water. 4.97 g (50%) of HDLAE was obtained as a white powder (m.p. 80-82°C).

^{1}H NMR (DMSO-d_6): δ (ppm) = 7.36 and 6.94 (t, J = 5.6 Hz, 2H, NH), 4.81 (q, J = 7.0 Hz, 2H, CH), 4.09 (q, J = 7.0 Hz, 4H, C$\underline{H}_2$-CH_3), 2.93 (q, J = 6.1 Hz, 4H, CH_2-N), 1.33 (d, J = 7.0 Hz, 6H, C$\underline{H}_3$-CH), 1.17 (t, J = 7.1 Hz, 6H, C$\underline{H}_3$-CH_2), 1.45-1.09 (m, 8H, CH_2),

^{13}C NMR (DMSO-d_6): δ (ppm) = 171.40, 155.30, 155.24, 68.03, 29.28, 25.84, 16.99, 13.98.

2.3.1.4. 3,14-Dioxa-5,12-diazahexadecanediocic acid-2,15-dimethyl-4,13-dioxo (HDLA)

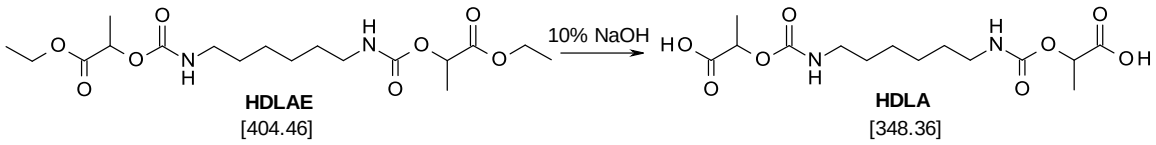

Reagents	Ethyl 2-[6-[(2-ethoxy-1-methyl-2-oxo-ethoxy)carbonylamino] hexylcarbamoyloxy]-propanoate	1.50 g	3.71 mmol

Procedure

HDLAE was dissolved in 15 mL THF and cooled with ice/water. 20 mL of an aqueous solution of NaOH (10% (w/w)) was added under stirring. After 1h the reaction mixture was acidified with a 2N aqueous solution of HCl and the product precipitated. Filtration and recrystallization from water gave 0.45 g (35%) of HDLA as a pale yellow powder (m.p. 153-155°C, decomposition).

^{1}H NMR (200 MHz, DMSO-d_6): δ (ppm) = 12.78 (bs, 2H, COOH), 7.29 and 6.88 (t, J = 5.6 Hz, 2H, NH), 4.75 (q, J = 7.0 Hz, 2H, CH), 3.00-2.85 (m, 4H, C$\underline{H}_2$-NH), 1.40-1.16 (m, 8H, CH_2), 1.31 (d, J = 7.0 Hz, 6H, CH_3),

^{13}C NMR (DMSO-d_6): δ (ppm) = 172.82, 155.32, 67.79, 29.25, 25.83, 17.00.

2.3.1.5. Acetic acid-2,2'-dimethyl-2,2'[methylenebis(4,1-phenyleneiminocarbonyloxy)] diethyl ester (MDLAE)

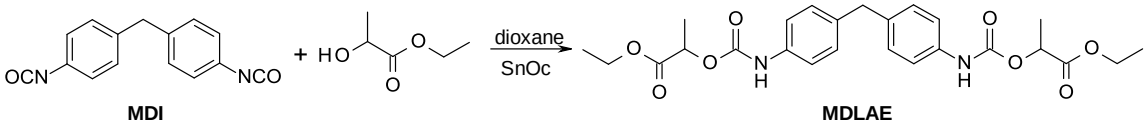

MDI [250.26] [118.13] **MDLAE** [486.51]

Reagents	ethyl lactate	7.86 g	66.5 mmol
	methane 4,4'-diphenyl diisocyanate	3.72 g	26.4 mmol

Procedure

Freshly distilled ethyl lactate was dissolved in 10 mL dry dioxane under Ar atmosphere. Freshly distilled methane 4,4'-diphenyl diisocyanate in 10 mL dry dioxane and 3 drops of SnOct were added and the reaction mixture was stirred at 90°C overnight. The product was precipitated in 200 mL ice/water, filtrated, dried and purified by silica gel flash-chromatography (PE:EE=3:2). 11.81 g (92%) of MDLAE was obtained as a white powder (m.p. 114-116°C, Rf value 0.73 (PE:EE=1:1)),

^{1}H NMR (DMSO-d_6): δ (ppm) = 9.82 (s, 2H, NH), 7.34 (d, J = 8.0 Hz, 4H, ar-H), 7.09 (d, J = 8.0 Hz, 4H, ar-H), 4.96 (q, J = 6.9 Hz, 2H, CH), 4.13 (q, J = 7.1 Hz, 4H, C$\underline{H}_2$-CH_3), 3.78 (s, 2H, CH_2-ar), 1.42 (d, J = 7.0 Hz, C$\underline{H}_3$-CH), 1.18 (t, J = 7.0 Hz, 6H, C$\underline{H}_3$-CH_2),

^{13}C NMR (DMSO-d_6): δ (ppm) = 171.10, 152.64, 136.69, 135.75, 128.90, 118.39, 68.46, 60.74, 16.89, 13.99.

2.3.1.6. Acetic acid-2,2'-dimethyl-2,2'[methylenebis(4,1-phenyleneiminocarbonyloxy)] (MDLA)

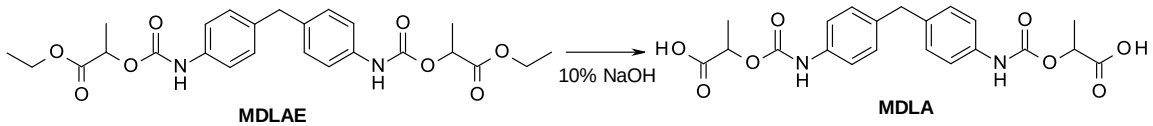

MDLAE [486.51] **MDLA** [430.41]

Reagents	Acetic acid-2,2'-dimethyl-2,2'[methylenebis-(4,1-phenyleneimino-carbonyloxy)] diethyl ester	1.50 g	3.08 mmol

Procedure

MDLAE was dissolved in 15 mL THF. 15 mL of an aqueous solution of NaOH (10% (w/v)) was added under stirring. The reaction was stirred over night and controlled by TLC ($CHCl_3$:MeOH=3:1, Rf value 0.43). The reaction mixture was acidified with a 2N aqueous solution of HCl and the product precipitated. Recrystallization from methanol gave 0.73 g (55%) of MDLA as a white powder (m.p. 184-186°C, decomposition),

^{1}H NMR (DMSO-d_6): δ (ppm) = 9.76 (s, 2H, NH), 7.34 (d, J = 8.0 Hz, 4H, ar-H), 7.09 (d, J = 8.2 Hz, 4H, ar-H) 4.90 (q, J = 7.0 Hz, 2H, CH), 3.78 (s, 2H, CH_2),

^{13}C NMR (DMSO-d_6): δ (ppm) = 172.59, 152.77, 136.85, 135.62, 128.25, 68.35, 16.96.

2.4. Cleavable chain extenders

2.4.1. Lactate based CCE

2.4.1.1. Synthesis of [2-(2-(2-(2-hydroxypropanoyloxy)propanoylamino)ethylamino)-1-methyl-2-oxo-ethyl]2-hydroxypropanoate (EDLA)

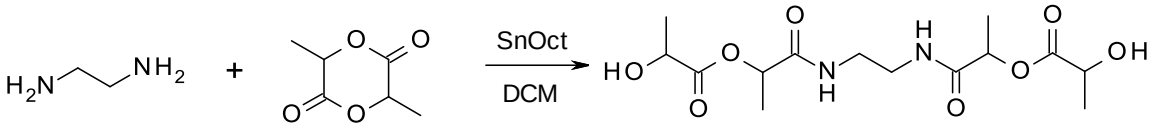

EDLA

[60.10] [144.13] [348.35]

Reagents	ethylene diamine	0.173 g	2.8 mmol
	lactide	0.826 g	5.7 mmol

Procedure

For the synthesis of EDLA a solution of ethylene diamine in 10 mL DCM with 1 drop of SnOct was cooled to -10°C. A solution of lactide in 5 mL DCM was added dropwise under Ar atmosphere. After 3 days at r.t. the solution was added dropwise to petroleum ether and the crude product settled as an oily substance. Purification by silica gel column chromatography using MeOH/$CHCl_3$ 1:15 as eluent yielded 0.202 g (20%) of EDLA as a pale yellow oil.

^{1}H NMR (200 MHz, $CDCl_3$): δ (ppm) = 7.41 and 7.31 (s, 2H, NH), 5.20 and 5.18 (q, J = 6.9 Hz, 2H, CH), 4.39 and 4.38 (q, J = 6.9 Hz, 2H, C<u>H</u>-OH), 3.97 (s, 2H, OH), 3.43 (s, 4H, CH_2), 1.48 (m, 12H, CH_3).

2.4.1.2. Synthesis of hydroxyethyl lactate (EGLA)

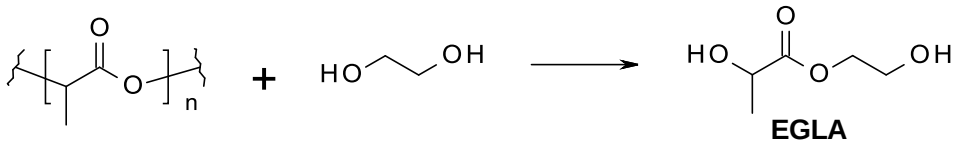

EGLA

[n*72.06] [62.07] [134.13]

Reagents	poly(lactic acid)	50 g	568 mmol*
	ethylene glycol	200 g	3225 mmol
			*units

Procedure

For the synthesis of **EGLA** poly(lactic acid) was heated with ethylene glycol to 180°C under stirring for 24h. The excess of ethylene glycol was distilled off before the product was fractionated in vacuo ($8 \cdot 10^{-3}$ mbar). 44 g (48%) of EGLA was obtained as the fraction 92-93°C as a colorless oil.

^{1}H NMR ($CDCl_3$): δ (ppm) = 4.31 (q, J = 7.0 Hz, 1H, CH), 4.22 (q, J = 4.0 Hz, 2H, CH_2-O), 3.92 (bs, 2H, OH), 3.78 (t, J = 4.7 Hz, 2H, C<u>H</u>$_2$-OH), 1.39 (d, J = 7.0 Hz, 3H, CH_3).

2.4.1.3. Synthesis of 2-[(2-ethoxy-2-oxo-ethyl)carbamoyloxy]ethyl 2-[(2-ethoxy-2-oxo-ethyl) carbamoyloxy]propanoate (ELAE)

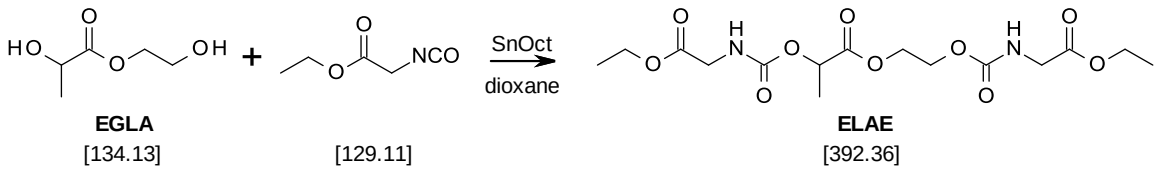

EGLA [134.13] [129.11] **ELAE** [392.36]

Reagents	hydroxyethyl lactate	2.00 g	14.9 mmol
	isocyanatoacetic acid ethyl ester	3.85 g	29.8 mmol

Procedure

Freshly distilled hydroxyethyl lactate was dissolved in 10 mL dry dioxane under Ar atmosphere. Isocyanatoacetic acid ethyl ester in 10 mL dry dioxane and 3 drops of SnOct were added and the reaction mixture was stirred at 70°C overnight. The product was precipitated in 200 mL petrol ether, filtrated and dried in vacuo. 5.1 g (87%) of **ELAE** was obtained as a white powder. Purification was not necessary because the reaction was only a model reaction for chain extension with **EGLA**.

^{1}H NMR ($CDCl_3$): δ (ppm) = 5.66-5.25 (m, 2H, NH), 5.08 (q, J = 7.0 Hz, 1H, CH), 4.43-4.27 (m, 4H, CH_2CO), 4.20 (q, J = 7.2 Hz, 4H, $C\underline{H}_2$-CH_3), 4.03-3.84 (m, 4H, CH_2-CH_2), 1.48 (d, J = 7.0 Hz, 3H, $C\underline{H}_3$-CH), 1.27 (t, J = 7.1 Hz, 6H, $C\underline{H}_3$-CH_2),

^{13}C NMR (DMSO-d_6): δ (ppm) = 171.14, 169.83, 155.38, 69.22, 63.04, 62.70, 61.53, 61.47, 42.73, 17.05, 14.11.

2.4.3. Synthesis of Michael adduct based CCE

Synthesis of N,N'-bis[(2-acryloyloxyethoxy)carbonyl]-1,6-hexanediamine (HDEA)

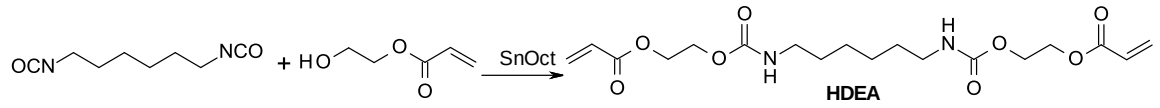

[168.19] [116.12] [400.42]

Reagents	hydroxyethyl acrylate	12.20 g	104.6 mmol
	hexamethylene diisocyanate	8.00 g	47.6 mmol

Procedure

For the synthesis of **HDEA**, freshly distilled hydroxyethyl acrylate was dissolved in 40 mL dry dioxane under Ar atmosphere. After the addition of 3 drops of SnOct the mixture was heated to 70°C and a solution of hexamethylene diisocyanate in 10 mL dry dioxane was added under stirring. After stirring overnight the product was precipitated in ice/water, filtered off and dried in vacuo. 17.45 g (86%) of HDEA was obtained as a white powder. The crude product was directly applied for the Michael addition reactions.

^{1}H NMR ($CDCl_3$): δ (ppm) = 6.43 (dd, J = 17.2, 1.6 Hz, 2H, $C\underline{H}_2$=CH), 6.13 (dd, J = 17.2, 10.2 Hz, 2H, CH_2=C$\underline{H}$), 5.85 (dd, J = 10.2, 1.6 Hz, 2H, $C\underline{H}_2$=CH), 4.79 (t, J = 5.0 Hz, 2H, NH), 4.47-4.19 (m, 8H, $C\underline{H}_2$-O), 3.16 (q4, J = 6.5 Hz, 4H, $C\underline{H}_2$-N), 1.60-1.24 (m, 8H, CH_2).

2.5. Concepts for cleavable soft blocks

2.5.1. Synthesis of lactate extended poly(tetrahydro furan)

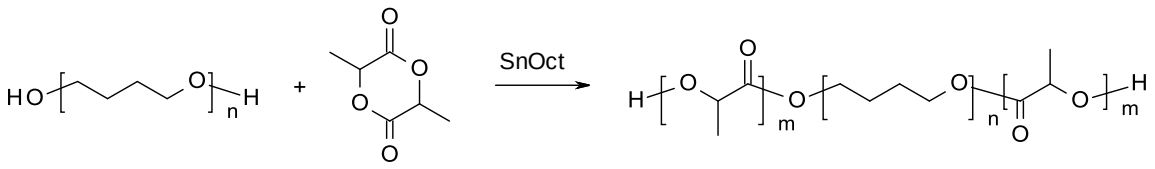

lactate extended poly(tetrahydro furan)

n = 28 [2000] | [144.12] | m = 3 [2400]

Reagents	poly(tetrahydro furan) (2000 g/mol)	25.77 g	12.9 mmol
	lactid	7.43 g	51.6 mmol

Procedure
poly(tetrahydro furan) was dried by azeotropic distillation from a toluene solution stored over $CaCl_2$ for 48 h. It was mixed with lactid and heated to 130°C in the presence of SnOct for 9h. The oily product was reprecipitated from a toluene solution in petrol ether twice, dissolved in dichloromethane, extracted thrice with 10% (w/v) aqueous sodium bicarbonate solution, washed with Brine, dried with sodium sulfate, filtrated and evaporated in vacuo. 20.20 g (64%) of the lactate extended poly(tetrahydro furan) was obtained as a clear oil (acid number <1).
^{1}H-NMR ($CDCl_3$): δ(ppm) = 5,25- 5,08 (6H, m, -O-CH-CO-), 4,23 - 4,08 (4H, m, -CO-O-CH_2-), 3,53 – 3,29 (approx 114H, m, -O-CH_2-), 1,66 - 1,51 (approx 118H, m, -CH_2-$C\underline{H}_2$-$C\underline{H}_2$-CH_2-).

2.5.2. Determination of the acid number

The acid number was determined according the standard DIN 53402. About 1 g of polymer (mg accuracy) was dissolved in 50 mL of acetone and titrated with 0.1 N methanolic potassium hydroxide titer solution against phenolphthalein. A blank sample of acetone, not containing polymer, was treated analogous. The acid number can be calculated by eq. 29.

$$acid\ number = 56.1 \cdot \frac{f \cdot c}{m} \cdot (A - B) \tag{29}$$

A.....consumption for sample [mL]
B..... consumption for blank [mL]
f.....titer factor [ ]
c.....concentration of titer solution [mol/L]
acid number.....[mg KOH/g polymer]
m .....weight [g]

2.6. Synthesis of degradable TPUs

Preparation of a polymer consisting of HMDI, pTHF1000 and TPEG

Reagents	poly(tetrahydrofuran) (1000 g/mol)	3.650 g	3.65 mmol
	hexamethylene diisocyanate	1.228 g	7.30 mmol
	bis(2-hydroxyethyl) terephthalate	0.928 g	3.65 mmol

Procedure
The poly(tetrahydrofuran) batch was dried overnight at 90°C in vacuo (5 mbar) under magnetic stirring. The appropriate amount of pTHF (mg accuracy) was weighted directly into the reaction flask and dried for another period of 60 min at same conditions. Hexamethylene diisocyanate in 5 mL dry DMF was added to pTHF under Ar atmosphere. The transfer syringe as well as the vessel were rinsed with 10 mL dry DMF in portions. 3 drops of SnOct were added to the reaction mixture. After 2 h of stirring at 90°C bis(2-hydroxyethyl) terephthalate (dried over $CaCl_2$), dissolved in 5 mL dry DMF was added with the same subsequent rinsing. After 1 h of stirring at 90°C the reaction mixture was stirred overnight. The viscous mixture was diluted with about 70 mL of DMF and the polymer was precipitated in about 1.5 L methanol, filtered and dried in vacuo.

2.7. Tests of the TPUs

2.7.1. Mechanical properties

2.7.1.1. Tensile tests

2.7.1.1.1. Non-degradable TPUs
The specimens to examine the mechanical properties of the non-degradable polymers were punched out of compression moulded sheets according to ISO 527-1 type 5A. The approximately 0.5 mm thick sheets were produced at a foil press (Collin P200P), with the following program:

- 10 K/min heating
- 200°C/10 min/10 bar
- 10 K/min cooling/100 bar

The dumbbell-shaped specimens were about 100 mm long and in the parallel region approximately 4 mm wide. The so prepared specimens were clamped in the tensile testing machine (Zwick Z050). No extensometer was used, so the crosshead travel was used directly to determine the strain. The dimensions were entered into the software shell and before the measurements with a crosshead velocity of 50 mm/min were started the specimens were pre-loaded with 0.1 N. The measurements were aborted when the specimens apparently were broken. Each sample was tested at least in quintuplicate.

2.7.1.1.2. Degradable TPUs
The specimens to examine the mechanical properties of the degradable polymers were punched out of solution casted films according to ISO 527-1 type 5B. About 10% (w/w) solutions of the TPUs in DMF were poured into moulds out of Teflon (60x40x2 mm^3 cavity). The moulds were covered with paper lids to avoid the deposition of dust particles during the slow evaporation of the solvent. After 24 h the films were dried in vacuo overnight at 60°C. The dumbbell-shaped specimens were about 35 mm long and in the 12 mm parallel region approximately 2 mm wide and were tested analogous to the procedure above.

2.7.1.2. Dynamic mechanical analysis (DMA)
Experiments were done on a Texas Instruments 2980DMA. Stripe specimens (20x2 mm^2) with thicknesses of about 150 µm were cut from the solution casted films described above. The samples were tested from -100°C to 50°C with a heating rate of 3 K/min, a frequency of 1 Hz, an amplitude of about 1.5µm (0.1% of the clamping distance). Results were obtained at least in duplicate.

2.7.2. Degradability

Degradability test procedure

The degradability tests were performed in phosphate buffered saline solution (PBS, consisting of 18.3 g $Na_2HPO_4 \cdot 2H_2O$, 2 g KH_2PO_4, 2 g KCl and 80 g NaCl in 1000 mL distilled water) at different elevated temperatures to accelerate the process. To prepare the specimens, small discs (5 mm) were punched out of the solution casted films described above. Degradation tests were performed at 110°C in an autoclave in covered eprouvettes for each specimen with 10 mL PBS. Samples were removed every 24 h. Heat-up and cool-down phase took about 2 h in sum and were conducted reproducible. The pH value of every sample was checked to be at 7.4 before the samples were extracted in distilled water, dried using a paper towel and weighed to assess the residual mass. In addition to the mass erosion the molecular weight of every polymer sample was determined by means of GPC. The mass erosion (m_{eros}) and the drop in the molecular weight (M_{drop}) were calculated by eq. 30 and 31. As reference surgical poly(lactic acid) (from the company Bionx implants, P(L/DL)LA (70:30)) was used.

$$m_{eros}(\mathrm{t}) = \frac{m_t - m_o}{m_o} \cdot 100\% \tag{30}$$

$$M_{drop}(\mathrm{t}) = \frac{M_t - M_o}{M_o} \cdot 100\% \tag{31}$$

Materials and General Methods

Reagents and solvents were – unless otherwise noted – all applied in a quality that is common for organic synthesis and – if necessary – purified as Armarego *et al.*[325] described.

For **thin layer chromatography** (TLC) aluminum foils, coated with silicagel 60 F254 from the company Merck were applied.

For **column and flash column chromatography**, silicagel 60, from the distributor VWR was applied.

^{1}H- NMR- and **^{13}C-NMR-spectra** were measured with a BRUKER AC-E-200 FT-NMR- spectrometer at 200 MHz. The chemical shift is displayed in ppm (s = sigulett, d = duplet, t = triplett, q = quartett, m = multiplett). Deutero-chloroform ($CDCl_3$) or deuterated dimethyl sulfoxid (d^6-DMSO) from the companies Aldrich and Eurisotop were used as solvents. The grade of deuteration was at least 99.8%.

UV-Vis spectroscopy was measured using a Hitachi U-2001 spectrometer with spectrophotometric grade acetonitrile as solvent and with the parameters layer thickness: 1 cm, wavelength range: 600 – 200 nm, scan speed: 200 nm s^{-1}, lamp change: 350 nm.

Melting points were determined with a "Zeiss Axioskop" microscope equipped with a heating device from Leitz. Melting points are not corrected.

GC-MS runs were performed on a Thermo Scientific GC-MS DSQ II using a BGB 5 column (L = 30 m, d = 0.32 mm, 1.0 µm film, achiral) with the following temperature method (injection volume: 1 µL): 2 min at 80°C, 20°C/min until 280°C, 2 min at 280°C. MS spectra were recorded using EI ionization (70 eV) and a quadrupole analyzer.

Thermal differential scanning calorimetry experiments were done on a Netzsch DSC 204 F1 Phoenix with a heating rate of 2°C/min under air.

Photo-differential scanning calorimetry experiments were done on a modified Shimadzu DSC50 using filtered UV-light (320-500 nm) from an Exfo OmniCure™ series 2000.

The curing of the photosensitive resins was performed with a **UV lamp** from the company UV-Technik Meyer with a special dysprosium UV lamp (UVH 2022 DY-0, 380V, 2.2kW, irradiation power 1kW, UV-A: 59 mW/cm^2, UV-B: 25 mW/cm^2, UV-C: 3 mW/cm^2, Vis: 45 mW/cm^2)

The **viscosimetry** measurements were performed on a Physica MCR 300 from the company Anton Paar with a plate-plate arrangement.

GPC measurements were carried out on a Viscotek GPCmax VE2001 equipped with a Waters Ultrahydrogel™ 250 and 1000 column equipped with a Viscotek VE3580 RI detector. Generally, polystyrene standards were used for calibration.

Dynamic mechanical analysis experiments were done on a Texas Instruments 2980DMA.

Tensile tests were measured on a Zwick Z050 tensile testing machine.

The fabrication of the 3D-parts structured by **digital light processing (DLP)** was done using an EnvisionTec Perfactory® Mini Multi Lens with a resolution of 1400 x 1050 and a PTFE vat.

The fabrication of the 3D-parts by **micro-stereolithography (µ-SLA)** was done using a system developed by the Laser Zentrum Hannover (LZH. The utilized laser (Electronics 355 nm Quasi-CW Laser System XCYTE) was a neodymium doped yttrium aluminum garnet ($Y_3Al_5O_{12}$) laser (Nd:YAG) with a frequency multiplied wavelength of 355 nm (tripled), equipped with an acousto-optic modulator (AOM, Isomet AO Modulator RFA9x0-110 Series) and a scanner (SCANLAB hurrySCAN 14).

The preparation and analysis of the photosensitive compounds and mixtures was conducted in a **yellow light lab**. This laboratory was placed in a window-less room to avoid admittance of day light. Adhesive foils of the company IFOHA (article nr. 11356, melon yellow) were used to cover fluorescent lamps.

Abbreviations

AMT	additive manufacturing technology
AOM	acousto-optic modulator
BA	butyl acrylate
BDO	1,4-butandiol
BEA	2-(acryloyloxy)ethyl N-butylcarbamate
BPO	Irgacure 819 (Ciba SC), phenyl¬bis(2,4,6-tri¬methyl-benzoyl) phosphine oxide
CABG	coronary artery bypass grafting
CAD	computer aided design
CCE	cleavable chain extender
CEA	2-cyanoethyl acrylate
CEMA	2-cyanoethyl methacrylate
CHD	coronary hearts disease
CL	ε-caprolactone
CQ	camphor quinone
CTA	chain transfer agent
DA	diacrylate
DB value	double bond value
DBA	di-n-butylamine
DBB	dihydroxy-4-tert-butylbenzene
DBC	double bond conversion
DI	diisocyanate
DLP	digital light procesing
DMAB	ethyl dimethylamino benzoate
DOD	3,6-dioxa-1,8-octan-dithiol
DPA	N,N-diisopropyl acrylamide
DSC	differential scanning calorimetry
E	elastic modulus
ε_b	elongation at break
EC	endothelial cell
ECM	extracellular matrix
EDLA	[2-(2-(2-(2-hydroxypropanoyloxy)propanoylamino)ethylamino)-1-methyl-2-oxo-ethyl]2-hydroxypropanoate
EGLA	hydroxyethyl lactate
EHA	2-ethylhexyl acrylate
ELAE	2-[(2-ethoxy-2-oxo-ethyl)carbamoyloxy]ethyl 2-[(2-ethoxy-2-oxo-ethyl) carbamoyloxy]propanoate
EPC	endothelial progenitor cell
ePTFE	expanded poly(tetrafluor ethylene)
ESC	embrionic stem cell

ETLA	ethyl lactate
FGF	fibroblast growth factor
FTIR	Fourier transformation infrared spectroscopy
GA	glycolic acid
GF	growth factors
HDDA	1,6-hexanediol diacrylate
HDEA	N,N'-bis[(2-acryloyloxyethoxy)carbonyl]-1,6-hexanediamine
HDHC	1,6-bis(hydroxyethyloxycarbonylamino)hexane
HDLA	3,14-dioxa-5,12-diazahexadecanediocic acid-2,15-dimethyl-4,13-dioxo
HDLAE	3,14-dioxa-5,12-diazahexadecanediocic acid-2,15-dimethyl-4,13-dioxo-1,16-diethylester
HEA	hydroxyethyl acrylate
HEMA	hydroxyethyl methacrylate
HMB	2,2'-hydroxy-4,4'-methoxybenzophenone
HPC	hematopoetic progenitor cells
HUVEC	human umbilical vein endothelial cells
IHD	ischemic heart disease
L	block length
LA	lactic acid
MA	monoacrylate
MDHC	4,4’-bis(hydroxyethyloxycarbonylamino)diphenyl methane
MDI	methylene diphenyl diisocyanate
MDLA	Acetic acid-2,2’-dimethyl-2,2’[methylenebis(4,1-phenyleneiminocarbonyloxy)]
MDLAE	Acetic acid-2,2’-dimethyl-2,2’[methylenebis(4,1-phenyleneiminocarbonyloxy)]-diethyl ester
Me_2CEA	2-cyano-1,1-dimethylethyl acrylate
Me_2CMA	1-cyano-1-methylethyl acrylate
MSC	mesenchymal stem cells
NCEA	N-methylcyanoethyl acrylamide
NMR	nuclear magnetic resonance
OH value	hydroxyl value
PBS	phosphate buffered saline
PCI	percutanous intervention
PEG	poly(ethylene glycol)
PEGDA	poly(ethylene glycol) diacrylate
Pell	Pellethane
PET	poly(ethylene terephthalate)
PGA	poly(glycolic acid)
photoDSC	photo differential scanning calorimetry
PI	photoinitiator
PLA	poly(lactic acid)
pTHF	poly(tetrahydro furan)

PU	polyurethane
Py	pyridine
R	diacrylate content
RP	rapid prototyping
RT-FTIR	real time Fourier transformation infrared spectroscopy
S	tensile strength
SFF	solif freeform fabrication
SLA	stereolithography
SMC	smooth muscle cells
TDI	toluene diisocyanate
TE	tissue engineering
Tg	glass transition temperature
TGEG	ethylene gylcol bisthioglycolate
TMC	tetramethylene carbonate
TPU	thermoplastic urethane elastomer
TTA	trimethylolpropane triacrylate
UDA	urethane oligomer diacrylate
UMA	urethane oligomer monoacrylate
UTA	urethane oligomer triacrylate
VEGF	vascular endothelial growth factors
VTE	vascular tissue engineering

Appendix

DMA measurements:

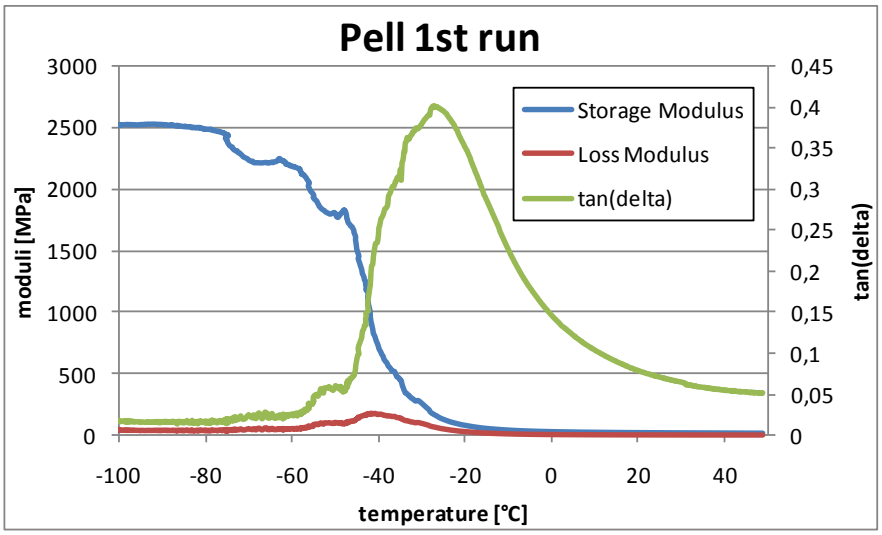

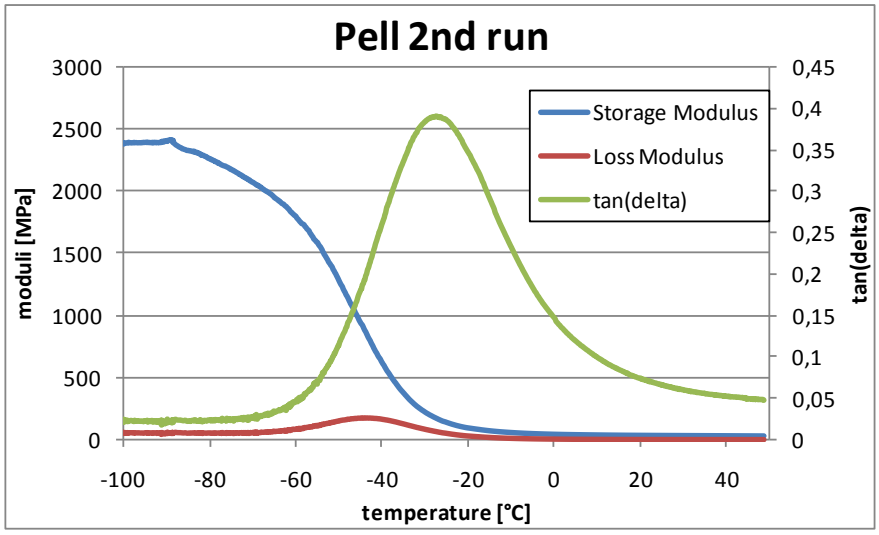

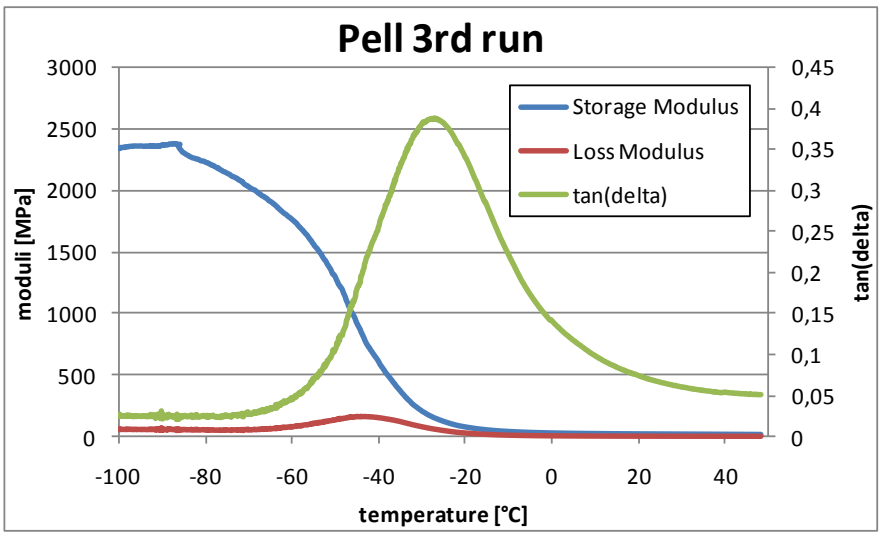

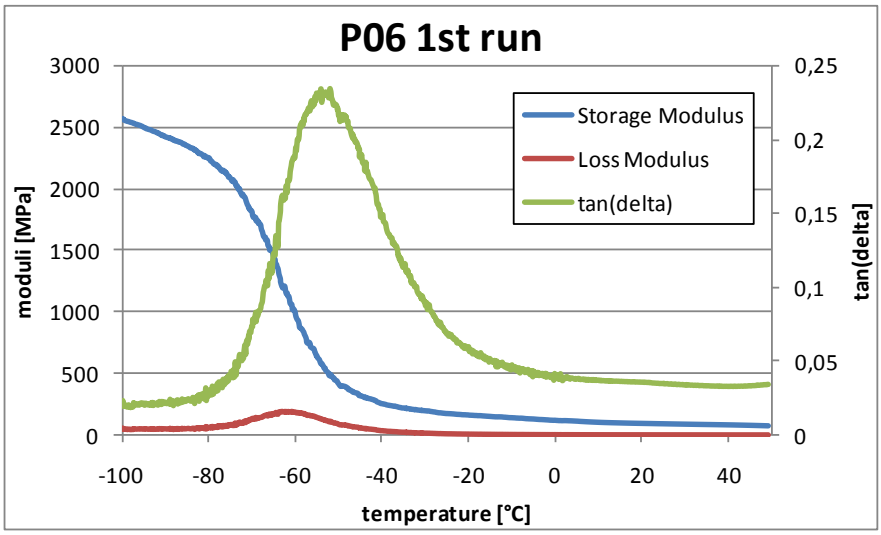
P06 1st run
moduli [MPa]
tan(delta)
temperature [°C]
Storage Modulus
Loss Modulus
tan(delta)
3000
2500
2000
1500
1000
500
0
0,25
0,2
0,15
0,1
0,05
0
-100
-80
-60
-40
-20
0
20
40

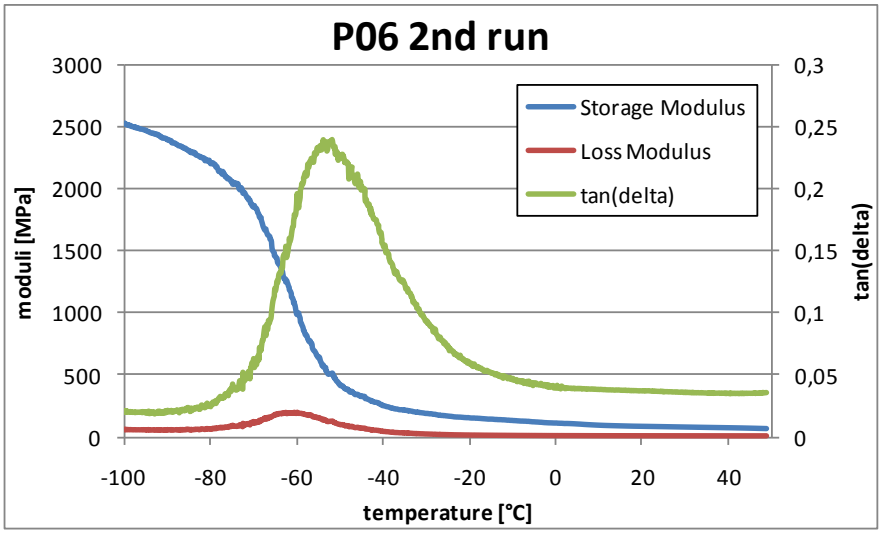
P06 2nd run
moduli [MPa]
tan(delta)
temperature [°C]
Storage Modulus
Loss Modulus
tan(delta)
3000
2500
2000
1500
1000
500
0
0,3
0,25
0,2
0,15
0,1
0,05
0
-100
-80
-60
-40
-20
0
20
40

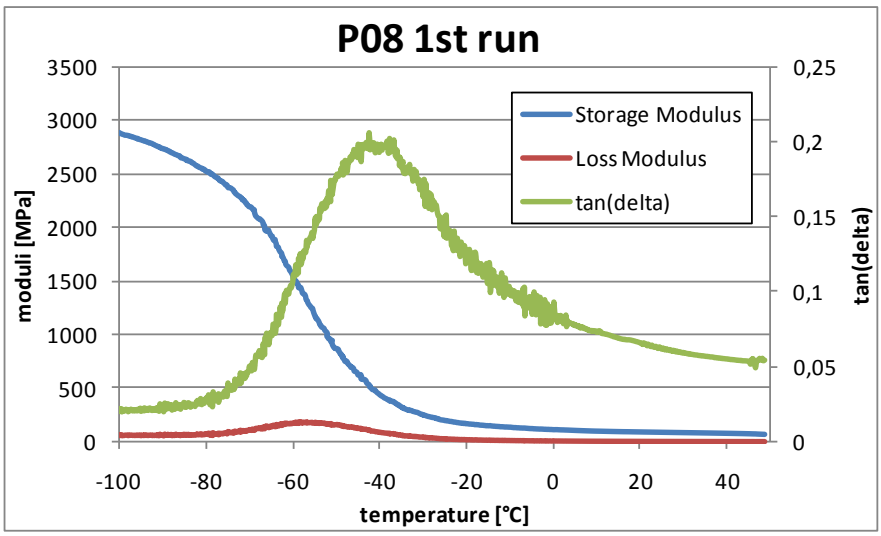
P08 1st run
moduli [MPa]
tan(delta)
temperature [°C]
Storage Modulus
Loss Modulus
tan(delta)
3500
3000
2500
2000
1500
1000
500
0
0,25
0,2
0,15
0,1
0,05
0
-100
-80
-60
-40
-20
0
20
40

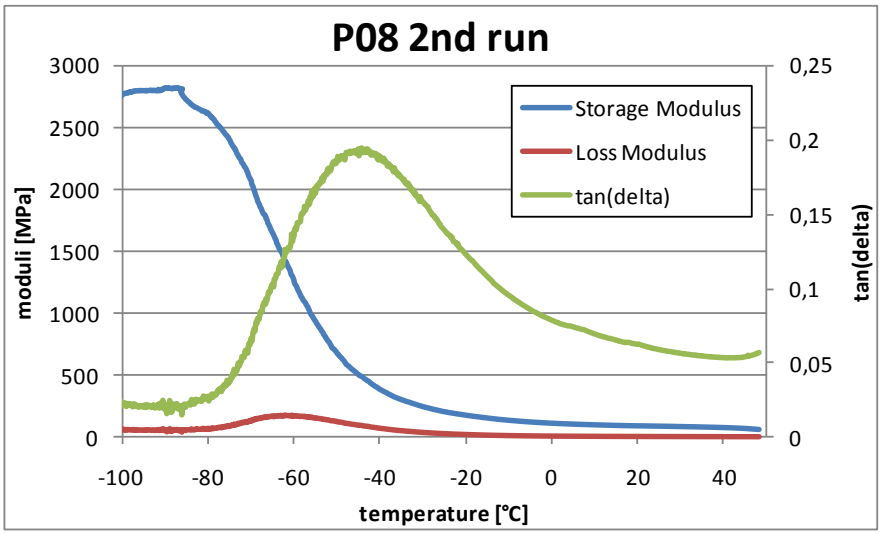
P08 2nd run
moduli [MPa]
tan(delta)
temperature [°C]
Storage Modulus
Loss Modulus
tan(delta)
3000
2500
2000
1500
1000
500
0
0,25
0,2
0,15
0,1
0,05
0
-100
-80
-60
-40
-20
0
20
40

References

1. Chung, M. K.; Rich, M. W. *Alcohol Health and Research World* **1990,** 14, (4), 269-276.
2. Wikipedia.org http://en.wikipedia.org/wiki/Heart (10-11-02).
3. Parikh, S. A.; Edelman, E. R. *Advanced Drug Delivery Reviews* **2000,** 42, (1-2), 139-161.
4. Engler, A. J.; Richert, L.; Wong, J. Y.; Picart, C.; Discher, D. E. *Surface Science* **2004,** 570, (1-2), 142-154.
5. American-Heart-Association *Heart Disease and Stroke Statistics 2010 Update: A Report From the American Heart Association*; 2010.
6. Choi, D.; Hwang, K.-C.; Lee, K.-Y.; Kim, Y.-H. *J. Controlled Release* **2009,** 140, (3), 194-202.
7. Rao, V.; Al-Weshahy, A. *Curr. Atheroscler. Rep.* **2008,** 10, (6), 478-485.
8. Miller, E. R., III; Erlinger, T. P.; Appel, L. J. *Curr. Atheroscler. Rep.* **2006,** 8, (6), 460-465.
9. Fisher, M.; Lees, K.; Spence, J. D. *Stroke* **2006,** 37, (9), 2430-2435.
10. de Lorgeril, M.; Salen, P. *Clin. Invest. Med.* **2006,** 29, (3), 154-158.
11. Stein, Y. *Atherosclerosis (Shannon, Irel.)* **1994,** 110, (Suppl.), S41-S44.
12. Engelfriet, P.; Hoekstra, J.; Hoogenveen, R.; Buchner, F.; van, R. C.; Verschuren, M. *Eur J Cardiovasc Prev Rehabil* **2010,** 17, (1), 50-5.
13. Adams, R. L. C.; Bird, R. J. *Nephrology* **2009,** 14, (5), 462-470.
14. Bavry, A. A.; Bhatt, D. L. *Lancet* **2008,** 371, (9630), 2134-2143.
15. Romano, A.; Jensen, M. R.; McAlpine, J. *Curr. Opin. Drug Discovery Dev.* **2010,** 13, (2), 157-158.
16. nhlbi.nih.gov http://www.nhlbi.nih.gov/health/dci/Diseases/Angioplasty/Angioplasty_WhatIs.html (25-11-02).
17. Elsner, D. *Internist* **2006,** 47, (12), 1251-4, 1255-7.
18. Pereira, C. E.; Albers, M.; Romiti, M.; Brochado-Neto, F. C.; Pereira, C. A. B. *Journal of Vascular Surgery* **2006,** 44, (3), 510-517.
19. sts.org http://www.sts.org/sections/patientinformation/adultcardiacsurgery/cabg/ (10-11-04).
20. Nomi, M.; Atala, A.; De Coppi, P.; Soker, S. *Molecular Aspects of Medicine* **2002,** 23, (6), 463-483.
21. Van Craenenbroeck, E. M.; Conraads, V. M. *Microvasc. Res.* **2010,** 79, (3), 184-192.
22. Siddique, A.; Shantsila, E.; Lip, G. Y. H.; Varma, C. *J. Angiog. Res.* **2010,** 2, No pp. given.
23. Kirton, J. P.; Xu, Q. *Microvasc. Res.* **2010,** 79, (3), 193-199.
24. Avci-Adali, M.; Ziemer, G.; Wendel, H. P. *Biotechnology Advances* **2010,** 28, (1), 119-129.
25. Allen, J. B.; Khan, S.; Lapidos, K. A.; Ameer, G. A. *Stem Cells* **2010,** 28, (2), 318-328.
26. Yoder, M. C. *J. Thromb. Haemostasis* **2009,** 7, (Suppl. 1), 49-52.
27. Pearson, J. D. *J. Thromb. Haemostasis* **2009,** 7, (2), 255-262.
28. Pearson, J. D. *Microvasc. Res.* **2009,** 79, (3), 162-168.
29. Zampetaki, A.; Kirton, J. P.; Xu, Q. *Cardiovasc. Res.* **2008,** 78, (3), 413-421.
30. Umemura, T.; Higashi, Y. *J. Pharmacol. Sci. (Tokyo, Jpn.)* **2008,** 108, (1), 1-6.
31. Roncalli, J. G.; Tongers, J.; Renault, M.-A.; Losordo, D. W. *Trends Biotechnol.* **2008,** 26, (5), 276-283.
32. Marsboom, G.; Janssens, S. *Expert Rev. Cardiovasc. Ther.* **2008,** 6, (5), 687-701.
33. Kawamoto, A.; Losordo, D. W. *Trends Cardiovasc. Med.* **2008,** 18, (1), 33-37.
34. Jujo, K.; Ii, M.; Losordo, D. W. *J. Mol. Cell. Cardiol.* **2008,** 45, (4), 530-544.
35. de Mel, A.; Jell, G.; Stevens, M. M.; Seifalian, A. M. *Biomacromolecules* **2008,** 9, (11), 2969-2979.
36. Miller-Kasprzak, E.; Jagodzinski, P. P. *Arch. Immunol. Ther. Exp.* **2007,** 55, (4), 247-259.

37. Dotsenko, O. *Open Cardiovasc. Med. J.* **2010,** 4, 97-104.
38. Gonzales, C.; Pedrazzini, T. *Exp. Cell Res.* **2009,** 315, (18), 3077-3085.
39. Atala, A. *J Tissue Eng Regen Med* **2007,** 1, (2), 83-96.
40. Gomes, M. E.; Reis, R. L. *Macromol. Biosci.* **2004,** 4, (8), 737-742.
41. Gaffney, M. M.; Hynes, S. O.; Barry, F.; O'Brien, T. *Br. J. Pharmacol.* **2007,** 152, (2), 175-188.
42. Kasper, C. *Chemie in unserer Zeit* **2005,** 39, (6), 394-401.
43. Langer, R.; Vacanti, J. P. *Science* **1993,** 260, (5110), 920-6.
44. Laurencin, C. T.; Ambrosio, A. M. A.; Borden, M. D.; Cooper, J. A. *Annual Review of Biomedical Engineering* **1999,** 1, (1), 19-46.
45. Fuchs, J. R.; Nasseri, B. A.; Vacanti, J. P. *Ann Thorac Surg FIELD Full Journal Title:The Annals of thoracic surgery* **2001,** 72, (2), 577-91.
46. Ikada, Y. *Journal of the Royal Society Interface* **2006,** 3, (10), 589-601.
47. Nair, L. S.; Laurencin, C. T. *Progress in Polymer Science* **2007,** 32, (8-9), 762-798.
48. Eisenbarth, E. *Advanced Engineering Materials* **2007,** 9, (12), 1051-1060.
49. Buchmeiser, M. R. *Journal of Polymer Science: Part A: Polymer Chemistry* **2009,** 47, (9), 2219-27.
50. Polak, J.; Hench, L. *Gene Ther.* **2005,** 12, (24), 1725-1733.
51. Andreadis, S. T. *Adv. Biochem. Eng./Biotechnol.* **2007,** 103, (Tissue Engineering II), 241-274.
52. Heyde, M.; Partridge, K. A.; Oreffo, R. O. C.; Howdle, S. M.; Shakesheff, K. M.; Garnett, M. C. *J. Pharm. Pharmacol.* **2007,** 59, (3), 329-350.
53. van der Kraan, P. M.; van de Loo, F. A. J.; van den Berg, W. B. *Biomaterials* **2004,** 25, (9), 1497-1504.
54. Ratcliffe, A. *Matrix Biology* **2000,** 19, (4), 353-357.
55. Isenberg, B. C.; Williams, C.; Tranquillo, R. T. *Circulation Research* **2006,** 98, (1), 25-35.
56. L'Heureux, N.; Dusserre, N.; Marini, A.; Garrido, S.; de la Fuente, L.; McAllister, T. *Nat Clin Pract Cardiovasc Med* **2007,** 4, (7), 389-395.
57. L'Heureux, N.; Paquet, S.; Labbe, R.; Germain, L.; Auger, F. A. *FASEB J.* **1998,** 12, (1), 47-56.
58. Norotte, C.; Marga, F. S.; Niklason, L. E.; Forgacs, G. *Biomaterials* **2009,** 30, (30), 5910-5917.
59. Mironov, V.; Reis, N.; Derby, B. *Tissue engineering* **2006,** 12, (4), 631-4.
60. Fedorovich, N. E.; Alblas, J.; de Wijn, J. R.; Hennink, W. E.; Verbout, A. J.; Dhert, W. J. A. *Tissue Engineering* **2007,** 13, (8), 1905-1925.
61. Chan, B. P.; Leong, K. W. *European Spine Journal* **2008,** 17, (4), 467-479.
62. Niklason, L. E.; Gao, J.; Abbott, W. M.; Hirschi, K. K.; Houser, S.; Marini, R.; Langer, R. *Science (Washington, D. C.)* **1999,** 284, (5413), 489-493.
63. Gong, Z.; Niklason, L. E. *FASEB J.* **2008,** 22, (6), 1635-1648, 10.1096/fj.07-087924.
64. Roeder, R.; Wolfe, J.; Lianakis, N.; Hinson, T.; Geddes, L. A.; Obermiller, J. *Journal of Biomedical Materials Research* **1999,** 47, (1), 65-70.
65. Sarkar, S.; Salacinski, H. J.; Hamilton, G.; Seifalian, A. M. *European Journal of Vascular and Endovascular Surgery* **2006,** 31, (6), 627-636.
66. Santana, D. B.; Armentano, R. L.; Zócalo, Y.; Cámpos, H. P.; Cabrera Fischer, E. I.; Graf, S.; Saldías, M.; Walter, S.; Alvarez, I. *Cell and Tissue Banking* **2007,** 8, (1), 43-57.
67. Salacinski, H. J.; Goldner, S.; Giudiceandrea, A.; Hamilton, G.; Seifalian, A. M.; Edwards, A.; Carson, R. J. *Journal of Biomaterials Applications* **2001,** 15, (3), 241-278.
68. Lee, J.; Cuddihy, M. J.; Kotov, N. A. *Tissue Engineering, Part B: Reviews* **2008,** 14, (1), 61-86.
69. Hollister, S. J. *Nature Materials* **2005,** 4, (7), 518-524.
70. Zilla, P.; Bezuidenhout, D.; Human, P. *Biomaterials* **2007,** 28, (34), 5009-5027.
71. Chen, H.; Yuan, L.; Song, W.; Wu, Z.; Li, D. *Prog. Polym. Sci.* **2008,** 33, (11), 1059-1087.
72. Venkatraman, S.; Boey, F.; Lao, L. L. *Progress in Polymer Science* **2008,** 33, 853-874.
73. Roh, J. D.; Sawh-Martinez, R.; Brennan, M. P.; Jay, S. M.; Devine, L.; Rao, D. A.; Yi, T.; Mirensky, T. L.; Nalbandian, A.; Udelsman, B.; Hibino, N.; Shinoka, T.; Saltzman, W. M.; Snyder, E.; Kyriakides, T. R.; Pober, J. S.; Breuer, C. K. *Proceedings of the National Academy of Sciences* **2010,** 107, (10), 4669-4674.

74. Roh, J. D.; Nelson, G. N.; Brennan, M. P.; Mirensky, T. L.; Yi, T.; Hazlett, T. F.; Tellides, G.; Sinusas, A. J.; Pober, J. S.; Saltzman, W. M.; Kyriakides, T. R.; Breuer, C. K. *Biomaterials* **2008,** 29, (10), 1454-1463.
75. Egashira, K. *Hypertension* **2003,** 41, (3, Pt. 2), 834-841.
76. Fahner, P. J.; Idu, M. M.; van Gulik, T. M.; Legemate, D. A. *Journal of Vascular Surgery* **2006,** 44, (3), 518-524.
77. Kreitmann, B.; Riberi, A.; Zeranska, M.; Novakovitch, G.; Metras, D. *European Journal of Cardio-Thoracic Surgery* **1997,** 11, (5), 943-952.
78. Courtman, D. W.; Errett, B. F.; Wilson, G. J. *J. Biomed. Mater. Res.* **2001,** 55, (4), 576-586.
79. Costa, C. *Transplantation Immunology Research Trends* **2007**, 203-217.
80. Murayama, Y.; Sato, S.; Oka, T. *Surgery Today* **1991,** 21, (5), 533-541.
81. Teuschl, A. Establishment of an Isolation Method of Different Types of Atelocollagen from Human Placenta and a Basic Evaluation as Biomaterial. Diploma thesis, Vienna University of Technology, Vienna, 2008.
82. Charulatha, V.; Rajaram, A. *Biomaterials* **2003,** 24, (5), 759-767.
83. Rabaud, M.; Lefebvre, F.; Ducassou, D. *Biomaterials* **1991,** 12, (3), 313-319.
84. McClure, M. J.; Sell, S. A.; Simpson, D. G.; Walpoth, B. H.; Bowlin, G. L. *Acta Biomater.* **2010,** 6, (7), 2422-2433.
85. Caves, J. M.; Kumar, V. A.; Martinez, A. W.; Kim, J.; Ripberger, C. M.; Haller, C. A.; Chaikof, E. L. *Biomaterials* **2010,** 31, (27), 7175-7182.
86. Redl, H.; Schlag, G.; Stanek, G.; Hirschl, A.; Seelich, T. *Biomaterials* **1983,** 4, (1), 29-32.
87. Tschoeke, B.; Flanagan, T. C.; Koch, S.; Harwoko, M. S.; Deichmann, T.; Ellae, V.; Sachweh, J. S.; Kellomaeki, M.; Gries, T.; Schmitz-Rode, T.; Jockenhoevel, S. *Tissue Eng., Part A* **2009,** 15, (8), 1909-1918.
88. Koch, S.; Flanagan, T. C.; Sachweh, J. S.; Tanios, F.; Schnoering, H.; Deichmann, T.; Ellä, V.; Kellomäki, M.; Gronloh, N.; Gries, T.; Tolba, R.; Schmitz-Rode, T.; Jockenhoevel, S. *Biomaterials* **2010,** 31, (17), 4731-4739.
89. Meinhart, J. G.; Deutsch, M.; Fischlein, T.; Howanietz, N.; Froschl, A.; Zilla, P. *The Annals of Thoracic Surgery* **2001,** 71, (90050), S327-331.
90. Huang, Y.; Onyeri, S.; Siewe, M.; Moshfeghian, A.; Madihally, S. V. *Biomaterials* **2005,** 26, (36), 7616-7627.
91. Sarasam, A.; Madihally, S. V. *Biomaterials* **2005,** 26, (27), 5500-5508.
92. Grigolo, B.; Roseti, L.; Fiorini, M.; Fini, M.; Giavaresi, G.; Nicoli Aldini, N.; Giardino, R.; Facchini, A. *Biomaterials* **2001,** 22, (17), 2417-2424.
93. Allison, D. D.; Grande-Allen, K. J. *Tissue Engineering* **2006,** 12, (8), 2131-2140.
94. Shu, X. Z.; Liu, Y.; Palumbo, F.; Prestwich, G. D. *Biomaterials* **2003,** 24, (21), 3825-3834.
95. Lee, K. Y.; Peters, M. C.; Mooney, D. J. *J. Controlled Release* **2003,** 87, (1-3), 49-56.
96. Kakisis, J. D.; Liapis, C. D.; Breuer, C.; Sumpio, B. E. *Journal of Vascular Surgery* **2005,** 41, (2), 349-54.
97. Trubel, W.; Moritz, A.; Schima, H.; Raderer, F.; Scherer, R.; Ullrich, R.; Losert, U.; Polterauer, P. *ASAIO Journal* **1994,** 40, (3), M273-M278.
98. Klinkert, P.; Schepers, A.; Burger Desiree, H. C.; van Bockel, J. H.; Breslau Paul, J. *Journal of Vascular Surgery* **2003,** 37, (1), 149-55.
99. Roach, P.; Eglin, D.; Rohde, K.; Perry, C. C. *J. Mater. Sci.: Mater. Med.* **2007,** 18, (7), 1263-1277.
100. Walpoth, B. H.; Rogulenko, R.; Tikhvinskaia, E.; Gogolewski, S.; Schaffner, T.; Hess, O. M.; Althaus, U. *Circulation* **1998,** 98, (19 Suppl), II319-23; discussion II324.
101. Chandra, R.; Rustgi, R. *Progress in Polymer Science* **1998,** 23, (7), 1273-1335.
102. Shalaby, S. W.; Burg, K. J. L., *Absorbable and Biodegradable Polymers*. CRC press: Boca Raton; London; New York; Washington, D.C., 2004; p 175-189.
103. Atala, A.; Mooney, D. J.; Vacanti, J. P.; Langer, R., *Synthetic Biodegradable Polymer Scaffolds*. Birkhäuser: Bosten, Basel, Berlin, 1997; p 165-185.
104. Middleton, J. C.; Tipton, A. J. *Biomaterials* **2000,** 21, (23), 2335-2346.

105. Gautier, E.; Fuertes, P.; Cassagnau, P.; Pascault, J.-P.; Fleury, E. *Journal of Polymer Science Part A: Polymer Chemistry* **2009,** 47, (5), 1440-1449.
106. Rezwan, K.; Chen, Q. Z.; Blaker, J. J.; Boccaccini, A. R. *Biomaterials* **2006,** 27, (18), 3413-3431.
107. Burkersroda, F. v.; Schedl, L.; Göpferich, A. *Biomaterials* **2002,** 23, (21), 4221-4231.
108. Jeong, S. I.; Kim, B.-S.; Kang, S. W.; Kwon, J. H.; Lee, Y. M.; Kim, S. H.; Kim, Y. H. *Biomaterials* **2004,** 25, (28), 5939-5946.
109. Soo-Hong, L.; Byung-Soo, K.; Soo Hyun, K.; Sung Won, C.; Sung In, J.; Il Keun, K.; Sun Woong, K.; Janeta, N.; David, J. M.; Yang-Kyoo, H.; Young Ha, K. *Journal of Biomedical Materials Research Part A* **2003,** 66A, (1), 29-37.
110. Smith, M. J.; McClure, M. J.; Sell, S. A.; Barnes, C. P.; Walpoth, B. H.; Simpson, D. G.; Bowlin, G. L. *Acta Biomater.* **2008,** 4, (1), 58-66.
111. Aldenhoff, Y. B. J.; Van der Veen, F. H.; ter Woorst, J.; Habets, J.; Poole-Warren, L. A.; Koole, L. H. *J. Biomed. Mater. Res.* **2000,** 54, (2), 224-233.
112. Becker, G. W.; Braun, D.; Oertel, G., *Kunststoff Handbuch Polyurethane*. 2.Auflage ed.; Carl Hanser Verlag München Wien, 1983; Vol. 7, p 664.
113. Santerre, J. P.; Woodhouse, K.; Laroche, G.; Labow, R. S. *Biomaterials* **2005,** 26, (35), 7457-7470.
114. Affrossman, S.; Barbenel, J. C.; Forbes, C. D.; MacAllister, J. M. R.; Meng, J.; Pethrick, R. A.; Scott, R. A. *Clinical Materials* **1991,** 8, (1-2), 25-31.
115. Zhao, Q.; Agger, M. P.; Fitzpatrick, M.; Anderson, J. M.; Hiltner, A.; Stokes, K.; Urbanski, P. *J. Biomed. Mater. Res.* **1990,** 24, (5), 621-637.
116. Labow, R. S.; Meek, E.; Matheson, L. A.; Santerre, J. P. **2002,** 23, (19), 3969-3975.
117. Howard, G. T. *Int. Biodeterior. Biodegrad.* **2002,** 49, (4), 245-252.
118. Khan, I.; Smith, N.; Jones, E.; Finch Dudley, S.; Cameron Ruth, E. *Biomaterials* **2005,** 26, (6), 633-43.
119. Khan, I.; Smith, N.; Jones, E.; Finch Dudley, S.; Cameron Ruth, E. *Biomaterials* **2005,** 26, (6), 621-31.
120. Schuster, M.; Turecek, C.; Kaiser, B.; Stampfl, J.; Liska, R.; Varga, F. *Journal of Macromolecular Science, Part A: Pure and Applied Chemistry* **2007,** 44, (5), 547-557.
121. Schuster, M.; Turecek, C.; Mateos, A.; Stampfl, J.; Liska, R.; Varga, F. *Monatsh. Chem.* **2007,** 138, (4), 261-268.
122. Schuster, M.; Turecek, C.; Varga, F.; Lichtenegger, H.; Stampfl, J.; Liska, R. *Appl. Surf. Sci.* **2007,** 254, (4), 1131-1134.
123. Mann, B. K.; Gobin, A. S.; Tsai, A. T.; Schmedlen, R. H.; West, J. L. *Biomaterials* **2001,** 22, (22), 3045-3051.
124. Arcaute, K.; Mann Brenda, K.; Wicker Ryan, B. *Annals of biomedical engineering* **2006,** 34, (9), 1429-41.
125. Stosich, M. S.; Bastian, B.; Marion, N. W.; Clark, P. A.; Reilly, G.; Mao, J. J. *Tissue Engineering* **2007,** 13, (12), 2881-2890.
126. Hubbell, J. A.; Massia, S. P.; Desai, N. P.; Drumheller, P. D. *Bio/Technology* **1991,** 9, (6), 568-72.
127. Drumheller, P. D.; Hubbell, J. A. *Analytical Biochemistry* **1994,** 222, (2), 380-8.
128. Heller, C.; Schwentenwein, M.; Russmueller, G.; Varga, F.; Stampfl, J.; Liska, R. *Journal of Polymer Science Part A: Polymer Chemistry* **2009,** 47, (24), 6941-6954.
129. Heller, C. Biocompatible and Biodegradable Photopolymers by Additive Manufacturing: From Synthesis to In-Vivo Studies. Dissertation, Vienna University of Technology, Vienna, 2010.
130. Stampfl, J.; Baudis, S.; Heller, C.; Liska, R.; Neumeister, A.; Kling, R.; Ostendorf, A.; Spitzbart, M. *Journal of Micromechanics and Microengineering* **2008,** 18, 125014.
131. Baudis, S.; Heller, C.; Liska, R.; Stampfl, J.; Bergmeister, H.; Weigel, G. *Journal of Polymer Science, Part A: Polymer Chemistry* **2009,** 47, (10), 2664-2676.

132. Liska, R.; Schuster, M.; Inführ, R.; Turecek, C.; Fritscher, C.; Seidl, B.; Schmidt, V.; Kuna, L.; Haase, A.; Varga, F.; Lichtenegger, H.; Stampfl, J. *Journal of Coatings Technology and Research* **2007,** 4, (4), 505-510.
133. Ho, W.; Tawil, B.; Dunn, J. C. Y.; Wu, B. M. *Tissue Eng.* **2006,** 12, (6), 1587-1595.
134. Agrawal, C. M.; Carter, J.; Ong, J. L. *Journal of ASTM International* **2006,** 3, (9).
135. Lim, L. T.; Auras, R.; Rubino, M. *Prog. Polym. Sci.* **2008,** 33, (8), 820-852.
136. Carampin, P.; Conconi, M. T.; Lora, S.; Menti, A. M.; Baiguera, S.; Bellini, S.; Grandi, C.; Parnigotto, P. P. *Journal of Biomedical Materials Research Part A* **2007,** 80A, (3), 661-668.
137. Sell, S. A.; Bowlin, G. L. *J. Mater. Chem.* **2008,** 18, (3), 260-263.
138. Baudis, S.; Schwarz, M.; Grasl, C.; Bergmeister, H.; Weigel, G.; Schima, H.; Liska, R. *MRS Symposium Proceedings* **2010,** 1235, RR03-30.
139. Sell, S. A.; McClure, M. J.; Garg, K.; Wolfe, P. S.; Bowlin, G. L. *Advanced Drug Delivery Reviews* **2009,** 61, (12), 1007-1019.
140. Yanyin, Y.; Durgadas, B.; Matthew, L. B.; Joachim, K.; Diana, N. Z.; Carl, G. S., Jr. *Advanced Materials* **2008,** 20, (11), 2037-2043.
141. Hacker, M.; Ringhofer, M.; Appel, B.; Neubauer, M.; Vogel, T.; Young, S.; Mikos, A. G.; Blunk, T.; Göpferich, A.; Schulz, M. B. *Biomaterials* **2007,** 28, (24), 3497-3507.
142. Nazarov, R.; Jin, H.-J.; Kaplan, D. L. *Biomacromolecules* **2004,** 5, (3), 718-726.
143. Melchels, F. P. W.; Feijen, J.; Grijpma, D. W. *Biomaterials* **2009,** 30, (23-24), 3801-3809.
144. Yang, S.; Leong, K.-F.; Du, Z.; Chua, C.-K. *Tissue Engineering* **2002,** 8, (1), 1-11.
145. Sodian, R.; Fu, P.; Lueders, C.; Szymanski, D.; Fritsche, C.; Gutberlet, M.; Hoerstrup, S. P.; Hausmann, H.; Lueth, T.; Hetzer, R. *The Thoracic and cardiovascular surgeon* **2005,** 53, (3), 144-9.
146. Gebhardt, A., *Rapid Prototyping - Werkzeuge für die schnelle Produktentstehung*. 2. Auflage ed.; Carl Hanser Verlag: München-Wien, 2000.
147. Leong, K. F.; Cheah, C. M.; Chua, C. K. *Biomaterials* **2003,** 24, (13), 2363-2378.
148. Hutmacher, D. W.; Sittinger, M.; Risbud, M. V. *Trends Biotechnol.* **2004,** 22, (7), 354-362.
149. Ricci, A.; Dietliker, K. *Spectrum (Bowling Green, OH, U. S.)* **2006,** 19, (1), 12-15.
150. Davis, K. A.; Burdick, J. A.; Anseth, K. S. *Biomaterials* **2003,** 24, (14), 2485-2495.
151. Moszner, N.; Salz, U. *Progress in Polymer Science* **2001,** 26, (4), 535-576.
152. Pham, Q. P.; Sharma, U.; Mikos, A. G. *Tissue engineering* **2006,** 12, (5), 1197-1211.
153. Sill, T. J.; von Recum, H. A. *Biomaterials* **2008,** 29, (13), 1989-2006.
154. Doshi, J.; Reneker, D. H. *Journal of Electrostatics* **1995,** 35, (2-3), 151-160.
155. Detta, N.; Errico, C.; Dinucci, D.; Puppi, D.; Clarke, D. A.; Reilly, G. C.; Chiellini, F. *J. Mater. Sci.: Mater. Med.* **2010,** 21, (5), 1761-1769.
156. Prabhakar, V.; Grinstaff, M. W.; Alarcon, J.; Knors, C.; Solan, A. K.; Niklason, L. E. *J. Biomed. Mater. Res., Part A* **2003,** 67A, (1), 303-311.
157. Boland, E. D.; Coleman, B. D.; Barnes, C. P.; Simpson, D. G.; Wnek, G. E.; Bowlin, G. L. *Acta Biomaterialia* **2005,** 1, (1), 115-123.
158. Sell, S. A.; McClure, M. J.; Barnes, C. P.; Knapp, D. C.; Walpoth, B. H.; Simpson, D. G.; Bowlin, G. L. *Biomed. Mater.* **2006,** 1, (2), 72-80.
159. Tan, A. R.; Ifkovits, J. L.; Baker, B. M.; Brey, D. M.; Mauck, R. L.; Burdick, J. A. *J. Biomed. Mater. Res., Part A* **2008,** 87A, (4), 1034-1043.
160. Ifkovits, J. L.; Padera, R. F.; Burdick, J. A. *Biomedical Materials* **2008,** 3, (3), 034104.
161. Sato, M.; Nakazawa, Y.; Takahashi, R.; Tanaka, K.; Sata, M.; Aytemiz, D.; Asakura, T. *Materials Letters* **2010,** 64, (16), 1786-1788.
162. Crapo, P. M.; Wang, Y. *Biomaterials* **2010,** 31, (7), 1626-1635.
163. Yilgor, I.; Yilgor, E. *Polymer Reviews (Philadelphia, PA, United States)* **2007,** 47, (4), 487-510.
164. Soldani, G.; Losi, P.; Bernabei, M.; Burchielli, S.; Chiappino, D.; Kull, S.; Briganti, E.; Spiller, D. *Biomaterials* **2010,** 31, (9), 2592-2605.
165. Zhang, Z.; Wang, Z.; Liu, S.; Kodama, M. *Biomaterials* **2004,** 25, (1), 177-187.
166. Xue, L.; Greisler Howard, P. *Journal of vascular surgery* **2003,** 37, (2), 472-80.

167. Farè, S.; Valtulina, V.; Petrini, P.; Alessandrini, E.; Pietrocola, G.; Tanzi, M. C.; Speziale, P.; Visai, L. *Journal of Biomedical Materials Research Part A* **2005,** 73A, (1), 1-11.
168. Harris, L. G.; Gorna, K.; Gogolewski, S.; Richards, R. G. *J. Biomed. Mater. Res., Part A* **2006,** 77A, (2), 304-312.
169. Courtney, T.; Sacks, M. S.; Stankus, J.; Guan, J.; Wagner, W. R. *Biomaterials* **2006,** 27, (19), 3631-3638.
170. Grenier, S.; Sandig, M.; Mequanint, K. *J. Biomed. Mater. Res., Part A* **2007,** 82A, (4), 802-809.
171. Grasl, C.; Bergmeister, H.; Stoiber, M.; Schima, H.; Weigel, G. *Journal of Biomedical Materials Research Part A* **2010,** 93A, (2), 716-723.
172. Gogolewski, S.; Galletti, G.; Ussia, G. *Colloid Polym. Sci.* **1987,** 265, (9), 774-8.
173. Burdick, J. A.; Anseth, K. S. *Biomaterials* **2002,** 23, (22), 4315-4323.
174. Hahn, M. S.; Taite, L. J.; Moon, J. J.; Rowland, M. C.; Ruffino, K. A.; West, J. L. *Biomaterials* **2006,** 27, (12), 2519-2524.
175. Hahn, M. S.; Miller, J. S.; West, J. L. *Advanced Materials (Weinheim, Germany)* **2006,** 18, (20), 2679-2684.
176. Rydholm, A. E.; Reddy, S. K.; Anseth, K. S.; Bowman, C. N. *Polymer* **2007,** 48, (15), 4589-4600.
177. Breusch, S. J.; Kühn, K. D. *Der Orthopäde* **2003,** 32, (1), 41-50.
178. Melchels, F. P. W.; Feijen, J.; Grijpma, D. W. *Biomaterials* **2010,** 31, (24), 6121-6130.
179. Schuster, M. Photopolymers for Bone Tissue Engineering. Dissertation, Vienna University of Technology, Vienna, 2008.
180. Schuster, M.; Turecek, C.; Weigel, G.; Saf, R.; Stampfl, J.; Varga, F.; Liska, R. *J. Polym. Sci., Part A: Polym. Chem.* **2009,** 47, (24), 7078-7089.
181. Baudis, S.; Steyrer, B.; Pulka, T.; Wilhelm, H.; Weigel, G.; Bergmeister, H.; Stampfl, J.; Liska, R. *Macromolecular Symposia* **2010,** ASAP.
182. Merrill, E. W.; Salzman, E. W. *ASAIO Journal (1978-1985)* **1983,** 6, (2), 60-4.
183. Tessmar, J. K.; Goepferich, A. M. *Macromolecular Bioscience* **2007,** 7, (1), 23-39.
184. Bryant, S.; Anseth, K., Photopolymerization of Hydrogel Scaffolds. In *Scaffolding In Tissue Engineering*, CRC Press: 2005.
185. Nguyen, K. T.; West, J. L. *Biomaterials* **2002,** 23, (22), 4307-4314.
186. Metters, A. T.; Lin, C.-C. *Biomaterials* **2007**, 5/1-5/44.
187. Bryant, S. J.; Anseth, K. S. *Biomaterials* **2001,** 22, (6), 619-626.
188. DeLong, S. A.; Moon, J. J.; West, J. L. *Biomaterials* **2005,** 26, (16), 3227-3234.
189. Nuttelman, C. R.; Tripodi, M. C.; Anseth, K. S. *Journal of Biomedical Materials Research Part A* **2004,** 68A, (4), 773-782.
190. Nuttelman, C. R.; Rice, M. A.; Rydholm, A. E.; Salinas, C. N.; Shah, D. N.; Anseth, K. S. *Progress in Polymer Science* **2008,** 33, (2), 167-179.
191. Weber, L. M.; Hayda, K. N.; Haskins, K.; Anseth, K. S. *Biomaterials* **2007,** 28, (19), 3004-3011.
192. Hern, D. L.; Hubbell, J. A. *J. Biomed. Mater. Res.* **1998,** 39, (2), 266-276.
193. Lee, S.-H.; Moon, J. J.; West, J. L. *Biomaterials* **2008,** 29, (20), 2962-2968.
194. Shu, X. Z.; Ghosh, K.; Liu, Y.; Palumbo, F. S.; Luo, Y.; Clark, R. A.; Prestwich, G. D. *Journal of Biomedical Materials Research, Part A* **2004,** 68A, (2), 365-375.
195. Anderson, D. G.; Tweedie, C. A.; Hossain, N.; Navarro, S. M.; Brey, D. M.; Van Vliet, K. J.; Langer, R.; Burdick, J. A. *Advanced Materials (Weinheim, Germany)* **2006,** 18, (19), 2614-2618.
196. Pedrón, S.; Anseth, K.; Benton, J. A.; Bosch, P.; Peinado, C. *Macromolecular Symposia* **2010,** 291-292, (1), 307-313.
197. Ifkovits, J. L.; Burdick, J. A. *Tissue Engineering* **2007,** 13, (10), 2369-2385.
198. Baroli, B. *Journal of Chemical Technology & Biotechnology* **2006,** 81, (4), 491-499.
199. Mason, M. N.; Metters, A. T.; Bowman, C. N.; Anseth, K. S. *Macromolecules* **2001,** 34, (13), 4630-4635.

200. Declercq, H.; Cornelissen, M.; Gorskiy, T.; Schacht, E. *J. Mater. Sci.: Mater. Med.* **2006,** 17, (2), 113-122.
201. Matsuda, T.; Kwon, I. K.; Kidoaki, S. *Biomacromolecules* **2003,** 5, (2), 295-305.
202. Vaida, C.; Mela, P.; Keul, H.; Möller, M. *Journal of Polymer Science Part A: Polymer Chemistry* **2008,** 46, (20), 6789-6800.
203. Timbart, L.; Amsden, B. *Journal of Polymer Science: Part A: Polymer Chemistry* **2008,** 46, 8191-8199.
204. Marvel, C. S.; Chambers, R. R. *J. Am. Chem. Soc.* **1948,** 70, (3), 993-998.
205. Marvel, C. S.; Caesar, P. D. *J. Am. Chem. Soc.* **1951,** 73, (3), 1097-1099.
206. Hoyle, C. E.; Lee, T. Y.; Roper, T. M. *Journal of Polymer Science Part A: Polymer Chemistry* **2004,** 42, (21), 5301-5338.
207. Hoyle, Charles E.; Bowman, Christopher N. *Angewandte Chemie International Edition* **2010,** 49, (9), 1540-1573.
208. Lecamp, L.; Houllier, F.; Youssef, B.; Bunel, C. *Polymer* **2001,** 42, (7), 2727-2736.
209. Aimetti, A. A.; Machen, A. J.; Anseth, K. S. *Biomaterials* **2009,** 30, (30), 6048-6054.
210. DeForest, C. A.; Polizzotti, B. D.; Anseth, K. S. *Nat. Mater.* **2009,** 8, (8), 659-664.
211. DeForest, C. A.; Sims, E. A.; Anseth, K. S. *Chem. Mater.* **2010,** 22, (16), 4783-4790.
212. DeForest, C. A.; Sims, E. A.; Anseth, K. S. *Polym. Prepr. (Am. Chem. Soc., Div. Polym. Chem.)* **2010,** 51, (1), 62-63.
213. Fairbanks, B. D.; Schwartz, M. P.; Halevi, A. E.; Nuttelman, C. R.; Bowman, C. N.; Anseth, K. S. *Adv. Mater. (Weinheim, Ger.)* **2009,** 21, (48), 5005-5010.
214. Guelcher, S. A. *Tissue Eng., Part B* **2008,** 14, (1), 3-17.
215. Netzel-Arnett, S.; Fields, G. B.; Birkedal-Hansen, H.; Van Wart, H. E.; Fields, G. *Journal of Biological Chemistry* **1991,** 266, (11), 6747-6755.
216. Sottrup-Jensen, L.; Birkedal-Hansen, H. *Journal of Biological Chemistry* **1989,** 264, (1), 393-401.
217. West, J. L.; Hubbell, J. A. *Macromolecules* **1999,** 32, (1), 241-244.
218. Madsen, J.; Armes, S. P.; Bertal, K.; Lomas, H.; MacNeil, S.; Lewis, A. L. *Biomacromolecules* **2008,** 9, (8), 2265-2275.
219. Meng, F.; Hennink, W. E.; Zhong, Z. *Biomaterials* **2009,** 30, (12), 2180-2198.
220. de Paz, V. M.; Zamora, F.; Begines, B.; Ferris, C.; Galbis, J. A. *Biomacromolecules* **2010,** 11, (1), 269-276.
221. Soeda, Y.; Toshima, K.; Matsumura, S. *Macromol. Biosci.* **2005,** 5, (4), 277-288.
222. Matsumura, S.; Soeda, Y.; Toshima, K. *Appl. Microbiol. Biotechnol.* **2006,** 70, (1), 12-20.
223. Pawlowski, P.; Rokicki, G. *Polymer* **2004,** 45, (10), 3125-3137.
224. Coulembier, O.; Degée, P.; Hedrick, J. L.; Dubois, P. *Progress in Polymer Science* **2006,** 31, (8), 723-747.
225. Biela, T.; Kowalski, A.; Libiszowski, J.; Duda, A.; Penczek, S. *Macromolecular Symposia* **2006,** 240, (1), 47-55.
226. Helou, M.; Miserque, O.; Brusson, J. M.; Carpentier, J. F.; Guillaume, S. *Advanced Synthesis & Catalysis* **2009,** 351, (9), 1312-1324.
227. Pamula, E.; Dobrzynski, P.; Szot, B.; Kretek, M.; Krawciow, J.; Plytycz, B.; Chadzinska, M. *Journal of Biomedical Materials Research Part A* **2008,** 87A, (2), 524-535.
228. Morakot, N.; Threeprom, J.; Baimark, Y. *e-Polym.* **2008**, (92).
229. Gorna, K.; Polowinski, S.; Gogolewski, S. *J. Polym. Sci., Part A: Polym. Chem.* **2001,** 40, (1), 156-170.
230. Gorna, K.; Gogolewski, S. *Polym. Degrad. Stab.* **2001,** 75, (1), 113-122.
231. Gorna, K.; Gogolewski, S. *J. Biomed. Mater. Res.* **2002,** 60, (4), 592-606.
232. Skarja, G. A.; Woodhouse, K. A. *J. Biomater. Sci., Polym. Ed.* **2001,** 12, (8), 851-873.
233. Guan, J.; Sacks, M. S.; Beckman, E. J.; Wagner, W. R. *J. Biomed. Mater. Res.* **2002,** 61, (3), 493-503.
234. Gorna, K.; Gogolewski, S. *J. Biomed. Mater. Res., Part A* **2006,** 79A, (1), 128-138.

235. Marcos-Fernandez, A.; Abraham, G. A.; Valentin, J. L.; San Roman, J. *Polymer* **2006,** 47, (3), 785-798.
236. Zhang, C.; Zhang, N.; Wen, X. *J. Biomed. Mater. Res., Part B* **2006,** 79B, (2), 335-344.
237. Jiang, X.; Li, J.; Ding, M.; Tan, H.; Ling, Q.; Zhong, Y.; Fu, Q. *Eur. Polym. J.* **2007,** 43, (5), 1838-1846.
238. Tatai, L.; Moore, T. G.; Adhikari, R.; Malherbe, F.; Jayasekara, R.; Griffiths, I.; Gunatillake, P. A. *Biomaterials* **2007,** 28, (36), 5407-5417.
239. Wisse, E.; Renken, R. A. E.; Roosma, J. R.; Palmans, A. R. A.; Meijer, E. W. *Biomacromolecules* **2007,** 8, (9), 2739-2745.
240. Walinska, K.; Iwan, A.; Gorna, K.; Gogolewski, S. *J. Mater. Sci.: Mater. Med.* **2008,** 19, (1), 129-135.
241. Zhang, C.; Wen, X.; Vyavahare, N. R.; Boland, T. *Biomaterials* **2008,** 29, (28), 3781-3791.
242. Bil, M.; Ryszkowska, J.; Kurzydłowski, K. *Journal of Materials Science* **2009,** 44, (6), 1469-1476.
243. Rodrigues-da Silva, G.; da Silva-Cunha, A. J.; Ayres, E.; Orefice, R. L. *J Mater Sci Mater Med* **2009,** 20, (2), 481-7.
244. Sarkar, D.; Yang, J.-C.; Gupta, A. S.; Lopina, S. T. *J. Biomed. Mater. Res., Part A* **2009,** 90A, (1), 263-271.
245. Soletti, L.; Hong, Y.; Guan, J.; Stankus, J. J.; El-Kurdi, M. S.; Wagner, W. R.; Vorp, D. A. *Acta Biomaterialia* **2010,** 6, (1), 110-122.
246. Lendlein, A.; Neuenschwander, P.; Suter, U. W. *Macromolecular Chemistry and Physics* **1998,** 199, (12), 2785-2796.
247. Cohn, D.; Hotovely-Salomon, A. *Polymer* **2005,** 46, (7), 2068-2075.
248. Cohn, D.; Hotovely Salomon, A. *Biomaterials* **2005,** 26, (15), 2297-2305.
249. van Minnen, B.; Leeuwen, M. B. M. v.; Stegenga, B.; Zuidema, J.; Hissink, C. E.; van Kooten, T. G.; Bos, R. R. M. *Journal of Material Science: Materials in Medicine* **2005,** 16, (3), 221-227.
250. Guo, Q.; Knight, P. T.; Mather, P. T. *J. Controlled Release* **2009,** 137, (3), 224-233.
251. Cao, J.; Chen, N.; Chen, Y.; Luo, X. *Int. J. Mol. Sci.* **2010,** 11, 1870-1877.
252. Kricheldorf, H. R.; Rost, S. *Macromolecules* **2005,** 38, (20), 8220-8226.
253. Asplund, J. O. B.; Bowden, T.; Mathisen, T.; Hilborn, J. *Biomacromolecules* **2007,** 8, (3), 905-911.
254. Lee, S.-I.; Yu, S.-C.; Lee, Y.-S. *Polym. Degrad. Stab.* **2001,** 72, (1), 81-87.
255. Ambs, S.; Neumann, H.-G. *Toxicology and Applied Pharmacology* **1996,** 139, (1), 186-194.
256. Cunningham, M. L.; Matthews, H. B. *Toxicology Letters* **1995,** 82-83, 9-14.
257. Kenyon, S. H.; Bhattacharyya, J.; Benson, C. J.; Carmichael, P. L. *Toxicology* **2004,** 196, (1-2), 65-75.
258. Wozniak, P.; Bil, M.; Ryszkowska, J.; Wychowanski, P.; Wróbel, E.; Ratajska, A.; Hoser, G.; Przybylski, J.; Kurzydlowski, K. J.; Lewandowska-Szumiel, M. *Acta Biomaterialia* **2010,** 6, (7), 2484-2493.
259. Eglin, D.; Grad, S.; Gogolewski, S.; Alini, M. *J. Biomed. Mater. Res., Part A* **2009,** 92A, (1), 393-408.
260. Guan, J.; Wagner, W. R. *Biomacromolecules* **2005,** 6, (5), 2833-2842.
261. Alperin, C.; Zandstra, P. W.; Woodhouse, K. A. *Biomaterials* **2005,** 26, (35), 7377-7386.
262. Kenawy, E.-R.; Al-Deyab, S. S.; El-Newehy, M. H. *Molecules* **2010,** 15, (4), 2257-2268.
263. Mahkam, M.; Sharifi-Sanjani, N. *Polym. Degrad. Stab.* **2003,** 80, (2), 199-202.
264. Rodrigues-da Silva, G.; da Silva-Cunha Jr, A.; Behar-Cohen, F.; Ayres, E.; Oréfice, R. L. *Polym. Degrad. Stab.* **2010,** 95, (4), 491-499.
265. Spaans, C. J.; De Groot, J. H.; Dekens, F. G.; Pennings, A. J. *Polym. Bull. (Berlin)* **1998,** 41, (2), 131-138.
266. Guo, Q.; Knight, P. T.; Wu, J.; Mather, P. T. *Macromolecules* **2010,** ASAP.
267. Tran, R. T.; Thevenot, P.; Zhang, Y.; Gyawali, D.; Tang, L.; Yang, J. *Materials* **2010,** 3, 1375-1389.

268. Dey, J.; Xu, H.; Shen, J.; Thevenot, P.; Gondi, S. R.; Nguyen, K. T.; Sumerlin, B. S.; Tang, L.; Yang, J. *Biomaterials* **2008,** 29, (35), 4637-4649.
269. Adhikari, R.; Danon, S. J.; Bean, P.; Le, T.; Gunatillake, P.; Ramshaw, J. A. M.; Werkmeister, J. A. *J. Mater. Sci.: Mater. Med.* **2010,** 21, (4), 1081-1089.
270. Shi, R.; Chen, D.; Liu, Q.; Wu, Y.; Xu, X.; Zhang, L.; Tian, W. *Int. J. Mol. Sci.* **2009,** 10, (10), 4223-4256.
271. Voda, A.; Beck, K.; Schauber, T.; Adler, M.; Dabisch, T.; Bescher, M.; Viol, M.; Demco, D. E.; Blümich, B. *Polymer Testing* **2006,** 25, (2), 203-213.
272. Grellmann, W.; Seidler, S., *Kunststoffprüfung*. Carl Hanser Verlag: München, 2005.
273. Williams, C. G.; Malik, A. N.; Kim, T. K.; Manson, P. N.; Elisseeff, J. H. *Biomaterials* **2005,** 26, (11), 1211-8.
274. Schmaljohann, D.; Gramm, S. *Polymer Preprints* **2002,** 43, (2), 758-759.
275. Mortimer, G. A. *J. Appl. Polym. Sci.* **1971,** 15, (5), 1231-5.
276. Ando, H.; Takahashi, N. Cyanoacrylate-based adhesive. 11,302,602, April 23, 1998, 1999.
277. Edelmann, K.; Reiche, A.; Sandner, B.; Marstalerz, J.; Mueller, H. *Polymer* **2005,** 46, (2), 407-417.
278. Mandeville, W. H., III; Holmes-Farley, S. R. Oral administration of iron-binding crosslinked amine polymers. 5,702,696, June 12, 1995, 1997.
279. Mandeville, W. H., III; Holmes-Farley, S. R. Iron-binding polymers for oral administration. 9,427,621, May 16, 1994, 1994.
280. Fouassier, J.-P.; Rabek, J. F., *Radiation Curing in Polymer Science and Technology, Vol. 1: Fundamentals and Methods*. Elsevier: 1993; p 563 pp.
281. Liska, R.; Herzog, D. *J. Polym. Sci., Part A: Polym. Chem.* **2004,** 42, (3), 752-764.
282. Karasu, F.; Dworak, C.; Kopeinig, S.; Hummer, E.; Arsu, N.; Liska, R. *Macromolecules* **2008,** 41, (21), 7953-7958.
283. Brandrup, J.; Immergut, E. H.; Grulke, E. A., *Polymer Handbook*. 3 ed.; John Wiley & Sons: New York, Chichester, Weinheim, Brisbane, Singapore, Toronto, 1999.
284. Menczel, J. D.; Prime , R. B., *Thermal Analysis of Polymers, Fundamentals and Applications*. Wiley: New Jersey, 2009.
285. Dhariwala, B.; Hunt, E.; Boland, T. *Tissue Engineering* **2004,** 10, (9/10), 1316-1322.
286. Gombotz, W. R.; Wang, G.; Horbett, T. A.; Hoffman, A. S. *Journal of Biomedical Materials Research* **1991,** 25, (12), 1547-62.
287. Puskas, J. E.; Chen, Y. *Biomacromolecules* **2004,** 5, (4), 1141-1154.
288. Kneubühl, F. K.; Sigrist, M. W., *Laser*. B.G. Teubner Verlag: Wiesbaden, 2005; Vol. 6.
289. Pedrotti, F.; Pedrotti, L.; Bausch, W.; Schmidt, H., *Optik für Ingenieure, Grundlagen*. Springer-Verlag: Heidelberg, 2005.
290. Rahn-AG, Datenblatt Genomer 4215. In 2007; p 5.
291. Rahn-AG, Data sheet Genomer 4188/EHA. In 2005; p 5.
292. Cognis, Data sheet Photomer 6210. In 2009; p 5.
293. *Polymer in Genomer 4215 (Full public report)*; LTD/1425; National Idustrial Chemicals Notification and Assessment Scheme: Sydney, 01/29/2010 2010; p 12.
294. Smith, K. E.; Temenoff, J. S.; Gall, K. *J. Appl. Polym. Sci.* **2009,** 114, (5), 2711-2722.
295. Mine, Y.; Mitsui, H.; Oshima, Y.; Noishiki, Y.; Nakai, M.; Sano, S. *Acta Med. Okayama* **2010,** 64, (2), 121-128.
296. Senyurt, A. F.; Hoyle, C. E.; Wei, H.; Piland, S. G.; Gould, T. E. *Macromolecules* **2007,** 40, (9), 3174-3182.
297. Good, B. T.; Reddy, S.; Davis, R. H.; Bowman, C. N. *Sens. Actuators, B* **2007,** B120, (2), 473-480.
298. Kade, M. J.; Burke, D. J.; Hawker, C. J. *Journal of Polymer Science Part A: Polymer Chemistry* **2010,** 48, (4), 743-750.
299. Klemm, E.; Sensfuß, S.; Holfter, U.; Flammersheim, H. J. *Die Angewandte Makromolekulare Chemie* **1993,** 212, (1), 121-127.

300. Blondel, W. C.; Didelon, J.; Maurice, G.; Carteaux, J. P.; Wang, X.; Stoltz, J. F. *IEEE Trans Biomed Eng* **2001,** 48, (4), 442-51.
301. Gabella, G. *The Anatomical record* **1995,** 243, (3), 376-83.
302. Envisiontec, Technical Data: Envisiontec R05/R11. In.
303. Hinczewski, C.; Corbel, S.; Chartier, T. *J. Eur. Ceram. Soc.* **1998,** 18, (6), 583-590.
304. Biomedica-Vienna, EZ4U: Non-radioactive cell proliferation and toxicity assay. Assay protocol. In.
305. Metters, A. T.; Bowman, C. N.; Anseth, K. S. *J. Phys. Chem. B* **2000,** 104, (30), 7043-7049.
306. Eisenbach, C. D.; Baumgartner, M.; Guenter, C. *Polym. Prepr. (Am. Chem. Soc., Div. Polym. Chem.)* **1985,** 26, (2), 7-9.
307. Marand, A.; Dahlin, J.; Karlsson, D.; Skarping, G.; Dalene, M. *J. Environ. Monit.* **2004,** 6, (7), 606-614.
308. Rokicki, G.; Piotrowska, A. *Polymer* **2002,** 43, (10), 2927-2935.
309. Assumption, H. J.; Mathias, L. J. *Polymer* **2003,** 44, (18), 5131-5136.
310. Pham, S. V.; Pham, P.-C. T.; Pham, P.-M. T.; Miller, J. M.; Pham, P.-T. T.; Pham, P.-A. T. *Drug Des., Dev. Ther.* **2010,** 4, 203-220.
311. Hankey, G. J.; Eikelboom, J. W. *The Lancet Neurology* **2010,** 9, (3), 273-284.
312. Kim, J.; Lee, K.-W.; Hefferan, T. E.; Currier, B. L.; Yaszemski, M. J.; Lu, L. *Biomacromolecules* **2008,** 9, (1), 149-157.
313. Cai, Y.; Armes, S. P. *Macromolecules* **2005,** 38, (2), 271-279.
314. Ochs, C.; Hahn, F. E.; Fröhlich, R. *Chemistry - A European Journal* **2000,** 6, (12), 2193-2199.
315. Hurd, C. D.; Gershbein, L. L. *J. Am. Chem. Soc.* **1947,** 69, (10), 2328-2335.
316. Papenburg, B. J.; Schüller-Ravoo, S.; Bolhuis-Versteeg, L. A. M.; Hartsuiker, L.; Grijpma, D. W.; Feijen, J.; Wessling, M.; Stamatialis, D. *Acta Biomaterialia* **2009,** 5, (9), 3281-3294.
317. Zhang, Z.; Kuijer, R.; Bulstra, S. K.; Grijpma, D. W.; Feijen, J. *Biomaterials* **2006,** 27, (9), 1741-1748.
318. Korley, L. T. J.; Pate, B. D.; Thomas, E. L.; Hammond, P. T. *Polymer* **2006,** 47, (9), 3073-3082.
319. Siemann, U. *Prog. Colloid Polym. Sci.* **2005,** 130, 1-14.
320. Yuan, X.; Mak, A. F. T.; Yao, K. *Polym. Degrad. Stab.* **2001,** 75, (1), 45-53.
321. Yang, J.; Webb, A. R.; Ameer, G. A. *Advanced Materials* **2004,** 16, (6), 511-516.
322. Bat, E.; van, K. T. G.; Feijen, J.; Grijpma, D. W. *Biomaterials* **2009,** 30, (22), 3652-3661.
323. Rehberg, C. E.; Dixon, M. B.; Faucette, W. A. *Journal of the American Chemical Society* **1950,** 72, 5199-5200.
324. Ueda, M.; Suzuki, T.; Imai, Y.; Pittman, C. U., Jr.; Wallace, E., Jr. *Journal of Polymer Science, Polymer Chemistry Edition* **1983,** 21, (10), 2997-3008.
325. Armarego, W. L. F.; Lin Lin Chai, C., *Purification of Laboratory Chemicals*. Fifth Edition ed.; Butterworth Heinemann: 2003.